ISSN 2518-718X

№ 2(90)/2018

ХИМИЯ сериясы

Серия ХИМИЯ

CHEMISTRY Series

ҚАРАҒАНДЫ УНИВЕРСИТЕТІНІҢ ХАБАРШЫСЫ

ВЕСТНИК КАРАГАНДИНСКОГО УНИВЕРСИТЕТА

BULLETIN OF THE KARAGANDA UNIVERSITY

ISSN 2518-718X
Индексі 74617
Индекс 74617

ҚАРАҒАНДЫ УНИВЕРСИТЕТІНІҢ ХАБАРШЫСЫ

ВЕСТНИК КАРАГАНДИНСКОГО УНИВЕРСИТЕТА

BULLETIN OF THE KARAGANDA UNIVERSITY

ХИМИЯ сериясы

Серия ХИМИЯ

CHEMISTRY Series

№ 2(90)/2018

Сәуір–мамыр–маусым
30 маусым 2018 ж.

Апрель–май–июнь
30 июня 2018 г.

April–May–June
June, 30, 2018

1996 жылдан бастап шығады
Издается с 1996 года
Founded in 1996

Жылына 4 рет шығады
Выходит 4 раза в год
Published 4 times a year

Қарағанды, 2018
Караганда, 2018
Karaganda, 2018

Редакцияның мекенжайы: 100028, Қазақстан, Қарағанды қ., Университет к-сі, 28
Тел.: (7212) 77-03-69 (ішкі 1026); факс: (7212) 77-03-84.
E-mail: vestnick_kargu@ksu.kz. Сайты: vestnik.ksu.kz

Редакторы

Ж.Т. Нурмуханова

Компьютерде беттеген

В.В. Бутяйкин

Қарағанды университетінің хабаршысы. «Химия» сериясы.

ISSN 2518-718X.

Меншік иесі: «Академик Е.А. Бөкетов атындағы Қарағанды мемлекеттік университеті» РММ.

Қазақстан Республикасының Мәдениет және ақпарат министрлігімен тіркелген. 23.10.2012 ж. № 13110–Ж тіркеу куәлігі.

Басуға 29.06.2018 ж. қол қойылды. Пішімі 60×84 1/8. Қағазы офсеттік. Көлемі 15,37 б.т. Таралымы 300 дана. Бағасы келісім бойынша. Тапсырыс № 69.

Е.А. Бөкетов атындағы ҚарМУ баспасының баспаханасында басылып шықты.
100012, Қазақстан, Қарағанды қ., Гоголь к-сі, 38. Тел. 51-38-20. E-mail: izd_kargu@mail.ru

Адрес редакции: 100028, Казахстан, г. Караганда, ул. Университетская, 28
Тел.: (7212) 77-03-69 (внутр. 1026); факс: (7212) 77-03-84.
E-mail: vestnick_kargu@ksu.kz. Сайт: vestnik.ksu.kz

Редактор
Ж.Т. Нурмуханова

Компьютерная верстка
В.В. Бутяйкин

Вестник Карагандинского университета. Серия «Химия».
ISSN 2518-718X.
Собственник: РГП «Карагандинский государственный университет имени академика Е.А. Букетова».
Зарегистрирован Министерством культуры и информации Республики Казахстан. Регистрационное свидетельство № 13110–Ж от 23.10.2012 г.

Подписано в печать 29.06.2018 г. Формат 60×84 1/8. Бумага офсетная. Объем 15,37 п.л. Тираж 300 экз. Цена договорная. Заказ № 69.
Отпечатано в типографии издательства КарГУ им. Е.А. Букетова.
100012, Казахстан, г. Караганда, ул. Гоголя, 38, тел.: (7212) 51-38-20. E-mail: izd_kargu@mail.ru

Postal address: 28, University Str., Karaganda, 100028, Kazakhstan
Tel.: (7212) 77-03-69 (add. 1026); fax: (7212) 77-03-84.
E-mail: vestnick_kargu@ksu.kz. Web-site: vestnik.ksu.kz

Editor
Zh.T. Nurmukhanova

Computer layout
V.V. Butyaikin

Bulletin of the Karaganda University. «Chemistry» series.
ISSN 2518-718X.
Proprietary: RSE «Academician Ye.A. Buketov Karaganda State University».
Registered by the Ministry of Culture and Information of the Republic of Kazakhstan. Registration certificate No. 13110–Zh from 23.10.2012.
Signed in print 29.06.2018. Format 60×84 1/8. Offset paper. Volume 15,37 p.sh. Circulation 300 copies. Price upon request. Order № 69.
Printed in the Ye.A. Buketov Karaganda State University Publishing house.
38, Gogol Str., Karaganda, 100012, Kazakhstan. Tel.: (7212) 51-38-20. E-mail: izd_kargu@mail.ru

МАЗМҰНЫ

ОРГАНИКАЛЫҚ ХИМИЯ

ФИЗИКАЛЫҚ ЖӘНЕ АНАЛИТИКАЛЫҚ ХИМИЯ

БЕЙОРГАНИКАЛЫҚ ХИМИЯ

ХИМИЯЛЫҚ ТЕХНОЛОГИЯ

ХИМИЯНЫ ОҚЫТУ ӘДІСТЕМЕСІ

СОДЕРЖАНИЕ

ОРГАНИЧЕСКАЯ ХИМИЯ

ФИЗИЧЕСКАЯ И АНАЛИТИЧЕСКАЯ ХИМИЯ

НЕОРГАНИЧЕСКАЯ ХИМИЯ

ХИМИЧЕСКАЯ ТЕХНОЛОГИЯ

МЕТОДИКА ОБУЧЕНИЯ ХИМИИ

CONTENTS

ORGANIC CHEMISTRY

PHYSICAL AND ANALYTICAL CHEMISTRY

INORGANIC CHEMISTRY

CHEMICAL TECHNOLOGY

METHODS OF TEACHING CHEMISTRY

ОРГАНИКАЛЫҚ ХИМИЯ
ОРГАНИЧЕСКАЯ ХИМИЯ
ORGANIC CHEMISTRY

UDC 541.64:678.744

Ye.V. Blagikh[1], Zh.K. Sadakbayeva[2], A.N. Klivenko[3],
Zh.A. Nurakhmetova[1], V.B. Sigitov[1], S.E. Kudaibergenov[1]

[1]Institute of Polymer Materials and Technology, Almaty, Kazakhstan;
[2]Institute of Macromolecular Chemistry of the Academy of Sciences, Prague, Czech Republic;
[3]Shakarim State University of Semey, Kazakhstan
(E-mail: skudai@mail.ru)

Development of composite hydrogel materials for cleaning the inner surface of pipelines

Flexible, mechanically strong composite hydrogel materials based on polyacrylamide hydrogel (PAAH), clay minerals (kaolin, bentonite and montmorillonite), poly-N-vinylpyrrolidone (PVP) and SiO_2 were developed for cleaning the inner surface of pipelines. The mechanical strength of composite hydrogels increases in the following order: PAAH-PVP > PAAH-Montmorillonite > PAAH-SiO_2 > PAAH-Bentonite. The results showed that the composite hydrogel samples are able to sustain more than 200 cycles of vertical deformation without damage. The hydrogel «pigs» selected according to the values of tensile strength and Young's modulus were tested on model «small» and «big» pipelines. The application of hydrogel «pigs» for cleaning the model pipelines proved to be successful. In contrast to mechanical analogues, hydrogel «pigs» pass freely through the pipelines of various shape and size, ensure necessary hydraulic pressure in the inner surface, provide explosion and fire safety, and absorb water along in the course of movement inside the pipeline. Their cleaning efficiency of the model pipelines from the asphaltene-resin-paraffin deposits (ARPD) was evaluated as 93–95 %. The scaled up hydrogel «pigs» were fabricated for cleaning of oilfield pipes. The proposed materials would be of interest for oil transportation companies due to cost-efficiency and technological feasibility.

Keywords: hydrogels, clay minerals, polyacrylamide hydrogel, composite materials, hydrogel «pigs», Young's modulus, model pipeline, cleaning effectiveness, asphaltene-resin-paraffin deposits.

Introduction

During the last decade, technical policies of oil transportation companies became more demanding regarding the longevity of the pipelines [1]. In the process of pipeline exploitation, the debris, sand and a mixture of asphaltene-resin-paraffin deposition (ARPD) are accumulated and deposited on the inner surface of the pipeline, leading to reduced capacity of the pipeline, low velocity of oil stream and increased pressure in the pipeline [1,2]. Additionally, water retention that occurs in the lower sections of the pipeline can cause corrosion process while accumulation of gas-air mixture in the upper sections of the pipeline can lead to explosion problems. The simultaneous transportation of crude oil and petroleum products in one and the same pipe is also a challenging task [3–5]. Periodic cleaning of pipelines by hydrogel «pigs» can significantly increase their productivity, prevent corrosion and extend their lifetime [6–8].

The pioneering works to strengthen the mechanical properties of hydrogels adding inorganic components were performed by Haraguchi [9, 10]. Composite gel is made from N-isopropylacrylamide; in its matrix, montmorillonite particles are immobilized. Mechanical characteristics of a gel with inorganic fillers are much better than that of a conventional gel. Mechanism of formation of the composite structures can be represented as a diffusion of acrylamide monomers to the layered clay structure [11–15]. After monomers are intercalated to the minerals, polymerization with simultaneous crosslinking of composite hydrogel materials

takes place. Nano- and microsized clay particles play the role of additional physical crosslinking centers. It leads to a significant increase in quality of mechanical properties of the composite materials.

Osada and co. [16–18] designed a series of double-network hydrogels with extremely high mechanical strength. This kind of nanocomposite hydrogel exhibited high transparency, high deswelling rate and extraordinary mechanical properties with up to 10^3 % of elongation ratio at break. Recently [19], physical hydrogels composed of polyampholytes demonstrating high toughness and viscoelasticity were developed.

In our earlier works [20–22], we have described the preparation and characteristics of composite materials based on PAAH and clay minerals. The present paper highlights the applicability of the composite hydrogel materials for purposes of cleaning the inner surface of pipeline from ARPD.

Experimental

Materials

Preparation of composite materials based on polyacrylamide hydrogel (PAAH), clay minerals, SiO_2 and PVP is reported elsewhere [20–22] (Fig. 1).

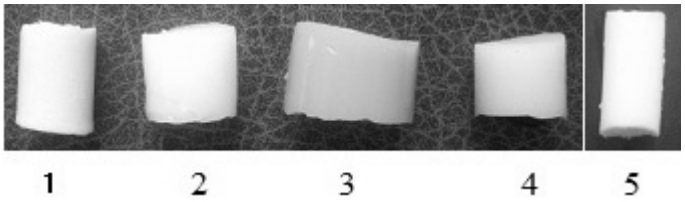

Figure 1. Samples of the composite materials based on PAAH and kaolin (1), SiO_2 (2), bentonite (3) montmorillonite (4) and PVP (5)

Two model pipelines with different length and diameter of the pipes, «Small» pipeline with L = 3 m, d = 20 mm) and «Big» pipeline with L = 15 m, d = 40 mm, were used for laboratory test of hydrogel «pigs» (Figs. 2 and 3).

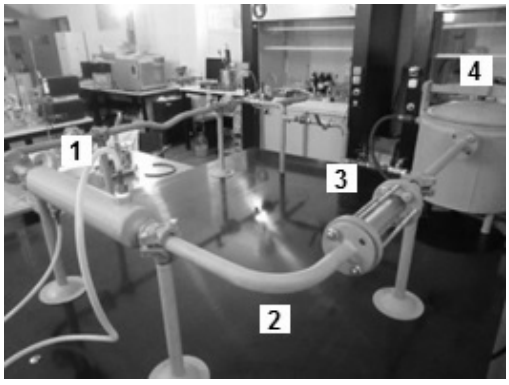

1 — section for cooling of oil; *2* — steel pipe; *3* — section for visualization of oil flow; *4* — oil reservoir

Figure 2. «Small» model pipeline

1 — steel pipe; *2* — oil reservoir; *3* — pump; *4* — inlet for hydrogel «pigs»

Figure 3. «Big» model pipeline

Both «Small» and «Big» pipelines consist of oil reservoir, pump, steel pipe of different cross-section, equipped with valves and monometers, sections for cooling of oil and visualization of oil flow, inlet and outlet for hydrogel «pigs». In order to have the ARP deposited, the crude oil was heated up to 60 ºC and circulated inside of a pipe for 2, 4 and 6 hours. The temperature of the cooling section was maintained at 5 ºC. The heating and cooling regimes of oil in model pipe correspond to real conditions of oil transportation. As anticipated, some ARPD was deposited on the inner part of steel pipe leading to the reduction of the pipeline's capacity. After cleaning a pipe by hydrogel «pigs», the solid ARPD was weighed and its amount was calculated.

After circulation of crude oil inside of «Small» model pipeline during 2, 4 and 6 hours, the section was cooled at 5 ºC, then dismantled and weighed. The amount of deposited ARP was calculated, and the efficiency of pipe cleaning (E) by hydrogel «pigs» was estimated using the formula (1):

$$E = \frac{m_2}{m_1} \times 100\ \%, \quad (1)$$

where m_1 — is the mass of the pipe before ARP deposition (g); m_2 — is the mass of the pipe after ARP deposition at definite time (g).

Scaling-up of hydrogel «pigs» was performed in reinforced plastic oilfield pipe with internal diameter of 220 mm and length of 230 mm. The bottom of plastic oilfield pipe was plugged and filled with the mixture of acrylamide, crosslinker, initiator, appropriate clay minerals dispersed in distilled water. The polymerization reaction was initiated by addition of accelerator — N,N,N',N'-tetramethylethylenediamine and carried out at room temperature during 3–4 hours. The scaled-up composite hydrogel «pigs» are presented in Figure 4.

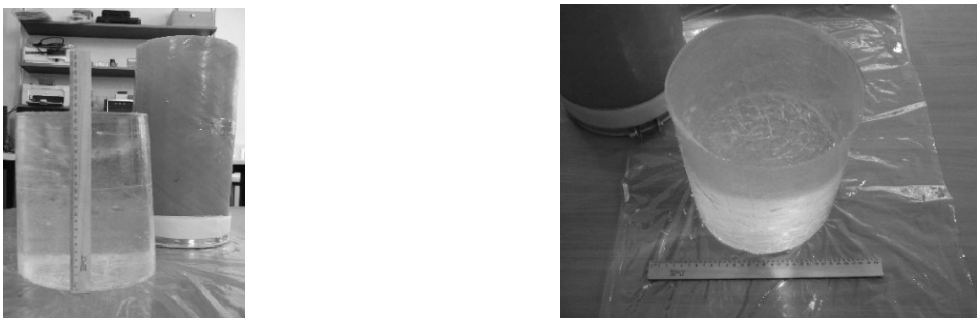

Figure 4. Scaled up composite hydrogel «pigs»

Results and Discussion

Testing on model pipeline

It should be noted that both «Small» and «Big» model pipelines were set up according to technical documentations of regular oilfield pipelines. As illustrated in Figure 5*a*, the gel «pig» successfully cleaned the inner surface of the pipe from corrosion deposits and mechanical impurities. Figure 5*b* shows the case when the «pigs» were used for cleaning the pipeline from ARPD.

Figure 5. Cleaning of pipe from mechanical impurities and corrosion deposits (*a*) and from ARPD (*b*)

The effectiveness of cleaning the model pipeline was compared with other composite hydrogel materials. As indicated in Table 1, the cleaning of the deposited ARP from Kumkol and Usen oil (Western Kazakhstan) with composite hydrogel «pigs» in dynamic regime showed 92–95 % effectiveness. The advantages of the proposed materials in comparison with mechanical scrapers are: the smooth passage through pipe sections with complex profile, the good hydraulic pressure inside of pipe, the sorption of water-salt mixtures accumulated inside of pipe, and explosion safety.

Table 1

Cleaning effectiveness of hydrogel «pigs»

Composite hydrogels	ARPD deposition time, hour	ARPD deposited, g	ARPD removed, g	Effectiveness, %
PAAH/PVP-Bentonite	2	281±5	265±5	90±2
PAAm/PVP-SiO_2	4	269±5	244±5	91±2
PAAm/PVP	6	255±5	238±5	92±2

From practical point of view, the most important parameter of hydrogel «pigs» is their mechanical properties. The selected samples exhibit a high stability and good tolerance towards mechanical stress. As illustrated in Figure 6, the mechanical strength of composite hydrogels increases in the following order: PAAH-PVP > PAAH-Montmorillonite > PAAH-SiO_2 > PAAH-Bentonite.

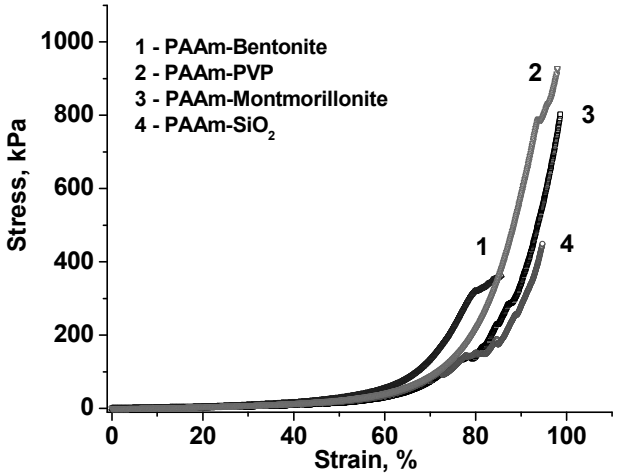

Figure 6. Compressive stress-strain curves of polyacrylamide hydrogels containing bentonite (1), PVP (2), montmorillonite (3) and SiO_2 (4)

The optimal hydrogel «pigs» selected for testing on model pipelines according to the values of tensile strength and Young's modulus are presented in Table 2.

Table 2

The Young's modulus and tensile strength of composite hydrogels used for model pipeline cleaning

Composite hydrogels	Mechanical properties	
	Young's modulus, kPa	Compressive strength, kPa
PAAH/PVP	5.89	791.3
PAAH/PVP-Bentonite	3.30	120.0
PAAH/PVP-SiO_2	2.60	96.1

Usually inside of the real pipeline, the hydrogel «pigs» are subjected to high pressure during the movement. Therefore the stability of composite hydrogel materials under vertical stress was evaluated at constant cyclic deformation. The results showed that the samples are able to sustain more than 200 cycles of vertical deformation without damage (Fig. 7). It indicates that the materials have advanced mechanical properties and can be applied under oilfield conditions.

The cost of developed composite hydrogel «pigs» is compared with commercial available gel samples in Table 3. The diameter of gel «pigs» corresponds to diameter of the pipe used for oil transportation. Evidently, the composite hydrogel «pigs» developed at the Institute of Polymer Materials and Technology are more cost-effective than that of «SamTechnoOil» (Russia) and «Aubin» (UK) companies. At present the manufacturing instructions for production of hydrogel «pigs» were developed. In 2015, the Committee of industrial development and safety of the Ministry of investment and development of the Republic of Kazakhstan issued a permission for the production and application of hydrogel «pigs» («PIG-1») for cleaning of real pipelines.

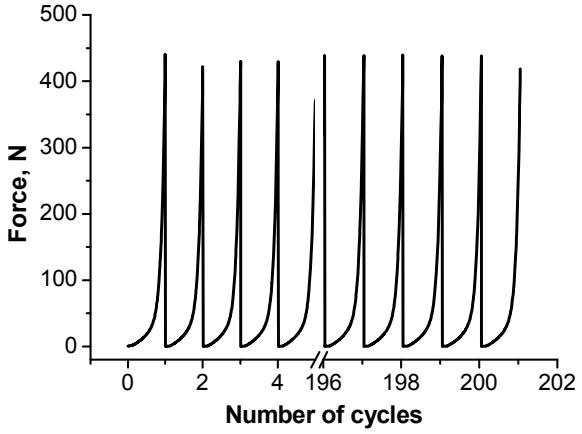

Figure 7. The effect of the number of compression cycles
on the elastic deformation of PAAH-PVP composite hydrogel

Table 3

Characteristics and costs of hydrogel «pigs» developed by various companies

Company	Diameter of gel «pigs», mm	Volume of gel «pigs», mm^3	Price, USD
«SamTechnoOil» (Russia)	1200	100	295
«Aubin» (UK)	700	1000	4912
«PIG-1» (IPMT «Kazakhstan»)	377	750	455

Conclusions

Flexible, mechanically stable composite hydrogel materials based on crosslinked polyacrylamide, clay minerals and PVP were developed. The mechanical strength of composite hydrogels increases in the following order: PAAH-PVP > PAAH-Montmorillonite > PAAH-SiO_2 > PAAH-Bentonite and demonstrates that PAAH-PVP semi-interpenetrating networks withstand the highest compressive load. Particularly, the PAAH-PVP can sustain more than 200 cycles of vertical deformation without damage. Composite hydrogel «pigs» were tested for their cleaning properties on «Small» and «Big» model pipelines; the efficiency of ARPD, corrosion deposition and mechanical admixtures removal from the inner surface of the pipe was in the range of 93–95 %. Additionally, permission for production and application of hydrogel «pigs» («PIG-1») for cleaning of real pipelines was issued.

Acknowledgements

This work was supported by the Ministry of Education and Science of the Republic of Kazakhstan and the World Bank in the frame of «Technology Commercialization» project (Grant agreement No. 197 from 05.03.2014).

References

1 Kudaibergenov S. Composite Hydrogel Materials / S. Kudaibergenov, Zh. Ibraeva, M. Yashkarova, S. Kabdrakhmanova, G. Tatykhanova // Advanced Separations by Specialized Sorbents. Chapter 1. / Ecaterina Stela Dragan Ed. New York: CRC Press, 2014. — P. 1–37.

2 Aiyejina A. Wax formation in oil pipelines: A critical review / A. Aiyejina, D. Chakrabarti, A. Pilgrim, M. Sastry // International Journal of Multiphase Flow. — 2011. — Vol. 37. — P. 671–694.

3 Misra S. Paraffin problems in crude-oil production and transportation — a review / S. Misra, S. Baruah, K. Singh // SPE Production & Facilities. — 1995. — Vol. 10. — P. 50–54.

4 Wang W. Identifying optimal pigging frequency for oil pipelines subject to non-uniform wax deposition distribution / W. Wang, Q. Huang, S. Li, C. Wang, X. Wang // Proceedings of the 2014 10th International Pipeline Conference IPC2014, (September 29 — October 3, 2014). — Calgary, Alberta, Canada. IPC2014–33064.

5 Fung G. To pig or not to pig: the marlin experience with stuck pig / G. Fung, W. Backhaus, S. McDaniel, M. Erdogmus // Offshore Technology Conference, Houston. — 2006.

6 Williamson D. Polyurethane and pipeline pigs make a perfect match / D. Williamson, J. Ranklin, L. Payne // Pipeline and Gas Journal & PPSA. — 2010. — Vol. 29. — P. 42–44.

7 Lee K. Hydrogels for tissue engineering / K. Lee, D. Mooney // Chemical Reviews. — 2001. — Vol. 101. — P. 1869–1879.

8 Qiu Y. Environment-sensitive hydrogels for drug delivery / Y. Qiu, K. Park // Advanced Drug Delivery Reviews. — 2001. — Vol. 53. — P. 321–339.

9 Haraguchi K. Nanocomposite hydrogels: a unique organic–inorganic network structure with extraordinary mechanical, optical, and swelling/de-swelling properties / K. Haraguchi, T.Takehisa // Advanced Materials. — 2002. –Vol. 16. — P. 1120–1124.

10 Haraguchi K. Compositional effects on mechanical properties of nanocomposite hydrogels composed of poly(N,N-dimethylacrylamide) and clay / K. Haraguchi, R. Farnworth, A. Ohbayashi, T. Takehisa // Macromolecules. — 2003. — Vol. 36. — P. 5732–5741.

11 Kopecek J. Hydrogels: from soft contact lenses and implants to self-assembled nanomaterials / J. Kopecek // Journal of Polymer Science: Part A: Polymer Chemistry. — 2009. — Vol. 47. — P. 5929–5946.

12 Lina J. Synthesis and properties of a novel double network nanocomposite hydrogel / J. Lina, Sh. Xua, X. Shia, S. Fenga, J. Wang // Polymers for Advanced Technologies. — 2009. — Vol. 20. — P. 645–649.

13 Sperling L. Interpenetrating polymer networks: An overview / L. Sperling // Advances in Chemistry. — 1994. — Vol. 239. — P. 3–38.

14 Haque M. Super tough double network hydrogels and their application as biomaterials / M. Haque, T. Kurokawa, J.P. Gong // Polymers. — 2012. — Vol. 53. — P. 1805–1822.

15 Myung D. Progress in the development of interpenetrating polymer network hydrogel / D. Myung, D. Waters, M. Wiseman, P.E. Duhamel, J. Noolandi, C.N. Ta, et al. // Polymers for Advanced Technologies. — 2008. — Vol. 19. — P. 647–657.

16 Gong J.P. Double-network hydrogels with extremely high mechanical strength / J.P. Gong, Y. Katsuyama, T. Kurokawa, Y. Osada // Adv. Mater. — 2003. — Vol. 15. — P. 1155–1158.

17 Nakayama A. High mechanical strength double-network hydrogel with bacterial cellulose / A. Nakayama, A. Kakugo, J.P. Gong, Y. Osada, M. Takai, T. Erata, et al. // Adv. Fun. Mater. — 2004. — Vol. 14. — P. 1124–1128.

18 Tanaka Y. Novel hydrogels with excellent mechanical performance / Y. Tanaka, J.P. Gong, Y. Osada // Prog. Polym. Sci. – 2005. — Vol. 30. — P. 1–9.

19 Sun T.L. Physical hydrogels composed of polyampholytes demonstrate high toughness and viscoselasticity / T.L. Sun, T. Kurokawa, S.Kuroda, A.B. Ihsan, T. Akasaki, K. Sato et al. // Nature Materials. — 2013. — Vol. 12. — P. 932–937.

20 Ibraeva Zh. Preparation and characterization of organic-inorganic composite materials based on poly(acrylamide) hydrogels and clay minerals / Zh. Ibraeva, A. Zhumaly, E. Blagikh, S. Kudaibergenov // Macromol. Symp. — 2015. — Vol. 351. — P. 97–111.

21 Ibraeva Zh. Mechanical properties of composite hydrogel materials based on poly(acrylamide) and clay minerals and their potential application for cleaning of the internal surface of pipes / Zh. Ibraeva, E. Blagikh, S. Kudaibergenov // Advances in Engineering Mechanics and Materials. — 2014. — P. 80–84.

22 Кудайбергенов С.Е. Получение и свойства композиционных материалов на основе гидрогеля полиакриламида и природных минералов для очистки внутренней полости трубопровода / С.Е. Кудайбергенов, А.А. Жумалы, Е.В. Благих, Ж.Е. Ибраева, Т.К. Алдыяров, М.Д. Насибуллин и др. // Наука и технологии трубопроводного транспорта нефти и нефтепродуктов. — 2016. — Т. 1. — С. 44–49.

Е.В. Благих, Ж.К. Садақбаева, А.Н. Кливенко,
Ж.А. Нұрахметова, В.Б. Сигитов, С.Е. Құдайбергенов

Құбырөткізгіштердің ішкі беттерін тазартуға арналған композициялық гидрогель материалдардарын жасап шығару

Полиакриламид (ПААГ), поли-N-винилпирролидон (ПВП) және сазды минералдар (каолин, бентонит және монтмориллонит) негізінде композициялық гидрогель материалдарын жасап шығару, олардың механикалық қасиеттерін зерттеу және мұнай құбырларының ішкі қабатын тазарту үшін механикалық берік, иілгіш және майысқақ қырғыштар ретінде қолдану нәтижелері берілген. Композиттік гидрогельдердің механикалық касиеттері келесідей артатыны анықталды: ПААГ-ПВП > ПААГ-монтмориллонит > ПААГ-SiO_2 > ПААГ-бентонит. Нәтижелер көрсеткендей, композиттік гидрогельдердің үлгілері жоғарғы механикалық төзімділікке ие, олар айтарлықтай, бүлінусіз 200 тік деформациядан артыққа төзе алады. «Үлкен» және «кіші» құбырларды тазартуға арналған гидрогельдік материалдарды таңдау мен тестілеу сығылу мен созылудағы төзімділік шектеулігі мен Юнг модулінің оңтайлы мәндеріне сәйкес жасалған. Композициялық гидрогель материалдары тазарту құрылғылары ретінде модельді мұнай құбырында ұтымды қолданылды. Механикалық аналогтарына қарағанда, гидрогельді тазартқыштар әр түрлі пішіндегі және өлшемдегі құбырлар арқылы оңай өтеді, ішкі бетке қажетті гидравликалық қысымды қамтамасыз етеді, жарылу қауіпсіздігін қамтамасыз етеді және құбырлардың ішкі бетіндегі суды өзіне сіңіреді. Модельді құбыроткізгіштерді асфальтенді шайырлы парафинді қалдықтардан (ARPD) және механикалық қоспалардан коррозиялық қалдықтардан тазартуда олардың тиімділігі 93–95 % құрады. Өндірістік мұнай құбырларын тазартуға арналған гидрогельдік материалдарды масштабтау жүргізілді. Ұсынылып отырған материалдар экономикалық тиімділігі және технологиялық жүзеге асырылуына байланысты мұнай тасымалдаумен айналысатын компаниялардың қызығушылығын тудырады.

Кілт сөздер: сазды минералдар, полиакриламид гидрогелдері, композициялық материалдар, гидрогелді «қырғыш», Юнг модулі, модельді құбырөткізгіш, тазарту дәрежесі, асфальтен-шайыр-парафин шөгінділері.

Е.В. Благих, Ж.К. Садакбаева, А.Н. Кливенко,
Ж.А. Нурахметова, В.Б. Сигитов, С.Е. Кудайбергенов

Разработка композиционных гидрогельных материалов для очистки внутренней поверхности трубопроводов

Разработаны гибкие, эластичные и механически прочные композиционные гидрогелевые материалы на основе полиакриламидного гидрогеля (ПААГ), глинистых минералов (каолин, бентонит и монтмориллонит), поли-N-винилпирролидона (ПВП) и SiO_2 для очистки внутренней поверхности трубопроводов. Механические свойства композитных гидрогелей увеличиваются в следующем порядке: ПААГ-ПВП > ПААГ-монтмориллонит > ПААГ-SiO_2 > ПААГ-бентонит. Результаты показали, что образцы композитных гидрогелей обладают высокой механической прочностью и без существенных разрушений могут выдержать более 200 вертикальных деформаций. Тестирование и отбор гидрогелевых «скребков» для очистки «малого» и «большого» трубопроводов осуществлялись в соответствии с оптимальными значениями предела прочности при сжатии или растяжении и модуля Юнга. В лабораторных условиях использование композитных материалов в качестве гидрогелевых «скребков» для очистки модельного трубопровода оказалось успешным. В отличие от механических аналогов, гидрогелевые «скребки» свободно проходят через трубопроводы различной формы и размера, обеспечивают необходимое гидравлическое давление на внутреннюю поверхность, обеспечивают взрывобезопасность и поглощают воду при движении по трубопроводу. Эффективность гидрогелевых «скребков» при очистке модельного трубопровода от механических примесей, коррозионных отложений и асфальтен-смоло-парафиновых отложений (АСПО) составила 93–95 %. Проведено масштабирование гидрогелевых «скребков» для очистки промысловых нефтепроводов. Предлагаемые материалы будут представлять интерес для нефтяных компаний, занимающихся транспортировкой нефти, благодаря экономической эффективности и технологической осуществимости.

Ключевые слова: глинистые минералы, полиакриламидные гидрогели, композиционные материалы, гидрогелевый «скребок», модуль Юнга, модельный трубопровод, эффективность очистки, асфальтен-смоло-парафиновые отложения.

References

1 Kudaibergenov, S., Ibrayeva, Zh., Yashkarova, M., Kabdrakhmanova, S., & Tatykhanova, G. (2014). Composite Hydrogel Materials. *Advanced Separations by Specialized Sorbents*. New York: CRC Press, 1–37.

2 Aiyejina, A., Chakrabarti, D., Pilgrim, A., & Sastry, M. (2011). Wax formation in oil pipelines: A critical review. *International Journal of Multiphase Flow, 37*(7), 671–694.

3 Misra, S., Baruah, S., & Singh, K. (1995). Paraffin problems in crude-oil production and transportation — a review. *SPE Production & Facilities*, *10*(1), 50–54.

4 Wang, W., Huang, Q., Li, S., Wang, C., & Wang, X. (2014). Identifying optimal pigging frequency for oil pipelines subject to non-uniform wax deposition distribution. Proceedings from the *10th International Pipeline Conference IPC2014*, Calgary, Alberta, Canada (September 29 — October 3). IPC2014–33064.

5 Fung, G., Backhaus, W., McDaniel, S., & Erdogmus, M. (2006). To pig or not to pig: the marlin experience with stuck pig. *Offshore Technology Conference*, Houston.

6 Williamson, D., Ranklin, J., & Payne, L. (2010). Polyurethane and pipeline pigs make a perfect match. *Pipeline and Gas Journal & PPSA*, *29*, 42–44.

7 Lee, K., & Mooney, D. (2001). Hydrogels for tissue engineering. *Chemical Reviews, 101*, 1869–1879.

8 Qiu, Y., & Park, K. (2001). Environment-sensitive hydrogels for drug delivery. *Advanced Drug Delivery Reviews, 53*, 321–339.

9 Haraguchi, K., & Takehisa, T. (2002). Nanocomposite hydrogels: a unique organic–inorganic network structure with extraordinary mechanical, optical, and swelling/de-swelling properties. *Advanced Materials*, *16*, 1120–1124.

10 Haraguchi, K., Farnworth, R., Ohbayashi, A., & Takehisa, T. (2003). Compositional effects on mechanical properties of nanocomposite hydrogels composed of poly(N,N-dimethylacrylamide) and clay. *Macromolecules*, *36*, 5732–41.

11 Kopecek, J. (2009). Hydrogels: from soft contact lenses and implants to self-assembled nanomaterials. *Journal of Polymer Science: Part A: Polymer Chemistry*, *47*, 5929–5946.

12 Lina, J., Xua, Sh., Shia, X., Fenga S., & Wang J. (2009). Synthesis and properties of a novel double network nanocomposite hydrogel. *Polymers for Advanced Technologies*, *20*, 645–649.

13 Sperling, L. (1994). Interpenetrating polymer networks: An overview. *Advances in Chemistry*, *239*, 3–38.

14 Haque, M., Kurokawa, T., & Gong, J.P. (2012). Super tough double network hydrogels and their application as biomaterials. *Polymers*, *53*, 1805–1822.

15 Myung, D., Waters, D., Wiseman, M., Duhamel, P.E., Noolandi, J., & Ta, C.N. et al. (2008). Progress in the development of interpenetrating polymer network hydrogels. *Polymers for Advanced Technologies*, *19*, 647–657.

16 Gong, J.P., Katsuyama, Y., Kurokawa, T., & Osada, Y. (2003). Double-network hydrogels with extremely high mechanical strength. *Advanced Materials*, *15*, 1155–1158.

17 Nakayama, A., Kakugo, A., Gong, J.P., Osada, Y., Takai, M., & Erata, T. et al. (2004). High mechanical strength double-network hydrogel with bacterial cellulose. *Advanced Functional Materials*, *14*, 1124–1128.

18 Tanaka, Y., Gong, J.P., & Osada, Y. (2005). Novel hydrogels with excellent mechanical performance. *Progress in Polymer Science, 30*, 1–9.

19 Sun, T.L., Kurokawa, T., Kuroda, S., Ihsan, A.B., Akasaki, T., & Sato, K. et al. (2013). Physical hydrogels composed of polyampholytes demonstrate high toughness and viscoselasticity. *Nature Materials*, *12*, 932–937.

20 Ibraeva, Zh., Zhumaly, A., Blagikh, E., & Kudaibergenov, S. (2015). Preparation and characterization of organic-inorganic composite materials based on poly(acrylamide) hydrogels and clay minerals. *Macromolecular Symposia, 351*, 97–111.

21 Ibraeva, Zh., Blagikh, E., & Kudaibergenov, S. (2014). Mechanical properties of composite hydrogel materials based on poly(acrylamide) and clay minerals and their potential application for cleaning of the internal surface of pipes. *Advances in Engineering Mechanics and Materials*, 80–84.

22 Kudaibergenov, S.E., Zhumaly, A.A., Blagikh, E.V., Ibraeva, Zh.E., Aldyarov, T.K., & Nasibullin M.D. et al. (2016). Poluchenie i svoistva kompozitsionnykh materialov na osnove hidrohelia poliakrilamida i prirodnykh mineralov dlia ochistki vnutrennei polosti truboprovoda [Synthesis and properties of composite materials based on polyacrylamide hydrogel and natural minerals intended for cleaning of the internal surface of pipelines]. *Nauka i Tekhnolohii truboprovodnoho transporta nefti i nefteproduktov — Science and technologies of pipeline transport of oil and oil products, 1*, 44–49 [in Russian].

UDC 547.37

M.Zh. Burkeyev, G.K. Kudaibergen, Ye.M. Tazhbayev,
G.K. Burkeyeva, A.V. Omasheva, N.A. Yesentayeva, A.N. Bolatbay

Ye.A. Buketov Karaganda State University, Kazakhstan
(E-mail: gulshahar90@mail.ru)

The number average and mass average molar masses of polyethylene(propylene)glycol fumarates

Unsaturated polyesters are interesting for theoretical and practical studies, since along with the simplicity of economical production, contain in their composition unsaturated double bonds, which makes it possible to obtain spatially crosslinked structures on their basis. In this work polyethylene glycol fumarate, polypropylene glycol fumarate were synthesized by the step-growth polymerization of ethylene(propylene)glycol and fumaric acid. The compositions of polyethylene(propylene)glycol fumarates were determined using elemental analysis and IR spectroscopy. Some physicochemical characteristics of synthesized polyethylene(propylene)-glycol fumarates were established. In order to state the correlation between the molar masses of polyethylene(propylene)glycol fumarates, the number average and mass average molar masses were found. As follows from the results presented in this paper mass average molecular masses of polyethylene glycol fumarate and polypropylene glycol fumarate calculated by the light scattering were around 2500 and 1488 a.e.m., the number average molar masses determined by the method of end groups were 2010 and 1245 a.e.m., respectively. It is shown that the methods of light scattering and end-group assay give good convergence and have a high degree of correlation. As a result of the study the correctness the light scattering method for the estimation of molecular masses of polyethylene(propylene)glycol fumarates was shown.

Keywords: unsaturated polyester resins, polyethylene glycol fumarate, polypropylene glycol fumarate, the number average molar mass, mass average molar mass, light scattering, titration, step-growth polymerization.

Introduction

The molar mass, which is one of the main characteristics of any chemical substance, plays a special role in case of high-molecular compounds, since it serves as a measure of length of the chain molecule. The latter is also characterized by the number of repeating units or the degree of polymerization of macromolecule. It should be noted that the molar mass of the polymer is the average statistical value, which refers to the molar masses of the macromolecules constituting the polymer. Polymers, unlike low-molecular substances, are polydisperse; they dissolve via preliminary swelling and in rare cases form colloidal solutions. A very large molar mass is typical for polymeric compounds and itoften changes from 8–10 thousand to several millions. Determination of the molecular mass of polymers is possible by using the classical methods (osmometry, ebullioscopy, cryoscopy, viscosimetry, etc.) and modern methods of investigation such as gel permeation chromatography, nephelometry, etc. Knowing the molar mass of the polymer necessary information on its structural features and properties can be obtained; also it is possible to carry out directed synthesis of substances based on properties.

Unsaturated polyesters due to the simplicity of economical production, availability of raw materials attract the attention of researchers, practitioners and have found wide practical use. The main and unique feature of unsaturated polyesters is the ability to copolymerize with various monomers to form valuable products that have special physicochemical and mechanical properties; they are characterized by low toxicity and relative availability. As the literature analysis shows, only co-monomers of hydrophobic nature are involved in the copolymerization with unsaturated polyesters [1–3] and synthesized polymeric materials can be use construction products. The problems of copolymerization of unsaturated polyesters with hydrophilic ionic monomers remain relevant until recently. It opens up prospects for the synthesis of new so-called «intelligent» polymers capable of reversibly reacting in response to insignificant changes in the environment. An important factor affecting the properties of synthesized copolymers is the molar masses of the initial unsaturated polyester resins. In literature there are contradictory data on the values of molar masses of unsaturated polyester resins. In this regard, it seemed interesting to compare the molar masses obtained by different methods.

With the aim of evaluation of the molar masses of synthesized polyethylene(propylene)glycol fumarate (p-EGF, p-PGF), this study presents the results on the determination of the number average and mass average molar masses obtained using light scattering method and end-group assay.

Method

Polyethylene(propylene)glycol fumarates were obtained by step-growth polymerization of ethylene (propylene)glycol and fumaric acid of the ratio 1.05:1 mol by heating and stirring them in a nitrogen medium [4]. After the reaction mixture reaches a temperature of 153 ºC, a catalyst ($AlCl_3$) is introduced into it at an amount of 0,2 % on total mass of the original monomer mixture. Stirring was continued for 6–8 hours until water was completely removed; after which the reaction mixture was cooled to room temperature. The route of the reaction was monitored by determining the acid number. The resulting resin was purified from the starting monomers by washing with acetone.

The number average molar mass of unsaturated polyesters was determined by acid number (AN) and hydroxyl number (HN) by direct titration with 0.1N and 0.5N KOH where phenolphthalein is used as an indicator.

$$M_n = \frac{56.11 \cdot 2 \cdot 1000}{AN + HN};$$

$$AN = \frac{(V_1 - V_2) \cdot f \cdot 0.00561 \cdot 1000}{g},$$

where V_1 and V_2 — the volume of 0.1N KOH, consumed for the titration of sample with a polymer and a control sample, ml.

$$HN = \frac{(V_1 - V_2) \cdot f \cdot 0.028 \cdot 1000}{g},$$

where V_1 and V_2 — the volume of 0.5N KOH, consumed for the titration of sample with a polymer and a control sample, ml.

The Debye method (light scattering) was used to estimate the mass average molar mass [5]. Determination of the turbidity of polymer solutions was carried out by light scattering using a 2100 AN nephelometer from HACH at λ = 5460 Å.

The degree of scattering of monochromatic light by a solution (turbidity) τ^0 is related to the osmotic pressure of the true solution by the following relation, known as the Debye equation:

$$\tau^0 = \frac{32(3.14)^3 n_0^2 (n - n_0)^2}{3\lambda^4 N_A C \left[\frac{\partial\left(\frac{\pi_0}{RT}\right)}{\partial C}\right]},$$

where n and n_0 — the refractive indexes of the solvent and solution, respectively; N_A — Avogadro constant, mol^{-1}; π_0 — osmotic pressure, atm; C — concentration of solution, g/cm^3; λ — wavelength, nm.

The accuracy of determining the molar mass and conformational features of molecules depends on the nephelometric features of the solvent used [5].

It was noted above that the osmotic pressure is a characteristic of the change in chemical potential of the solution and is due to the activity of the dissolved substance a^0. It can be shown that the turbidity of the system increases with the increasing the activity of dissolved particles. In another words, with increasing a^0, the proportion of scattered light increases. The intensity of the scattered light I_0 observed at an angle θ to the incident monochromatic ray is called the optical anisotropy of the dissolved polymer particles and varies with the angle of observation. The optical anisotropy of these particles is that the intensity of the scattering is not the same along the different axes of the molecular coil. The dependence of the intensity of the scattered light on the angle of observation of the scattered ray is called the Rayleigh ratio (number), or the reduced intensity.

$$R_{\theta i} = r^2 I_{\theta i} / I_0,$$

where $I_{\theta i}$ and I_0 — the intensity of scattered and incident light, respectively; r — distance from particle to observer.

In practice, when determining the turbidity often a value $R_{\theta i}$ is calculated, but not τ^0. Therefore:

$$\frac{HC}{R_{\theta i}} = \frac{1}{\bar{M}_w} + \frac{2BC}{RT}.$$

At small values of C, the dependence $HC / R_{\theta i} = f(C)$ is expressed by a straight line that cuts off $C \to 0$ on the *y*-axis is a segment equal to the reciprocal of the molar mass.

$$\left[\frac{HC}{R_{\theta i}}\right]_{c\to 0} = \frac{1}{\bar{M}_i}.$$

The concentration of the initial solution for the determination of the polymer at the wavelength region 10^5–10^7 nm is of the order of $2 \cdot 10^{-3}$ g/ml (0.2 g/l). For this, a sample of unsaturated polyester of 0.1 g (accurate to 0.0001) was placed in a pre-weighed volumetric flask (~50 ml) with a clogged cork. Further it was dissolved in an increasing volume of a thoroughly purified and repeatedly distilled solvent, then brought to a mark and weighed. The concentration of the solution C_1 (g/cm^3) was calculated using the formula

$$C_1 = m_p \rho / m_s,$$

where m_p — polymer mass, g; ρ — density of solvent, g/cm^3; m_s — mass of solvent, g.

Then, 30 ml of the prepared solution was transferred to a cuvette of the instrument; the turbidity of the solution and the refractive indexes were determined until complete reproducibility.

A series of solutions were prepared from the available solution by successively diluting an aliquot (~30 ml) of each previous solution to 50 ml in a volumetric flask, then turbidity and refractive indexes were measured. The concentration of the subsequent solutions was calculated according to the above formula. Based on the calculated values, a plot of the dependence $HC/R_{\theta i} - f(C)$. Extrapolating the resulting straight line to $C = 0$, we obtained a segment that corresponds to the limiting value $HC/R_{\theta i} = 1/\bar{M}_w$.

Results and Discussion

Polyethylene(propylene)glycol fumarates were obtained by step-growth polymerization of fumaric acid and ethylene glycol according to the following scheme [4]:

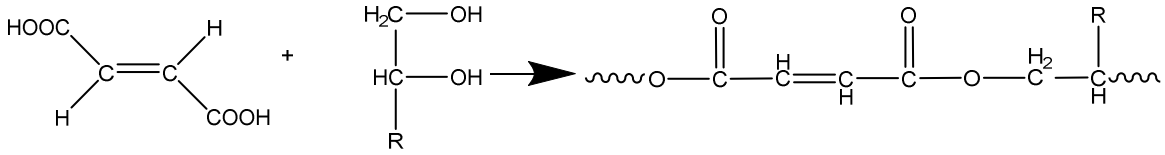

R — H, CH_3

Polyethylene(propylene)glycol fumarates were identified by IR spectroscopy (Fig. 1). In the IR spectra of synthesized polyethylene(propylene)glycol fumarates, the absorption bands at 755 cm^{-1} due to pendulum oscillations of –CH_2– bonds are observed, and absorption bands at 1162 cm^{-1} region confirm the presence of the –C–O–C– bond of the ester. The intense absorption band at 1461 cm^{-1} indicates the vibrations of –C–H bonds. The presence of –C=O bond and symmetrically located –CH bonds in the CH_2 and CH_3 groups are characterized by absorption bands at 1736 cm^{-1} and 2985 cm^{-1}, respectively. The spectra exhibit an intense peak at 1306 cm^{-1} reflecting the presence of the –C=C–group of the polyester. The presence of p-EGF and p-PGF–C=C– bonds in the structure indicates the formation of an unsaturated polyester.

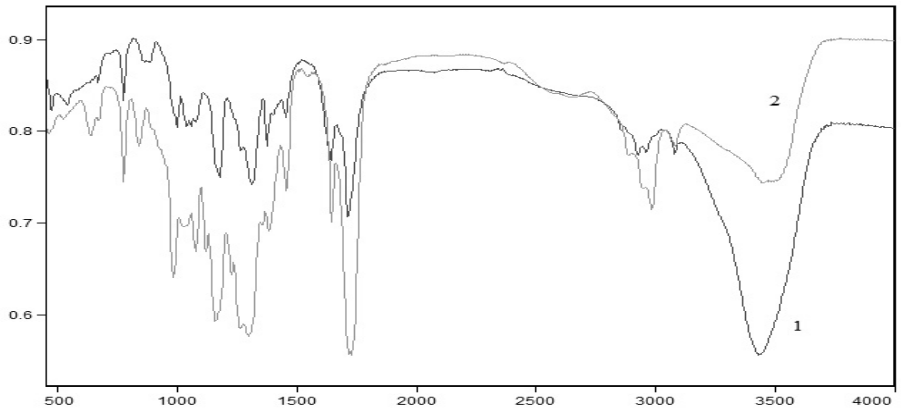

1 — p-EGF; *2* — p-PGF

Figure 1. IR spectra

The light scattering method is the most reliable and convenient out of the few absolute methods for the determination of the mass average molar masses of polymers, covering an exceptionally wide range of molecular masses. In addition, it is a direct method for measuring the size of macromolecules in solution, used for approbation and calibration of other, indirect methods (in particular, hydrodynamic methods).

The results of metrological processing of straight lines and calculated values of molar mass are given in Table. The data obtained were confirmed by a mathematical study and a graph of the accuracy of the coordinate $HC/R_{\theta i} - f(C)$ (Figs. 2, 3). Extrapolation of the $HC/R_{\theta i}$ dependence on C is determined by the formula extrapolated to the zero scattering angle θ in accordance with equation.

Thus, the molar mass of the polymer is calculated and determined by the intersection values. As follows from the results presented in Table, polyethylene glycol fumarate and polypropylene glycol fumarate have molar masses of the order of 2500 and 1488, respectively, and the values of the molar masses studied in the three units of turbidity are in good agreement. The values of $\bar{M}_w$ listed in Table are in good accordance with the data calculated from the titration [3].

Table

Molar mass features of an unsaturated polyester resin

Object	$H \times 10^{-5}$	$\left(\frac{HC}{R_{\theta i}}\right)_{c\to 0} = \frac{1}{\bar{M}_w} \times 10^{-3}$	$\bar{M}_w$	$\bar{M}_n$	D_m
p-EGF	6.401	0.400	2500.00	2010.59	1.24
p-PGF	3.3010	0.6720	1488.00	1245.34	1.19

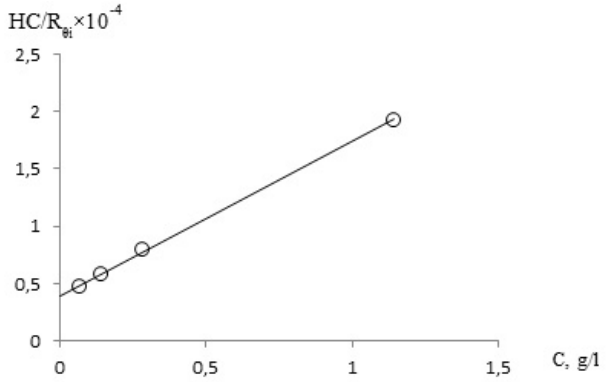

Figure 2. Dependence of $HC/R_{\theta i}$ on the concentration (C) for solutions of p-EGF in chloroform

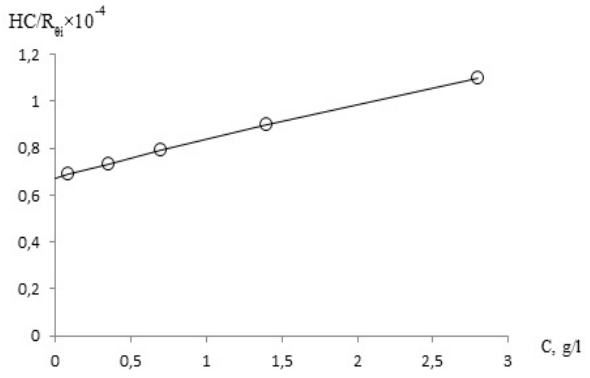

Figure 3. Dependence of $HC/R_{\theta i}$ on the concentration (C) for solutions of p-EGF in chloroform

In the literature, it is noted that the light scattering method is most applicable for polymers with a high molar mass (above 10,000). To confirm the correctness of the use of the light scattering method for the estimation of the molar masses of polyethylene(propylene)glycol fumarates, we additionally determined the numberaverage molar mass by the method of determining the end groups. This method is most effective forlinear condensation polymers of which the molar mass is usually below 20,000.

Conclusions

The set of experimental results on the establishment of the mass-average and number-average molar masses obtained by light-scattering and the determination of end groups have similar values, indicating the oligomeric nature of p-EGF and p-PGF. Thus, as a result of the study, the correctness of the light scattering method for the estimation of molecular masses of polyethylene(propylene)glycol fumarate were shown.

References

1 Бениг Г.В. Ненасыщенные полиэфиры: строение и свойства / Г.В. Бениг. — М.: Химия, 1968. — 253 с.

2 Седов Л.Н. Модифицирование химической структуры полималеинатов и полифумаратов для регулирования свойств сополимеров на их основе / Л.Н. Седов, Г.М. Авдеева, Е.Г. Зильберман, Н.Ф. Пугачевская, О.И. Савичева // Вестн. техн. и эконом. информации. — 1970. — № 2. — С. 16.

3 Анисимов Ю.Н. Привитая сополимеризация винилацетата с ненасыщенной олигоэфирной смолой и характеристики отвержденных композиций / Ю.Н. Анисимов, Н.А. Вонсович, О.Б. Грехова // ЖПХ. — 1996. — Т. 69, № 2. — С. 312–316.

4 Патент № 31052. Казахстан. Способ получения ненасыщенных полиэфирных смол на основе пропиленгликоля, фталевого ангидрида и фумаровой кислоты / М.Ж. Буркеев, Е.М. Тажбаев и др. Опубл. 16.03.2016.

5 Козлов Н.А. Физика полимеров / Н.А. Козлов, А.Д. Митрофанов. — Владимир: ВлГУ, 2001. — 345 с.

М.Ж. Бүркеев, Г.Қ. Құдайберген, Е.М. Тажбаев,
Г.К. Бүркеева, А.В. Омашева, Н.А. Есентаева, А.Н. Болатбай

Полиэтилен(пропилен)гликольфумараттардың ортасандық және ортамассалық молекулярлық массалары

Қанықпаған полиэифрлі шайырлар теориялық және практикалық жағынан қызықты болып табылады, себебі алудың қарапайымдылығы мен экономикалық тиімділігіне қарамастан, құрамында қос байланыстың болуынан олардың негізінде кеңістікті-тігілген құрылымды қосылыстарды алуға мүмкіндік береді. Мақалада этилен(пропилен)гликоль мен фумаратты поликонденсациялау реакциялары арқылы полиэтиленгликольфумарат, полипропиленгликольфумарат синтезделінді. Полиэтилен(пропилен)гликольфумараттардың құрамы элементтік талдау, ИҚ-спектроскопия көмегімен анықталды. Синтезделген полиэтилен(пропилен)гликольфумараттардың кейбір физика-химиялық сипаттамалары белгілі болды. Полиэтилен(пропилен)гликольфумараттардың молекулалық массалары арасындағы арақатынастылық дәрежесін анықтау мақсатында ортасандық және ортамассалық молекулалық массалары табылды. Авторлар көрсеткен мәліметтерден полиэтиленгликольфумарат және полипропиленгликольфумарат жарық шашырату әдісі бойынша ортамассалық молекулалық массалары 2500 пен 1488 а.е.м., ал шеткі топтардың мөлшерін анықтау әдісі бойынша ортасандық молекулалық массалары сәйкесінше 2010 а.е.м. және 1245 а.е.м. тең екені көрсетілді. Сонымен қатар жарық шашырату мен шеткі топтардың үлесін анықтау әдістерінің мәндері жақсы сәйкестік және жоғары арақатынастылық дәрежесіне ие. Жүргізілген зерттеулер нәтижесінде полиэтилен(пропилен)-гликольфумараттардың молекулалық массасын анықтау кезінде жарық шашырату әдісінің қолданылуының дұрыстылығы дәлелденді.

Кілт сөздер: қанықпаған полиэфирлі шайырлар, полиэтиленгликольфумарат, полипропиленгликольфумарат, ортасандық молекулалық масса, ортамассалық молекулалық масса, жарық шашырату, титрлеу, поликонденсация.

М.Ж. Буркеев, Г.К. Кудайберген, Е.М. Тажбаев,
Г.К. Буркеева, А.В. Омашева, Н.А. Есентаева, А.Н. Болатбай

Среднечисловая и среднемассовая молекулярные массы полиэтилен(пропилен)гликольфумаратов

Ненасыщенные полиэфиры интересны для теоретических и практических исследований, поскольку, наряду с простотой, экономичностью получения, содержат в своем составе ненасыщенные двойные связи, что делает возможным получение на их основе пространственно-сшитых структур. В статье показано, что реакцией поликонденсации этилен(пропилен)гликоля и фумаровой кислоты синтезированы полиэтиленгликольфумарат и полипропиленгликольфумарат. Составы полиэтилен(пропилен)гликольфумаратов были установлены по данным элементного анализа, ИК-спектроскопии. Определены некоторые физико-химические характеристики синтезированных полиэтилен(пропилен)гликольфумаратов. С целью определения корреляции между значениями молекулярных масс полиэтилен(пропилен)гликольфумаратов найдены среднечисловые и среднемассовые значения последних. Как следует из представленных в данной работе результатов, полиэтиленгликольфумарат и полипропиленгликольфумарат имеют среднемассовую молекулярную массу, рассчитанную методом светорассеяния, порядка 2500 и 1488 а.е.м. соответственно, среднечисловая молекулярная масса по методу определения доли концевых групп составляет 2010 и 1245 а.е.м. соответственно. Показано, что методы светорассеяния и определения концевых групп дают хорошую сходимость и имеют высокую степень корреляции. В результате проведенных исследований показана корректность применения метода светорассеяния для оценки молекулярной массы полиэтилен(пропилен)гликольфумаратов.

Ключевые слова: ненасыщенные полиэфирные смолы, полиэтиленгликольфумарат, полипропиленгликольфумарат, среднечисловая молекулярная масса, среднемассовая молекулярная масса, светорассеяние, титрование, поликонденсация.

References

1 Benig, G.V. (1968). *Nenasyshchennye poliefiry: stroenie i svoistva [Unsaturated polyesters: structure and properties]*. Moscow: Khimiia [in Russian].

2 Sedov, L.N., Avdeyeva, G.M., Zilberman, Ye.G., Pugachevskaya, N.F., & Savicheva, O.I. (1970). Modifitsirovanie khimicheskoi struktury polimaleinatov i polifumaratov dlia rehulirovaniia svoistv sopolimerov na ikh osnove [Modification of the chemical structure of polymaleinates and polyfumarates to regulate the properties of copolymers based on them]. *Vestnik tekhnicheskoi i ekonomicheskoi informatsii — Technical and Economic Information Bulletin*, *2*, 16 [in Russian].

3 Anisimov, Yu.N., Vonsovich, N.A., & Grekhova, O.B. (1996). Privitaia sopolimerizatsiia vinilatsetata s nenasyshchennoi olihoefirnoi smoloi i kharakteristiki otverzhdennykh kompozitsii [Graft copolymerization of vinyl acetate with an unsaturated polyester resin and characteristics of cured compositions]. *Zhurnal prikladnoi khimii — Journal of Applied Chemistry*, *69*, 2, 312–316 [in Russian].

4 Burkeyev, M.Zh., & Tazhbayev, Ye.M., et al. (16.03.2016). Patent No. 31052 Kazakhstan. *Sposob polucheniia nenasyshchennykh poliefirnykh smol na osnove propilenhlikolia, ftalevoho anhidrida i fumarovoi kisloty [Method for the preparation of unsaturated polyester resins based on propylene glycol, phthalic anhydride and fumaric acid]* [in Russian].

5 Kozlov, N.A., & Mitrafanov, A.D. (2001). *Fizika polimerov [Physics of Polymers]*. Vladimir: VlGU [in Russian].

UDC 554.02

J. Klimentova, P. Vojtisek

Charles University, Prague, Czech Republic
(E-mail: pavojt@natur.cuni)

Variation of the stereoparameters for description geometry of calix[4]arenes — more suitable solution for «flat systems»

This article deals with a variation of previously introduced parameters α, β, and δ which were used to describing the all possible conformations of these compounds, cone, partial cone, 1,2- and 1,3-alternate conformers of methylene- and heteroatom-bridged calix[4]arenes. Usefulness of these parameters α, β, δ have been already demonstrated, but, it seems, to be more suitable to do any variations them for flat systems. The background for the parameters α, β, δ lies in the representation of the scale of the angles of the calix[4]arene rings towards the reference plane. The original scale 0° — 360° for these angles depicts very well the differences between the calix[4]arene conformations but has two significant disadvantages. The first one is the discontinuity of the scale. The angles α_i range approximately from 0° to 110° and from 250° to 360° because of the sterical hindrance that would occur should the calixarene phenyl ring enter the cavity. The second disadvantage is the discontinuity at the point $\alpha_i = 0°$, it means the case of flat systems. These flat systems are usually the ‘transitions states‘ between the calixarene conformations and cannot be observed using parameters α, β, δ. To eliminate the difficulties in describing the 'transition states' between the calix[4]arene conformations caused by the discontinuities of the original scale, the new scale should be introduced. New parameters α´, β´, δ´ were introduced by subtracting 360° for each 'negative' ring present in the structure (one for partial cone conformers, two for 1,2- and 1,3-alternate conformers); after the parameters α, β, δ are calculated.

Keywords: supramolecular chemistry, stereochemistry of calix[4]arene, conformation, transition states, torsion angles, distorsion parameters, analysis of structural data from CCDC, cluster analysis.

Variation of the parameters α, β, δ

The background for the parameters α, β, δ lies in the representation of the scale of the angles of the calix[4]arene rings towards the reference plane [1–3]. The original scale 0°–360° (see Fig. 3 in [2]) for these angles depicts very well the differences between the calix[4]arene conformations (separation into the distinct 'clusters') [3, 4] but has two significant disadvantages. The first one is the discontinuity of the scale. The angles α_i range approximately from 0° to 110° and from 250° to 360° because of the sterical hindrance that would occur should the calixarene phenyl ring enter the cavity [3, 4].

The second disadvantage is the discontinuity at the point $\alpha_i = 0°$, it means the case of flat systems. This discontinuity is principally responsible for the distinct separation into the 'clusters' observed in [3, 4] on Fig. 4–7, but as a result the ‘transitions states‘ between the calixarene conformations cannot be observed. And mainly these ‘transitions states‘ are flat systems.

To eliminate the difficulties in describing the 'transition states' between the calix[4]arene conformations caused by the discontinuities of the original scale, the new scale, depicted in the second part of Figure 1, should be introduced. This scale differs from the first one in the values of the 'negative' phenyl ring angles; these angles are calculated from those in the first scale by subtracting 360°. However, the negative values of some phenyl ring angles might cause difficulties in parameter α, β, δ calculation. Therefore we decided for transformation of the existing parameters α, β, δ by subtracting 360° for each 'negative' ring present in the structure (one for *partial cone* conformers, two for *1,2-* and *1,3-alternate* conformers); *after* the parameters α, β, δ are calculated. The formulae for the resulting parameters α´, β´, δ´ are given in the next paragraph.

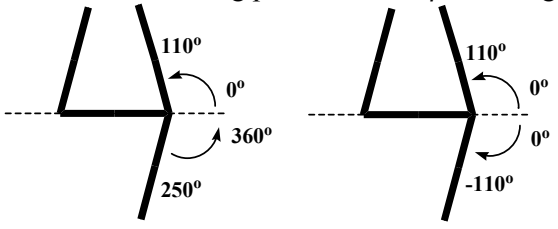

Figure 1. The dual representation of the scale of phenyl ring angles α_i

A new set of parameters, α′, β′, δ′ was therefore introduced to describe the 'transition states' between the calix[4]arene conformations. These parameters are defined using the original α, β, δ parameters for four conformers of calix[4]arenes as follows:

cone calix[4]arenes: $\alpha' = \alpha$; $\beta' = \beta$; $\delta' = \delta$; (1)

partial cone calix[4]arenes: $\alpha' = \alpha - 90°$; $\beta' = \beta$ — $360°$; $\delta' = \delta - 360°$; (2)

1,2-alternate calix[4]arenes: $\alpha' = \alpha - 180°$; $\beta' = \beta$; $\delta' = \delta - 720°$; (3)

1,3-alternate calix[4]arenes: $\alpha' = \alpha - 180°$; $\beta' = \beta$ — $720°$; $\delta' = \delta$. (4)

Aplication of the new parameters α′, β′, δ′

The α′-β′ and α′-δ′ plots for the group of calix[4]arenes with methylene bridges are depicted on Figures 2 and 3.

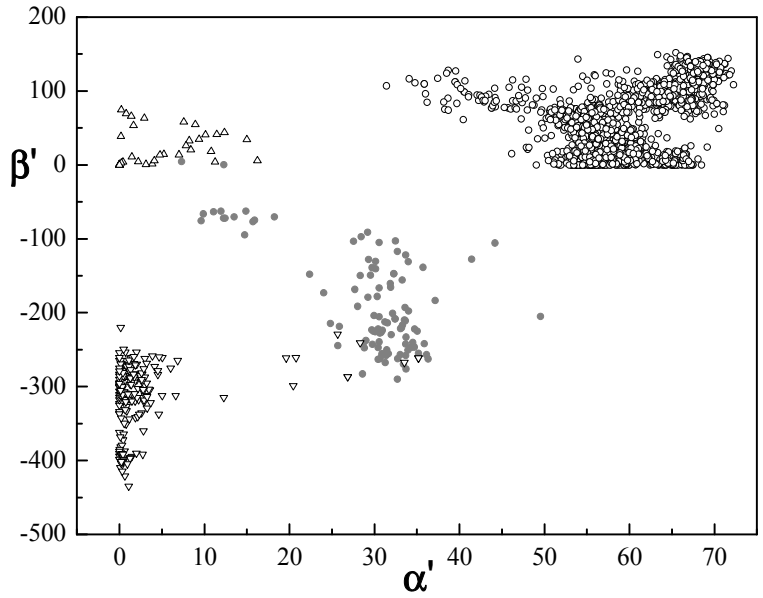

○ — cone; ● — partial cone; Δ — 1,2-alternate; ▽ — 1,3-alternate conformation

Figure 2. The α′-β′plot for the group of calix[4]arenes with methylene bridge groups

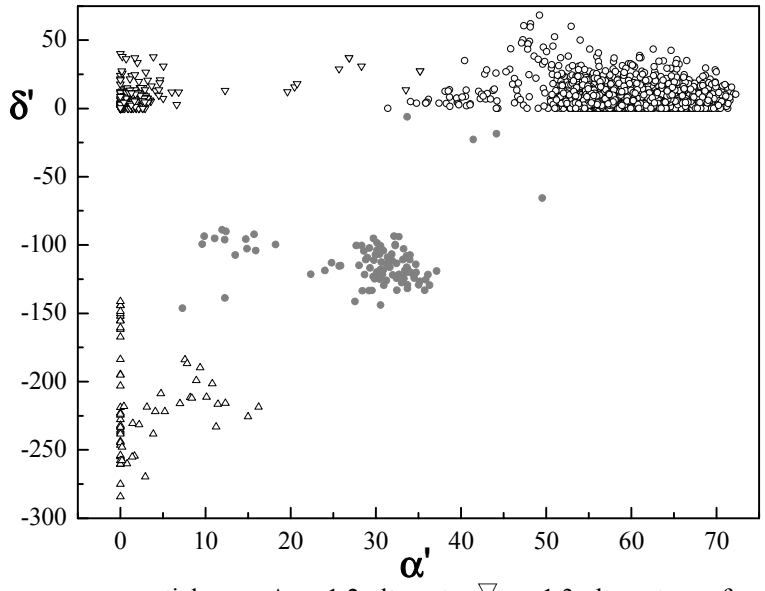

○ — cone; ● — partial cone; Δ — 1,2-alternate; ▽ — 1,3-alternate conformation

Figure 3. The α′-δ′ plot for the group of calix[4]arenes with methylene bridge groups

From the α′-β′ plot, it is obvious that two hits from the *partial cone* group lie within the *1,2-alternate* group. The plot is more transparent and better than using parameters α-β. These structures are ZALGOI (Fig. 4) and a very open structure KOCQIC (Fig. 5). The similarity of these structures to the *1,2-alternate* group is readily observable. The distinct group separated from the *partial cone* conformers ('on the path' to the *1,2-alternate* conformers) is the group of single atom 'triple-bridged' structures which possess very opened cavities (see structure ABIHIC, Fig. 4). These structures have been already discussed.

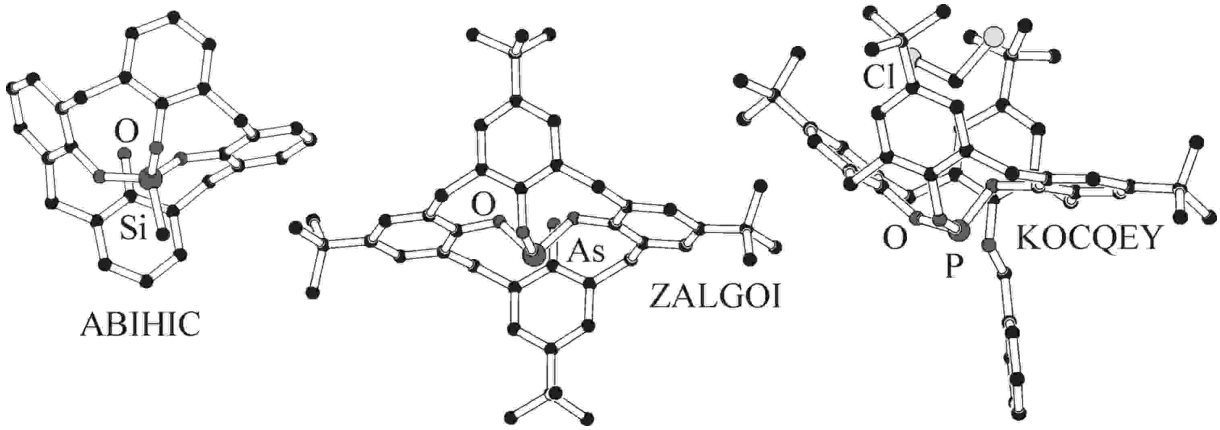

Figure 4. Structures ABIHIC, ZALGOI and KOCQEY [5]

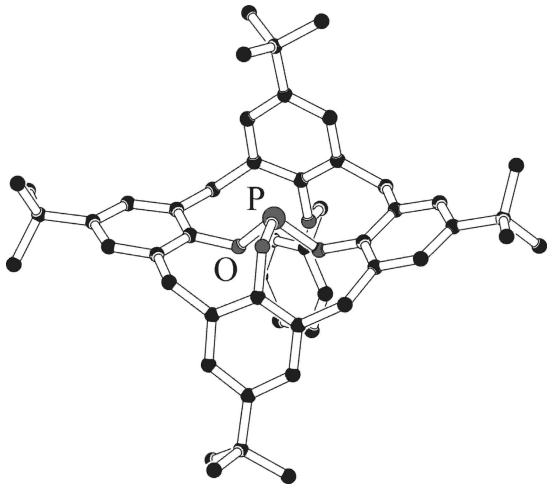

Figure 5. Structure KOCQIC [5]

From the α′-β′ plot it can be clearly seen that four hits from the *partial cone* group are close to the *cone* group. The structures GUBTAY (no Fig.) and KOCQEY [4] (Fig. 4) belong to this group.

From the two plots it is obvious that several hits from the *1,3-alternate* group are very close to both *cone* and *partial cone* group (hits with α′ > 10°). The unifying feature of these structures is the presence of calix[4]arene skeleton strongly deformed towards C_{2v} geometry; close to that of *saddle* shaped calix[4]resorcinarenes. The main reason behind this deformation is missing of two opposite phenolic oxygen atoms at the lower rim and the resulting π,π-stacking between the other opposite calix[4]arene phenyl rings (e.g. structure GUCYUY, Fig. 6). The π,π-stacking might occur even between calix[4]arene phenyl rings from different molecules. Representative example of this group of structures is the structure GUCYUY (the deformation in this case is due to the presence of π,π-stacking between the opposite calix[4]arene phenyl rings and between one calix[4]arene phenyl ring and the phenyl ring from the crown ether bridge).

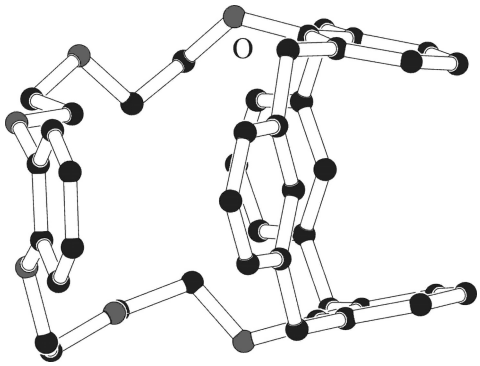

Figure 6. Structure GUCYUY [5]

The α′-β′ and α′-δ′ plots for the group of calix[4]arenes with heteroatom bridges are depicted on Figures 7 and 8. From both plots, it is obvious that several structures from the *partial cone* group (structures with α′ ~ 10–20°) are close to the *1,2-alternate* group. These structures possess relatively opened cavities; structure SEBZEE [5] is a clathrate with a trimeric structure, the other two structures possess open cavities due to the presence of π, π-stacking between one calix[4]arene phenyl ring and an aromatic moiety from complex ligand molecule (see structure YAQKAD, Fig. 9 and VAVRAM, Fig. II-5 in [4]).

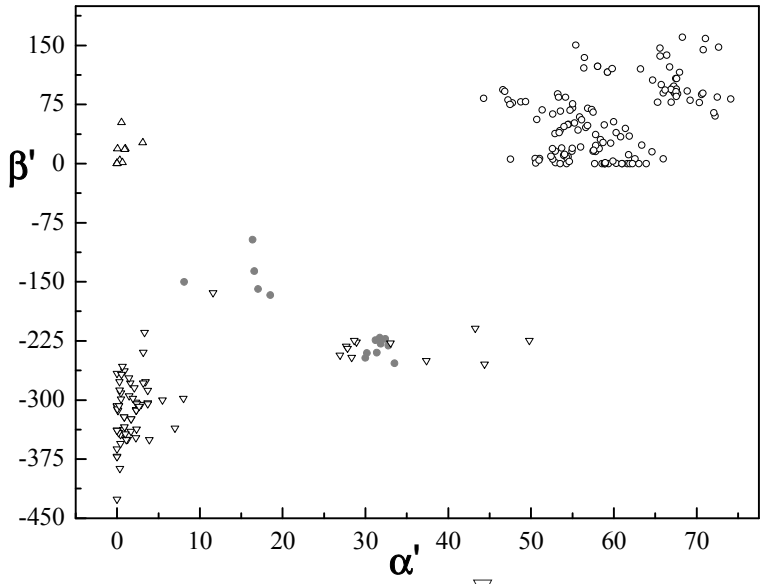

Figure 7. The α′-β′ plot for the group of calix[4]arenes with heteroatom bridges

From the α′-β′ plot it can be observed that several *cone* structures are 'on the path' to the *1,3-alternate* group (structures with α′ ~ 45°). These structures (e.g. structure ACAJAQ see Fig. 10) all exist in a very flat *pinched cone* conformation (a remarkable deformation towards C_{2v} symmetry) because of a distal *cis*- coordination of a metal ion to the four phenolic oxygen atoms. Structure TETQEO [5] also belongs to this group. In this case proximal *cis*- coordination of two potassium ions causes a marked opening of the calixarene cavity (symmetry approximately C_{4v}) and therefore lower value of the parameter α′. Examples of the distal *cis*- coordination are given on the structure ACAJAQ (Fig. 10) and BEPKOX (see [3]).

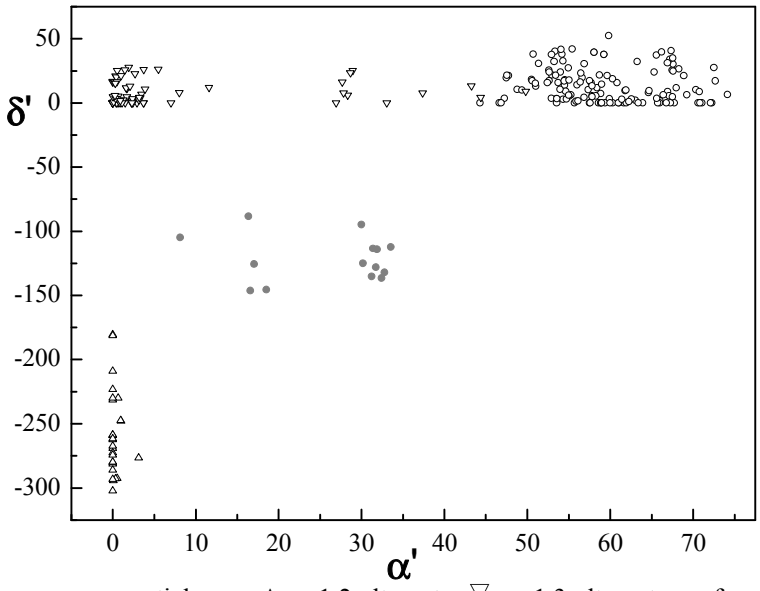

○ — cone; ● — partial cone; Δ — 1,2-alternate; ▽ — 1,3-alternate conformation

Figure 8. The α′-δ′ plot for the group of calix[4]arenes with heteroatom bridges

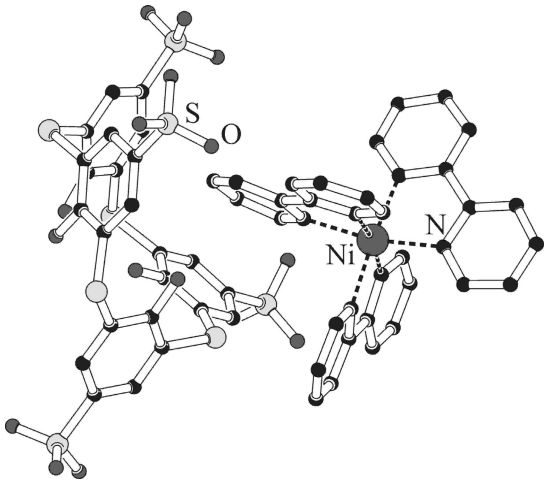

Figure 9. Structure YAQKAD [5]

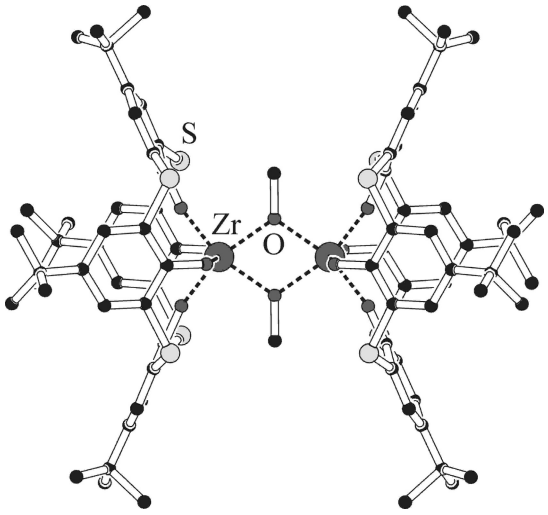

Figure 10. Structure ACAJAQ [5]

It is obvious from the two plots, that several hits from the *1,3-alternate* group are very close to both *cone* and *partial cone* group (hits with α′ > 20°). The unifying feature of these structures is the presence of calix[4]arene skeleton strongly deformed towards C_{2v} geometry; close to that of *saddle* shaped calix[4]resorcinarenes. All these structures (e.g. FEZZIU, HAXGAP, NODJOF, SAXJEG [5]) lack at least two distal phenolic oxygen atoms at the lower rim and with the only exception of SAXJEG (Fig. II-25 in [4]) have distally *m*- substituted two phenyl rings. The geometry of these structures is governed by the presence of π,π-stacking between the two other opposite calix[4]arene phenyl rings; sometimes even between calix[4]arene phenyl rings from different molecules (structures FEZZIU, HAXGAP [5]). The representative examples of this group are the structures FEZZIU (Fig. II-23 in [4] and HAXGAP (Fig. 11).

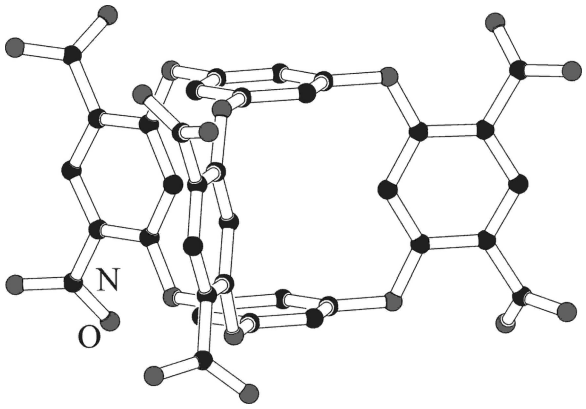

Figure 11. Structure HAXGAP [5]

The only hit from this group with α′~ 10° close to the 'renegade' group of *partial cone* structures (structure TAZMEN, see the α′-β′ plot) has a very open structure probably due to *m*-substitution of two opposite calix[4]arene rings (Fig. 12).

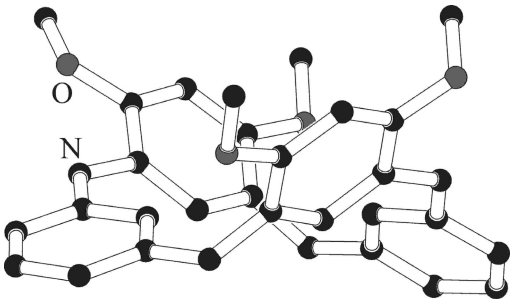

Figure 12. Structure TAZMEN [5]

Conclusion

The utility of parameters α, β, δ in describing the conformation of calix[4]arenes and the impact of inter/intramolecular interactions present in the structure on the symmetry of the *cone* calix[4]arene base frame has been evaluated in review [3, 4]. These parameters can describe deformations of the scaffold symmetry. A deformation towards C_{2v} (*flattened cone* structures) is reflected by the parameter β; a deformation towards C_s symmetry is best reflected by the parameter δ. The parameter αreflects the degree of 'opening' of the calix[4]arene cavity.

The «original» parameters α, β, δ are based on the angles at the scale from 0° to 360° for α_i, having two significant disadvantages. The first one is the discontinuity of the scale (see Fig. 1). The angles α_i range approximately from 0° to 110° and from 250° to 360° because of the sterical hindrance that would occur should the calixarene phenyl ring enter the cavity. The second disadvantage is the discontinuity at the point $\alpha_i = 0°$, it means the case of flat systems. But these flat systems are usually the ‘transitions states‘ between the calixarene conformations and cannot be acceptable described using the parameters α, β, δ**.**

To eliminate the difficulties in describing the 'transition states' between the calix[4]arene conformations caused by the discontinuities of the original scale, the new scale for α_i (see Fig. 1) should be introduced. New

parameters α´, β´, δ´ were introduced easily by subtracting 360° for each 'negative' ring present in the structure (one for partial cone conformers, two for 1,2- and 1,3-alternate conformers); after the parameters α, β, δarecalculated.

These new parameters are not quite different approach, their properties and connections with a symmetry of calixarenescafold are remained. They are able to reflect same effect as the original parameters α, β, δ**.** It is only small «correction», but it seems to be useful for description and modelling flat systems and for studying transitions between calixarene conformations.

Acknowledgements

We thank RNDr. Ivana Císařová, CSc. for the provision of CSD data. Access to the Cambridge Crystallographic Data Centre was sponsored by the Grant Agency of the Czech Republic (grant No. 203/99/0067). We thank Dr. Ye. Minayeva for her help with Russian part of text. We thank Professor S. Kenzhetayeva for her help with Kazakh part of text.

References

1 Klimentová, J., & Vojtíšek, P. (2005). Stereochemistry of calix[4]arenes. *Materials Structrure*, *12*, 151–152.

2 Klimentová, J., & Vojtíšek, P. (2007). New receptors for anions in water: Synthesis, characterization, X-ray structures of new derivatives of 5,11,17,23-tetraamino-25,26,27,28-tetrapropyloxycalix[4]arene. *Journal of Molecular Structure*, *826*(1), 48–63 and references therein.

3 Klimentová, J., Mádlová, M., Němečková, P., Palatinusová, L., Vojtíšek, P., & Lukeš, I. (2017). Conformations of calix[4]arenes — an investigation based on CSD data. Part I. Cone conformers of methylene- and heteroatom-bridged calix[4]arenes. *Bulletin of the Karaganda University. Ser. Chemistry, 85*(1), 21–46.

4 Klimentová, J., Mádlová, M., Němečková, P., Palatinusová, L., Vojtíšek, P., & Lukeš, I. (2017). Conformations of calix[4]arenes — an investigation based on CSD data. Part II. Partial cone, 1,2-alternate and 1,3-alternate conformers of methylene- and heteroatom-bridged calix[4]arenes. *Bulletin of the Karaganda University. Ser. Chemistry*, *88*(4), 8–38.

5 CSD Version 2.3.6 (update August 2006), Cambridge Crystallographic Data Centre (CCDC).

Я. Климентова, П. Войтишек

Каликс[4]арендердің геометриясын сипаттау үшін стереопараметрлерін өзгерту — «жазық жүйелер» үшін қолайлы шешім

Мақалада каликс[4]арендер барлық мүмкін болатын конформацияларын, нақтылап айтқанда, жартылай конустың, метиленді және гетероатомды көпіршелері бар 1,2- және 1,3-альтернантты конфермелерін, сипаттау үшін қолданылған, алдында енгізілген α, β және δ параметрлерін өзгерту қарастырылды. Осы α, β, δ параметрлерінің жарамдылығы көрсетілген, бірақ оларды жазық жүйелер үшін қолданған дұрыстау болады. α, β, δ параметрлері үшін алғышарт каликс[4]арендердің сақина бұрыштарына салыстыру жазықтығына қатысты шкала ұсыну болып тұр. Осы бұрыштар үшін бастапқы масштаб 0°–360° каликс[4]арендердің конформациялары арасындағы өзгешеліктерді жақсы көрсетеді, бірақ екі елеулі кемшілік бар. Біріншісі — ол шкаланың үзілуі. Кеңістіктік кедергілер салдарынан, бұрыштар α_i 0° дан 110° және 250° ден 360° шектеуінде жатыр. Егер қуысқа каликсарендік фенил сақинасы енсе, осы іске асады. Екінші кемшілік — α_i = 0° нүктесіндегі үзілу, бұл жазық жүйелерінің жағдайлары. Осы жазық жүйелер, әдетте, каликсарендер конформациялары арасындағы «ауысу күйлері» болып табылады және α, β, δ параметрлерін қолданғанда байқалмайды. Бастапқы шкаланың үзілуі нәтижесінде пайда болатын, каликс[4]арендер конформациялары арасындағы «ауыспалы күйлерді» сипаттауда байқалатын осындай қиындықтарды жою үшін жаңа масштаб енгізу қажет. Жаңа параметрлер α', β', δ' құрылымдағы әрбір «теріс» сақина үшін 360° алып тастау арқылы енгізілген (біреуі конустың жартылай конформерлері үшін, екеуі 1,2- және 1,3-альтернантты конформер үшін); соңынан α, β, δ параметрлері есептелген.

Кілт сөздер: супрамолекулалық химия, каликс[4]арендердің стереохимиясы, конформациялар, ауыспалы күйлер, торсионды бұрыштар, ауытқу параметрлері, CCDC құрылымдық мәліметтерінің талдауы, кластерлік талдау.

Я. Климентова, П. Войтишек

Изменение стереопараметров для описания геометрии каликс[4]аренов — более подходящее решение для «плоских систем»

В статье рассмотрено изменение ранее введенных параметров α, β и δ, которые были использованы для описания всех возможных конформаций, а именно: конуса, частичного конуса, 1,2- и 1,3-альтернантных конформеров каликс[4]аренов с метиленовыми и гетероатомными мостиками. Пригодность параметров α, β, δ была продемонстрирована, но, по-видимому, более целесообразно использовать их для плоских систем. Предпосылка для параметров α, β, δ лежит в представлении шкалы углов колец каликс[4]аренов по отношению к плоскости сравнения. Исходный масштаб 0°–360° для этих углов очень хорошо показывает различия между конформациями каликс[4]аренов, но имеет два существенных недостатка. Первый — это разрыв шкалы. Углы α_i лежат в пределах от 0° до 110° и от 250° до 360° из-за стерических препятствий, которые произойдут, если в полость войдет каликсареновое фенильное кольцо. Второй недостаток — разрыв в точке $\alpha_i = 0°$, это означает случай плоских систем. Эти плоские системы обычно являются «состояниями переходов» между конформациями каликсарена и не могут наблюдаться с использованием параметров α, β, δ. Чтобы устранить трудности при описании «переходных состояний» между конформациями каликс[4]арена, вызванными разрывами исходной шкалы, следует ввести новый масштаб. Новые параметры α', β', δ' были введены путем вычитания 360° для каждого «отрицательного» кольца, присутствующего в структуре (один — для частичных конформеров конуса, два — для 1,2- и 1,3-альтернантных конформеров), далее были рассчитаны параметры α, β, δ.

Ключевые слова: супрамолекулярная химия, стереохимия каликс[4]аренов, конформации, переходные состояния, торсионные углы, параметры отклонения, анализ структурных данных CCDC, кластерный анализ.

UDC 541.64

Ye.M. Tazhbayev, M.Zh. Burkeyev, L.Zh. Zhaparova,
T.S. Zhumagalieva, Zh.T. Arystanova

Ye.A. Buketov Karaganda State University, Kazakhstan
(E-mail: lyazzh@mail.ru)

Nanoparticles on the basis of polylactic acid and polylactic-co-glycolic acids loaded with drugs

In this article a brief review on the research works devoted to the synthesis and investigation of polymeric nanoparticles and nanocapsules on the basis of polylactic acid and its copolymer with polyglycolic acid is given. Nanoparticles based on biocompatible and biodergadable polylactic acid and polylactic-co-glycolic acids gained special interest in pharmaceutical field as the carriers of different drug preparations. General methods of synthesizing nanosomal formulations of polylactic acid and polylactic-co-glycolic acids were described in this work. Among the perspective methods of obtaining the polymeric nanoparticles and nanocapsules of polylactides and its copolymer with glycolic acid loaded with drugs the nanoprecipitation and emulsion methods were found to be the most suitable for the systems used. Another method of synthesizing the nanosized systems of polylactic-co-glycolic acid is a double emulsion method which makes possible to obtain nanocapsules with optimal characteristics. The possibilities of immobilization of nanoparticulate systems based on these polymers with antitumor and antituberculosis drugs were considered. Some examples of polylactic acid and polylactic-co-glycolic acids' nanoparticles and nanocapsules loaded with drugs which have applications in medicine for the treatment of tumor and tuberculosis diseases were shown.

Keywords: polylactic acid, polylactic-co-glycolic acid, nanoparticles, antitumor drugs, antituberculosis drug, drug delivery, polymers, nanocapsules.

One of the promising drug carriers used in developing controlled drug delivery systems is polylactic acid (PLA) [1–13]. Polylactide or polylactic acid was first found in 1932 by Carothers. PLA was the first polymer which was used together with polygycolic acid as a surgical suture [1–6]. PLA is not soluble in water and in water-ethanol mixtures: it possesses unique properties including high mechanical properties and very low toxicity [2–13]. Polylactide is biocompatible and biodegradable polymer which has been used in medicine for a long time not only as an auxiliary material, but as carrier for the targeted delivery of the drugs [7–12]. First synthetic polymer and bioabsorbing material was polyglycolic acid which opened this class of polymers in 1954. Since that time the derivatives of this polymer with polylactic acid (polylactide) and ε-caprolactone have been used for the drug delivery purposes [13–15]. Incorporation of the chains of glycolic acid allows controlling the biodegradation rate, hence the drug release rate can be regulated by obtaining the copolymers of poly-lactic-co-glycolic acid (PLGA) of wide range of composition [16].

The drug delivery systems are known to be constructed on the basis of biocompatible polymers in the forms of micro- and nanoparticles or nanocapsules [13–20]. Biodegradable nanoparticles gained much interest of scientists due to their unique properties and advantages over conventional drug dosing forms. The use of such forms is especially important in a treatment of long-termed diseases using high doses of potent drugs. So, micro- and nanoparticles based on polylactic, polyglycolic acids and their copolymers and ethers, are used for the delivery of various drug preparations [13–27]. The polymers of glycolic and lactic acids are widely used for the preparation of biodegradable medical devices and of drug-sustained release microspheres or implants marketed in Europe, Japan, and the USA [27].

The use of the copolymers of lactic acid with glycolic acid gives more opportunities in the creation of controlled delivery systems for potent drugs which are used in the treatment of tumors and tuberculosis. Antitumor drug preparations based on nanoparticles of the copolymers of lactic and glycolic acids have been worked out and they are allowed to be used in medicine practice in Russian Federation by the trade names dekapeptyl, zoladex, sandostatin and somatulin [17]. The copolymer of lactic and glycolic [50/50 Poly-(D,L-lactide-co-glycolide) (nominal)] acids is non-toxic and its catabolism in the organism ends up with the formation of CO_2 and H_2O [17, 25, 27].

Microspheres with controlled degradation were obtained on the basis of a copolymer of lactic and glycolic acids, polyethylene glycol (PEG) or polycaprolactam. An important feature of polylactides and polyglycolides is biocompatibility with the tissues of the body, enzymatic degradation by ethereal bonds to derivatives of lactic and glycolic acids.

As it was mentioned above depending on the ratio of lactic and glycolic acids it is possible to change such properties of the product as plasticity, durability, the biodegradation time and release rate of the drug. It was found that varying the ratio of the lactic and glycolic chains the release rate of the drug can be controlled [28]. With increasing the content of glycolic chains the release rate of hydrophilic drugs increases and the release rate of lipophilic drugs decreases provided that the drug excretion takes place as a result of polymer degradation. By this way the copolymers of PLGA with PEG and poly-ε-caprolactone (PCL) with controlled degradability were successfully synthesized in [28]. They degrade by the ester bonds to the derivatives of lactic and glycolic acids. It has been established that polylactides with hydrophobic end groups degrades 2.7 times faster *in vitro* and 4 times faster *in vivo* than the polymers with hydrophilic groups [29].

Different techniques can be used for the preparation of nanostructures of PLA and PLGA:

– double emulsion followed by solvent evaporation [18, 19];

– dialysis [18, 19];

– nanoprecipitation [18–21];

– the salting out [19–24];

– supercritical fluid technology [18, 19].

Detailed description of these methods and the examples of the polymeric nanoparticles obtained using these techniques can be found in [18].

Among the effective and reproducible methods of obtaining nanoparticles of PLA, polyglycolic acid or their copolymers is found to be nanoprecipitation [18–30]. This method was first developed by Fessi et al. for the preparation of polymeric nanoparticles [19]. It is also called as solvent displacement method [19]. J. Prasad Rao and E. Geckeler Kurt described this process in detail [18]. According to them the basic principle of this technique is based on the interfacial deposition of a polymer after displacement of a semi-polar solvent, miscible with water, from a lipophilic solution [19]. Rapid diffusion of the solvent into non-solvent phase results in the decrease of interfacial tension between the two phases, which increases the surface area and leads to the formation of small droplets of organic solvent [18, 19]. The authors inform that the nanoprecipitation system consists of three basic components: the polymer (synthetic, semi synthetic or natural), the polymer solvent and the non-solvent of the polymer [19]. Organic solvents such as ethanol, acetone, hexane, methylene chloride or dioxane which are miscible with water and easy to remove by evaporation can serve as a polymer solvent [19]. Due to this reason, acetone is the most frequently employed polymer solvent in this method [19]. Also there are some examples of using the solvent mixture (acetone-water, acetone-ethanol and methanol) [19]. J. Prasad Rao and Kurt E. Geckeler summarized the examples of the polymers, solvents and non-solvents used for the preparation of nanoparticles by nanoprecipitation method in Table 1 [18].

Table 1

Nanoprecipitation formulations for the preparation of polymer nanoparticles [18]

Polymer	Solvent	Non-solvent	Stabilizing agent	Particle size, nm	References
PLGA	Acetone	Water	PVA	95–560	[24]
Allylic starch	Acetone	Water	–	270	[16]
Dextran ester	Acetone	Water	–	77	[27]
PLGA	Acetone/ethanol	Water	Tween 20	63–90	[31]
PCL diol	Chloroform	Water	Pluronic F 127	17.4	[16]
Eudragit L100–155	Acetone/absolute ethanol	Water	–	120	[22]
PLGA	Acetone	Water	–	165±5	[27]
	Acetonitrile			164±4	[23]
PCL	Acetone	Water	PVA	365±5	
PLA	THF	Water	–	100–300	[24]
PCL	Acetone	Water	–	741–924	[21]
PCL	Acetone	Water	Span 20	266±11	[20]
PLA	Acetone	Water	Polysorbate 80	250±50	[25]
PCL	Acetone	Water	Poloxamer 188	308–352	[20]
			PE/F68		[27]

According to H. Fessi, et al. [19] when obtaining nanoparticles using nanoprecipitation method the process of particle formation consists of three stages: nucleation, growth and aggregation. The rate of each step determines the particle size and the driving force of these phenomena is the ratio of polymer concentration over the solubility of the polymer in the solvent mixture [19]. The separation between the nucleation and the growth stages is the key factor for uniform particle formation.

The system of nanoprecipitation mainly consists of three components; these are the polymer, the solvent of the polymer and non-solvent of the polymer [18, 19]. PLA nanoparticles with the range of particle size from 100 to 300 nm were obtained depending on the solvent and surfactant used in [19, 21]. So nanoprecipitation is a simple, fast and reproducible method which allows obtaining both nanoparticles and nanocapsules [18].

PLGA nanoparticles coated with transferrin with the size in the range 63–90 nm for the purpose of passing through blood-brain-barrier were successfully synthesized in the presence of Tween 20 using nanoprecipitation method [22]. B.J. Nehilla et al. synthesized coenzyme Q10-loaded PLGA nanoparticles without using surfactant with the average size 165 nm [23]. Nanoprecipitation method was also used for the encapsulation of curcumin into PLGA nanoparticles by M.M. Yallapu et al. [24] as a result of which the particles with the size ranging in 95–560 nm were obtained.

The mechanism of intracellular uptake of PLGA nanoparticles and their effect on therapeutic efficiency of the active compounds in cellular level when encapsulating DNA, proteins and different low molecular weight compounds are throhoughly considered by J. Panyam and V. Labhasetwar in [16].

There are also the examples of using PLA and PLGA nanoparticles for the treatment of tumor and tuberculosis diseases below.

Derakhshandeh K. et al. encapsulated 9-nitrocamphotericin in the copolymer of poly-lactic-co-glycolic acids using above said nanoprecipitation method. As a result the encapsulation efficiency 30 % [11]. Fonseca C. with colleagues synthesized PLGA nanoparticles loaded with Paclitaxel using solvent evaporation followed by extraction [12]. In this case the authors achieved the encapsulation efficiency of 100 % with complete maintenance of antitumor activity in *in vitro* study [31]. In [30] PLGA nanospheres immobilized with triptorelin were synthesized using the double emulsion technique followed by solvent evaporation. As a result the encapsulation efficiency varied from 4 to 83 % depending on initial drug concentration [30]. The authors of the work [31] successfully encapsulated poorly water-soluble xantones into PLGA nanoparticles.

Helle A. et al. investigated the possibility of using capillary electrophoresis for the quantitative determination of model drugs (salbutamol sulphate, sodium chromoglycate and beclomethasone dipropionate) which were encapsulated in PLA nanoparticles by nanoprecipitation method [26]. A quantitative capillary electrophoresis method was developed for salbutamol sulphate and sodium chromoglycate by the authors. It was found out that the encapsulation of beclomethasone dipropionate in the PLA nanoparticles was more efficient than in case of more hydrophilic model drugs (salbutamol sulphate and sodium chromoglycate) [26].

It is necessary to note that there are works on obtaining nanoparticles from the commercial polymers and load them with drugs. For instance, Jae-Woon Nah et al. prepared nanoparticles of PLGA using dialysis method without surfactant [32] and loaded them with a model drug clonazepam. The authors investigated the effect of different solvents on physicochemical characteristics of the nanoparticles and found that the drug-loading contents were dependent on the copolymer composition and initial feeding amount of the drug [32].

R. Jalil and J.R. Nixon prepared the microcapsules of PLA containing phenobarbitone using a w/o emulsion-evaporation method [33]. The authors used the polymer of three different molar masses, 20.200, 13.300 and 5.200 to obtain microcapsules and they studied the in vitro release kinetics of phenobarbitone from prepared microcapsules at different pH values (pH 2, pH 7 and pH 9) [34]. They have found that the release follows in a square root of time dependent release mechanism [34]. M. Dutt, et al. used the same technique to obtain PLGA microparticles and load them with the antiTB drugs isoniazid and rifampicin. It resulted in PLGA nanoparticles with the drugs with the size around 200–300 nm and with the encapsulation efficiency of 50–65 % [35]. The authors investigated the in vitro and in vivo drug release on CaCo-2 cells and established that obtained nanoparticles had a slower release kinetics compared to free drugs [35].

During the last decades various polymeric systems have been developed for the targeted delivery of antitumor drug preparations. The examples of nanoparticles on the basis of PLA and PLGA, PEG-PLGA for passive transport of antitumor drugs are given in Table 2 [36].

Table 2

Polymeric nanoparticles developed for the delivery of drugs to treat various tumors [36]

Polymer	Drug	Tumor cell line	In vitro and in vivo study	References
PLGA	Paclitaxel	Human cervical carcinoma cells (HeLa)	In vitro and in vivo	37
	Cisplastin	Colon adenocarcinoma cells	In vitro and in vivo in mice	38, 39
	5-Fluorouracil	Glioma (U87MG) and breast and adenocacinoma (MCF-7) cell lines	In vitro	40
	Doxorubicin	MDA-MB-231 breast tumor cells HeLa cells Fibroblust cells Lung epithelial tumor cells (A549)	In vitro In vitro In vitro In vitro	41 42 43 44
	Gemcitabine	Pancreatic tumor cells (PANCl)	In vitro	45
PLGA-mPEG	Cisplastin	Prostate tumor (LNCaP) cells	In vitro	46
PLGA-b-PEG	Docetaxel	Prostate tumor (LNCaP) cells	In vivo in nude mice	47
	Cisplastin	Breast (MCF-7) and prostate tumor (PC-3 and DU145) cells	In vitro and in vivo in nude mice	48
PLGA-mPEG+ carboxymethyl cellulose	Cisplastin	Ovarian tumor (IGROVI-CP) cells	In vitro and in vivo in mice	49
hyaluronic acid-PEG-PLGA	5-Fluorouracil	EAT cell lines	In vitro and in vivo in mice	50
l-PLGA-human serum albumin	Doxorubicin	Rat glioblastoma	In vivo in rat	51

Isoniasid is a first-line drug to treat tuberculosis which can be administered perorally as well as intramuscularly. However the drug dose used for healing the disease is high compared to the required minimum inhibitory concentration of the drugs [52]. Therefore the attention of scientists is concentrated on prolongation the effect of isoniazid together with other antiTB drug preparations by encapsulation them in different matrices. M.Zh. Burkeev et al. used the same method (nanoprecipitation) for the encapsulation of widely used antituberculosis drugs isoniasid and p-aminosalicylic acid (PASA) in PLA and PLGA nanoparticles [53]. Optimal conditions (solvent, the ratio polymer: drug, etc.) for synthesizing PLA nanocapsules loaded with the drugs were found. The best results were obtained when acetone was used as a solvent. Nanoparticles of PLA loaded with isoniazid with the average diameter 200–300 nm and high meaning of binding degree (50 %) have been successfully synthesized. Immobilization of PLA nanoparticles with antituberculosis drug isoniazid have been performed with the ratio of the polymer to drug as 1:10, 1:5, 1:4. As a result of the experiments the last proportion was chosen as an optimal one. The procedure can be described briefly as follows: 5 mg of drug was dissolved in 0.2 ml of water and then 0.5 ml of acetone was added. 20 mg of PLA was dissolved in 1 ml of acetone and was mixed with the solution containing the drug. After that organic solvent was evaporated within 40 min at low pressure. The volume of the dispersion was made to 20 ml with water and filtered from aggregated particles. Obtained nanoparticles were characterized using photon correlation spectroscopy which have shown that the system consists of rather small particles with the size 253.7 nm and obtained particles have narrow particle size distribution (PDI = 0.241). The yield of PLA nanoparticles with isoniazid was 78.4 %. The system was found to be stable within the time which was confirmed by measurement of the surface charge of nanoparticles (–30–35 mV) [53].

PASA and its sodium salt are commonly used in tuberculosis therapy together with aminoglycosides. It is specifically to treat active drug resistant tuberculosis. Having high activity against strains of Mycobacterium tuberculosis it has side effects typical to antituberculosis drug preparations, which needs to be reduced. Therefore with the aim of increasing the efficiency of this drug and decreasing its therapeutic concentration the possibility of binding antituberculosis drug PASA with PLA nanoparticles was studied further by our research group. Data on physicochemical characteristics of synthesized empty PLA nanoparticles and polymeric particles loaded with antituberculosis drugs isoniazid and PASA are summarized in Table 3.

Table 3

Physicochemical characteristics of empty and drug loaded PLA nanoparticles

Characterization of nanoparticles		Empty PLA nanoparticles	PLA nanoparticles loaded with drugs	
			with isoniazid	with PASA
Average particle diameter, d, nm		290.1	253.7	310.7
PDI		0.316	0.241	0.515
Zeta potential, mV		–35.0	–30.4	–32.6
Fraction of nanoparticles, %		98.8	97.5	100.0
Yield of nanoparticles, %		76.6	78.4	76.0
Binding (%)	conductometry	–	50.5	68.7
	spectrophotometry	–	-	70.4

From data given in Table 3 it is obvious that the particle size (determined by dynamic light scattering (DLS) of PLA nanoparticles increased after incorporation of the drug which probably took place because of the adsorption of some part of the PASA on the surface of PLA nanoparticles. The yields of the nanoparticles with and without drug (determined using gravimetry) were high in both cases (Table 3). Data on binding obtained by two methods (conductometry and spectrophotometry) show that the meanings of binding degree of PASA with PLA nanoparticles correlates with each other and equal to 68.7 % and 70.4 % accordingly.

Poor solubility of some potent drugs in water is one of the major obstacles in using such drug preparations. In this regard the scientific group under supervision of prof. M.Zh. Burkeev investigated the possibility of loading the nanoparticles on the basis of PLA and PLGA with poorly-water soluble drug silymarin. Silymarin is known to be a potent antioxidant, liver protector and anti-cancer agent. Its hepatoprotective effectiveness is due to its antioxidant and anti-inflammatory properties. Being such an effective drug it has a problem of low bioavailability caused by its poor solubility in water, which means that high dose of the drug is needed for achieving therapeutic level in plasma. Its solubility in distilled water is 58 mkg/ml at 25 ºC, therefore this drug is considered as a preparation insoluble in water [54]. With the aim of synthesizing novel form of silymarin which provides sustained release Y. Ma et al. encapsulated it in self-assembled nanoparticles of Bletilla striata polysaccharide conjugates modified with stearic acid [54, 55]. Obtained nanoparticles of a mean diameter of 200 nm exhibited a sustained-release profile for nearly 1 week with no obvious initial burst and they showed a lower viability and higher uptake intensity on HepG2 cell lines compared to drug solutions [55].

With the aim of overcoming low bioavailability of silymarin the attempts to bind this drug with PLA nanoparticles was made by our research group. Nanoparticles of PLA loaded with silymarin were synthesized using nanoprecipitation method. As a result PLA nanoparticles containing the drug with the mean diameter 206.9 nm and PDI 0.291 were obtained. To observe the surface of the drug-loaded PLA nanoparticles they were analyzed using electron microscopy (SEM and REM). The images of PLA nanoparticles immobilized with silymarin are shown in Figure.

From given pictures it is seen that the system is not stable at a time and the particles have aggregated; however there are separate nanoparticles the meaning of mean diameter of which is in good accordance with data obtained by DLS. The binding degree of PLA with the drug determined using UV-Vis-spectroscopy (λ=325 nm) was 75 % which is a high value.

The nanoparticles on the basis of PLGA can be obtained by various methods: by mixing aqueous and organic solvents containing polymer and drug substance and then removing first the organic and then the aqueous phase [18, 19, 56–64]. The methods for obtaining nanoparticles are based on the ability to form films at the water/solvent interface. Thus, with intensive mixing of the polymer solution in chloroform or methylene chloride with a small amount of water, particles with a polymer shell containing water or a solution of the drug substance are formed. When the water: solvent ratio is reversed, it is possible to obtain nanoparticles with a solvent incorporated therein.

Most of the methods used to incorporate active substances into the polymer matrix are based on the use of emulsions. The method of obtaining nanoparticles using emulsions consists in dispersing and stabilizing one liquid by another, in which it is insoluble. The key criterion for creating an emulsion is the insolubility (or weak solubility) of the dispersed phase in a homogeneous dispersion medium. Further, the resulting emulsion is mixed with a surfactant solution and the solvent and water are removed.

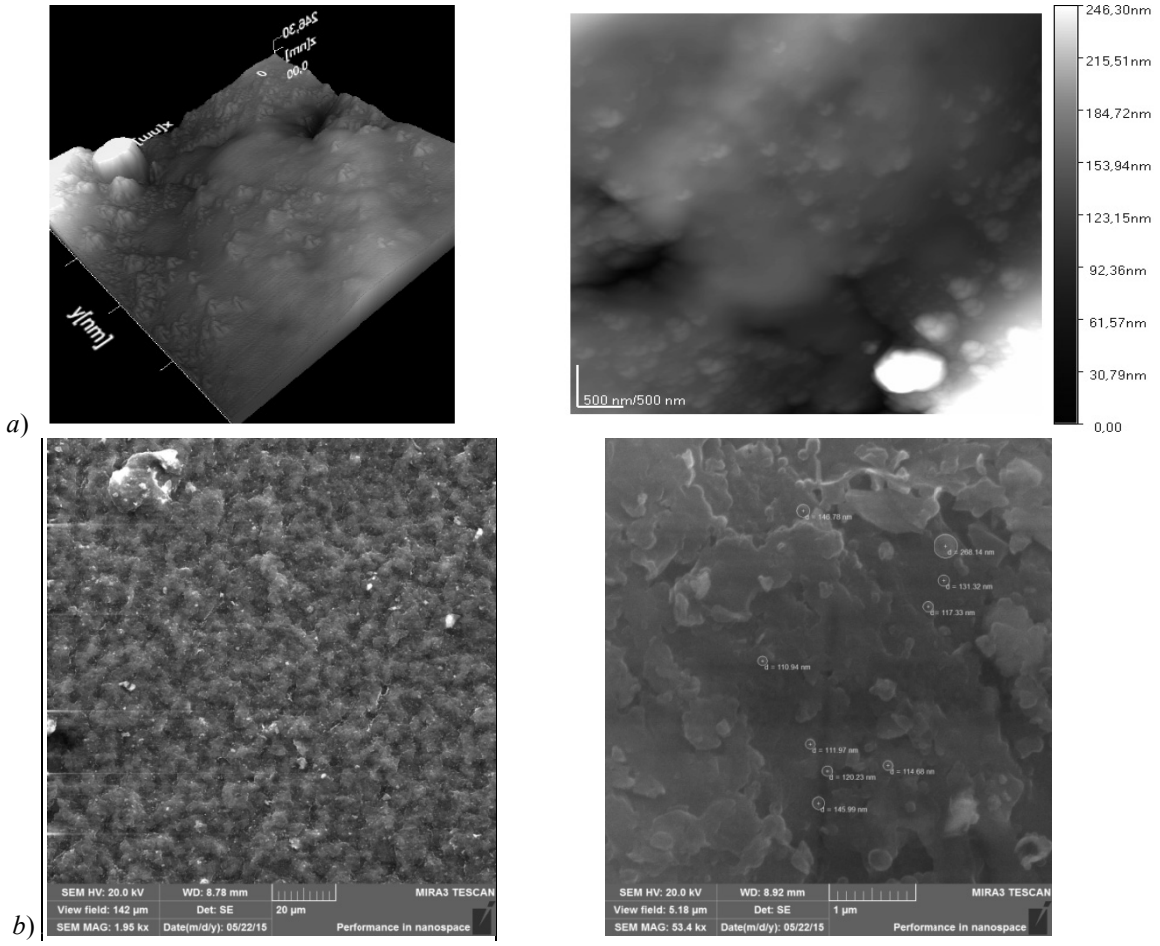

Figure. SEM (*a*) and REM (*b*) images of PLA nanoparticles loaded with silymarin

In this regard the attempts to immobilize the antituberculosis drug p-aminosalicylic acid into the polymer matrix of PLGA using the emulsion method were made by our research group. The ratio of 1:8 of the drug to the polymer and the concentration of surfactant 5 % (polyvinyl alcohol) were found to be optimal for synthesizing nanoparticles with satisfactory characteristics and with high meaning of binding degree (78 %).

Conclusions

Advances of nanotechnology in medicine, especially in the field of applying nanoparticulate systems for the controlled drug delivery are obvious. Nowadays there are the systems which have already passed preclinical and clinical trials and are allowed to be used in therapy of different tumors and tuberculosis diseases.

The review on the use of PLA and PLGA as drug carriers for the last two decades shows the increase of the number of publications in this area; hence the works on synthesizing nanoparticles and nanocapsules on the basis of these polymers for the drug delivery purposes are gaining much interest. The results of the studies points on the importance and potential of application of such systems on the basis of PLA and its copolymer with glycolic acid in the treatment of long-termed diseases such as tumors and tuberculosis.

The review given in this article is far from being comprehensive, however the authors tried to cover all aspects of synthesizing and characterization of nanoparticulate systems on the basis of such polymers as PLA and PLGA loaded with drugs.

References

1 Okada, M. (2002). Chemical synthesis of biodegradable polymers. *Prog. Polym. Sci., 27,* 87–133.

2 Qiu, L.Y, & Bae, Y.H. (2006). Polymer architecture and drug delivery. *Pharm. Res., 23*(1), 1–30.

3 Drumright, R.E., Gruber, P.R., & Henton, D.E. (2000). Polylactic acid technology. *Advanced Materials, 12*(23), 1841–1846.

4 Dechy-Cabaret, O., Martin-Vaca, B., & Bourissou, D. (2004). Controlled ring-opening polymerization of lactide and glycolide. *Chemical Reviews., 104*(12), 6147–6176.

5 Kricheldorf, H.R., & Kreiser-Saunders, I. (1996). Polylactides — synthesis, characterization and medical application. *Macromolecular Symposia, 103,* 85–102.

6 Vert, M. (2000). Lactide polymerization faced with therapeutic application requirements. *Macromolecular Symposia, 153,* 333–342.

7 Slomkovski, S. (2006). Biodegradable nano- and microparticles as carriers of bioactive compounds. *Acta Pol. Pharm., 63*(5), 351–358.

8 Nair, L.S., & Laurencin, C.T. (2007). Biodegradable polymers as biomaterials. *Prog. Polym. Sci., 32,* 762–789.

9 Mehta, R., Kumar, V., Bhunia, H., & Upadhyay, S.N. (2005). Synthesis of poly(lactic acid): a review. J. *Macromol. Sci. Polym. Rev., 45,* 325–49.

10 Dorgan, J.R., Lehermeier, H., & Mang, M. (2000). Thermal and rheological properties of commercial-grade poly(lactic acids)s. *J. Polym. Environ., 8,* 1–9.

11 Derakhshandeh, K., Erfan, M., & Dadashzadeh, S. (2007). Encapsulation of 9-nitrocamptothecin, a novel anticancer drug, in biodegradable nanoparticles: factorial design, characterization and release kinetics. *Eur. J. Pharm. Biopharm., 66*(1), 34–41.

12 Fonseca, C., Simoes, S., & Gaspar, R. (2002). Paclitaxel-loaded PLGA nanoparticles: preparation, physicochemical characterization and in vitro anti-tumoral activity. *J. Control. Rel., 83*(2), 273–286.

13 Avgoustakis, K., Beletsi, A., & Panagi, Z., et al. (2002). PLGA–mPEG nanoparticles of cisplatin: in vitro nanoparticle degradation, in vitro drug release and in vivo drug residence in blood properties. J. *Control. Rel., 79*(1–3), 123–35.

14 Gao, H., Wang, Y.N., & Fan, Y.G., et al. (2005). Synthesis of a biodegradable tadpole-shaped polymer via the coupling reaction of polylactide onto mono(6-(2-aminoethyl)amino-6-deoxy)-beta-cyclodextrin and its properties as the new carrier of protein delivery system. *J. Control. Rel., 107*(1), 158–73.

15 Avgoustakis, K. (2004). Pegylated poly(lactide) and poly(lactide-coglycolide) nanoparticles: preparation, properties and possible applications in drug delivery. *Curr. Drug Deliv., 1*(4), 321–333.

16 Panyam, J., & Labhasetwar, V. (2003). Biodegradable nanoparticles for drug and gene delivery to cells and tissue. *Adv. Drug Del. Reviews, 55,* 329–47.

17 Charles, E.L., & Buffalo, N.Y. (1954). *United States patent No. US 3297033*. Preparation Method of Poly-(D,L-lactide-co-glycolide) Nanoparticles with drugs.

18 Prasad Rao J., & Geckeler Kurt E. (2011). Polymer Nanoparticles: Preparation techniques and size control parameters. *Progr. Polymer Sci., 36,* 887–913.

19 Fessi, H., Puisieux, F., & Devissaguet, J.P., et al. (1989). Nanocapsule formation by interfacial polymer deposition following solvent displacement. *Int. J. Pharm., 55,* 1–4.

20 Seyler, I., Appel, M., & Devissaguet, J.P., et al. (1999). Macrophage activation by a lipophilic derivative of muramyldipeptide within nanocapsules: investigation of the mechanism of drug delivery. *J. Nanopart. Res., 1,* 91–97.

21 Legrand, P., Lesieur, S., & Bochot, A., et al. (2007). Influence of polymer behaviour in organic solution on the production of polylactide nanoparticles by nanoprecipitation. *Int. J. Pharm., 344,* 33–43.

22 Chang, J., Jallouli, Y., & Kroubi, M., et al. (2009). Characterization of endocytosis of transferrin-coated PLGA nanoparticles by the blood–brain barrier. *Int. J. Pharm., 379,* 285–292.

23 Nehilla, B.J., Bergkvist, M., & Popat, K.C., et al. (2008). Purified and surfactant-free coenzyme Q10-loaded biodegradable nanoparticles. *Int. J. Pharm., 348,* 107–114.

24 Yallapu, M.M., Gupta, B.K., & Jaggi, M., et al. (2010). Fabrication of curcumin encapsulated PLGA nanoparticles for improved therapeutic effects in metastatic cancer cells. *J. Colloid. Interface Sci., 351,* 19–29.

25 Li, H., Tran, W., & Hu, Y., et al. (2006). A PEDF N-terminal peptide protects the retina from ischemic injury when delivered in PLGA nanospheres. *Exp. Eye Res., 83*(4), 824–833.

26 Helle, A., Hirsjarvi, S., & Peltonen, L., et al. (2008). Quantitative determination of drug encapsulation in poly(lactic acid) nanoparticles by capillary electrophoresis. *J. Chromatography. A., 1178,* 248–55.

27 Moghimi, S.M., Hunter, A.C., & Murray, J.C. (2005). Nanomedicine: current status and future prospects. *FASEB J., 19,* 311–322.

28 Fenske, D.B., Chonn, A., & Cullis, P.R. (2008). Liposomal nanomedicines: an emerging field. *Toxicol. Pathol., 36*(1), 21–29.

29 Shaitan, K., Tourleigh, Y., & Golik, D., et al. (2006). Computer-aided molecular design of nanocontainers for inclusion and targeted delivery of bioactive compounds. *J. Drug Del. Sci. Tech., 16,* 253–258.

30 Nicoli, S. (2001). Design of triptorelin loaded nanospheres for transdermal iontophoretic administration. *Int. J. Pharm., 214* (1–2), 31–35.

31 Pinto, M.M., & Sousa, E.P. (2003). Natural and synthetic xanthonolignoids: chemistry and biological activities. *Curr. Med. Chem., 10*(1), 1–12.

32 Nah, J.-W., Young, J.J., & Koh, J.-J. (2000). Drug release from nanoparticles of poly-D,L-lactide-co-glycolide. *Korean J. Chem. Eng.*, *17*(2), 230–236.

33 Jalil, R., & Nixon, J.R. (1990). Microencapsulation using poly-D, L-lactic acid III: Effect of polymer molecular weight on the release kinetics. *J. Microencapsulation, 7*(3), 357–374.

34 Jalil, R., & Nixon, J.R. (1990). Microencapsulation using poly-D,L-lactic acid IV: Effect of storage on the microcapsules' characteristics. *J. Microencapsulation, 7*(3), 375–383.

35 Dutt, M., & Khuller, G.K. (2001). Chemotherapy of Mycobacterium tuberculosis infections in mice with a combination of isoniazid and rifampicin entrapped in poly(D,L-lactide-co-glycolide) microparticles. *Journal of Antimicrobial Chemotherapy, 47,* 829–835.

36 Prabhu, R.H., Patravale, V.B., & Joshi, M.D. (2015). Polymeric nanoparticles for targeted treatment in oncology: Current Insights. *International Journal of Nanomedicine, 10*, 1001–1018.

37 Danhier, F., Lecouturier, N., & Vroman, B., et al. (2009). Paclitaxel-loaded PEGylated PLGA-based nanoparticles: in vitro and in vivo evaluation. *J. Control. Rel.*, *133*(1), 11–17.

38 Moreno, D., de Hardaya, C.T., & Bandries, E., et al. (2008). Characterization of cysplastin toxicity delivered from PLGA-systems. *Eur. J. Pharm. Biopharm., 68*(3), 503–512.

39 Moreno, D., Zalba, S., & Navarro, I., et al. (2010). Pharmacodynamics of cysplastin-loaded PLGA nanoparticles adminestered to tumor-bearing mice. *Eur. J. Pharm. Biopharm., 74*(2), 265–274.

40 Nair, K.L., Jagadeeshan, S., Nair, S.A., & Kumar, G.S. (2011). Biological evaluation of 5-fluororacil nanoparticles for cancer therapy and its dependence on the carrier, PLGA. *Int. J. Nanomed., 6,* 1685–1697.

41 Betancourt, T., Brown, B., & Brannon-Peppas, L. (2007). Doxorubicin-loaded PLGA nanoparticles by nanoprecipitation: preparation, characterization and in vitro evaluation. *Nanomed., 2*(2), 219–232.

42 Park, H., Yang, J., & Lee J., et al. (2009). Multifunctional nanoparticles for combined doxorubicin and photothermal treatments. *ACS Nano., 3*(10), 2919–2926.

43 Amjadi, I., Rabiee, M., & Hosseini, M.S., et al. (2012). Synthesis and characterization of doxorubicin-loaded PLGA nanoparticles as a sustained release anticancer drug delivery system. *Appl. Biochem. Biotech., 168*(6), 1434–1447.

44 Chittasupho, C., Xie, S.X., & Baoum, A., et al. (2009). ICAM-1 targeting of doxorubicin-loaded PLGA nanoparticles to lung epithelial cells. *Eur. J. Pharm., 37*(2), 141–150.

45 Aggarwal, S., Yadav, S., & Gupta S. EGFR targeted PLGA nanoparticles using gemcitabine for treatment of pancreatic cancer. *J. Biomed. Nanotechnol., 7*(1), 137–138.

46 Gryparis, E.S., Hatziapostolou, M., & Paradimitriou E., et al. (2007). Anticancer activity of ciplastin-loaded PLGA-mPEG nanoparticles on LNCaP prostate cancer cells. *Eur.J. Pharm. Biopharm., 67*(1), 1–8.

47 Cheng, J., Teply, B.A., & Sherifi, I., et al. (2007). Formulation of functionalized PLGA-PEG nanoparticles for in vivo targeted drug delivery. *Biomaterials., 28*(5), 869–876.

48 Graf, N., Bielenberg, D.R., & Kolishetti, N., et al. (2012). α(V)β(3) Integrin-targeted PLGA-PEG nanoparticles for enhanced antitumor efficiency of a Pt (IV) prodrug. *ACS Nano., 6(*5), 4530–4539.

49 Cheng, L., Jin, C., & Lu, W., et al. (2011). Developing a highly stable PLGA-mPEG nanoparticle loaded with cisplastin for chemotherapy of ovarian cancer. *PLoS One., 6*(9), 425–433.

50 Yadav, A.K., Agarwal, A., & Rai G., et al. (2010). Development and characterization of hyaluronic acid decorated PLGA nanoparticles for delivery of 5-fluororacil. *Drug. Del., 17*(8), 561–572.

51 Wohlfart, S., Khalansky, A.S., & Gelperina, S., et al. (2011). Efficient chemotherapy of rat glioblastoma using doxorubicin loaded PLGA nanoparticles with different stabilizers. *PLoS One., 6*(5), 119–121.

52 Bui, K.T., & Alyautdin, R.N. (2008). Polylactide nanoparticles with antituberculosis drugs adsorbed on them. *Exp. Clin. Pharmacology, 3,* 7–11.

53 Burkeev, M.Zh., Tazhbayev, Ye.M., Zhaparova, L.Zh., Zhumagalieva, T.S., & Zhappar, N.K. (2016). Synthesis and characterization of poly(DL-lactic acid) nanoparticles loaded with the antituberculosis drug Isoniazid. *Pharm. Chem. J., 50*(9), 608–612.

54 Ma, Y., He, S., & Ma, X., et al. (2016). Silymarin-loaded nanoparticles based on stearic acid-modified Bletilla striata polysaccharide for hepatic targeting. *Biomed. Pharmacotherapy, 81,* 93–103.

55 Kwan, Y. Y., Du, H. H., & Yousaf, A. M., et al. (2013). Silymarin-loaded solid nanoparticles provide excellent hepatic protection: physicochemical characterization and in vivo evaluation. *Int. J. Nanomed., 8,* 3332–3343.

56 Quintanar-Guerrero, D., Allémann, E., Doelker, E., & Fessi, H. (1997). A mechanistic study of the formation of polymer nanoparticles by the emulsification-diffusion technique. *Colloid Polym. Sci., 275,* 640–647.

57 Quintanar-Guerrero, D., Allémann, E., Doelker, E., & Fessi, H. (1996). Influence of stabilizing agents and preparative variables on the formation of poly(lactic acid) nanoparticles by an emulsification-diffusion technique. *Int. J. Pharm., 143,* 133–141.

58 Allémann, E., Gurny, R., & Doelker, E. (1993). Drug loaded nanoparticles. Preparation, methods and drug targeting issues. *Eur. J. Pharm. Biopharm., 39,* 173–191.

59 Gurny, R., Peppas, N.A., Harrington, D.D., & Banker, G.S. (1981). Development of biodegradable and injectable lattices for controlled release potent drugs. *Drug. Dev. Ind. Pharm., 7,* pp. 1–25.

60 Allémann, E., Gurny, R., & Doelker, E. (1992). Preparation of aqueous polymeric nanodispersions by a reversible salting-out process: influence of process parameters on particle size. *Int. J. Pharm., 87*(1–3), 247–253.

61 Dong, W.Y., Körber, M., López Esguerra, V., & Bodmeier, R. (2006). Stability of poly(D,L-lactide-co-glycolide) and leuprolide acetate in in-situ forming drug delivery systems. *J. Control. Release, 115*(2), 158–167.

62 Delie, F., Berton, M., Allémann, E., & Gurny, R. (2001). Comparison of two methods of encapsulation of an oligonucleotide into poly(D,L-Lactic Acid) particles. *Int. J. Pharm., 214,* 25–30.

63 Bilati, U., Allémann, E., & Doelker, E. (2005). Poly(D, L-lactide-coglycolide) protein-loaded nanoparticles prepared by the double emulsion method — processing and formulation issues for enhanced entrapment efficiency. *J. Microencapsul., 22*(2), 205–214.

64 Olivier, J.-Ch. (2005). Drug Transport to Brain with Targeted Nanoparticles. J. Amer. Soc. for Exp. Neurotherapeutics, *2*, 108–119.

Е.М. Тажбаев, М.Ж. Буркеев, Л.Ж. Жапарова,
Т.С. Жұмағалиева, Ж.Т. Арыстанова

Дәрілік заттармен иммобилизацияланған полисүт қышқылы мен полилактидгликолид негізіндегі нанобөлшектер

Мақалада полисүт қышқылы мен оның гликоль қышқылымен сополимерінің негізінде полимерлі нанобөлшектер мен нанокапсулаларды алуға бағытталған зерттеу жұмыстарына қысқаша шолу жасалған. Биоүйлесімді және биоыдырамалы полисүтқышқылы мен полилактидгликолид қышқылы полимерлерінің нанобөлшектері фармацевтика саласында дәрілік заттардың тасымалдаушылары ретінде ғалымдардың назарын ерекше аударып отыр. Авторлар полилактид және полилактидгликолид қышқылдарының наноөлшемді үлгілерін алу әдістерін сипаттаған. Оның ішінде нанотұндыру және эмульсия әдістерінің полисүт қышқылы мен оның гликоль қышқылымен сополимерінің нанобөлшектері мен нанокапсулаларын синтездеуде болашағы зор екендігі көрсетілді. Полилактидгликолидтің наноөлшемді жүйелерін синтездеудің тағы бір әдісі қосарланған эмульсия әдісі болып табылады. Бұл әдіс ықшамды сипаттамаларға ие нанокапсулаларды алуға мүмкіндік береді. Аталған полимерлердің негізінде наносомалы жүйелерді қатерлі ісікке және түберкулезге қарсы дәрілік препараттармен иммобилизациялау мүмкіндігін қарастырды. Қатерлі ісік және туберкулез ауруларын емдеуде дәрілік заттармен иммобилизацияланған полисүт қышқылы мен полилактидгликолидті нанобөлшектері мен нанокапсулаларының медицинада қолданыс тапқан кейбір мысалдары келтірілген.

Кілт сөздер: полисүт қышқылы, полилактидгликолид, нанобөлшектер, қатерлі ісікке қарсы препараттар, туберкулезге қарсы препараттар, дәрілік заттарды жеткізу, полимерлер, нанокапсулалар.

Е.М. Тажбаев, М.Ж. Буркеев, Л.Ж. Жапарова,
Т.С. Жумагалиева, Ж.Т. Арыстанова

Наночастицы на основе полимолочной кислоты и полилактидгликолида, иммобилизованные лекарственными препаратами

В статье приведен краткий обзор исследований, посвященных синтезу и изучению полимерных наночастиц и нанокапсул на основе полимолочной кислоты и ее сополимера с гликолевой кислотой. Наночастицы на основе биосовместимых и биодеградируемых полимеров молочной и гликолевой кислот привлекают внимание ученых при использовании их в качестве носителей лекарственных препаратов. В статье описаны методы синтеза наносомальных форм полилактида и полимолочной и гликолевой кислот. Методы наноосаждения и эмульсии показаны как перспективные способы получения полимерных наночастиц и нанокапсул полимолочной кислоты и ее сополимера с гликолевой кислотой для иммобилизации их лекарственными препаратами. Еще одним методом синтеза наноразмерных систем полилактид-со-гликолида является метод двойной эмульсии, который позволяет получить нанокапсулы с оптимальными характеристиками. Рассмотрены возможности иммобилизации наночастиц и нанокапсул на основе этих полимеров противоопухолевыми и противотуберкулезными препаратами. Показаны некоторые примеры наночастиц и нанокапсул полилактида и полимолочной и гликолевой кислот с лекарственными препаратами, которые уже нашли применение в медицине в лечении раковых заболеваний и туберкулеза.

Ключевые слова: полимолочная кислота, полилактидгликолид, наночастицы, противоопухолевые препараты, противотуберкулезные препараты, доставка лекарств, полимеры, нанокапсулы.

UDC 541.64

Ye.M. Tazhbayev[1], M.Zh. Burkeyev[1], L.Zh. Zhaparova[1],
T.S. Zhumagalieva[1], Zh.T. Arystanova[1], D.A. Mukhanova[2]

[1]*Ye.A. Buketov Karaganda State University, Kazakhstan;*
[2]*LLP Biotron Group, Stepnogorsk, Kazakhstan*
(*E-mail: lyazzh@mail.ru*)

Preparation and characterization of empty nanoparticles of poly-D,L-lactic acid and serum albumin

The methods of preparation of polymeric nanoparticles and nanocapsules on the basis of such polymers as human serum albumin and poly-D,L-lactic acid are shown in this article. Human serum albumin and poly-D,L-lactic acid are well-known polymers used in medicine for different purposes including delivery of some potent drugs in the forms of nanoparticles. Empty nanoparticles of human serum albumin and poly-D,L-lactic acid have been successfully synthesized using desolvation and nanoprecipitation methods correspondingly. Optimal conditions of synthesizing the nanoparticles of human serum albumin and poly-D,L-lactic acid have been worked out. Obtained nanoparticles of the polymers have satisfactory physicochemical characteristics: the particle sizes were in the interval of 100–300 nm with narrow particle size distribution which points on the formation of nanoparticles of similar size. The surface charge of the particles was defined as it is the parameter that determines the stability of the system. The meanings of zetapotential were around –30 mV for both systems which justifies the stability of particles within the time. So the results of this study have shown that synthesized nanoparticles of human serum albumin and poly-D,L-lactic acid have good characteristics and hence they can further be used for loading them with different drugs.

Keywords: polymers, polylactic acid, human serum albumin, nanoparticles, drug delivery, nanocapsules, nanoprecipitation, desolvation.

Introduction

Nanoparticulate systems such as nanoparticles and nanocapsules based on biocompatible polymers are becoming the subject of interest both for scientists and doctors. Such characteristics as small size, large surface area and stability within the time, make these systems unique and promising, especially in the controlled delivery of drugs. Nanocarriers were found to be accumulated in tumor tissues and in the inflamed tissues [1] and the particles of certain size are able to find the infected cells or tissues and act selectively without damaging healthy tissues. Also nano-size of such colloidal particles allows them to penetrate through narrow blood capillaries [2].

Nanosomal forms are constructed on the basis of commonly used biocompatible and biodegradable polymers. Human serum albumin (HSA) and poly-D,L-lactic acid (PLA) (Fig. 1) are well-known polymers which have found wide application in medicine as an auxiliary materials as well as polymeric carriers for different drug preparations. In this regard, the aim of this study was to synthesize empty polymeric nanoparticles of HSA and PLA with satisfactory physicochemical characteristics for loading them with drugs.

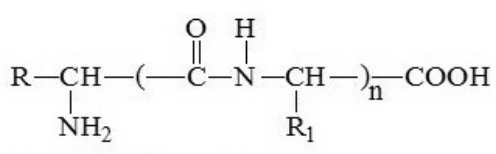

(1)

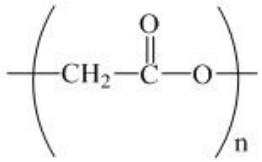

(2)

Figure 1. Structural formula of human serum albumin (*1*) and poly-D,L-lactic acid (*2*)

Method

Preparation of empty nanoparticles of poly(D,L-lactic acid)

Nanoparticles of PLA were obtained using the method of nanoprecipitation. Briefly, 0.2 ml of water was added to 0.5 ml of acetone. Then PLA was dissolved in 1 ml of acetone and mixed with the solution prepared before. The polymer solution was added with a syringe to 5 ml of the external phase (water) with

slight stirring. The residual organic solvent was evaporated for 40 minutes under reduced pressure on a vacuum rotary evaporator «Vacuum controller V-855» (Buchi, Switzerland) and the dispersion of the nanoparticles was diluted with water to 20 ml and filtered (paper filter) to remove any large formations.

Preparation of empty HSA nanoparticles

Empty HSA nanoparticles were prepared using a desolvation method [3]. The pH of HSA solution of albumin (2 %) was adjusted to 8.3 with buffer solution. Then under constant stirring (600 rpm) at room temperature 8 ml of ethanol (96 %) was added to the mixture (1 ml/min) using a tubing pump. After the desolvation process the particles were stabilized by the addition of an aqueous 8 % glutaraldehyde solution (1.175 μl per ml HSA). After that the suspension was stirred for 24 h. The nanoparticles were separated from low molecular components by repeated centrifugation with the Centrifuge MiniSpin Plus 14500 (Eppendorf, Hamburg, Germany) at 14500 rpm and washing them with water.

Measurement of particle size, zeta potential (ζ) and particle size distribution

Average particle diameter and the particle size distribution of PLA and HSA nanoparticles were determined at 25 ºC by dynamic light scattering (DLS) on a Malvern Zetasizer Nano ZS instrument at a scattering angle of 173º. The zeta potential was also measured on this device. Nanoparticles were previously diluted with a phosphate-buffer (pH 7.4) and the zeta potential was determined by Laser Doppler micro electrophoresis.

Results and Discussion

There are a number of methods for synthesizing nanoparticles: emulsion polymerization, emulsification-diffusion, interfacial deposition, desolvation, nanoprecipitation, solvent evaporation/extraction and solvent displacement methods there [1, 2, 4–7]. The method of preparation of polymeric nanoparticles and nanocapsules can be chosen depending on the goals, technological advantages, the properties of the substances entrapped and the polymeric materials to be used [1, 2, 4–7].

Nanoparticles of HSA can be synthesized by protein denaturation in an water-in-oil emulsion and applying desolvation (coacervation) methods as shown in [1, 3]. When obtaining albumin nanoparticles by desolvation, HSA is dissolved in water and then desolvated with ethanol and stabilized by addition of a cross-linker which is glutaraldehyde. Particle size of the synthesized nanoparticles usually varies between 80–300 nm. Therefore empty HSA nanoparticles have been obtained using desolvation method at a pH meaning of 8.3. In this case the particles of optimal size and relatively big surface area are formed. It allows high degree of adsorption of the drug on the surface of particles. In this method the addition of amphiphilic solvent, i.e. ethanol drop-wise to the concentrated solution of albumin is relevant, as the volume of ethanol is 4–5 fold higher than water and addition of the whole amount of ethanol may lead to the formation of insoluble aggregates of albumin or albumin nanoparticles of non-spherical structure. Slow addition of ethanol is also necessary to stabilize the system and homogeneous formation of albumin nanoparticles, hence colloidal particles of spherical shape with monomodal distribution can be obtained. Afterwards the HSA nanoparticles are crosslinked with the help of small amount of glutaraldehyde. Hardened nanoparticles of albumin do not change their shape and physical state even after multifold centrifugation and dissolving.

Physicochemical characteristics of synthesized empty HSA nanoparticles were determined using photon correlation spectroscopy, of which the results are given in Figure 2.

From Figure 2 it is seen that obtained nanoparticles have very good characteristics: optimal size (d = 151.2 nm) and narrow particle size distribution (PDI = 0.094). The portion of particles of nanometer size is 100 %, which meets the requirements of polymeric carriers.

Another interesting polymer from the point of view of carriers for different active agents is poly-D,L-lacitc acid. Polymeric nanoparticles based on PLA are gaining interest among the scientists as this polymer possesses such properties as biocompatibility and biodegradability.

One of the methods of synthesizing nanoparticles of PLA is nanoprecipitation. A number of experiments on the selection of optimal conditions of synthesizing PLA nanoparticles have been carried using THF, acetone and the mixture of acetone with ethanol as solvents. The choice of these solvents is due to the solubility of PLA in these solvents and by their ability to mix with water. The study on selection of optimal solvent has shown that acetone was the best one for the formation of nanoparticles. In this case the nanoparticles with satisfactory characteristics were obtained (Fig. 3).

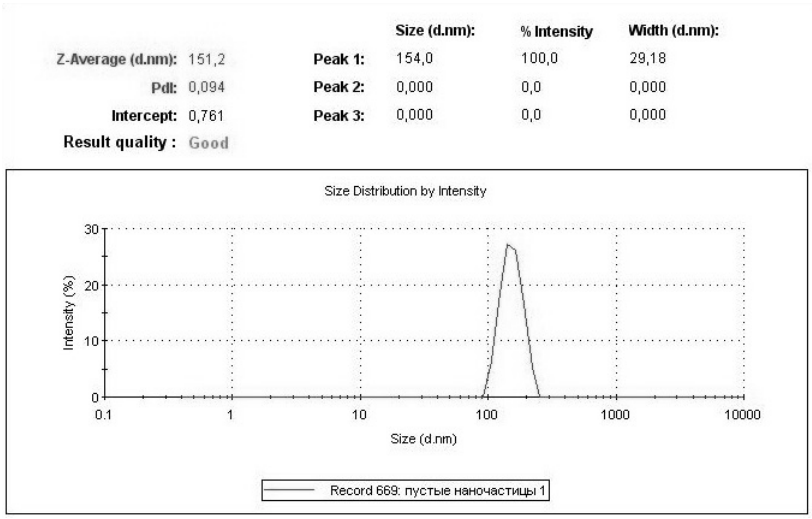

Figure 2. Particle size distribution of empty HSA nanoparticles

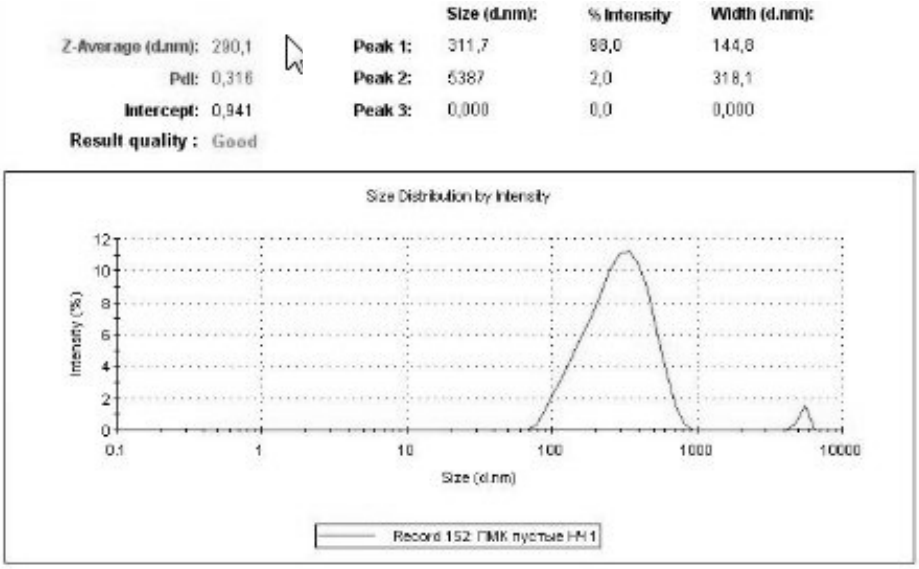

Figure 3. Particle size distribution of empty PLA nanoparticles

It is clear from Figure 3, that the system mainly consists of the particles with nanometer size and only 2 % of the system is microparticles.

Physicochemical characteristics of empty PLA and HSA nanoparticles are summarized in Table.

T a b l e

Physicochemical characteristics of empty PLA and HSA nanoparticles

Parameter	Empty PLA nanoparticles	Empty HSA nanoparticles
Average particle size, *d*, nm	290.1	151.2
PDI	0.316	0.094
Zetapotential, mV	–35.0	–31.0
Molecular mass	1520.0	–
Yield of nanoparticles, %	76.6	98.2

Together with particle size and size distribution such parameter as the surface charge of the particles needs to be evaluated. In addition, better targeting can be accomplished by obtaining monodisperse systems and/or by attaching antibodies or ligands on the surface of nanoparticles [7, 8]. When synthesizing polymeric nanoparticles one of the important parameters is the surface charge as together with the meaning of size and

particle size distribution it defines the biodistribution of nanoparticles after administering them into the body. Surface charge of the particles is characterized by zeta potential which is an indicator of the stability of the colloidal system. In this case the absence of excess counter ions is important because it may lead to aggregation; the latter is not acceptable when using polymeric nanoparticles for the drug delivery purposes. According to the results of measuring zetapotential in both cases the systems are stable (Table) as the meanings of surface charge were not close to 0.

Conclusions

So at this stage of the research empty nanoparticles of PLA and HSA with high yield have been successfully synthesized. Physicochemical characteristics of obtained particles meet the requirements of the polymeric carriers of drug preparations; therefore they are aimed to be used for loading with such antitumor drugs as tamoxifen and cyclophosphamide.

References

1 Kreuter, J. (1994). *Nanoparticles: Colloidal Drug Delivery Systems.* New-York: Marcel Dekker, USA.

2 Kreuter, J. (2007). Nanoparticles — a historical Perspectives. *Int. J. Pharm. 331,* 1–10.

3 Dreis, S., Rothweiler, F., Michaelis, M., Cinatl, Jr., Kreuter, J., & Langer, K. (2007). Preparation, characterization and maintenance of drug efficacy of doxorubicin-loaded human serum albumin nanoparticles. *Int. J. Pharm.*, *341,* 207–214.

4 Prasad, R.J., & Geckeler, K.E. (2011). Polymer Nanoparticles: Preparation techniques and size control parameters. *Progr. Polymer Sci., 36,* 887–913.

5 Fessi, H., Puisieux, F., & Devissaguet, J.P., et al. (1989). Nanocapsule formation by interfacial polymer deposition following solvent displacement. *Int. J. Pharm., 55*, 1–4.

6 Alleman, E., Gurny, R., & Doelker, E. (1993). Drug-loaded nanoparticles — preparation methods and drug targeting issues. Review. *Eur. J. Pharm. Biopharm*. *39*(5), 173–191.

7 Moghimi, S.M., Hunter, A.C., & Murray, J.C. (2005). Nanomedicine: current status and future prospects. *FASEB J.*, *19,* 311–322.

Е.М. Тажбаев, М.Ж. Буркеев, Л.Ж. Жапарова,
Т.С. Жұмағалиева, Ж.Т. Арыстанова, Д.А. Мұханова

Поли-D,L-сүт қышқылы мен сарысу альбуминнің бос нанобөлшектерін синтездеу және сипаттау

Мақалада сарысу альбумин мен поли-D,L-сүт қышқылының полимерлі нанобөлшектері мен нанокапсулаларын алу әдістері көрсетілген. Адамның сарысу альбумині және поли-D,L-сүт қышқылы медицинада әртүрлі мақсатта, соның ішінде кейбір әсері күшті дәрілік заттарды нанобөлшектер түріндегі жеткізуші ретінде қолданылатын белгілі полимерлер болып табылады. Альбумин мен поли-D,L-сүт қышқылының нанобөлшектерін синтездеудің ықшамды жағдайлары табылды. Сарысу альбуминнің және поли-D,L-сүт қышқылының бос нанобөлшектері сәйкесінше десольваттау және нанотұндыру әдістерімен синтезделді. Алынған полимерлі нанобөлшектер қанағаттанарлық физика-химиялық сипаттамаларға ие: бөлшектердің өлшемі 100–300 нм аралығында, ал бөлшектердің өлшем бойынша таралуы тар болды, бұл өлшемі жағынан біртекті бөлшектердің түзілгенін көрсетеді. Бөлшектердің беттік заряды анықталды, себебі бұл өлшем жүйенің тұрақтылығына жауап береді. Дзетапотенциал өлшемдері екі жүйе үшін де шамамен –30мВ-қа тең болды, бұл бөлшектердің уақыт бойынша тұрақтылығын білдіреді. Осылайша, бұл зерттеулердің нәтижесі синтезделген сарысу альбумин және поли-D,L-сүт қышқылының нанобөлшектерінің жақсы сипаттамаларға ие екендігін және оларды әрі қарай әртүрлі дәрілік препараттармен иммобилизациялауға болатындығын көрсетті.

Кілт сөздер: полимерлер, полисүт қышқылы, адамның сарысу альбумині, нанобөлшектер, дәрілік заттарды тасымалдау, нанотұндыру, десольвация.

Е.М. Тажбаев, М.Ж. Буркеев, Л.Ж. Жапарова,
Т.С. Жумагалиева, Ж.Т. Арыстанова, Д.А. Муханова

Получение и характеристика пустых наночастиц поли-D,L-молочной кислоты и сывороточного альбумина

В статье показаны способы синтеза полимерных наночастиц и нанокапсул на основе сывороточного альбумина человека и поли-D,L-молочной кислоты. Сывороточный альбумин человека и поли-D,L-молочная кислота являются хорошо известными полимерами, используемыми в медицине для различных целей, в том числе для доставки некоторых сильнодействующих лекарств в форме наночастиц. Найдены оптимальные условия синтеза полимерных наночастиц сывороточного альбумина и поли-D,L-молочной кислоты. Пустые наночастицы человеческого сывороточного альбумина и поли-D,L-молочной кислоты синтезированы методами десольвации и наноосаждения соответственно. Полученные полимерные наночастицы имели удовлетворительные физико-химические характеристики: размеры частиц варьировали в интервале 100–300 нм с узким распределением частиц по размерам, что указывает на образование частиц одного размера. Определен поверхностный заряд частиц, так как эта величина отвечает за стабильность системы. Значения дзетапотенциалов равнялись около –30 мВ для обеих систем, что свидетельствует о стабильности частиц во времени. Таким образом, результаты данного исследования показали, что синтезированные наночастицы сывороточного альбумина человека и поли-D,L-молочной кислоты имеют хорошие характеристики и, следовательно, могут быть в дальнейшем использованы для иммобилизации их различными лекарственными препаратами.

Ключевые слова: полимеры, полимолочная кислота, сывороточный альбумин человека, наночастицы, доставка лекарств, нанокапсулы, наноосаждение, десольвация.

UDC 582: 542.61: 543.544.5

B.S. Temirgaziev[1,2], U.B. Tuleuov[2], E.A. Baizhigit[1], Ye.V. Minayeva[2],
L.K. Salkeyeva[2], B.I. Tuleuov[1], S.M. Adekenov[1]

[1]*JSC «International Research and Production Holding «Phytochemistry», Karaganda, Kazakhstan;*
[2]*Ye.A. Buketov Karaganda State University, Kazakhstan*
(E-mail: yelenaminayeva@mail.ru)

Optimization of the technology for obtaining ecdysterone from *Serratula coronata* L. by varying the extraction methods and growth phases

A complex study of the aerial part of *Serratula coronata* L. cultivated in the collection area of medicinal plants of the IRPH «Phytochemistry» (Karaganda) in different phases of growth and using the most optimal extraction methods has been carried out. The content of the main active component of ecdysterone (20E)has been studied. Investigation of the seasonal dynamics of ecdysterone distribution under conditions of varying extraction methods shows that its maximum accumulation is observed during the vegetative phase, and the optimal method in this phase is extraction with isobutyl alcohol, the extract of which contains 13.86 % of ecdysterone and the maceration method with 96.2 % ethyl alcohol with a 20E content of 12.03 %, respectively. It is shown that the maceration with 96.2 % ethyl alcohol is technologically optimal, which fully complies with the international standards of good manufacturing practice (GMP) under pharmaceutical production conditions and excludes the use of toxic and expensive isobutyl alcohol solvent. It has been found that the content of ecdysterone from the beginning of vegetation to the final phase goes down, which is confirmed by the data of high-performance liquid chromatography (HPLC). It is assumed that there is an outflow of ecdysterone to the root system, and then its redistribution occurs as the plant develops further with a partial discharge into the soil. Based on the data on the quantitative content of the target component by the HPLC method, it is recommended that for the preparation of the ecdysterone substance of many actoprotective phytopreparations and valuable WS, the preparation of the above-ground biomass of *Serratula coronata* L. should be carried out during the vegetation phase of this taxon.

Keywords: Serratula coronata L., aerial part, 20-hydroxyecdysone, high-performance liquid chromatography, extraction, ethyl alcohol, growth phase, vegetation.

Introduction

Serratula coronata L. of Asteraceae Dumort family is known in folk medicine as a remedy for treatment of inflammatory and infectious diseases (dyspepsia, pharyngitis, tonsillitis and others), as well as neuroses and mental illnesses [1, 2]. This plant attracted the attention of scientific medicine due the presence of phytoecdysteroids that are vegetable hormones [3].

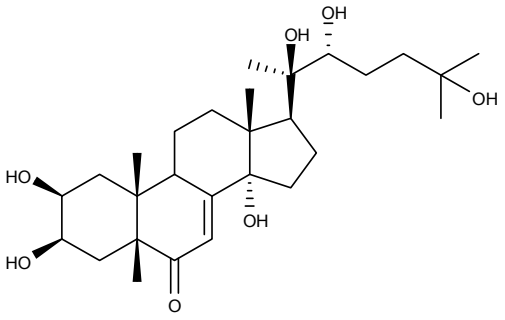

Figure 1. Structural formula of 20-hydroxyecdysone

The extensive chemical screening showed that *Serratula coronata* L. is worthy of special attention as a pharmacologically promising and industrially significant plant raw material for the isolation of adaptogens from the class of phytoecdysteroids. It was found that content of phytoecdysteroids, in particular, ecdysterone-2β, 3β, 14α, 20R, 22R, 25-hexahydroxy-5β (H) -cholest-7-en-6-one (20-hydroxyecdysone or 20E, Fig. 1) in the terrestrial organs of *Serratula coronata* L. is an order of magnitude higher than in the known medicinal plant *Rhaponticum carthamoides* (Willd) Iljin of Asteraceae Dumort family [4]. Leuzea (or maral root) is traditionally considered to be one of the strongest natural adaptogens. A substance containing

20E was isolated from the underground organs of the Leuzea at the end of the last century at the Institute of Plant Compounds Chemistry of the Academy of Sciences of the Uzbek SSR, on the basis of which the preparation «Ekdisten» was developed, which possesses specific adaptogenic properties. This drug was registered as a medicinal tonic [5].

At the present time, the composition of ecdysteroids of *Serratula coronata* L. is most thoroughly studied, which is used as the main pharmacological raw material for obtaining new adaptogenic, anabolic, and tonic agents [6]. So, on the basis of the above taxon, the preparation «Ecdyphyt» was developed in JSC «International Research and Production Holding» Phytochemistry» (IRPH «Phytochemistry»), which is the sum of extractives with the main active component 20E and the sum of ecdysteroids and flavonoids [7, 8].

«Serpisten» created by Volodin et al. [9,10] at the Institute of Biology of the Komiin the Science Center of the Ural Branch of the Russian Academy of Sciences is a mixture of ecdysteroids such as 20-E (80 %), 25S-inocosterone (11 %), α-ecdysone (5 %), and some other minor components isolated from the aerial part of *Serratula coronata* L. Biologically active compound «Serpisten» shows a high ergotropic, CNS-tonic, stress-protective, hematoprotective action as well as the action on the background of a slight anabolic effect.

It is known that the complex processing of wild and cultivated medicinal plant material as a renewable material is one of the priority approaches in the chemical study of plants in terms of obtaining practically valuable substances and new working standards (WS) for the fast-growing pharmaceutical industry in the Republic of Kazakhstan. In the IRPH «Phytochemistry», there was recently carried out study of the ecdysteroid and flavonoid composition of the extract of the aboveground part of the freshly harvested plants of the plant *Serratula coronata* L. growing on the site of medicinal plants of IRPH «Phytochemistry» in order to develop an effective method for the separation of ecdysterone, the main component of the composition of ecdysteroids, and WS, as well as other minor phytoecdysteroids and flavonoids for their use as a new WS [11]. Plants grown in culture surpass natural specimens on the accumulation of biomass [7].

In this regard, the purpose of this work was to determine the most productive phase of growth, and the optimal method for extracting the aerial part of the *Serratula coronata* L., data that can be used in the future to produce the above preparations with a high content of the active main component of ecdysterone.

Experimental

Plant raw material (the aerial part of the *Serratula coronata* L.) was harvested from the middle of May to the end of September 2017 in the collection plot of medicinal plants of the IRPH «Phytochemistry» (Karaganda) during the vegetation-withering phases.

The plant was dried to an air-dry state in a dry, cool place. The average sample of the raw material was ground to a particle size of 2–3 mm for the chemical screening of the plant. Each sample for extraction was 5 g. Various methods were used to extract 20-hydroxyecdysone, such as extraction with a water bath, maceration method, extraction using a Soxhlet apparatus using ethyl alcohol and its 70 % aqueous solution, isobutyl alcohol. These methods were applied in accordance with the earlier used ones. Each extraction method was carried out three times. The extracts were evaporated using a «BuchiRotavaporR-3» rotary evaporator. The resulting thickened samples weighing an average of 0.2 g were placed in a glass container and investigated using the HPLC method.

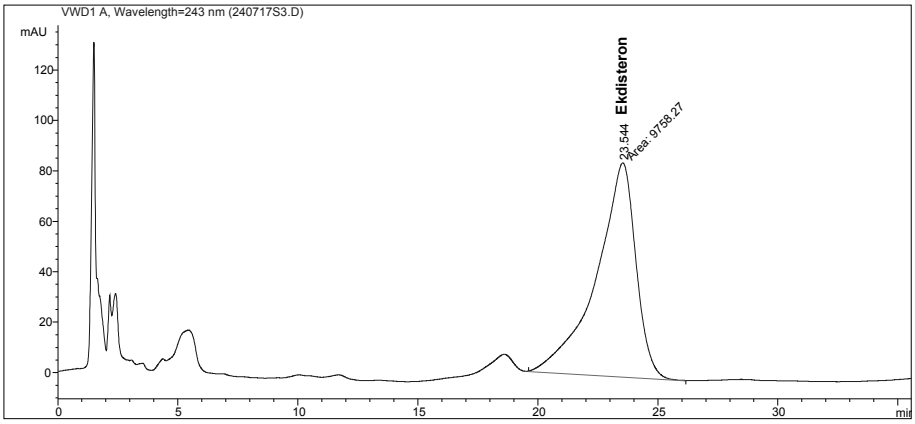

Isobutyl alcohol, yield of 20E is 13.86 %

Figure 2. Chromatogram of the extract of *Serratula coronata* L.

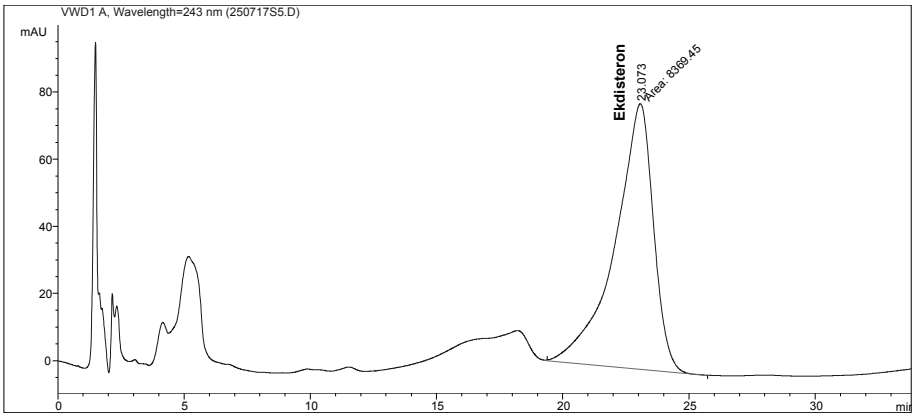

Maceration method, 96.2 % ethyl alcohol, yield of 20E is 12.03 %

Figure 3. Chromatogram of the extract of *Serratula coronata* L.

The extracts were analyzed by reversed-phase HPLC (HPLC, HEWLETT PACKARD Agilent 1100 Series, analytical column 4.6×150 mm, Zorbax SB-C18, mobile phase (MP): 10 % isopropyl alcohol, UV detection at wavelength 254 nm, column temperature 20 ºC, flow rate of the eluent 0.75 ml/min, sample volume 20 μl). The content of 20E was studied (Figs. 2, 3).

Results and discussion

It is known that the content of ecdysterone in a number of species of the genus *Serratula* L. strongly varies depending on the phenophase and their age status [7]. In this connection, a study was carried out to determine the distribution of ecdysterone in the cultivated plant of *Serratula coronata* L. at various stages of development such as vegetation, start of budding, budding, start of flowering, flowering, start of fruiting, fruiting, start of withering away and dying out.

The results of a quantitative analysis of the ecdysterone content depending on the extraction methods and on the species and concentration of the extractant in the studied taxon are presented in the Table below.

T a b l e

The content of ecdysterone in the aerial part of *Serratula coronata* L. depending on the method of extraction and the phase of plant development (in % of the weight of absolutely dry raw material) according to HPLC

Methods for extraction of 20E and the phase of development of the *Serratula coronata* L. plant	The quantitative content (20E) in %
1	2
Vegetation phase	
Extraction with 96.2 % ethyl alcohol	8.88
Extraction with 70 % ethyl alcohol	4.51
Extraction with isobutyl alcohol	13.86
Extraction with 96.2 % ethanol on a Soxhlet apparatus	11.03
Maceration with 96.2 % ethyl alcohol	12.03
Maceration with 70 % ethyl alcohol	5.94
Start of buddingphase	
Extraction with 96.2 % ethyl alcohol	5.51
Extraction with 70 % ethyl alcohol	3.51
Extraction with 96.2 % ethanol on a Soxhlet apparatus	4.11
Extraction with isobutyl alcohol	4.99
Maceration with 96.2 % ethyl alcohol	4.56
Maceration with 70 % ethyl alcohol	2.83
Budding phase	
Extraction with 96.2 % ethyl alcohol	2.56
Extraction with 70 % ethyl alcohol	1.89
Extraction with isobutyl alcohol	5.04
Extraction with 96.2 % ethanol on a Soxhlet apparatus	2.38
Maceration with 96.2 % ethyl alcohol	3.27

Continuation of Table

1	2
Maceration with 70 % ethyl alcohol	2.08
Start of flowering phase	
Extraction with 96.2 % ethyl alcohol	3.19
Extraction with 70 % ethyl alcohol	1.19
Extraction with isobutyl alcohol	1.83
Extraction with 96.2 % ethanol on a Soxhlet apparatus	2.81
Maceration with 96.2 % ethyl alcohol	2.52
Maceration with 70 % ethyl alcohol	1.89
Flowering phase	
Extraction with 96.2 % ethyl alcohol	2.35
Extraction with 70 % ethyl alcohol	1.91
Extraction with isobutyl alcohol	3.25
Extraction with 96.2 % ethanol on a Soxhlet apparatus	2.17
Maceration with 96.2 % ethyl alcohol	2.77
Maceration with 70 % ethyl alcohol	2.50
Start of fruiting phase	
Extraction with 96.2 % ethyl alcohol	2.83
Extraction with 70 % ethyl alcohol	2.87
Extraction with isobutyl alcohol	4.00
Extraction with 96.2 % ethanol on a Soxhlet apparatus	2.44
Maceration with 96.2 % ethyl alcohol	2.80
Maceration with 70 % ethyl alcohol	3.01
Fruitingphase	
Extraction with 96.2 % ethyl alcohol	1.77
Extraction with 70 % ethyl alcohol	2.01
Extraction with isobutyl alcohol	2.44
Extraction with 96.2 % ethanol on a Soxhlet apparatus	2.64
Maceration with 96.2 % ethyl alcohol	2.91
Maceration with 70 % ethyl alcohol	2.45
Start of withering away phase	
Extraction with 96.2 % ethyl alcohol	2.48
Extraction with 70 % ethyl alcohol	2.79
Extraction with isobutyl alcohol	1.35
Extraction with 96.2 % ethanol on a Soxhlet apparatus	3.85
Maceration with 96.2 % ethyl alcohol	1.84
Maceration with 70 % ethyl alcohol	2.08
Dying out phase	
Extraction with 96.2 % ethyl alcohol	2.09
Extraction with 70 % ethyl alcohol	1.12
Extraction with isobutyl alcohol	2.35
Extraction with 96.2 % ethanol on a Soxhlet apparatus	3.17
Maceration with 96.2 % ethyl alcohol	1.03
Maceration with 70 % ethyl alcohol	1.37

As can be seen from the table above, almost all 6 extracts of the vegetative phase found a high content of ecdysterone, which proves the high efficiency of using *Serratula coronata* L. as the main industrially significant source of the above-mentioned substance.

Thus, the study of seasonal dynamics of ecdysterone distribution under conditions of varying extraction methods has showed that its maximum accumulation is observed during the vegetative phase, and the optimal method in this phase is extraction with isobutyl alcohol, the extract of which contains 13.86 % of ecdysterone and maceration method with 96.2 % ethyl alcohol with a content of 20E 12.03 %, respectively. But, in our view, the maceration with 96.2 % ethanol is optimal, which fully complies with the international standards of good manufacturing practice (GMP) under pharmaceutical production conditions and excludes the use of toxic and expensive isobutyl alcohol solvent.

The relatively low yield of ecdysterone at other stages of development of the taxon under investigation suggests that there is an outflow of ecdysterone to the root system, and then its redistribution occurs as the plant develops further with a partial discharge into the soil.

Thus, we recommend the preparation of the aboveground biomass of *Serratula coronata* L. at the collection site of medicinal plants of the «IRPH «Phytochemistry» for obtaining the ecdysterone substance of many actoprotective phytopreparations and valuable WS based on the data provided by HPLC analysis. In general, a study of *Serratula coronata* L. in the conditions of culture, biological, phytochemical and technological features of plant material with the aim of creating an industrial base of the valuable taxon seems promising.

References

1 Крылов Г.В. Растения здоровья / Г.В. Крылов, Н.Ф. Казаков, А.А. Лагерь. — Новосибирск: Новосиб. кн. изд-во, 1989. — 303 с.

2 Завражнов В.И. Лекарственные растения: лечебное и профилактическое использование / В.И. Завражнов, Р.И. Китаева, К.Ф. Хмелев. — Воронеж: Изд-во Воронеж. ун-та, 1993. — 479 с.

3 Абубакиров Н.К. Экдистероиды цветковых растений (Angiospermae) / Н.К. Абубакиров // Химия природных соединений. — 1981. — № 6. — С. 685–702.

4 Володин В.В. Экдистероиды в интактных растениях и клеточных культурах: автореф. дис. … д-ра. биол. наук: 08.00.12 — «Физиология растений» / В.В. Володин. — М., 1999. — 49 с.

5 А.с. 1312774 СССР. Тонизирующее средство / Н.К. Абубакиров, М.Б. Султанов, В.Н. Сыров, А.Г. Курмуков и др. // Б.И. 1988. — № 17.

6 Зибарева Л.Н. Фитоэкдистероиды: распространение в мировой флоре, биологическая активность / Л.Н. Зибарева // Фармацевтический бюллетень. — 2015. — № 3–4. — С. 40–48.

7 Тулеуов Б.И. Стероидные соединения растений и лекарственные препараты на их основе. Поиск, химическая модификация и практические аспекты применения: монография / Б.И. Тулеуов. — Караганда: Гласир, 2009. — 208 с.

8 Тулеуов Б.И. Технология фитостероидных препаратов: монография / Б.И. Тулеуов. — Караганда: Гласир, 2017. — 112 с.

9 Володин В.В. Фитоэкдистероиды / В.В. Володин. — СПб.: Наука, 2003. — 293 с.

10 Володин В.В. Фитоэкдистероиды и адаптогены. Новая экдистероидсодержащая субстанция Серпистен / В.В. Володин, С.О. Володина // Фармацевтический бюллетень. — 2015. — № 3–4. — С. 69–82.

11 Темиргазиев Б.С. Комплексная переработка лекарственного сырья *Serratula coronata* L. / Б.С. Темиргазиев, О.У. Куатбаев, П.К. Кудабаева, Б.И. Тулеуов, С.М. Адекенов // Фармацевтический бюллетень. — 2015. — № 3–4. — С. 119–124.

Б.С. Темірғазиев, Ұ.Б. Төлеуов, Е.А. Байжігіт, Е.В. Минаева,
Л.К. Сәлкеева, Б.И. Төлеуов, С.М. Әдекенов

Экстракция әдістері мен өсу фазаларын түрлендіру арқылы тәжді түймебас өсімдігінен экдистерон алу технологиясын оңтайландыру

«Фитохимия» ХҒӨХ» (Қарағанды қ.) дәрілік өсімдіктер коллекциялық учаскесінде дақылға енгізілген тәжді түймебас *Serratula coronata* L. өсімдігінің жер үсті бөлігіне, негізгі әсер етуші компонент экдистерон (20Е) мөлшерін әртүрлі өсу фазалары және оңтайлы әдістер арқылы бөліп алып аңықтау үшін кешенді зерттеу жүргізілді. Экдистеронды бөліп алу әдістерін түрлендіру жағдайында таралуының мезгілдік динамикасын зерттеу оның барынша жинақталуы вегетация фазасында байқалатынын, ал осы фазадағы оңтайлы әдісіне экстрактта 13,86 % экдистерон болатын изобутил спиртімен экстракция және 20Е мөлшері 12,03 % болатын 96,2 % этил спиртімен мацерациялау әдісі жататынын көрсетті. Технологиялық оңтайлы әдіс ретінде фармацевтикалық өндіріс жағдайында дұрыс өндірістік тәжірибенің (GMP) халықаралық стандарттарына толық сәйкес келетін және зарарлы әрі қымбат еріткіш изобутил спиртін қолдануды қажет етпейтін тәжді түймебасты 96,2 % этил спиртімен мацерациялау әдісі көрсетілді. Экдистерон мөлшерінің вегетация басынан соңғы фазасына дейін төмендейтіні жоғарыэффектілі сұйықтық хроматография (ЖЭСХ) әдісі арқылы дәлелденді. Экдистеронның тамырлық жүйеге қарай жылжуы, ал оның кейін өсімдіктің одан әрі даму кезеңінде біраз бөлігінің топыраққа өтуі арқылы қайта таралуы болжанды. ЖЭСХ әдісі арқылы мақсатты компоненттің сандық құрамы бойынша мәліметтер негізінде, экдистеронды көптеген актопротекторлы фитопрепараттар субстанциясын және бағалы стандарттық үлгіні алу үшін тәжді түймебастың жер үстілік биомассасын дайындауды осы таксонның вегетация фазасында жүргізілуі ұсынылды.

Кілт сөздер: *Serratula coronata* L., жер үсті бөлігі, 20-гидроксиэкдизон, жоғарытиімді сұйықтық хроматография, экстракция, этил спирті, өсу фазалары, вегетация.

Б.С. Темиргазиев, У.Б. Тулеуов, Е.А. Байжигит, Е.В. Минаева,
Л.К. Салькеева, Б.И. Тулеуов, С.М. Адекенов

Оптимизация технологии получения экдистерона из серпухи венценосной варьированием методов экстракции и фаз произрастания

Проведено комплексное исследование надземной части серпухи венценосной *Serratula coronata* L., культивируемой на коллекционном участке лекарственных растений МНПХ «Фитохимия» (г. Караганда), в различных фазах произрастания и с применением наиболее оптимальных методов извлечения на содержание основного действующего компонента экдистерона (20Е). Изучение сезонной динамики распределения экдистерона в условиях варьирования методов извлечения показало, что максимальное его накопление наблюдается в фазу вегетации, а оптимальным способом в данной фазе являются экстракция изобутиловым спиртом, в экстракте которого содержится 13,86 % экдистерона, и метод мацерации 96,2 % этиловым спиртом с содержанием 20Е 12,03 % соответственно. Показано, что технологически оптимальным является метод мацерации серпухи венценосной 96,2 % этиловым спиртом, который полностью соответствует международным стандартам надлежащей производственной практики (GMP) в условиях фармацевтического производства и исключает использование токсичного и дорогостоящего растворителя — изобутилового спирта. Установлено, что содержание экдистерона от начала вегетации до завершающей фазы идет на спад, что подтверждается данными высокоэффективной жидкостной хроматографии (ВЭЖХ). Предполагается, что имеет место отток экдистерона в корневую систему, а затем происходит его перераспределение по мере дальнейшего развития растения с частичным сбросом в почву. На основе данных по количественному содержанию целевого компонента методом ВЭЖХ рекомендуется для получения экдистерона — субстанции многих актопротекторных фитопрепаратов и ценного РСО заготовку надземной биомассы серпухи венценосной вести в фазе вегетации указанного таксона.

Ключевые слова: Serratula coronata L., надземная часть, 20-гидроксиэкдизон, высокоэффективная жидкостная хроматография, экстракция, этиловый спирт, фазы произрастания, вегетация.

References

1 Krylov, G.V. (1989). *Rasteniia zdorovia [Plants of health]*. Novosibirsk: Novosibirsk book publ. house [in Russian].

2 Zavrazhnov, V.I., Kitaieva, R.I., & Khmelev, K.F. (1993). *Lekarstvennye rasteniia: lechebnoe i profilakticheskoe ispolzovanie [Medicinal plants: therapeutic and preventive use]*. Voronezh: Voronezh University publ. [in Russian].

3 Abubakirov, N.K. (1981). Ekdisteroidy tsvetkovykh rastenii (Angiospermae) [Ecdysteroids of flowering plants (Angiospermae)]. *Khimiia prirodnykh soedinenii — Chemistry of natural compounds*, *6,* 685–702 [in Russian].

4 Volodin, V.V. (1999). Ekdisteroidy v intaktnykh rasteniiakh i kletochnykh strukturakh [Ecdysteroids in intact plants and cell cultures]. *Extended abstract of candidate's thesis.* Moscow [in Russian].

5 Abubakirov, N.K., Sultanov, M.B., Syrov, V.N., & Kurmukov, A.G. et al. (1988). *USSR Patent*. No. 1312774.

6 Zibareva, L.N. (2015). Fitoekdisteroidy: rasprostranenie v mirovoi flore, biolohicheskaia aktivnost [Phytoecdysteroids: distribution in the world flora, biological activity]. *Farmatsevticheskii bulleten — Pharmaceutical Bulletin*, *3–4,* 40–48 [in Russian].

7 Tuleuov, B.I. (2009). *Steroidnye soedineniia rastenii i lekarstvennye preparaty na ikh osnove. Poisk, khimicheskaia modifikatsiia i prakticheskie aspekty primeneniia [Steroid compounds of plants and drugs based on them. Search, chemical modification and practical aspects of the application]*. Karaganda: Hlasir [in Russian].

8 Tuleuov, B.I. (2017). *Tekhnolohiia fitoekdisteroidnykh preparatov [Technology of phytosteroid preparations*]. Karaganda: Hlasir [in Russian].

9 Volodin, V.V. (2003). *Fitoekdisteroidy [Phytoecdysteroids]*. Saint Petersburg: Nauka [in Russian].

10 Volodin, V.V., & Volodina, S.O. (2015). Fitoekdisteroidy i adaptoheny. Novaia ekdisteroidsoderzhashchaia substantsiia «Serpisten» [Phytoecdysteroids and adaptogens. New ecdysteroid-containing substance Serpisten]. *Farmatsevticheskii bulleten — Pharmaceutical Bulletin*, *3–4*, 69–82 [in Russian].

11 Temirgaziev, B.S., Kuatbaev, O.U., Kudabaeva, P.K., Tuleuov, B.I., & Adekenov, S.M. (2015). Kompleksnaia pererabotka lekarstvennoho syria *Serratula coronata* L. [Complex processing of medicinal raw materials Serratulacoronate L.]. *Farmatsevticheskii bulleten — Pharmaceutical Bulleti*n, *3–4*, 119–124.

UDC 539.19+541.27

A.Z. Issagulov, S.Sh. Kazhikenova, G.S. Shaikhova, G.Sh. Makhmetova, L.G. Kasymova

Karaganda State Technical University, Kazakhstan
(E-mail: shaikxova_2011@mail.ru)

Evaluation of pressure and volumetric modules in melted systems

In the article there were estimated the pair potential and pressure of bulk modules in molten systems. There are given appropriate formulas for calculating the compressibility of electron melts. The polytherms of compressibility for selenium, tellurium, germanium and silicon are calculated. For the calculation of bulk modules, melts of metals and semiconductors are considered as a two-component liquid consisting of ions and electrons. According to the virial theorem, a part of the pressure associated with the dynamics and interaction of the ion subsystem is estimated. Since the isothermal bulk modulus is a static exponent, we determined it under conditions where the pressure and volume in the system change slowly, and the temperature of the melt changes very slowly or remains constant. The adiabatic bulk modulus, i.e. dynamic, was determined under conditions of heating of the melt caused by compression. Under adiabatic compression a change in temperature and pressure is allowed. This phenomenon occurs in fast processes, i.e. when there is no heat exchange due to the inertia of the thermal properties of the melts. This behavior of adiabatic compressibility is characteristic of metallic melts. We have found that the instantaneous dynamic modulus calculated in the pair approximation model is identical to the dynamic modulus calculated in the full theory in the second order, and also differs markedly from the statistical module. The explanation of this fact consists in neglecting the members of the electron-ion interaction of a higher order than the second, and also the unsatisfactory modification of the pseudopotential by means of an amendment to the Hartree energy. We obtained the relationships that make possible to calculate the compressibility of melts. Theoretical calculated polytherms of compressibility for semiconductors are given in the article.

Keywords: cluster structure, polyterms of compressibility, semiconductor, function of radial distribution, structural factor, adiabatic compressibility, paired potential, of the pressure of volumetric modules.

The molten metals and their alloys are widely used in the national economy. This interest is especially great in heating engineering, nuclear energy technology, electronic engineering and in other industrial sectors, as well as for meeting the needs of the metallurgical production and in the engineering design of new technology in this field. The greatest attention devoted to the molten metals is in the metallurgy, which is conditioned by the necessity of passing the liquid phase before crystallization. The practical significance of the expected results of the work lies in the possibility of using new ideas about the structure of melts, based on computer simulation, which allows modeling the properties of the melt at the atomic level. This is important for the development of optimal technological processes in non-ferrous and ferrous metallurgy, in pyrometallurgy in general, occurring at the phase interface, as well as for similar processes in the technology of inorganic materials (silicon, selenium, tellurium, germanium, etc.), including number for nanocoatings, films and other special technologies.

It is necessary to consider some correlations for the calculation of the solid modules in the molted systems. Metal melts and melts of semiconductors can be considered as double-base liquid consisting of ions and electrons, then according to the virial theorem, a part of pressure which is connected with dynamics and interaction of ionic subsystem can be evaluated, i.e.

$$P_{ion} = \frac{1}{3\Omega}\left\{2K - \sum_{i<j}\left[R_{ij}\frac{\partial V_{eff}(R_{ij})}{\partial R_{ij}} + R_S\frac{\partial V_{eff}(R_{ij})}{\partial R_S}\right]\right\}, \quad (1)$$

where K — is kinetic energy.

For the calculation of the total pressure per size P_{ion} it is necessary to add the pressure, which is created by the fermi-gas that is equal to the sum of the derivative energy $E_0(\Omega)$ and $E_P(\Omega)$ with the opposite sign $P_{eg} = -(\partial E_0/\partial\Omega) - (\partial E_P/\partial\Omega)$.

One may rewrite the pressure P_{ion} in the integral form, containing explicitly dependence on the structure $g(R)$. If we represent the kinetic energy through the temperature, then

$$P_{ion} = \frac{1}{6\Omega}\int_0^\infty g(R)\left[R\frac{\partial V_{eff}(R,R_C)}{\partial R} + R_S\frac{\partial_{eff}(R,R_S)}{\partial R_S}\right]dR + \frac{kT}{\Omega}. \quad (2)$$

The derivative $\frac{\partial V_{eff}}{\partial R_S}$ in the expression for pressure is specific for the melts so far as $V_{eff}(R,R_S)$ is not only the distance function but also the function $\Omega = \Omega(R_S)$. It points out that the result is an effect of dielectric dependence of penetration function, which defines indirect interaction of ions from the compactness of shielding electronic subsystem nz, at the same time $n = \frac{N}{\Omega} = \frac{3}{4\pi z R_S^3}$. The calculation done for Na [1] shows that thecomponents P_{ion} and P_S^0 which are parts of pressure P_{eg}, have the values close to zero.

If one neglects changes of the pair potential $V_{eff}(R)$ of solidity during the pressure estimation, the result turns out to be overstated. It follows that in the models with stiff fixed compactness which reproduce complex N,Q,T one have to do with the great positive pressures. Such situation is observed while calculating the force coefficients in a crystal. The shown conclusion doesn't indicate the inexactness of mentioned models for a hot metal. The equilibrium should be considered simultaneously for its both subsystems — ionic and electronic, as far as the positive pressure of ionic subsystem defines bulk effects in the electronic subsystem.

As is known, in the theory of condensed systems there is «compressibility sums rule» which describes how much up-build model of the system is self-consistent. The reciprocal value of the volumetric module is equal to the mentioned compressibility. These sizes are important at the consideration of the property of condensed systems. In the crystal the quiescent volumetric module β_{st} equal to the second derivative energy by volume, must be consistent with the dynamic bulkmodulus β_{din}, which is a combination of the elastic constants calculated from the phonon dispersion relation by the «long» wave method [2].

Indicated correlation is defined by the interatomic interaction with the constant volume and doesn't depend on the volume-dependent components of energy. In this self-consistent model correlation between the form of the effective interaction if Q = const and derivatives of the energy in volume, contains mentioned components and defines the «compressibility sums rule».

As is shown in the work [3], the properties are examined well in case of crystalline Na. Subsequently it turned out that the sum rule is not satisfied because of the non-self-consistency of the metal model constructed on the basis of the assumption of perturbation theory in the second order in terms of the pseudopotential.

It gives the reason to assert that the components which emerge in the dynamic matrix in the third and fourth orders in the long-waved limit give the contribution of the second order. This inconsistency results from the inclusion of this contributions while calculating the statistic modules and neglecting them in dynamic modules. But the inclusion of these highest terms at the dynamic arraying, which correspond to the triplet and quadrupole interaction, is possible in essence [2]. Conducted calculations with the crystalline Na [3] have shown that it is necessary to vary Hartree energyfor bringing into concordance of evaluable static module to the experimental β_{st}. But in such variation the dynamic modulus β_{din}, which is well consistent with the experiment, turns out to be too overstated.

The feasible explanation of this is in the fact that the components of the third and the fourth orders become more important in the dynamic matrix, in the field with the little q. In the present case to preserve the

consent with the experiment there is necessary the modification of the pseudo-potential itself in this mentioned field. In such case the Hartree energy variation will correspond to this modified pseudo-potential.

The statistic isothermal modulus of flexibility of the liquid phase is the following pressure derivative by volume:

$$\overline{\beta}_{st} = -\Omega\left(\frac{\partial P}{\partial \Omega}\right)_T . \tag{3}$$

The dynamic isothermal modulus is identified by the long-wave by the structural factor range $S(q)$:

$$\overline{\beta}_{din} = \frac{kT}{\Omega S(0)} . \tag{4}$$

Both of these modules must match in the consistency theory. However, application of the perturbation theory in the second order on the pseudo-potential and definition of the dynamic modulus through $S(q)$ in the model with the potential that is independent on the compactness will lead to the diversions like in the case of the crystal. The exact formula for the static modulus is like this:

$$\overline{\beta}_{st} = \overline{\beta}_{ion} + \overline{\beta}^0_{stp} + \overline{\beta}_e + \frac{kT}{\Omega} , \tag{5}$$

where

$$\overline{\beta}_{ion} = \frac{1}{18\Omega}\int D(g(R))D(V_{eff}(R))dR + \frac{1}{18\Omega}\int g(R)D^2V_{eff}(R)dR ,$$

where D is a statement which is input to shorten the writing:

$$D = R\frac{\partial}{R} + R_S\frac{\partial}{\partial R_S} .$$

The physical value of the derivatives remains the same like in the case of the equation (2). Summing up all, one may write:

$$\overline{\beta}^0_{stp} = \frac{1}{18\Omega}R_S\frac{\partial}{\partial R_S}R_S\frac{\partial}{\partial R_S}\left[V\ (R=0)\right] + P^0_{stp} ; \tag{6}$$

$$\overline{\beta}^0_e = \frac{1}{9\Omega}R_S\frac{\partial}{\partial R_S}R_S\frac{\partial E}{\partial R_S} + P'_e . \tag{7}$$

One may write the analogous formula for the dynamic modulus $\overline{\beta}_{din}$, as long as it is also calculated in the model with the potential independent on the compactness. Since the model is self-consistent, the dynamic and static modules calculated in it coincide. The analogous conclusion may be done even in the case of calculation of the crystal compressibility, which is realized in the reciprocal space. Thus, it is expected the following correlation to be accomplished:

$$\overline{\beta}_{din} = \overline{\beta}'_{ion} + kT/\Omega , \tag{8}$$

where

$$\overline{\beta}_{ion} = \frac{1}{18\Omega}\int Dg(R)\frac{R\partial}{\partial R}V_{eff}dR + \frac{1}{18\Omega}\int g(R)\frac{R\partial}{\partial R}V_{eff}dR .$$

The equation (4) gives more simple formula for $\overline{\beta}_{din}$. The equivalence of the equations (4) and (6) is in essence particular case of the matched condition between n and $n+1$ the partial distribution functions. The equation (8) doesn't contain the direction to the calculation of the statistic calculation (5). However, in the calculations on the equation (5) one has to face the following problems: for the calculation such the function of the radial distribution is required $q(R)$ which would coincide with the complete theory, i.e. for that the identity was realized:

$$S(0) = \int\left\{\left[g(R)-1\right]/\Omega\right\}dR , \tag{9}$$

equal $\frac{kT}{\Omega\overline{\beta}_{st}}$. It requires the consideration of the components of the third and the fourth orders in the field of the minor $q-s$. As these components coincide to the calculation of the effective interactions between the

tree and four ions, it is an awkward task. It is therefore natural to make the assumption that the function $q(R)$, calculated in a computer experiment with a pair effective potential at Q = const, does not lead to large errors, excluding the long-wave region.

Just this very function $q(R)$ is put in the equation (5) and (8); the equations (5) and (8) require the values of the derivatives of functions $q(R)$ in volume which can be taken by the repetition of the computer experiment with different source compactness.

It is therefore natural to make the assumption that the function $g(R)$, calculated in a computer experiment with a pair effective potential at Ω = const, does not lead to large errors, excluding the long-wave region.

The present situation is the extreme laborious task. So it is more convenient to confine with the approach:

$$g(R, R_S T) = \frac{1}{\Omega} f(R/R_S, T), \tag{10}$$

where $f(R/R_S, T)$ is the function which provides similar change of the structure with the compactness in at the constant temperature.

However, the assumption (10) is correct for the crystal structure, but is not obligatory for a liquid. That is why this approach follows to:

$$Dg(R) = \frac{R\partial g(R/R_S)}{\partial R} + R_S \frac{\partial g(R/R_S)}{\partial R_S} = -3g(R). \tag{11}$$

Taking into account the derived result let's rewrite the equation (4) as in this way:

$$\overline{\beta}_{ion} = \frac{1}{18\Omega} \int g(R)(D^2 - 3D) V_{eff}(R) dR \ . \tag{12}$$

The value for $\overline{\beta}_{ion}$ = 0,097 which has been found without variation of Hartree energy conforms with experimental which is equal to 0.0973 as in case of the crystal. The value which is determined by the computer experiment amounts 0.032±0,002 that leads to $\overline{\beta}_{abc}\Omega = 0.078 \pm 0.005$.

Equation (10) indicates that the modulus obtained by Eq. (12) is an «instantaneous» bulk modulus, which, as shown in [4], is the upper limit of the adiabatic bulk modulus and is approximately 10 % larger than the isothermal bulk modulus Na. The results which are given in the work coincide with abovementioned ones. Besides that, the low differences are indicative of that the approach (10) is acceptable for such differences. Further one may calculate with the help of the equation (12) in the same approach. The variation of Hartree energy gives a result of 0.105 and it also coincides with the experiment, if we take into account the upper limit of the real compressibility. In case of crystalline state the correction of Hartee energy gives the considerable contribution that is necessary to achieve the concordance with the experiment.

The accuracy which is taken from the calculation as a whole is note worse than for the crystal [5] and can be explained approximately in the same way like before. One of the possible explanations applies to the substantial modification of the pseudo-potential at low $q - s$, what about it was told above. It is corroborated by the calculation with the components of the third and fourth order, i.e. including the triplet and quadrupole effective interactions. It is corroborated by the calculated polyterms of adiabatic compressibility for the liquid lead (Fig. 1). Adiabatic compressibility in this process increases monotonously. Such the behavior of the compressibility basically is typical for the metal melts. Thus, one may conclude that the instantaneous dynamic modulus, which is calculated in the modulus of pair approach, is identical with the dynamic modulus, that is calculated in the complete theory on the second order, and also is distinctly differs from the static modulus, on the one hand, and from that one which is calculated in the theory of the second order, on the other hand. The first of them matches to the isometric experimental modulus, while the second one refers the correction to the Hartree energy. Thereby, the situation doesn't differ from that which was used at the analogical calculations for the crystalline condition of a substance [6].

The possible explanation is in the neglect of the components of electron-ion interaction of the higher order than the second one, also in the inadequacy of pseudo-potential modification by means of the correction to the Hartree energy that leads to the correct result only in the long-wave limit. The above relations enable us to calculate the compressibility of melts. The theoretical calculated polyterms of the compressibility to selenium, tellurium, germanium and silicon are shown on the Figures 1–5.

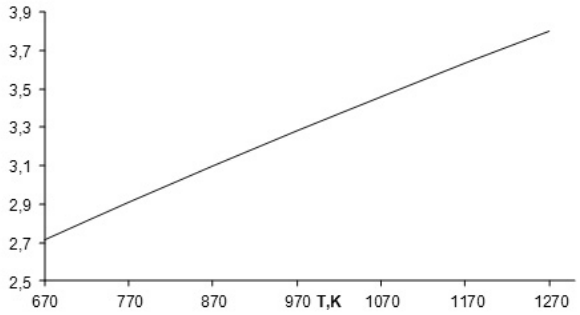

Figure 1. The compressibility polyterms of the lead melt

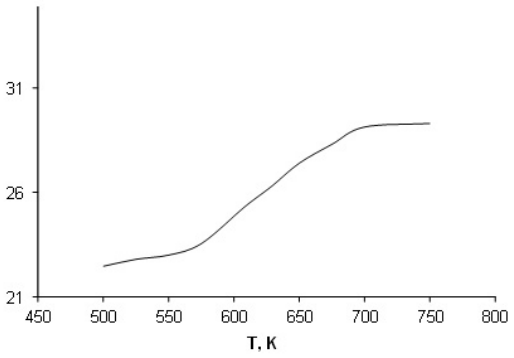

Figure 2. The compressibility polyterms of the selenium melt

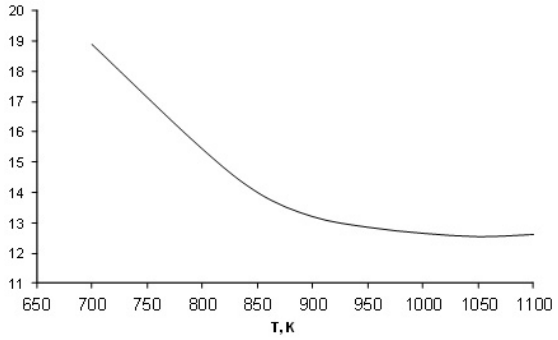

Figure 3. The compressibility polyterms of the tellurium melt

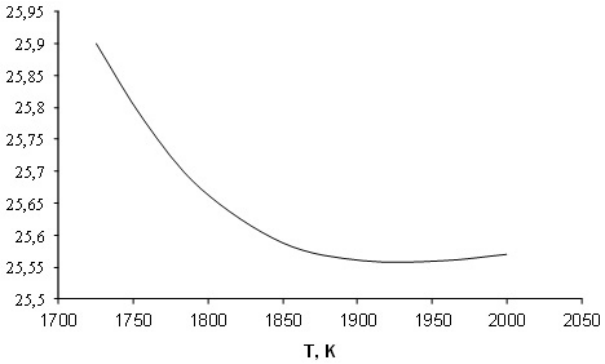

Figure 4. The compressibility polyterms of the silicon melt

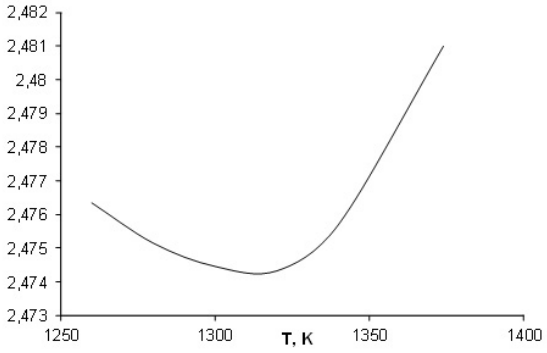

Figure 5. The compressibility polyterms of the germanium melt

The model of the micro-heterogeneous melt with the clusters of the similar size at fixed temperature is, certainly, idealized. In fact, in the real melt there can be the clusters of various sizes. The existence of the clusters not only close to the crystallization temperature, but also at the higher temperatures, in the melts of semimetals and semiconductors is conditioned on the presence in them the two types of the chemical bond — covalent and metallic [1].

The covalent bond type that is present and predominant in the crystal, while its passing to the liquid condition can disappear neither just after melting, nor at the further heating. These bonds are laid on the atomic nature itself, which constitute semimetals and semiconductors in the outer electron shell of the atoms and cannot disappear completely at any aggregate substance condition. The question only is in their manifestation degree. If these bonds exist together with the bounds that greatly differ in their energy, then they mani-

fest essentially. The example is the molecular liquids. If these bonds are dipped into the matrix of the other bond types, which is not much differ from them energetically, then their individuality levels on the equalized background of those allied by their energy, but differ in the bond nature, for example, metallic.

Thus, the double-structured melt cluster model (the model of the mixture of cluster and atomic component), reflecting the opportunity of equilibrium existence of the two types of chemical bound (covalent and metallic bonds), different by their nature, but close by their solidity (thermodynamic aspect) and the two mechanisms of the cluster decay (kinetic aspect) allow to explain quite right the main types of the experimental and theoretical polyterm compressibility in the melts of the semimetals and semiconductors.

The Variety of the forms of polyterms compressibility in the electronic melts requires typification, or their analysis allows clearing the mechanism of the aggregation processes and dissolution of extensive objects in the melts.

References

1 Регель А.Р. Периодический закон и физические свойства электронных расплавов: монография / А.Р. Регель, В.М. Глазов. — М.: Наука, 1982. — 296 с.

2 Onuki A. Viscosity enhancement by domians in phase-separating fluids near the critical point. Proposal of critical rheology / A. Onuki // Phys. Rev. A. Gen. Phys. — 1987. — Vol. 35, No. 12. — P. 5149–5155.

3 Torquato S. Computer simulation of nearest — neighbor distribution functions and related quantities for hard-sphere systems / S. Torquato, S.B. Lee // Physica A. — 1990. — Vol. 167, No. 2. — P. 361–383.

4 Medvedev N.N. Aggregation of tetrahedral and quartoctahedral Delaunay simplices in liquid and amorphous rubidium / N.N. Medvedev // J. Phys: Condens. Matter. — 1990. — Vol. 2, No. 46. — P. 9145–9154.

5 Sun T.F. An efficient algorithm for the solution of the correlation function for soft spherical repulsions / T.F. Sun, J.A. Schouten // Mol. Phys. — 1990. — Vol. 69, No. 4. — P. 604–614.

6 Takamiya M. Density functional approach to two-dimensional classical fluids / M. Takamiya, K. Nakanishi // Mol. Phys. — 1990. — Vol. 70, No. 5. — P. 767–781.

А.З. Исағұлов, С.Ш. Қажыкенова, Г.С. Шаихова, Г.Ш. Махметова, Л.Ж. Қасымова

Балқытылған жүйелердегі қысымды және көлемдік модульдарды бағалау

Мақалада балқытылған жүйелердегі көлемдік модульдер қысымы мен жұптық әлеуеті бағаланған. Электрондық балқымалардың сығылғыштығын есептеу үшін сәйкес формулалар келтірілген. Селен, теллур, германий және кремний үшін сығылғыштық политермалары есептелген. Көлемдік модульдердің есебі үшін металдар мен жартылайөткізгіштер балқымалары иондар мен электрондардан тұратын екі компонентті сұйықтық ретінде қарастырылған. Вириал теоремасы бойынша, иондық кішірек жүйенің динамикасы мен өзара әрекеттесуімен байланысты қысым бөлігі бағаланған. Көлемдік серпімділіктің изотермиялық модулі статикалық модуль болып табылғандықтан, оны біз жүйедегі қысым мен көлем баяу өзгерген жағдайда, ал балқыма температурасы өте баяу өзгергенде немесе тұрақты болып қалған жағдайда тауып алдық. Көлемдік серпімділіктің адиабаттық модулі, яғни динамикалық, сығумен туындаған балқыманы қыздыру жағдайында анықталды. Адиабаттық сығу кезінде температура мен қысымның өзгерісі орын алады. Бұл құбылыс тез жүретін үрдістер кезінде, яғни балқымалардың жылулық қасиеттерінің инерциондығы салдарынан жылу алмасу болмаған кезде орын алады. Адиабаттық сығылғыштықтың мұндай сипаты металл балқымаларға тән. Авторлар жұптық жуықтау моделінде есептелген лездік динамикалық модуль екінші тәртіппен толық теорияда есептелген динамикалық модульмен бірдей екендігін анықтады, сонымен қатар статикалық модульден елеулі өзгешелігі бар. Бұл факт неғұрлым жоғары тәртіптегі электрондық-иондық өзара әрекеттесу мүшелерін елемеу, сонымен қатар Хартри энергиясына түзету арқылы псевдопотенциал модификациясының қанағаттанбауымен түсіндіріледі. Авторлар шығарып алған қатынас балқымалардың сығылғыштығын есептеп алуға мүмкіндік береді. Жартылайөткізгіштер үшін сығылғыштықтың теориялық есептелген политермалары жұмыста келтірілген.

Кілт сөздер: кластерлік құрылым, сығылғыштық политермалары, жартылайөткізгіштер, радиалды үлестірім функциясы, құрылымдық фактор, адиабаталық сығылғыштық, жұптық потенциал, көлемдік модульдардың қысымы.

А.З. Исагулов, С.Ш. Кажикенова, Г.С. Шаихова, Г.Ш. Махметова, Л.Ж. Касымова

Оценка давления и объемных модулей в расплавленных системах

В статье оценены парный потенциал и давление объемных модулей в расплавленных системах. Приведены соответствующие формулы для расчета сжимаемости электронных расплавов. Вычислены политермы сжимаемости для селена, теллура, германия и кремния. Для расчёта объёмных модулей расплавы металлов и полупроводников рассмотрены как двухкомпонентная жидкость, состоящая из ионов и электронов. По теореме вириала оценена часть давления, связанная с динамикой и взаимодействием ионной подсистемы. Так как изотермический модуль объемной упругости является статическим показателем, он определен нами в условиях, когда давление и объем в системе изменяются медленно, а температура расплава очень медленно изменяется или остается постоянной. Адиабатический модуль объемной упругости, т.е. динамический, определен нами в условиях нагревания расплава, вызванного сжатием. При адиабатическом сжатии допускается изменение температуры и давления. Данное явление имеет место при быстропротекающих процессах, т.е. когда отсутствует теплообмен из-за инерционности тепловых свойств расплавов. Такое поведение адиабатической сжимаемости характерно для металлических расплавов. Авторы установили, что мгновенный динамический модуль, рассчитанный в модели парного приближения, идентичен динамическому модулю, вычисленному в полной теории во втором порядке, а также заметно отличается от статистического модуля. Объяснение данного факта состоит в пренебрежении членами электронно-ионного взаимодействия более высокого порядка, чем второй, а также неудовлетворительностью модификации псевдопотенциала посредством поправки к энергии Хартри. Полученные авторами соотношения позволяют вычислить сжимаемость расплавов. Теоретические вычисленные политермы сжимаемости для полупроводников приведены в работе.

Ключевые слова: кластерная структура, политермы сжимаемости, полупроводники, функция радиального распределения, структурный фактор, адиабатическая сжимаемость, парный потенциал, давление объемных модулей.

References

1 Regel, A.R., & Glazov, V.M. (1982). *Periodicheskii zakon i fizicheskie svoistva elektronnykh rasplavov [Periodic Law and Physical Properties of Electronic Melts]*. Moscow: Nauka [in Russian].

2 Onuki, A. (1987). Viscosity enhancement by domians in phase-separating fluids near the critical point. Proposal of critical rheology. *Phys. Rev. A. Gen. Phys., 35(12)*, 5149–5155.

3 Torquato, S., & Lee, S.B. (1990). Computer simulation of nearest — neighbor distribution functions and related quantities for hard-sphere systems. *Physica A, 167(2)*, 361–383.

4 Medvedev, N.N. (1990). Aggregation of tetrahedral and quartoctahedral Delaunay simplices in liquid and amorphous rubidium. *J. Phys: Condens. Matter, 2(46)*, 9145–9154.

5 Sun, T.F., & Schouten, J.A. (1990). An efficient algorithm for the solution of the correlation function for soft spherical repulsions. *Mol. Phys., 69(4)*, 604–614.

6 Takamiya, M., & Nakanishi, K. (1990). Density functional approach to two-dimensional classical fluids. *Mol.Phys, 70(5)*, 767–781.

UDC 541.515

K.Zh. Kutzhanova, A.F. Kurmanova, I.A. Pustolaikina, B.M. Ismagulov

Ye.A. Buketov Karaganda State University, Kazakhstan
(E-mail: kutzhanovak@mail.ru)

Nonempirical modeling of protolytic processes in dimeric molecules of amino acids

Quantum-chemical modeling of intermolecular proton exchange in dimers of aminoacetic acid was carried out using an unempirical unrestricted Hartree-Fock method using the 3–21G basis set. Three main structural isomers of dimeric molecules of aminoacetic acid have been quantum-chemically identified. For these isomers, the search for the structure of the transition state of the proton exchange reaction was carried out using the quadratic synchronous transit QST2 (Quadratic Synchronous Transit Approach) procedure. The symmetrical structure of the transition state for the dimer of aminoacetic acid is noted, in the formation of hydrogen bonds of which two carboxyl functional groups are involved. The kinetics and mechanism of intermolecular migration of a proton in the dimer of aminoacetic acid have been studied using the internal IRC (Intrinsic Reaction Coordinate method) method. Curves are obtained for the dependence of the total energy of the reaction system under consideration on the internal coordinate of the reaction. The activation energy of proton exchange in dimers of aminoacetic acid is estimated as the difference in the total energies of the transition and initial states of the reaction system. The minimum value of the activation energy (26 kJ/mol in the forward direction and 34 kJ/mol in the reverse direction) was obtained for the intermolecular proton exchange reaction in the dimer of aminoacetic acid, in the formation of the hydrogen bonds of which two carboxyl functional groups are involved. The maximum value of the activation energy (244 kJ/mol in the forward direction and 236 kJ/mol in the reverse direction) was obtained for the intermolecular proton exchange reaction in the dimer of aminoacetic acid, in the formation of hydrogen bonds of which two amino groups are involved.

Keywords: quantum chemical calculation, *ab initio* UHF 3–21G, hydrogen bond, aminoacetic acid, dimer, cyclic complexes by hydrogen bonding, geometric and energy parameters, complexation energy, hydrogen bond energy.

Most of the applied quantum chemical work is connected with the calculation of the geometry of organic compounds. Such researches are carried out for both stable molecules and short-lived intermediates and transition states. Analysis of the calculated data allows to obtain reliable information on their structure and therefore to be of independent interest from the point of view of organic chemists. In addition, knowledge of geometry is necessary for calculating the thermal formation, thermal effects and activation energies of the reactions [1].

In this paper, the process of proton exchange between molecules in dimers of aminoacetic acid by quantum chemical methods was considered. If the studiedmolecules contain two reaction centers [2, 3], it is possible to consider three main possible complexes formed by the hydrogen bond:

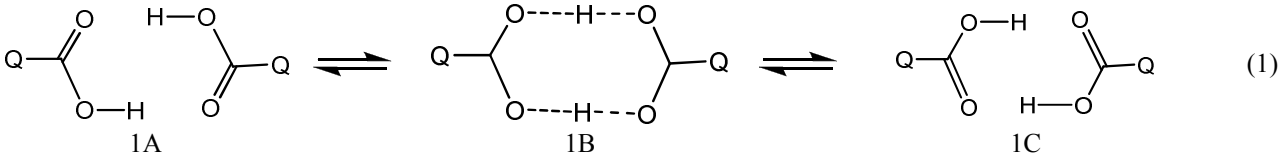

(1)

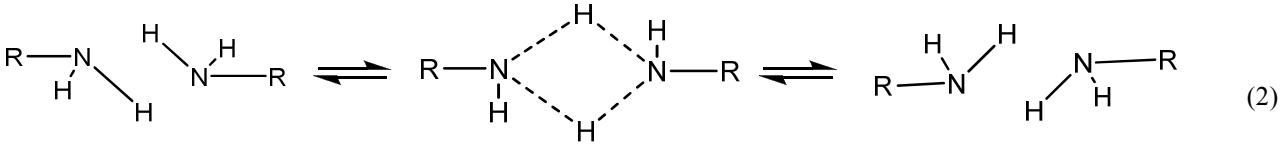

(2)

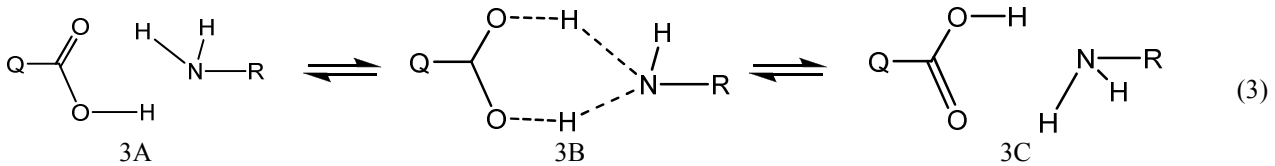

(3)

where Q — is $-CH_2-NH_2$; R — is $-CH_2-COOH$.

(1) is a complex due to the hydrogen bond in which carboxyl functional groups of an amino acid are involved in the formation of hydrogen bonds;

(2) is the complex due to the hydrogen bond, in which the amino groups of the amino acid are involved in the formation of hydrogen bonds;

(3) is a complex due to the hydrogen bond in which the carboxyl functional group of one molecule and the amino group of another amino acid molecule are involved in the formation of hydrogen bonds;

On the proposed scheme of intramolecular hydrogen transition inside the cyclic dimer of aminoacetic acid: A) the initial geometry of dimer 1; B) transition state; C) finite dimer geometry.

Simulation of the process of intermolecular proton exchange was carried out by an *ab initio* method in the 3–21G basis in the unrestricted Hartree-Fock approximation of the Gaussian09 Revision-B.01-SMP software package [4].

When creating the dimer molecule, the GaussView program was used — a visualizer program designed to create input files, as well as visualization of the output files generated during the Gaussian calculation.

To study the kinetics and mechanism of intermolecular migration of a proton in the dimer of aminoacetic acid, the quantum chemical procedure IRC was used [5].

The initial (A) and final (C) structures of the dimer of aminoacetic acid with full optimization of all geometric parameters are shown in Figure 1. It should be noted that the numbering of atoms in the molecules of the intended reagents and reaction products must be strictly preserved.

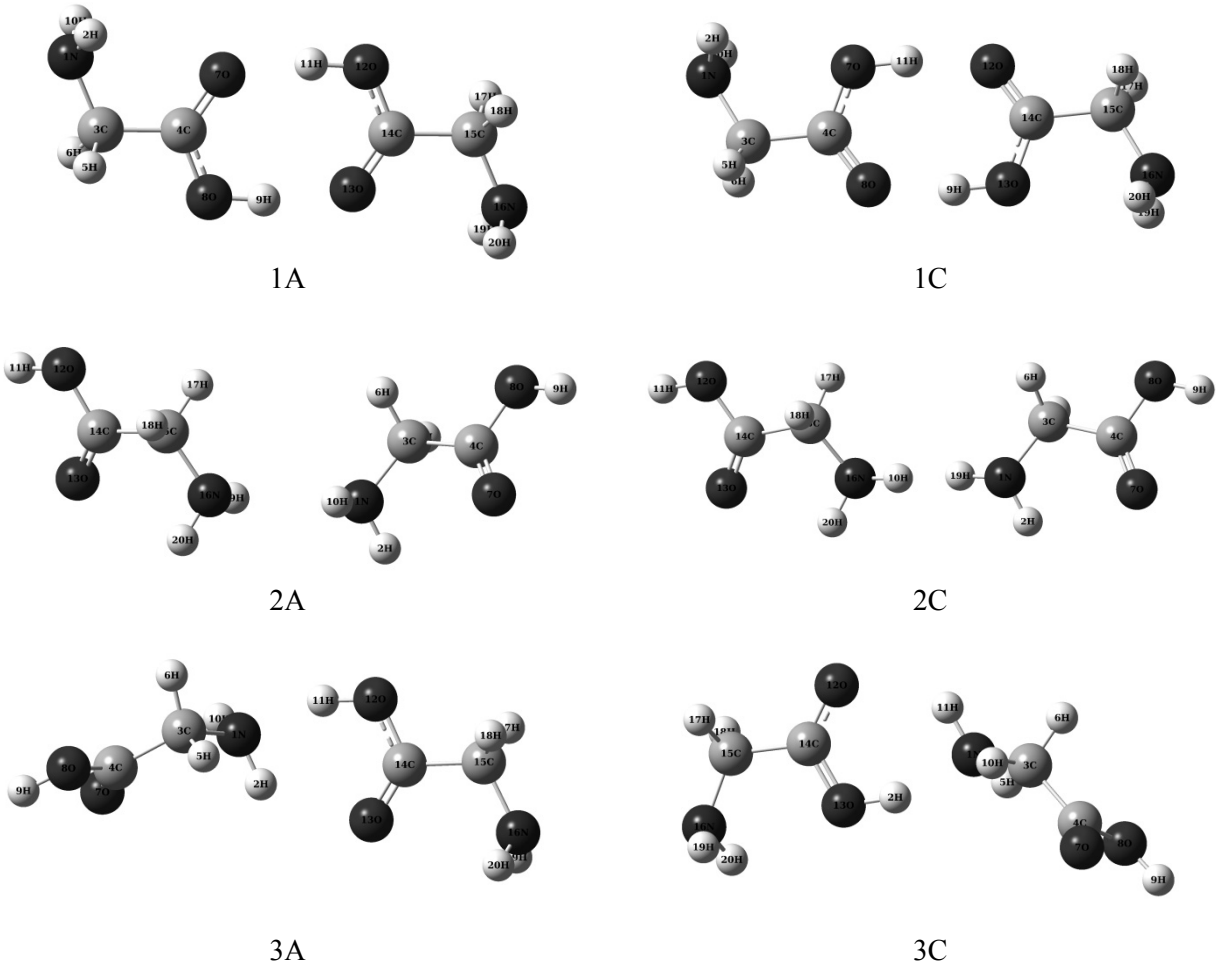

1A 1C

2A 2C

3A 3C

A — the structure of the reagents; C — product structures

Figure 1. Structures of intermolecular complexes due to the hydrogen bond of the dimer of aminoacetic acid

Next, a transition state was calculated using the keywords Opt (QST2) UHF 3–21G. The search for a transition state of intramoleculartautomerism was carried out by the quadratic synchronous linear transit method.

Figure 2 shows the transitional structures in a complex due to hydrogen bondingof various types for dimers of aminoacetic acid.

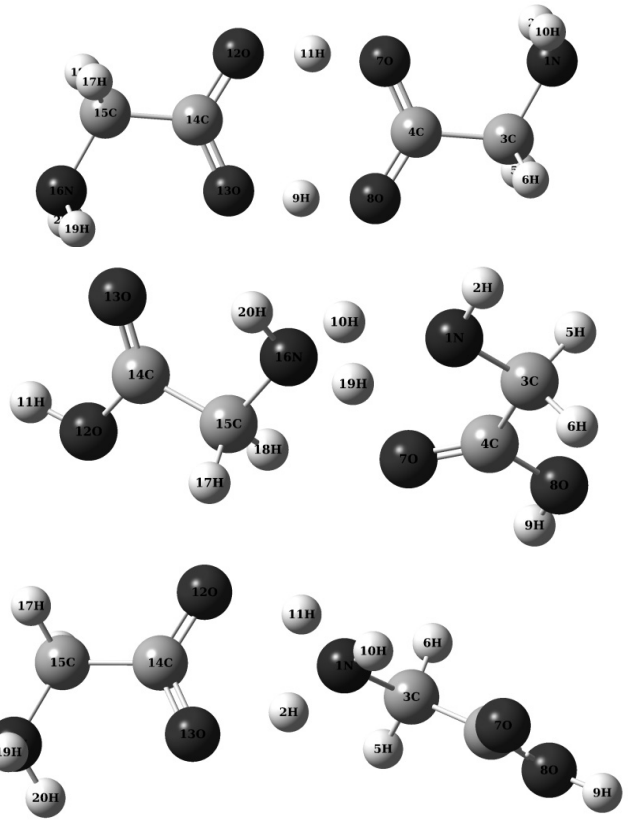

1B

2B

3B

Figure 2. The transition state of the proton transfer process in dimericaminoacetic acid complexes

Figures 3–5 depict the dependence of the total energy of the dimer systems and the RMS normal gradient on the internal coordinate of the RMS (root-mean-square) reaction.

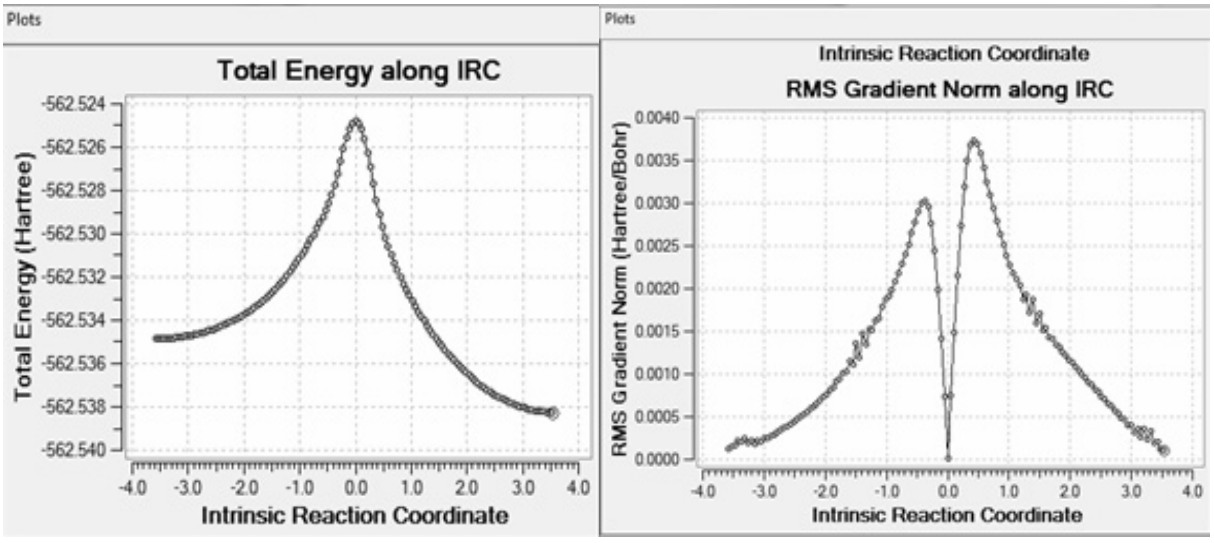

E_{total} *RMS*

Figure 3. Kinetic curves as a function of the reaction coordinate in the complex due to the hydrogen bond (1) of aminoacetic acid

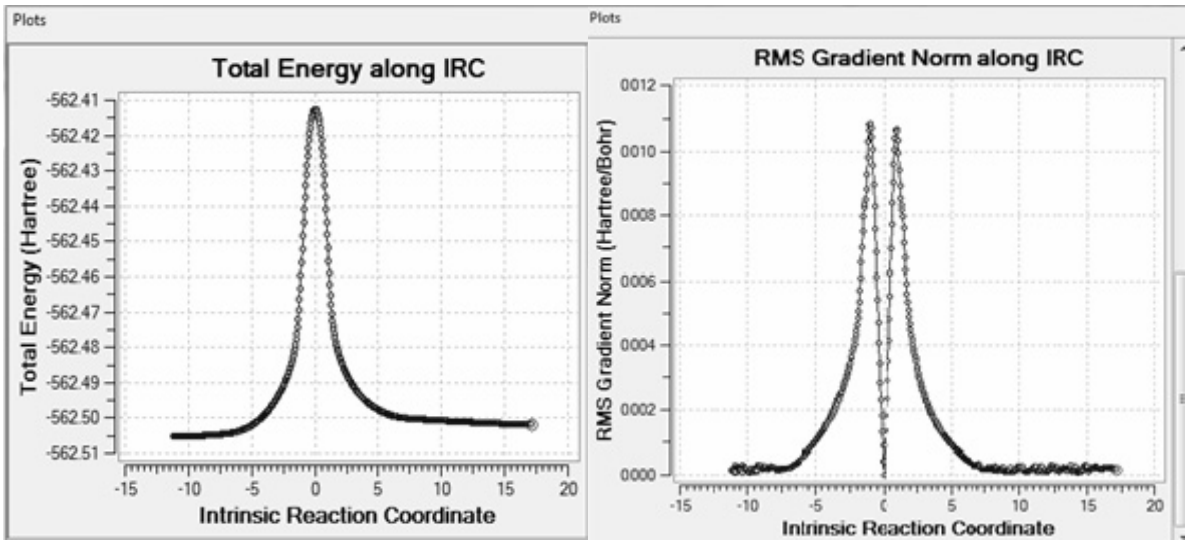

E_{total} *RMS*

Figure 4. Kinetic curves as a function of the reaction coordinate in the complex due to the hydrogen bond (2) of aminoacetic acid

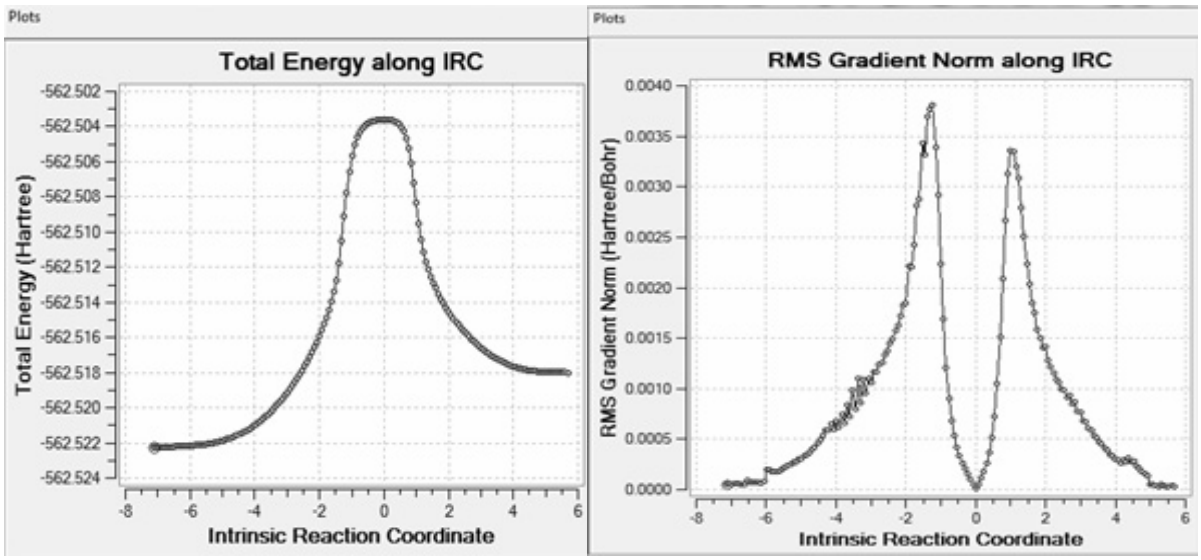

E_{total} *RMS*

Figure 5. Kinetic curves as a function of the reaction coordinate in the complex due to the hydrogen bond (3) of aminoacetic acid

As can be seen from Figures 3–5, the extreme points of the curves of kinetic dependencies are identical to the points on the graphical dependence of the root-mean-square deviation standard along the coordinates of the reaction path.

The program GaussianView allows you to determine the structure of each studied point of the curves examined, optimizing all the geometric parameters of the molecules. It should be noted that the calculation procedure for internal coordinates is carried out automatically, which significantly reduces the time required for calculation. So in the calculation of the complex due to the hydrogen bond (1), in the automatic mode 134 optimized structures are investigated, the complex due to the hydrogen bond (2) — 563 and the complex due to the hydrogen bond (3) — 168.

Table shows the energy values for all types of particles: A, B, and C for all the complexes under study due to the hydrogen bond.

Table

Kinetic characteristics of different types of complex due to the hydrogen bond of aminoacetic acid according to 3–21G UHF calculations

Complex due to the hydrogen bond	E_A, a.u.	E_B, a.u.	E_C, a.u.	ΔE_{AB}, a.u.	ΔE_{BC}, a.u.
(1)	–562.535	–562.525	–562.538	0.01	0.013
(2)	–562.505	–562.412	–562.502	0.093	0.09
(3)	–562.522	–562.504	–562.518	0.018	0.014

Note. E_A — is the total energy of the process reagent; E_B — is the total energy of the transition structures of the process; E_C — total energy of process products.

As shown by the analysis of the energy parameters presented in Table, the minimal activation energy accompanies the process of proton transfer in the complex due to the hydrogen bond (1) in the forward and reverse directions, respectively, 26 and 34 kJ/mol, the maximum activation energy for the process in the complex due to the hydrogen (2), where the parameter corresponds to 244 and 236 kJ/mol, the intermediate position is occupied by the activation energy in the complex due to hydrogen bonds (3): 47 and 36 kJ/mol, respectively. It should be remembered that in reactions where the activation energy is greater than 150 kJ the rate is very small or practically these reactions do not flow. In reactions where the activation energy is less than 60 kJ, the rate is very high.

Thus, by using non-empirical quantum chemical methods, kinetic curves and characteristics were obtained depending on the coordinate of the reaction of the complex due to the hydrogen bond of aminoacetic acid, their kinetic stability is shown, and the characteristic of the hydrogen bond is estimated.

References

1 Reiher M. Relativistic Quantum Chemistry. The Fundamental Theory of Molecular Science / M. Reiher, A. Wolf. — Wiley-VCH, 2009. — P. 694.

2 Владимиров Я.А. Физико-химические свойства аминокислот и пептидов / Я.А. Владимиров // Журнал общей химии. — 2010. — Т. 80, № 2. — С. 425–430.

3 Bonaccorsi R. Conformational energy of glycine in aqueous solutions and relative stability of the zwitterionic and neutral forms. An ab initio study / R. Bonaccorsi, P. Palla, J. Tomasi // Journal of the American Chemical Society. — 1984. — Vol. 106, No. 7. — P. 1945–1950.

4 Frisch M.J. Gaussian 09, Revision C.01 / M.J. Frisch, G.W. Trucks, H.B. Schlegel. — Wallingford: Gaussian, Inc., 2009. — 245 p.

5 Цышевский Р.В. Квантово-химические расчеты механизмов химических реакций: учеб.-метод. пособие / Р.В. Цышевский, Г.Г. Гарифзянова, Г.М. Храпковский. — Казань: Изд-во КНИТУ, 2012. — 82 с.

К.Ж. Кутжанова, А.Ф. Курманова, И.А. Пустолайкина, Б.М. Исмагулов

Аминқышқылдары димерлі молекулаларының протондану процестерін эмпирикалық емес модельдеу

Аминсірке қышқылының димерлеріндегі молекулааралық протон алмасуының квантты-химиялық модельдеуі 3–21G негізгі жиынтығын пайдалана отырып, шектеусіз Хартри-Фок әдісі арқылы жүзеге асырылды. Аминсірке қышқылы димерінің үш негізгі құрылымдық изомері квантты-химиялық түрде анықталған. Бұл изомерлер үшін протон алмасу реакциясының ауыспалы күйінің құрылымы QST2 (Quadratic Synchronous Transit Approach) квадраттық синхронды транзит процедурасы арқылы ізделінді. Аминсірке қышқылының димері үшін оның құрамында екі карбоксильді функционалды топтың сутектік байланыстары қалыптасатын өтпелі күйдің симметриялық құрылымы байқалады. Аминсірке қышқылының димеріндегі протонды молекулалы тасымалдануының кинетикасы мен механизмі IRC (Intrinsic Reaction Coordinate method) ішкі координат әдісімен зерттелінді. Реакцияның ішкі координатасымен қарастырылып отырған реакция жүйесінің толық энергияларының тәуелділік қисықтары алынды. Реакция жүйесінің ауыспалы және бастапқы күйлеріндегі айырымы ретінде аминсірке қышқылының димерлеріндегі протон алмасудың активтілік энергиясы бағаланды. Молекулааралық протон алмасу реакциясы үшін активтілік энергиясының минималды мәні (тура 26 кДж/моль және кері бағытта 34 кДж/моль), аминсірке қышқылының сутектік байланыстардың түзілуіне екі карбоксильді функционалды қатысатын димерінде алынды. Молекулааралық протон алмасу реакциясы үшін активтілік энергиясының максималды мәні (тура 244 кДж/моль және кері

бағытта 236 кДж/моль) аминсірке қышқылының сутектік байланыстардың түзілуіне екі амин тобы қатысатын димерінде алынды.

Кілт сөздер: квантты-химиялық есептеулер, *ab initio* UHF 3–21G, сутектік байланыс, аминсірке қышқылы, димер, сутектік байланыс арқылы түзілетін циклдік кешендер, геометриялық және энергиялық өлшемдер, кешен түзу энергиясы, сутектік байланыс энергиясы.

К.Ж. Кутжанова, А.Ф. Курманова, И.А. Пустолайкина, Б.М. Исмагулов

Неэмпирическое моделирование протолитических процессов в димерных молекулах аминокислот

Выполнено квантово-химическое моделирование межмолекулярного протонного обмена в димерах аминоуксусной кислоты с помощью неэмпирического неограниченного метода Хартри–Фока с использованием базисного набора 3–21G. Квантово-химически идентифицированы три основных структурных изомера димера аминоуксусной кислоты. Для данных изомеров с помощью процедуры квадратичного синхронного транзита QST2 (Quadratic Synchronous Transit Approach) осуществлен поиск структуры переходного состояния реакции протонного обмена. Отмечено симметричное строение переходного состояния для димера аминоуксусной кислоты, в образовании водородных связей которого задействованы две карбоксильные функциональные группы. Кинетика и механизм межмолекулярной миграции протона в димере аминоуксусной кислоты изучены с использованием метода внутренней координаты реакции IRC (Intrinsic Reaction Coordinate method). Получены кривые зависимости полной энергии рассматриваемой реакционной системы от внутренней координаты реакции. Оценена энергия активации протонного обмена в димерах аминоуксусной кислоты как разница в полных энергиях переходного и исходного состояний реакционной системы. Минимальное значение энергии активации (26 кДж/моль в прямом и 34 кДж/моль в обратном направлении) получено для реакции межмолекулярного протонного обмена в димере аминоуксусной кислоты, в образовании водородных связей которого задействованы две карбоксильные функциональные группы. Максимальное значение энергии активации (244 кДж/моль в прямом и 236 кДж/моль в обратном направлении) получено для реакции межмолекулярного протонного обмена в димере аминоуксусной кислоты, в образовании водородных связей которого задействованы две аминогруппы.

Ключевые слова: квантово-химические расчеты, *ab initio* UHF 3–21G, водородная связь, аминоуксусная кислота, димер, циклические комплексы за счет водородной связи, геометрические и энергетические параметры, энергия комплексообразования, энергия водородной связи.

References

1 Reiher, M., & Wolf, A. (2009). *Relativistic Quantum Chemistry. The Fundamental Theory of Molecular Science*. Wiley-VCH.

2 Vladimirov, Ya.A. (2010). Fiziko-khimicheskie svoistva aminokislot i peptidov [Physico-chemical properties of amino acids and peptides]. *Zhurnal obshchei khimii — Journal of General Chemistry, 2*, 425–430 [in Russian].

3 Bonaccorsi, R., Palla, P., &Tomasi, J. (1984). Conformational energy of glycine in aqueous solutions and relative stability of the zwitterionic and neutral forms. An ab initio study. *Journal of the American Chemical Society, 106(7)*, 1945–1950.

4 Frisch, M.J., Trucks, G.W., & Schlegel, H.B. (2009). *Gaussian 09, Revision C.01*. Wallingford: Gaussian, Inc.

5 Tsyshevsky, R.V., Garifzyanova, G.G., & Khrapkovsky, G.M. (2012). *Kvantovo-khimicheskie raschety mekhanizmov khimicheskikh reaktsii [Quantum-chemical calculations of the mechanisms of chemical reactions]*. Kazan: Izdatelstvovo Kazanskoho Nauchno-Issledovatelskoho Tekhnicheskoho Universiteta [in Russian].

UDC 541.515

I.A. Pustolaikina, K.Zh. Kutzhanova, A.V. Pushchina, A.F. Kurmanova

Ye.A. Buketov Karaganda State University, Kazakhstan
(E-mail: irinamorozo@mail.ru)

Proton exchange in ammonia, water and formic acid dimers: quantum-chemical calculation

Proton exchange in hydrogen-bounded complexes occupies an important place among dynamic processes taking place in molecular systems with hydrogen bond. However, despite numerous experimental and theoretical studies in this field, a single point of view on the mechanism of proton exchange has not yet been accepted by scientists. Ammonia, water and formic acid are small in size protolytes with widely differing acid-base properties. This makes them suitable and comfortable for theoretical modeling of proton exchange reaction. Quantum-chemical simulation of the proton exchange reaction in model dimers of ammonia, water and formic acid was carried out by AM1 and *ab initio* 6–31G, 6–31G++ methods of Gaussian-2009 program. The search of transition state structure was performed by using of QST2 procedure, the descent along the reaction coordinate was held by using of IRC procedure. The symmetrical structure of transition state in the case of formic acid dimer and the asymmetric structure of transition complex in the case of ammonia dimer were obtained for studied proton exchange reaction. A synchronous mechanism of proton exchange reaction is shown in the case of the formic acid dimer and a sequential mechanism is shown in the case of ammonia dimer. The dynamic shortening of the hydrogen bridge length was noted during proton exchange reaction in all model systems. It was suggested that the mechanism of proton exchange reaction is determined by the nature of the resulting transition state (symmetrical or asymmetrical). At the same time, the transition state structure is determined by the acid-base properties of reaction partners.

Keywords: proton exchange, dimer, sequential and synchronous reaction mechanism, hydrogen-bounded complex, AM1, *ab initio*, 6–31G, QST2, IRC.

Introduction

Proton exchange in hydrogen-bounded complexes occupies an important place among dynamic processes taking place in molecular systems with hydrogen bond [1]. Formation of the hydrogen bond can be considered as an intermediate stage of the proton exchange protolytic reaction in this case [2]. However, despite numerous experimental and theoretical studies in this field, a single point of view on the mechanism of proton exchange has notyetbeen accepted by scientists today [3]. Study of the proton exchange reaction mechanism by modern quantum chemistry methods can help us to clarify important aspects of the hydrogen bonding phenomenon, as well as specific features of a number of physical, chemical and biological phenomena.

It is assumed that the proton exchange reaction proceeds through the formation of intermediate cyclic complexes with H-bonds [4]. As we know, many nitrogen- and oxygen-containing organic compounds tend to form cyclic dimers both in solutions and in the gas phase. Geometry of dimers is favorable for the proton exchange reaction [5]. For example, formic acid exists in dimer form both in liquid and gaseous state. Strong H-bonds between molecules can be found in water and liquid ammonia. At the same timeammonia, water and formic acid molecules have small size and very different acid-base properties. This makes them suitable and comfortable for theoretical modeling of proton exchange reaction.

Methods

The purpose of the investigation was to study the proton exchange reaction mechanism in water, ammonia and formic acid cyclic dimmers by quantum-chemical methods.Cyclic complexes of objects have been treated *ab initio* using the 6–31G and 6–31G++ basis sets as well as by the semiempirical AM1 method. The choice of methods was determined by the desire to compare the results of semiempirical and non-empirical modeling with each other, as well as the specification of methods.Thus, the semiempirical method AM1 is applicable for organic molecules calculation, especially those containing nitrogen and oxygen, as well as for hydrogen bonded systems. Simultaneously high-level *ab initio* methods can be used as a standard for interatomic interaction accurate description at the quantum-chemical level. The search of transition state structure was performed by using of QST2 procedure, the descent along the reaction coordinate was held by using of IRC procedure. Calculations were made using the Gaussian 2009 package [6, 7].

Results

Proton exchange in dimers of protoliths is an energy-degenerate process. New products are not formed as a result of this exchange reaction:

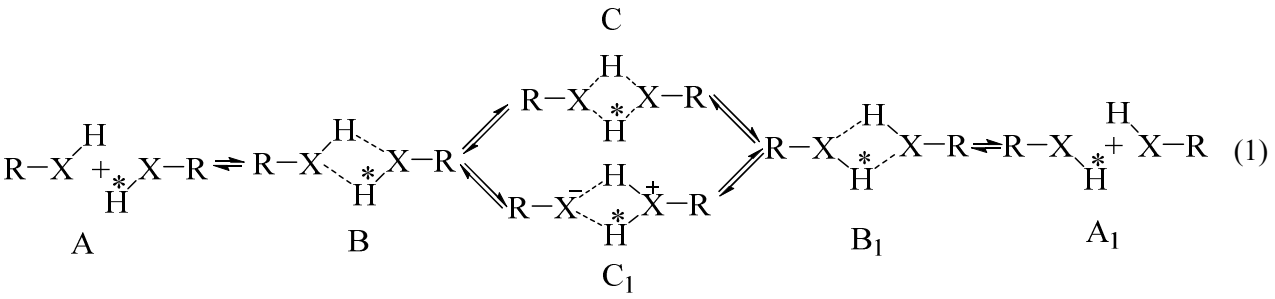

(1)

Scheme 1 shows that the initial A and final A_1 states are geometrically and energetically identical and correspond to two independent molecules of the protolith with intermolecular interaction. Hydrogen bonded cyclic complexes (dimers) B and B_1 were formed as a result of this type interaction. Synchronous double proton transfer can occur in the case of intermediate C formation -symmetric hydrogen bonded molecular complex (HBMC) and sequential proton transfer can occur in the case of intermediate C_1 formation — asymmetric hydrogen bonded ionic complex (HBIC). It was interesting to determine the proton exchange mechanism in ammonia, water and formic acid dimers by quantum chemical AM1 and *ab initio* methods and to perform their comparative analysis.

The calculation of ammonia, water and formic acidcyclic dimer structures was originally carried out (structures B and B_1 on Scheme 1). Regardless of the calculation method identical structure of the NH_3–NH_3, H_2O–H_2O, HCOOH–HCOOH cyclic complexes was obtained as a result of geometry optimization procedure. However, different length of hydrogen bridge in the same dimers were noted as a result of semiempirical or *ab initio* calculation method. Table 1 shows the structure and hydrogen bridge length R(X-X), Å, obtained as a result of quantum-chemical calculations for model associates. Table 1 also presents the literature experimental data of hydrogen bond lengths in studied cyclic associates. It can be seen from the experimental data that the hydrogen bridge length is maximal for ammonia dimer and minimal for formic acid dimer. The same relationship between the hydrogen bridge lengths was also obtained on the basis of quantum-chemical calculations.

Table 1

Structure and length of the hydrogen bridge for model dimers of ammonia, water and formic acid

Dimer	Structure of dimer	R(X-X), Å	AM1	6–31G	6–31G++	Exp./gas.p.
NH_3-NH_3	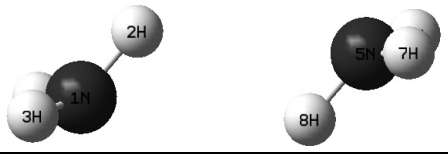	R(N1-N5)	3.48	3.27	3.32	3.27 [8]
H_2O-H_2O	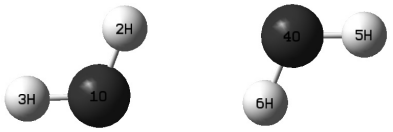	R(O1-O4)	2.68	2.67	2.68	2.76 [9]
HCOOH-HCOOH	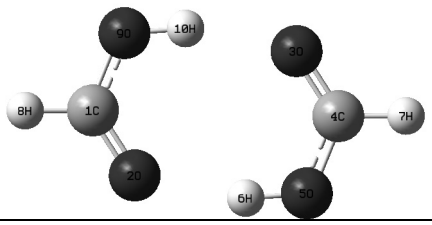	R(O9-O3)	3.06	2.72	2.74	2.73 [10]
		R(O2-O5)	3.06	2.72	2.74	2.72 [10]

It can be seen from the data presented in Table 1 that the best agreement with the experimental data on the hydrogen bridge length was obtained by *ab initio* Hartree-Fock method for ammonia and formic acid dimers. The semiempirical AM1 method gives highly overestimated distances between heteroatoms in model dimers in the same time. There is however, a large difference in the calculated and experimental data of hydrogen bridge length for water dimer. This may be a consequence of the discrepancy between the theoretical model of the dimer and the practical one. This can be cause by difference between theoretical and practical model of water dimer. Data for linear structure water associates are given in literature generally. We did not succeed in obtaining accurate experimental data about water cyclic dimer structure.

Obtained structures of dimers have been used to simulate the proton exchange reaction. It was taken that initial and final states of the reaction system (scheme 1) are geometrically and energetically identical. The search of transition state structure was carried out by using of QST2 procedure (Quadratic Synchronous Transit Approach) [11]. Table 2 shows obtained geometric structures of the proton exchange reaction transition states. It is interesting to note that the hydrogen bridge length in transition state is smaller than in original dimer in all cases.

Table 2

Geometric structures of transition states for proton exchange reaction in model dimers

Dimer	Structure of the transition state according to the method		
	AM1	6–31G	6–31G++
NH_3-NH_3	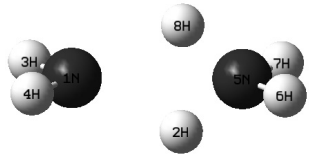 R(N1-N5) = 2.34 Å	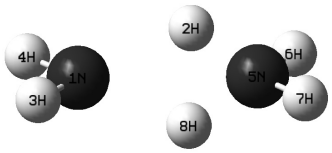 R(N1-N5) = 2.36 Å	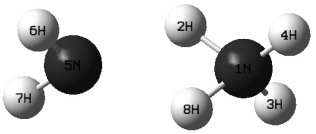 R(N1-N5) = 2.44 Å
H_2O-H_2O	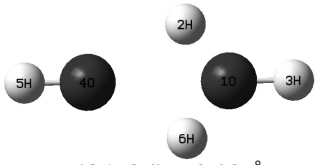 R(O1-O4) = 2.08 Å	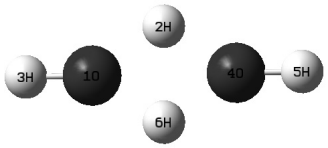 R(O1-O4) = 2.05 Å symmetrical	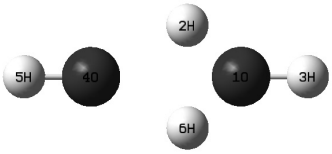 R(O1-O4) = 2.12 Å
HCOOH-HCOOH	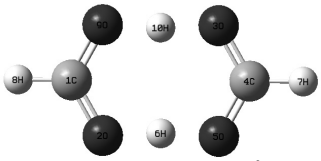 R(O2-O5) = 2.40 Å R(O3-O9) = 2.40 Å symmetrical	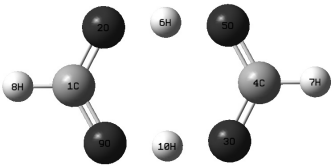 R(O2-O5) = 2.39 Å R(O3-O9) = 2.39 Å symmetrical	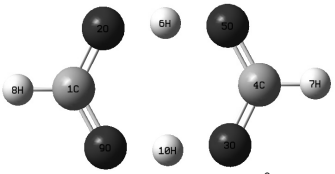 R(O2-O5) = 2.39 Å R(O3-O9) = 2.39 Å symmetrical

It can be seen from the data presented in Table 2, that there are two types of transition state: 1) symmetrical structure (structure C on scheme 1); 2) asymmetric structure (structure C_1 on scheme 1). Formation of an asymmetric structure of ion-type transition complex is observed for ammonia and water dimers (excepted for H_2O-H_2O complex calculated by 6–31G method). Formation of a symmetrical structure of molecular type transition complex is observed for dimers of formic acid. It can be assumed that symmetrical structure of transition state for proton exchange reaction is typical for dimers of acid type particles, and asymmetric structure of transition state is typical for basic type particles. Since water is ampholyte, it can form both types of transition state.

In the same time the mechanism of the proton exchange reaction will be determined by the molecular or ionic type of transition state. Synchronous double proton transfer should be expected in the case of symmetric type of transition state structure; sequential proton transfer should be expected in the case of asymmetric type of transition state structure.

The descent along the reaction coordinate was carried out by using of IRC procedure (Intrinsic Reaction Coordinate method) [11]. Figure 1 shows the reaction path diagram for proton exchange in model dimers, obtained by using of AM1 semiempirical calculation method.

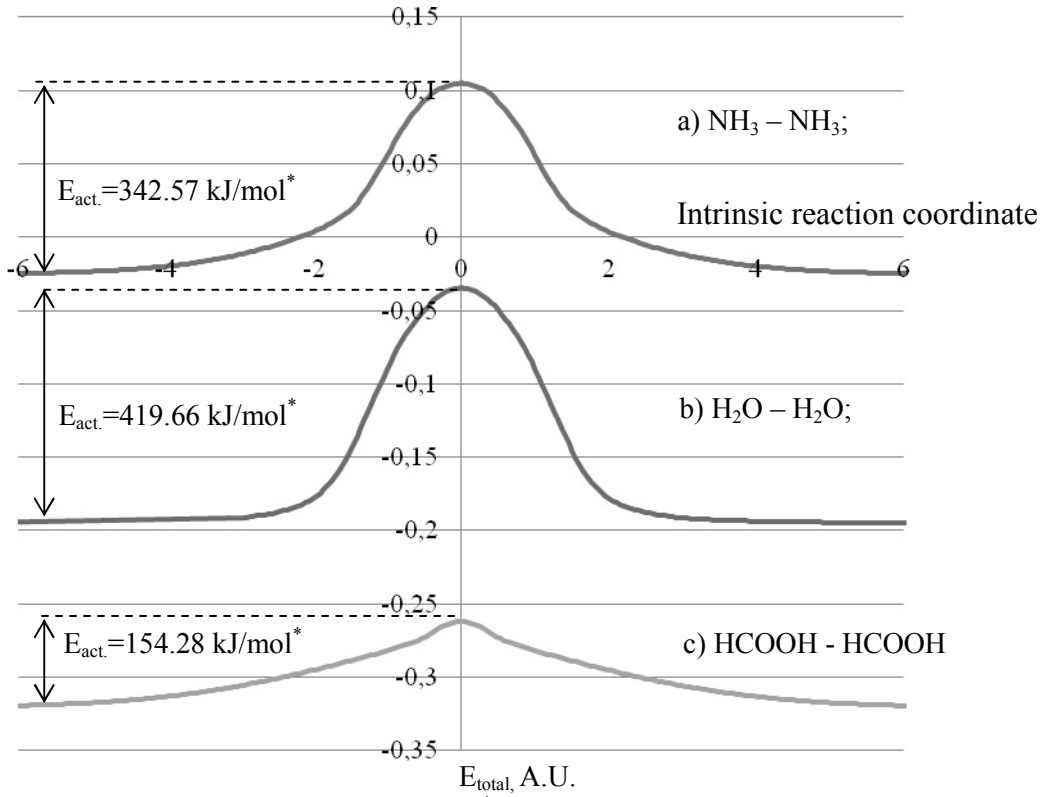

Calculation method: AM1 (*1 A.U.=2625.5 kJ/mol)

Figure 1. Reaction path diagram for proton exchange in model dimers

From graphs in Figure 1 we can see that the potential barrier height for proton exchange in water dimer is maximal, and in formic acid dimer is minimal. Activationenergyoftheproton exchange reaction was estimated as the difference in the total energies of the transition and initial states of the system. By AM1 activation energy calculations it was found 342.57 kJ/mol for ammonia dimer, 419.66 kJ/mol for water dimer and 154.28 kJ/mol for formic acid dimer. Calculated activation energy values are close to the covalent bond energy that indicates about overestimation of the hydrogen bond energy by the semiempirical AM1 method.

Reaction path diagrams for proton exchange in model dimers were obtained analogically by *ab initio* 6-31G, 6-31G++ calculations with the help of IRCprocedure. The results of calculations are shown in Figure 2.

Figure 2 shows that *ab initio* calculated curves have more acute energy peak in comparison with graphs obtained as a result of semiempirical AM1 calculation. The lower values of total energy were obtained as a result of 6–31G++ *ab initio* calculations. In the6–31G/ 6–31G++ basis set the barrier height of 282.84/272.20 kJ/mol for double proton transfer in ammonia dimer and 253.89/ 249.05 kJ/mol in water dimer and 65.40/68.18 kJ/mol in formic acid dimer was found. It should be noted that the barrier for the proton exchange in formic acid dimer obtained in the present investigation agree with the experimental results for the double proton transfer in DCOOH dimer (50.66 kJ/mol [12]). The difference in the values may be due to the difference in the phases: calculations were made for the gas phase, and the experiment was carried out for the liquid.

Thus, quantum-chemical simulation of the proton exchange reaction in model dimers of ammonia, water and formic acid was carried out by the AM1 and *ab initio* 6–31G, 6–31G++ methods. Activation energy, change of the reaction system geometry and of the hydrogen bridge length ΔR(X-X), Å were monitored during the calculations. Obtained characteristics are presented in Table 3.

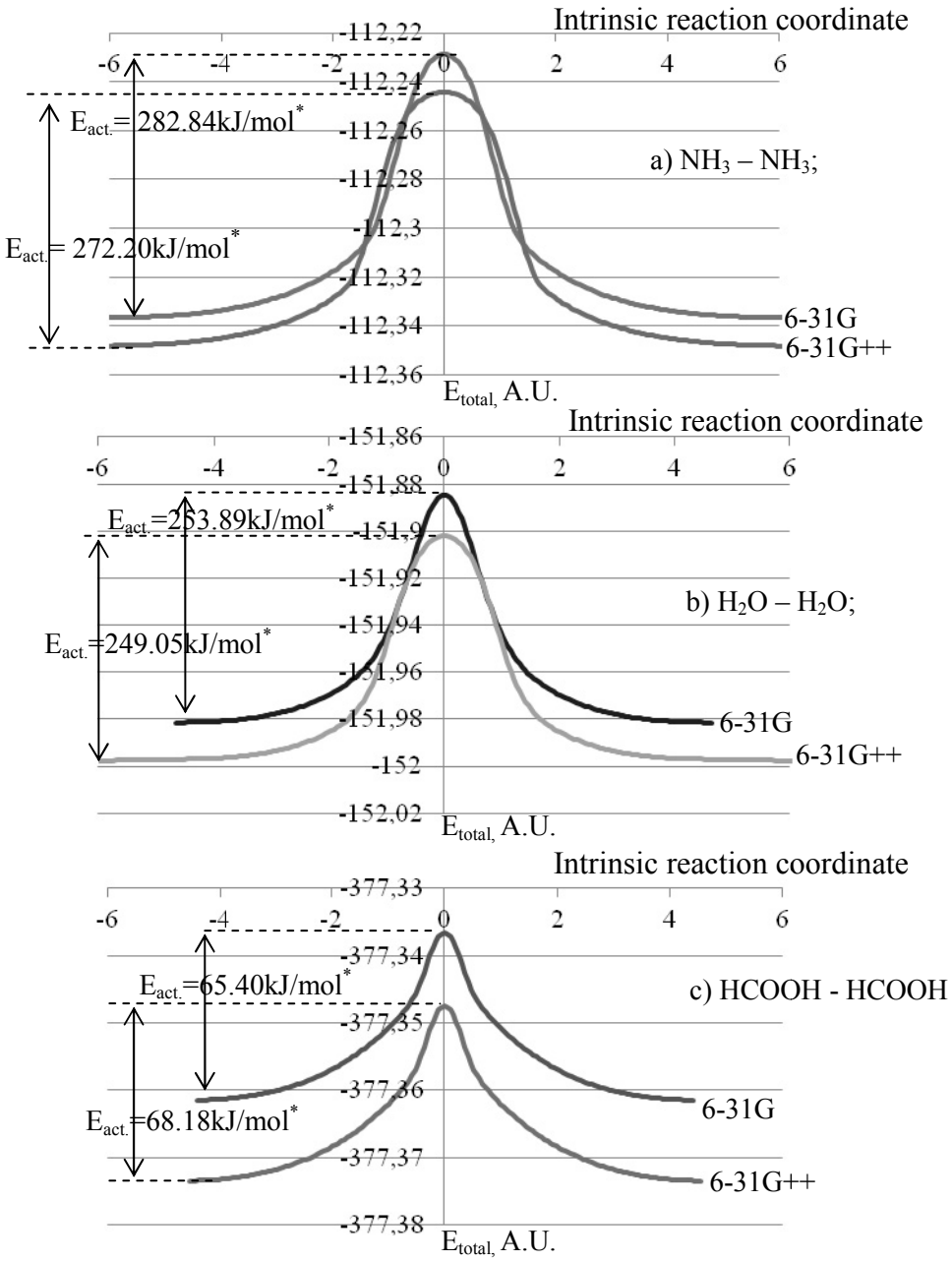

Calculation method: 6–31G, 6–31G++ (*1 A.U.=2625.5 kJ/mol)

Figure 2. Reaction path diagram for proton exchange in model dimers

Table 3

Calculated characteristics of proton exchange in model dimers of water, ammonia and formic acid

Dimer	Method					
	AM1		6–31G		6–31G++	
	$E_{act.}$, kJ/mol	ΔR(X-X), Å	$E_{act.}$, kJ/mol	ΔR(X-X), Å	$E_{act.}$, kJ/mol	ΔR(X-X), Å
Ammonia	342.57	1.14	282.84	0.91	272.20	0.88
Water	419.66	0.6	253.89	0.62	249.05	0.56
Formic acid	154.28	0.66	65.40	0.33	68.18	0.35

It can be seen from the data presented in Table 3, that the shortening of the hydrogen bridge length during the proton exchange reaction was fixed both by the semiempirical AM1 method and *ab initio* calcula-

tions. The maximum shortening of the hydrogen bridge length was observed for proton exchange in ammonia dimer (ΔR(N-N) = 0.88–1.14 Å). There are asymmetric types of transition state structure and sequential proton exchange mechanism was fixed. The minimum shortening of the hydrogen bridge length was observed for proton exchange in formic acid dimer (ΔR(O-O)=0.33–0.65 Å). There are symmetrical types of transition state structure and synchronous proton exchange mechanism was fixed.

It should be noted that the barrier height for the proton exchange in formic acid dimer is minimal. In the case of water, which is the ampholyte, a synchronous mechanism of proton exchange was recorded by 6-31G *ab initio* calculations and a sequential mechanism was showed by AM1 and 6–31G++ calculations. It was suggested that the mechanism of proton exchange reaction is determined by the nature of the resulting transition state (symmetrical or asymmetrical). At the same time, the transition state structure is determined by the acid-base properties of reaction partners.

References

1 Бурейко С.Ф. Кинетическая спектроскопия процессов протонного обмена в системах с водородной связью: дис. … д-ра физ.-мат. наук: 01.04.07 / С.Ф. Бурейко. — СПб., 2003. — 309 с.

2 Chojnacki H. Correlation effects in the double proton transfer of the formic acid dimer / H. Chojnacki // Molecular Engineering. — 1997. — No. 7. — P. 161–167.

3 Танасюк Д.А. Водородные связи и протонный обмен в системе вода-этанол / Д.А. Танасюк, В.М. Бяков, В.И. Ермаков // Успехи в химии и химической технологии. — 2014. — Т. 28, № 6 (155). — С. 111–114.

4 Буренин А.В. Классификация энергетических уровней димера аммиака / А.В. Буренин // Оптика и спектроскопия. — 2014. — Т. 116, № 4. — С. 568–572.

5 Клишин Ю.А. Строение димеров аммиака, метана, ацетилена и фтороводорода / Наука, образование, общество: тенденции и перспективы: сб. науч. тр. — М.: ООО «АР-Консалт», 2014. — С. 26–30.

6 Frisch M.J. Gaussian 09, Revision C.01 / M.J. Frisch, G.W. Trucks, H.B. Schlegel. — Wallingford: Gaussian, Inc., 2009. — 245 p.

7 Dennington R. GaussView, version 5 / R. Dennington, T. Keith, J. Millam. — Semichem Inc., Shawnee Mission, KS, 2009. — Retrieved from http://www.gaussian.com/g_tech/gv5ref/gv5citation.htm

8 Лебедев Н.Г. Устойчивые геометрические конфигурации основного и возбужденных состояний димеров воды / Н.Г. Лебедев // Вестн. Волгоград. гос. ун-та. Сер. 1. Мат., физ. — 2011. — № 1 (14). — С. 113–120.

9 Гречухина О.Н. Моделирование молекулярной динамики в димерах карбоновых кислот: автореф. дис. … канд. физ.-мат. наук: 05.13.18 — «Математическое моделирование, численные методы и комплексы программ» / О.Н. Гречухина. — Астрахань, 2009. — 22 с.

10 Даринский Б.М. Изомеры димера из молекул воды / Б.М. Даринский, В.Ф. Селеменев, Е.М. Флягина // Сорбционные и хроматографические процессы. — 2013. — Т. 13, Вып. 6. — С. 902–911.

11 Cook D.B. Handbook of Computational Quantum Chemistry / D.B. Cook. — New York: Dover Publications, 2005. — 832 p.

12 Shettya S. A quantitative and a qualitative study of the resonance assisted double proton transfer in formic acid dimer / S. Shettya, S. Pal, D.G. Kanhere, A. Goursot // Indian Journal of Chemistry. — 2006. — Vol. 45A. — P. 202–212.

И.А. Пустолайкина, К.Ж. Кутжанова, А.В. Пущина, А.Ф. Курманова

Аммиак, су және құмырсқа қышқылы димерлеріндегі протон алмасу: квантты-химиялық есептеулер

Сутегі арқылы түзілген комплекстердегі протон алмасу сутегі байланысы бар молекулалық жүйелердегі динамикалық процестерде маңызды орын алады. Бірақ осы облыстағы көптеген тәжірибелік және теориялық берілгендерге қарамастан, протон алмасудың механизмі туралы ғалымдарда бірдей көзқарас қалыптаспаған. Аммиак, су және құмырсқа қышқылы күшті қышқылнегіздік қасиеттерімен ерекшеленетін, өлшемі жағынан кішкене, протон алмасу реакцияларын теориялық модельдеуге ыңғайлы протолиттер болып табылады. Аммиак, су және құмырсқа қышқылы модельді димерлерінде протон алмасу реакцияларының квантты химиялық модельдеуі Gaussian-2009 бағдарламасының *ab initio* 6–31G, 6–31G++ базистерінде және AM1 әдістері арқылы орындалды. Ауыспалы күйдің құрылысы QST2 процедурасының көмегімен анықталды, реакция координатасы бойынша түсу IRC процедурасының көмегімен жүргізілді. Зерттеліп отырған протон алмасу реакцияларында құмырсқа қышқылы димерінің ауыспалы күйінің симметриялы құрылысы және аммиак димерінің ауыспалы күйінің асимметриялы құрылысы алынды. Протон алмасу механизмі құмырсқа қышқылы димерінде бір уақытта, ал аммиакта сатылап жүретіндігі көрсетілді. Барлық модельді жүйелерде протон алмасу реакциясы кезінде сутектік байланыс ұзындығы қысқарады. Протон алмасу механизмі түзілетін ауыспалы күйдің табиғатына (симметриялы немесе

асимметриялы) негізделген, ал оның құрылысы реакцияға түсетін заттардың қышқыл-негіздік қасиеттерімен анықталады деген болжам жасалынды.

Кілт сөздер: протон алмасу, димер, реакцияның сатылап және бір уақыттағы механизмі, сутегі байланысы арқылы түзілетін комплекс, AM1, *ab initio*, 6–31G, QST2, IRC.

И.А. Пустолайкина, К.Ж. Кутжанова, А.В. Пущина, А.Ф. Курманова

Обмен протонами в димерах аммиака, воды и муравьиной кислоты: квантово-химический расчет

Протонный обмен в водородносвязанных комплексах занимает важное место среди динамических процессов, имеющих место в молекулярных системах с водородной связью. Однако, несмотря на многочисленные экспериментальные и теоретические изыскания в данной области, единой точки зрения на механизм протонного обмена учеными не выработано. Аммиак, вода и муравьиная кислота являются небольшими по размеру протолитами с сильно различающимися кислотно-основными свойствами, удобными для теоретического моделирования реакции обмена протона. Методами AM1 и *ab initio* в базисах 6–31G, 6–31G++программы Gaussian-2009 выполнено квантово-химическое моделирование реакции протонного обмена в модельных димерах аммиака, воды и муравьиной кислоты. Поиск структуры переходного состояния осуществлен с помощью процедуры QST2, спуск по координате реакции — с помощью процедуры IRC. Для исследуемой реакции обмена протонами получено симметричное строение переходного состояния в случае димера муравьиной кислоты и асимметричное строение переходного комплекса в случае димера аммиака. Показан синхронный механизм обмена протонами в димере муравьиной кислоты, последовательный механизм в димере аммиака. Во всех модельных системах отмечено динамическое сокращение длины водородного мостика в ходе реакции протонного обмена. Сделано предположение, что механизм обмена протонами обусловливается характером образующегося переходного состояния (симметричное или асимметричное), структура которого, в свою очередь, определяется кислотно-основными свойствами реакционных партнеров.

Ключевые слова: протонный обмен, димер, последовательный и синхронный механизмы реакции, комплекс за счет водородной связи, AM1, *ab initio*, 6–31G, QST2, IRC.

References

1 Bureyko, S.F. (2003). Kineticheskaia spektroskopiia protsessov protonnoho obmena v sistemakh s vodorodnoi sviaziu [Kinetic spectroscopy of proton exchange processes in systems with a hydrogen bond]. *Doctor's thesis*. Saint Petersburg [in Russian].

2 Chojnacki, H. (1997). Correlation effects in the double proton transfer of the formic acid dimer. *Molecular Engineering*, 7, 161–167.

3 Tanasyuk, D.A., Byakov, V.M., & Ermakov, V.I. (2014). Vodorodnye sviazi i protonnyi obmen v sisteme voda – etanol [Hydrogen bonds and proton exchange in water-ethanol system]. *Uspekhi v khimii i khimicheskoi tekhnolohii. — Advances in chemistry and chemical technology, 6,* 111–114 [in Russian].

4 Burenin, A.V. (2014). Klassifikatsiia enerheticheskikh urovnei dimera ammiaka [Classification of energy levels of ammonia dimer]. *Optika i spektroskopiia. — Optics and spectroscopy, 116, 4,* 568–572 [in Russian].

5 Klishin, Yu.A. (2014). Stroenie dimerov ammiaka, metana, atsetilena i ftorovodoroda [The structure of the dimers of ammonia, methane, acetylene and hydrogen fluoride]. *Nauka, obrazovanie, obshchestvo: tendentsii i perspektivy — Science, Education, Society: Trends and Perspectives.* Moscow: OOO «AR-Konsalt» [in Russian].

6 Frisch, M.J., Trucks, G.W., & Schlegel, H.B. (2009). *Gaussian 09, Revision C.01.* Wallingford: Gaussian Inc.

7 Dennington, R., Keith, T., & Millam, J. (2009). GaussView, version 5. Semichem Inc., Shawnee Mission, KS. Retrieved from http://www.gaussian.com/g_tech/gv5ref/gv5citation.htm

8 Lebedev, N.G. (2011). Ustoichivye heometricheskie konfihuratsii osnovnoho i vozbuzhdennykh sostoianii dimerov vody [Stable geometric configurations of ground and excited states of water dimmers]. *Vestnik Volhohradskoho hosudarstvennoho universiteta. Seriia 1, Fizika i Matematika. — Volhohrad state University Bulletin. Ser. 1, Mat. and Phys, 1(14),* 113–120 [in Russian].

9 Grechukhina, O.N. (2009). Modelirovaniie molekuliarnoi dinamiki v dimerakh karbonovykh kislot [Modeling of molecular dynamics in carboxylic acids dimmers]. *Extended abstract of candidate'sthesis.* Astrakhan [in Russian].

10 Darinsky, B.M., Selemenev, V.F., & Flyagina, E.M. (2013). Izomery dimera iz molekul vody [Isomers of dimer from water molecules]. *Sorbtsionnyie i khromatohraficheskie protsessy. — Sorption and chromatographic processes, 13, 6*, 902–911 [in Russian].

11 Cook, D.B. (2005). *Handbook of Computational Quantum Chemistry*. New York: Dover Publ.

12 Shettya, S., Pal, S., Kanhere, D.G., & Goursot, A. (2006). A quantitative and a qualitative study of the resonance assisted double proton transfer in formic acid dimer. *Indian Journal of Chemistry, 45A,* 202–212.

UDC 537.531

I.E. Stas', V.Yu. Chirkova, I.A. Shtobbe

Altai State University, Barnaul, Russia
(E-mail: varvara.chirkova@gmail.com)

Experimental study of the electrical conductivity of water, dilute aqueous solutions of alkali metal chlorides and alcohols under the electromagnetic field influence

The article is devoted to the study of the influence of a high-frequency electromagnetic field on the electrical conductivity of water, aqueous solutions of alkali metal chlorides and dilute aqueous solutions of normal alcohols. A significant increase in the electrical conductivity of water and aqueous solutions under the influence of the electromagnetic field with a frequency varying in the range of 100–200 MHz is found. The effectiveness of the electromagnetic field impact depends on the frequency of the field and the time of its action. The electrical conductivity of water and aqueous solutions of alcohols increases to the greatest extent, more than twice. The effect of field influence on the electrolytes solutions is sufficiently lower and appears only for the solutions with concentrations of less than 0.01 mol/L. The maximum increase in electrical conductivity of is observed in 10^{-4}–10^{-3} M sodium chloride solutions and is 27–33 %. After the termination of the field action, the electrical conductivity of the electrolytes solutions slowly relaxes to the initial values, and the electrical conductivity of water and aqueous solutions of alcohols continues to increase for 7–10 days until a stationary value is established. The observed phenomena can be caused by a change in the structural organization of water as a result of electromagnetic interference.

Keywords: water, aqueous solutions, alkali metal chlorides, aqueous solutions of alcohols, specific conductivity, electromagnetic field, frequency, irradiation time.

Introduction

Water has a number of properties that sharply distinguish it from other liquids, and it is not yet deciphered, extremely flexible and variable structure, depending on the slightest changes in pressure, temperature, presence of impurities and various energy fields. The presence of low-energy hydrogen bonds between water molecules determines its sensitivity to external influences. However, so far, there are no theoretical and experimentally justified models and mechanisms that explain the short-term and long-term effects of energy and information impacts on water. In this connection, the actual task, in our opinion, is the identification of the mechanism of such phenomena, their relation to the structure and properties of water, and electromagnetic field influence on the water and water systems that is not directly related to changes in the chemical composition of water and aqueous solutions.

The repeatedly verified facts show that even small energy impacts and additives of various substances in a very small concentration lead to a significant change in the physicochemical properties of the systems and cause the shifts in the energy parameters of subsequent physicochemical processes tens of times higher than the energy of the activating action passed to the substance [1–4]. Changes in the structural, optical, kinetic, magnetic, and other physicochemical properties of the water systems studied have been recorded [5–11].

The purpose of this work is to study the effect of a high-frequency electromagnetic field with a frequency varying in the range of 100–200 MHz on the electrical conductivity of dilute aqueous solutions of electrolytes (alkali metal halides) and alcohols.

As the objects of investigation, solutions of lithium, sodium, potassium and cesium chlorides were chosen. According to O.Ya. Samoylov [12], the first two ions have positive hydration, and the last two ions have a negative hydration. According to the same theory, chlorine ions are negatively hydrated. Thus, it is possible to estimate the effectiveness of irradiation of solutions with different types of hydration. Solutions with a concentration of 0.001–0.0001 mol/L were studied in the work, so that the ion-ion interaction could be neglected.

Also, the solutions of propyl, butyl, and hexyl alcohols of normal structure, distinguished by the length of the hydrocarbon radical representing the hydrophobic part of the alcoholic diphilic molecule, were chosen as the objects of investigation. The structure of water-alcoholic solutions is largely determined by the structure of water and alcohols, as well as by the features of the interaction between the components in the solu-

tion. It is known that aliphatic alcohols dissolve in water in significant amounts, due to the formation of strong hydrogen bonds with water molecules. Studies show that when certain amounts of alcohol are added to water, the solution stabilization, which is mainly due to the association of particles, as well as the transition of less ordered structures to more ordered ones, is observed. Liquid water consists of areas of a certain structure, called clusters. When adding alcohol, first the voids between the clusters are filled, that leads to their stabilization, and then the molecules of alcohol begin to compete for hydrogen bonds within the clusters. Particularly easily in the structure of water small molecules of alcohol are introduced, which, falling into local molecular formations, retain the spatial arrangement of water molecules [13]. This confirms the fact that when adding alcohol to water, a decrease in the interlayer distances, compared to the same values for water, is observed. With the increasing alkyl radical, a gradual increase in the interlayer distances occurs, which proves the destructive effect of the more voluminous alcohol molecules, which is accompanied by more significant rearrangements of the molecules spatial arrangement in local water formations [14].

Electromagnetic conductivity was chosen as a response to electromagnetic interference. Previous studies have shown a significant increase of electromagnetic conductivity of water exposed to radiation [15]. In addition, previous studies indicate a change in the surface properties of normal structure aliphatic alcohols solutions [16]. The observed changes in the surface tension of these solutions may be a consequence of changes in intermolecular interactions in the volume of the solution. Alcohols are not electrolytes, therefore the electrical conductivity of water in their presence should not change. However, alcohol molecules change the supramolecular organization of water due to the so-called hydrophobic hydration that is an ordering of water structure near the hydrocarbon radical of the alcohol molecule [14]. Since a significant contribution to the electrical conductivity of water is due to the relay mechanism, which depending on a spatial orientation of water molecules, any reorientation of the solvent molecules both due to the addition of molecules of the dissolved substance (alcohol) and due to the external physical action should lead to a decrease in the activation energy of the proton hopping from this place to the next. Therefore, the study of the electrical conductivity of alcohols solutions and its changes as a result of physical effects seems to us a very promising task that allows us to expand our understanding of the physical picture of processes caused by intermolecular interaction.

Method

Deionized water purified with the deionizer of water WD-301, with an initial specific electric conductivity of $1.4–1.8 \cdot 10^{-4}$ S/m was used in this study. LiCl, NaCl, KCl, CsCl of the grade «chemically pure», propanol-1 (GOST 6006-78), butanol-1 (TU 6-09-3467) and hexanol-1 (TU 6-09-3499-87) were used. The purity of the alcohols was checked according to the values of the refractive index and surface tension, so the discrepancies between the found and tabulated values did not exceed 0.5–1.0 %.

The source of the electromagnetic field was a high-frequency generator G4–119A, which output power was 1 W and its frequency range was 30–200 MHz. The voltage at the high-frequency electrodes was 20–22 V. A cell of capacitive type was used to irradiation of water, aqueous solutions of electrolytes and alcohols. The cell consisted of a 20 ml teflon beaker, in the center of which an internal high-frequency electrode was located. The high-frequency electrode was a brass rod, isolated with teflon. The outer high-frequency electrode was an aluminum cup, closely fitting to the teflon surface. The electrodes through the bottom of the cup were connected to the generator by means of an high-frequency cable.

The conductometer CC-102/1 with platinum electrodes was used for measuring the electrical conductivity. The electrodes were stored in deionized water and periodically cleaned the surface by washing with dilute HNO_3. The cell constant, determined with use of a 0.01 M KCl solution, was equal to 51 m^{-1}. Before the experiments, the purity of the dishes (a cell, a cup) was checked according to the electrical conductivity of the deionized water.

Aqueous solutions of salts and alcohols were exposed to EMF with a variable frequency in the range of 100–200 MHz with step of 5–10 MHz. Each portion of the solution was irradiated with a field of only one predetermined frequency. The electrical conductivity values were measured every 10–30 minutes, pouring the solution into a conductometric cell.

Results and Discussion

Earlier, an increase in the specific electric conductivity (æ) of water as a result of the ultra-high-frequency electromagnetic waves influence was determined (the frequency range of 30–200 MHz was studied). The selectivity of the field action is shown. The maximum increase in æ is observed only at certain field

frequencies equal to 110, 150 and 170 MHz. The change in frequency by ± 1 MHz relative to the indicated values led to a sharp decrease in the effect.

In this paper, kinetic regularities of the field influence on water are investigated. It is established that changes in the electrical conductivity increase gradually to a certain limit, and it is the effect of «saturation». The rate of increase of the effect and the limiting values of æ depend on the frequency of the EMF. The maximum rate of increase in electrical conductivity corresponds to a frequency of 150 MHz, and its maximum value is 170 MHz. The settling time of $æ_{max}$ also varies depending on the frequency, so that is from 60 minutes for the frequency of 150 MHz, to 240 minutes for the frequency of 170 MHz (Fig. 1).

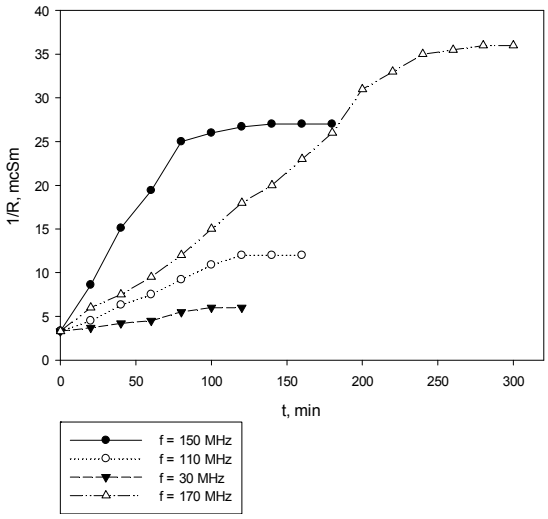

T = 296 K, cell constant a = 51 m^{-1}

Figure 1. Kinetic curves of the change in the electrical conductivity of water under the influence of the fixed frequency electromagnetic field

The values of the electrical conductivity of 10^{-4}–10^{-3}M solutions of LiCl, NaCl, KCl and CsCl are determined. Figures 2 and 3 shows the experimental values of the conductivity of solutions of these salts. Salts containing positively hydrated ions have a significantly lower electrical conductivity. At the transition from LiCl and NaCl to KCl and CsCl, the conductivity appreciably increases. The lower mobility of Li^+ and Na^+ ions is due to their high degree of hydration and, as a consequence, the large size of the hydrated ions. When the solutions are diluted 10 times, the electrical conductivity of solutions of LiCl and NaCl also decreases by approximately 10 times, and for solutions of KCl and CsCl conductivity decreases to a lesser degree.

An increase in the electrical conductivity of solutions as a result of EM impact is established. The degree of its increase depends on the nature of the electrolyte and its concentration, field frequency and duration of exposure. Proceeding from the assumption that as a result of the electromagnetic influence, the ion-dipole interaction can be weakened, which should affect the mobility of the ions, we should expect the greatest influence of the field on solutions of lithium and sodium salts. Indeed, as shown in Figure 2, the maximum increase in the electrical conductivity of millimolar solutions is observed in the case of lithium and sodium chlorides (11 and 27 %, respectively). For salts of K and Cs, the change in conductivity is negligible. The field has the least effect on the properties of KCl solutions.

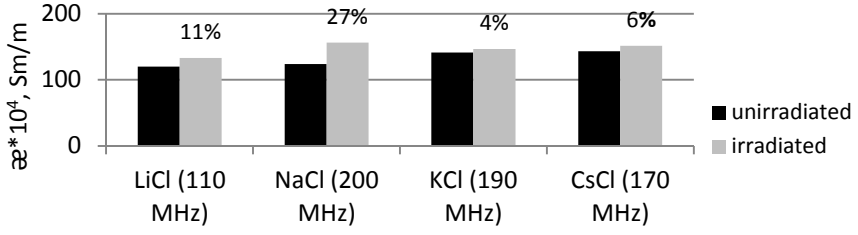

Figure 2. The maximum increase in electrical conductivity of 0.001M salt solutions as a result of electromagnetic influence (T = 295 K)

With a decrease in concentration by an order of magnitude, the effectiveness of the electromagnetic action significantly increases (Fig. 3). The effect is most noticed for NaCl.

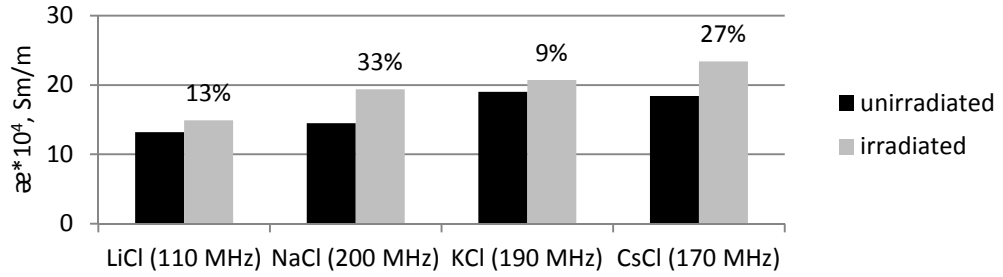

Figure 3. The maximum increase in electrical conductivity of 0.0001M salt solutions as a result of electromagnetic influence (T = 295 K)

As to the nature of the dependence of the electrical conductivity on the frequency of EMF, then clearly expressed maxima are observed for lithium and sodium salts at certain frequencies, while for potassium and cesium salts only small variations of the measured quantity are observed. At C = 10^{-4} mol/L for CsCl, a perceptible maximum of electrical conductivity for a frequency of 170 MHz is observed on this curve. Table 1 lists the frequencies of the electromagnetic field corresponding to the maximum increase in æ. They are individual for each electrolyte.

Table 1

Electromagnetic field frequencies corresponding to the maximum increase in electrical conductivity of alkali metal chlorides solutions

Electrolyte	f, MHz	
LiCl	110	160
NaCl	–	200
KCl	100	190
CsCl	90	170

Figures 4*a* and 4*b* show the concentration dependences of the effectiveness of the electromagnetic impact in the studied solutions. For the convenience of the graphical representation of the data, the molar conductivity values are given. The electrical conductivity of deci- and centimolar solutions as a result of the field action nearly does not change, and its maximum increase is observed at a concentration of 10^{-4} mol/L.

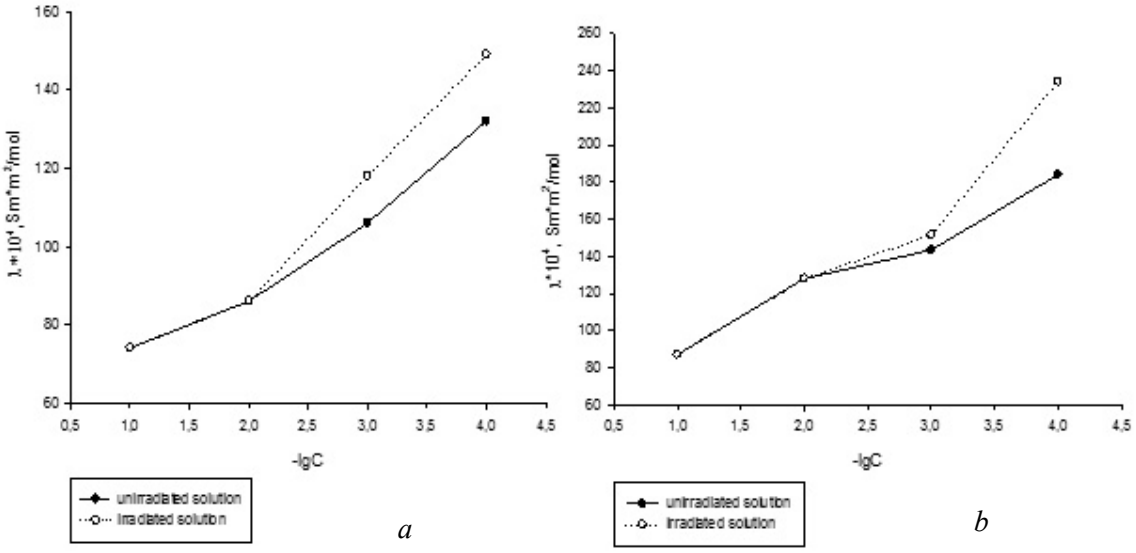

a — LiCl (f = 110 MHz); *b* — CsCl (f = 170 MHz); T = 295 K

Figure 4. The dependence of the molar conductivity on the concentration

It is established that, as in the case of water, the electrical conductivity of the solutions increases gradually over 100–110 minutes of EMF impact. Further irradiation does not affect its magnitude (Fig. 5*a*). After the termination of the action, relaxation of the conductivity to the initial value is observed (Fig. 5*b*), however, the relaxation time is a little longer than the time of the electrical conductivity increasing. It is 120–130 minutes. It should be noted that the electrical conductivity of irradiated water does not return to the initial value after the irradiation stops, but continues to increase for a week or more [7].

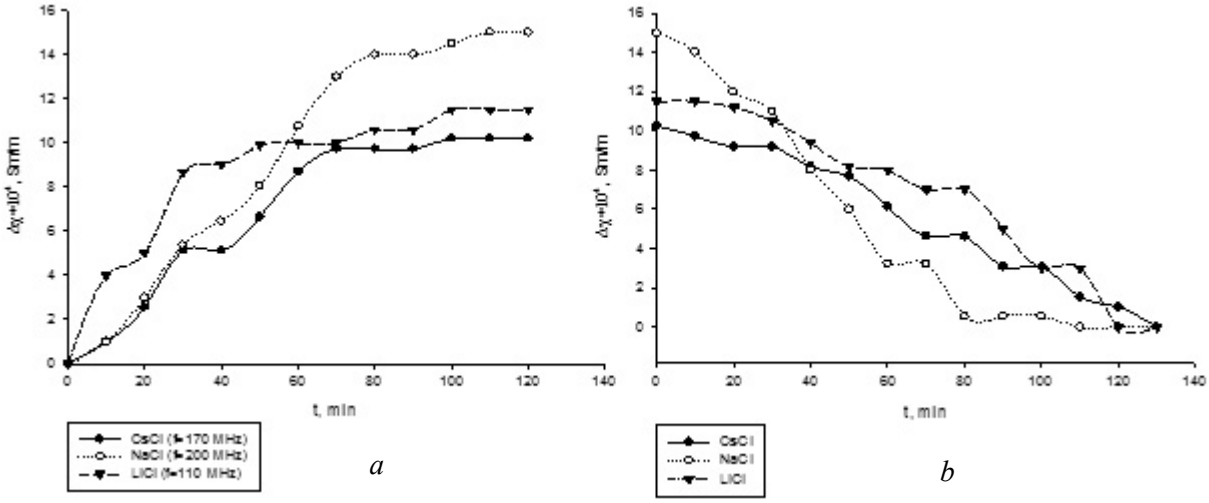

Figure 5. The change in the electrical conductivity of 0.001M electrolyte solutions ($æ_f$-$æ_0$) as a function of the irradiation time (*a*) and the time after irradiation (*b*)

Studies have shown that adding alcohols to water leads to an increase in its electrical conductivity. Table 2 gives data on the electrical conductivity of propanol-1 and butanol-1 solutions of various concentrations. It follows from the presented data that with the elongation of the hydrocarbon radical, there is slower increasing of the electrical conductivity.

Table 2

Electrical conductivity of aqueous solutions of propanol-1 and butanol-1 as a function of concentration at T = 296 K

C, mol/L	0	0.025	0.05	0.10	0.15	0.20
$æ \cdot 10^4$, S/m, propanol-1	1.25	1.73	2.09	2.29	2.61	3.21
$æ \cdot 10^4$, S/m, butanol-1	1.25	1.48	1.79	2.14	2.75	2.81

The influence of EMF leads to an increase in the conductivity of alcohols aqueous solutions. The effect is noticed only for certain field frequencies. Thus, the maximum increase in the electrical conductivity of the solution of butanol-1 is observed under the influence of EMF at a frequency of 130 and 170 MHz and is 54 % (170 MHz) at an irradiation time of 60 min (Fig. 6).

Increase in electrical conductivity during EMF influence occurs gradually. Its significant growth is observed in the first 30 minutes of EM impact. With further irradiation, a less noticed increase is observed. However, in 2 hours of irradiation, the value of the specific electrical conductivity became twice as high as its original value (Fig. 7*a*). After the field effect was stopped, the electrical conductivity of the solution was measured every day for 10 days. The electrical conductivity continued to increase and reached $11.6 \cdot 10^{-4}$ S/m (Fig. 7*b*). In the further time there were no changes. The relaxation effect was absent for 6 months. A similar picture is observed for propanol-1.

Hexanol is slightly soluble in water. Its saturated solution corresponds to a concentration of 0.03 mol/L. Studies were carried out with solutions of precisely this concentration. Tables 3 and 4 show the electrical conductivity of the hexanol solution and its variation as a function of the frequency and time of EMF influence.

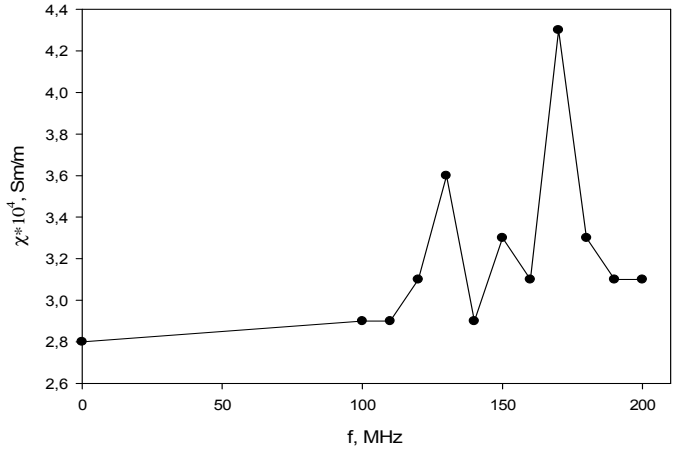

t_{irr} = 60 min, T = 296 K

Figure 6. The change in the specific electric conductivity of a 0.2 M butanol-1 solution as a result of the influence of different frequencies EMF

Table 5 presents the values of the relative electrical conductivity of water and alcohols solutions $æ_r = æ_f/æ_0$ ($æ_f$ is the specific electrical conductivity of the irradiated solution, $æ_0$ — specific electrical conductivity of the non-irradiated solution), showing the effectiveness of the electromagnetic influence, depending on its frequency. For water and butanol, the maximum increase in electrical conductivity for a 30-minute impact time corresponds to a frequency of 170 MHz, and for propanol and hexanol it is 150 MHz. In the presence of alcohol, the degree of increase in æ of water is lower.

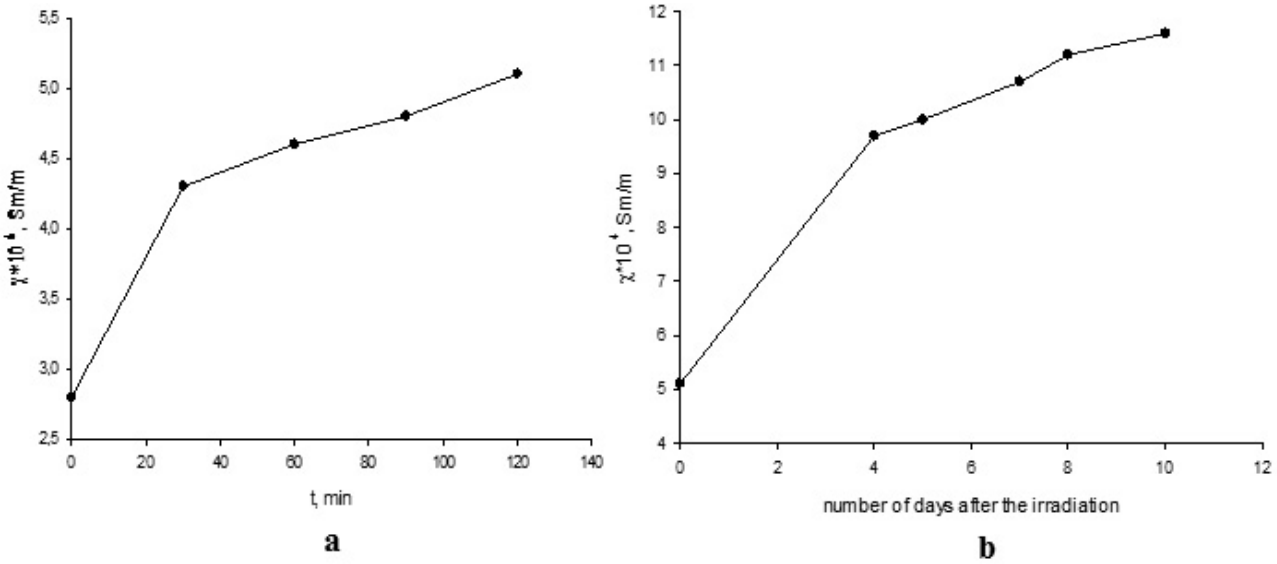

a — on the time of irradiation; *b* — on time after the irradiation; f = 170 MHz, T = 296 K

Figure 7. The dependence of the specific electrical conductivity of a 0.2 M butanol solution

Table 3

The changes in the electrical conductivity of a 0.03 M hexanol aqueous solution as a result of the influence of different frequencies EMF (t_{irr} = 30 min, T = 296 K)

f, MHz	0	130	150	155	170
$æ \cdot 10^4$, S/m	1.7	2.4	3.1	5.6	3.2

Table 4

The changes in the electrical conductivity of hexanol solutions as a function of the irradiation time (f=170 MHz, C = 0.03 M, T = 296 K)

t, min	0	30	60	90	120
æ·10^4, S/m	1.7	3.2	3.8	4.1	4.3

Table 5

The changes in the electrical conductivity of water and alcohols aqueous solutions as a result of the influence of different frequencies EMF (t_{irr} = 30 min, t = 298 K)

f, MHz	130	150	155	170
$æ_r$ water	1.13	1.22	2.65	**2.74**
$æ_r$ propanol-1(0,2M)	1.66	**2.54**	1.74	1.55
$æ_r$butanol-1 (0,2M)	1.29	1.18	1.28	**1.54**
$æ_r$ hexanol-1 (0,03M)	1.39	**2.06**	1.46	1.88

The increase in the conductivity of halides of salts solutions can be explained from the viewpoint of strengthening the structure of water as a result of electromagnetic influence. When the interaction energy of the water molecules increases, the interaction between them and the ions of the dissolved substance is weakened, so the degree of hydration of ions decreases. Since the mobility of the ions depends on their size, the ion, partially devoid of the hydrated shell, moves faster in the aqueous medium. This fact was confirmed in [17], where an increase in the diffusion coefficients of heavy metal ions as a result of the field action is shown. It is obvious that for the K^+ and Cs^+ ions with negative hydration the effect should appear to the minimum degree, which was experimentally detected (Fig. 2). This assumption seems to be contradicted by the data presented in Figure 3, where the maximum increase in electrical conductivity is observed in the presence of Cs^+ ions. However, at an electrolyte concentration of 10^{-4} mol/L, the electrical conductivity of its solution is comparable to the conductivity of water, and the experimentally recorded increase in it can be the consequence of the increase in the electrical conductivity of water, rather than the mobility of cesium ions. An increase in the electrical conductivity of water can be the result of a change in its structural organization, which changes the activation energy of the proton hopping from one position to another during the relay mechanism of water conductivity.

Since the acid properties of alcohols are less than in water, the observed increase in the electrical conductivity of their aqueous solutions can be due only to an increase in the mobility of hydrogen and hydroxyl ions formed as a result of partial dissociation of water molecules. As follows from the literature data [14], alcohols regulate the water structure as a result of hydrophobic hydration, which facilitates the movement of protons and hydroxyl ions along the hydrogen bond network. Hydrophobic hydration is the effect of interaction of nonpolar molecules or groups with the initial or transformed aqueous tetrahedral network. The most common case of hydrophobic hydration is solutions of substances, such as alcohols, whose molecules are heterofunctional. As follows from [2, 3], the hydrocarbon groups of alcohol molecules are located in the voids of the water structure, while the hydroxyl groups are integrated in the network of its hydrogen bonds. Stabilization of the water structure is primarily determined by the strengthening of hydrogen bonds near nonpolar groups, which is equivalent to lowering the water temperature. According to Anderson and Simons[18], the presence of tertiary butanol in water at a concentration of 0.06 mole fraction exerts the same effect on its lattice as a decrease in temperature by 15 °C. In the opinion of the authors of [5, 6], the introduction of dissolved non-electrolyte molecules into the water lattice leads to its complete restructuring and hardening of the water structure. Glew et al. [19] concluded that dilute aqueous solutions at low temperatures consist of molecules of a solute stabilizing the attached water and ordered hydrogen-bonded cells. This structuring of the solution, in the opinion of these authors, is the fundamental reason for the anomalous concentration dependence of enthalpy, heat capacity, sound absorption rate, solubility of inert gases, etc.

It can be assumed that the energy of the electromagnetic field absorbed by the solution is expended on strengthening the hydrogen bonds between water molecules. In the presence of alcohol, due to hydrophobic interactions, water is already partially structured, so the effectiveness of the field effect is lower. The ion-dipole interaction in electrolyte solutions is even stronger, so the energy of the electromagnetic field is sufficient to overcome it, only in extremely dilute solutions.

A distinctive feature of the field influence on water, aqueous solutions of alkali metal salts and alcohols is also the fact that after termination of field influence the electrical conductivity of saline solutions slowly relaxes to the initial values, and the electrical conductivity of water and alcohol solutions continues to increase throughout the week, maintaining its increased value over the 6 months and more. If the first effect can be explained by the thermal motion impact, which destroys the structure of the electrolyte solution changed as a result of the EMF influence, then the «aftereffect» is much more difficult to explain. Since water is not an absolutely pure liquid, it always contains a certain amount of dissolved gases, it can be assumed that as a result of EMF influence, not only changes in the structural organization of water occur, but also its degassing. The theory of degassing of water under the EMF influence was developed by Shatalov [20]. From the viewpoint of this theory, some experimental facts can be explained. The process of formation of gas bubbles and their reverse sedimentation proceed slowly enough. Gas bubbles adsorb on their surface ions, present in small amounts in water. When these bubbles are removed from the volume of the aqueous medium, desorption of the ions occurs, which increases the electrical conductivity of the water. In salt solutions, the solubility of gases decreases, and the effect of the field influence is much lower. However, this theory does not explain why in the presence of dissolved substances the maximum change in the electrical conductivity of water depends on the nature of the dissolved substance. Therefore, the «after effect» needs further careful study to identify its nature.

Conclusions

Thus, the research has shown that at the influence of an electromagnetic field the electrical conductivity of water changes to the greatest degree. Additions of electrolytes or non-electrolytes reduce the effectiveness of electromagnetic interference. The influence of EMF on the electrical conductivity of electrolytes solutions is to a much lesser degree as compared with alcohols solutions and increases with dilution of solutions. The effect of increasing the electrical conductivity disappears even at an electrolyte concentration $C \geq 0.01$ mole/L, while for non-electrolytes solutions it is significant at a concentration of 0.2 mol/L and is close in magnitude to the effect of the field influence on pure water.

References

1 Мокроусов Г.М. Физико-химические процессы в магнитном поле / Г.М. Мокроусов, Н.П. Горленко. — Томск: Изд-во ТГУ, 1988. — 128 с.

2 Классен В.И. Омагничивание водных систем / В.И. Классен. — М.: Химия, 1982. — 128 с.

3 Рахманин Ю.А. Вода — космическое явление / Ю.А. Рахманин, В.К. Кондратов. — М.: РАЕН, 2002. — 402 с.

4 Segtnan V.H. Studies on the structure of water using two-dimensional near-infrared correlation spectroscopy and principal component analysis / V.H. Segtnan, S. Sasic, T. Isaksson // Analitical Chem. — 2001. — Vol. 73, No.13. — P. 3153–3161.

5 Portier C.J. Assessment of Health Effects from Exposure to Power-Line Frequency Electric and Magnetic Fields / C.J. Portier, M.S. Wolfe. — USA: NIH Publ., 1998. — 67 p.

6 Гапочка Л.Д. Воздействие электромагнитного излучения КВЧ- и СВЧ-диапазонов на жидкую воду / Л.Д. Гапочка, М.Д. Гапочка, А.Ф. Королев // Вестник МГУ. Сер. Физика, астрономия. — 1994. — Т. 35, № 4. — С. 71–76.

7 Бучаченко А.Л. Химия на рубеже веков. Свершения и прогнозы / А.Л. Бучаченко // Успехи химии. — 1999. — Т. 68, № 2. — С. 99–118.

8 Киргинцев А.Н. К вопросу о влиянии магнитного поля на физико-химические свойства растворов / А.Н. Киргинцев, В.М. Соколов, В.И. Ханаев // Журнал физической химии. — 1968. — Т. 48. — С. 301–303.

9 Красиков Н.Н. Действие электромагнитного поля на жидкости, осуществляемое без контакта с потенциалозадающими электродами / Н.Н. Красиков, О.В. Шуваева // Журнал физической химии. — 2000. — Т. 74, № 6. — С. 1133–1135.

10 Лобанов А.И. Параметрический резонанс и формирование диссипативных структур в растворах электролитов при воздействии периодического электрического поля / А.И. Лобанов, Т.К. Старожилова, А.П. Черняев // Журнал физической химии. — 2000. — Т. 74, № 11. — С. 2087–2092.

11 Красиков Н.Н. Влияние электрического поля на ионный состав водных растворов / Н.Н. Красиков // Журнал физической химии. — 2002. — Т. 76, № 3. — С. 567–568.

12 Самойлов О.Я. Структура водных растворов электролитов и гидратация ионов / О.Я. Самойлов. — М.: Изд-во АН СССР, 1957. — 144 с.

13 Белоусов В.П. Термодинамика водных растворов неэлектролитов / В.П. Белоусов, М.Ю. Панов. — Л.: Химия, 1983. — 264 с.

14 Крестов Г.А. Термодинамика процессов в растворах / Г.А. Крестов. — Л.: Химия, 1984. — 272 с.

15 Бессонова А.П. Частотная дисперсия физико-химических свойств воды, подвергшейся ЭМ воздействию / А.П. Бессонова, И.Е. Стась // Известия вузов. Химия и химическая технология. — 2010. — Т. 53, № 4. — С. 48–50.

16 Стась И.Е. Влияние электромагнитного поля на величину адсорбции спиртов из водных растворов / И.Е. Стась, В.Ю. Чиркова // Известия АлтГУ. — 2012. — Т. 2, № 3. — С. 138–141.

17 Стась И.Е. Электродные процессы в высокочастотном электромагнитном поле / И.Е. Стась, Б.П. Шипунов, Т.С. Ивонина // Известия вузов. Сер. Химия и хим. технология. — 2003. — Т. 45, № 5. — С. 61–66.

18 Anderson R.C. Study of the influence of the presence of alcohols on water structure / R.C. Anderson, M.C.R. Simons // Trans. Faraday Soc. — 1969. — Vol. 65, No.10. — P. 2550–2557.

19 Glew D.N. Hydrogen-Bonded Solvent Systems / D.N. Glew, H.D.Mak; Ed. by A.K. Covington & P. Jones. — London, United Kingdom, 1968. — 264 p.

20 Шаталов В.М. Дегазация биожидкостей как механизм биологического действия слабых электромагнитных полей / В.М. Шаталов // Біофізичний вісник. — 2009. — Т. 23, № 2. — С. 74–86.

И.Е. Стась, В.Ю. Чиркова, И.А. Штоббе

Сілтілі металл хлоридінің су, сумен араластырған және спирттің электрөткізгіштігі және оның электрмагниттік өрістері әсерінен өзгеруі

Мақала жоғары жиілік электрмагнитті өрістің су, сілтілі металл хлоридтің сулы ерітінділердің құрылымды спирттік электрөткізгіштігіне әсерін зерттеуге арналған. Су ерітінділері мен су электрөткізгіштігі 100–200 МГц аралағында электромагнитті өріспен әсер еткенде су және сулы ерітінділердің электрөткізгіштігі едәуір өсетіні байқалады. Электрмагниттік ықпалдың тиімділігі өріс жиілігі мен оған әсер ету уақытынан тәуелді. Яғни, су және су ерітінділері электрөткізгіштігі екі есеге артады. 0,01 моль/л аз мөлшердегі ерітіндіде өріс тиімділігі көрініс табады және хлорид натриі ерітіндісінде 10^{-4}–10^{-3} М электрөткізгіштік едәуір жоғарылап, 27–33 % құрайды. Әсерді тоқтатқан жағдайда электролит ерітінділері электрөткізгіштігі өз бастапқы мәндеріне болады, ал су мен спиртті ерітінділерінің электрөткізгіштігі 7–10 күн аралығында артады. Байқалған құбылыстарды суқұрылымының өзгерісімен түсіндіруге болады.

Кілт сөздер: су, су ерітінділері, сілтілі металл хлоридтері, спирттердің су ерітінділері, электрөткізгіштік, электрмагниттік өріс, жиілік, сәулелену уақыты.

И.Е. Стась, В.Ю. Чиркова, И.А. Штоббе

Электропроводность воды, разбавленных водных растворов хлоридов щелочных металлов и спиртов и ее изменение в результате воздействия электромагнитного поля

Статья посвящена изучению влияния высокочастотного электромагнитного поля на электропроводность воды, водных растворов хлоридов щелочных металлов и разбавленных водных растворов спиртов нормального строения. Установлено, что при воздействии электромагнитного поля с варьируемой в диапазоне 100–200 МГц частотой наблюдается значимое увеличение электропроводности воды и водных растворов. Эффективность электромагнитного воздействия зависит от частоты поля и времени его воздействия. В наибольшей степени возрастает электропроводность воды и водных растворов спиртов — более, чем в два раза. Эффект полевого воздействия на растворы электролитов проявляется лишь при концентрации раствора, меньшей 0,01 моль/л, и выражен в меньшей степени — максимальное увеличение электропроводности наблюдается в 10^{-4}–10^{-3} М растворах хлорида натрия и составляет 27–33 %. После прекращения воздействия электропроводность растворов электролитов медленно релаксирует к исходным значениям, а электропроводность воды и водных растворов спиртов продолжает возрастать на протяжении 7–10 дней до установления стационарного значения. Наблюдаемые явления могут быть обусловлены изменением структурной организации воды в результате электромагнитного воздействия.

Ключевые слова: вода, водные растворы, хлориды щелочных металлов, водные растворы спиртов, удельная электропроводность, электромагнитное поле, частота, время облучения.

References

1 Mokrousov, G.M., & Gorlenko, N.P. (1988). *Fiziko-khimicheskie protsessy v mahnitnom pole [Physicochemical processes in a magnetic field]*. Tomsk: Tomsk State Univ. Publ. [in Russian].

2 Klassen, V.I. (1982). *Omahnichivanie vodnykh sistem [Magnetization of water systems]*. Moscow: Khimiia [in Russian].

3 Rahmanin, Yu.A., & Kondratov, V.K. (2002). *Voda — kosmicheskoe yavlenie [Water is a cosmic phenomenon]*. Moscow: RAEN [in Russian].

4 Segtnan, V.H., Sasic, S., Isaksson, T., & Ozaki, Y. (2001). Studies on the structure of water using two-dimensional near-infrared correlation spectroscopy and principal component analysis. *Analitical Chem., 73(13)*, 3153–3161.

5 Portier, C.J., & Wolfe, M.S. (1998). *Assessment of Health Effects from Exposure to Power-Line Frequency Electric and Magnetic Fields*. USA: NIH Publ., 67.

6 Gapochka, L.D., Gapochka, M.D., & Korolev, A.F. (1994). Vozdeistvie elektromahnitnoho izlucheniia KVCH- i SVCH-diapazonov na zhidkuiu vodu [Effect of electromagnetic radiation of EHF- and microwave ranges on liquid water]. *Vestnik MGU. Ser. Fiz. Astron. — Herald of Moscow University. Ser. Phys. and Astron., 35(4)*, 71–76.

7 Buchachenko, A.L. (1999). Khimiia na rubezhe vekov. Sversheniia i prohnozy [Chemistry at the turn of the century. Accomplishments and forecasts]. *Uspekhi khimii — Successes of chemistry, 68, 2,* 99–118 [in Russian].

8 Kirgincev, A.N., Sokolov, V.M., & Hanaev, V.I. (1968). K voprosu o vliianii mahnitnoho polia na fiziko-khimicheskie svoistva rastvorov [To the question of a magnetic field influence on the physicochemical properties of solutions]. *Zhurnal fizicheskoi khimii — Journal of Phys. Chem., 48,* 301–303 [in Russian].

9 Krasikov, N.N., & Shuvaeva, O.V. (2000). Deistvie elektromahnitnoho polia na zhidkosti, osushchestvliaemoe bez kontakta s potentsialozadaiushchimi elektrodami [The influence of an electromagnetic field on a liquid, realized without contact with potential-setting electrodes]. *Zhurnal fizicheskoi khimii — Journal of Phys. Chem., 74, 6,* 1133–1135 [in Russian].

10 Lobanov, A.I., Starozhilova, T.K., & Chernyaev, A.P. (2000). Parametricheskii rezonans i formirovanie dissipativnykh struktur v rastvorakh elektrolitov pri vozdeistvii periodicheskoho elektricheskoho polia [Parametric resonance and the formation of dissipative structures in electrolyte solutions under the action of a periodic electric field]. *Zhurnal fizicheskoi khimii — Journal of Phys. Chem., 74, 11,* 2087–2092 [in Russian].

11 Krasikov, N.N. (2002). Vliianie elektricheskoho polia na ionnyi sostav vodnykh rastvorov [Influence of the electric field on the ionic composition of aqueous solutions]. *Zhurnal fizicheskoi khimii — Journal of Phys. Chem., 76, 3,* 567–568 [in Russian].

12 Samoylov, O.Ya. (1957). *Struktura vodnykh rastvorov elektrolitov i hidratatsiia ionov [Structure of aqueous solutions of electrolytes and hydration of ions]*. Moscow: Izdatelstvo AN SSSR [in Russian].

13 Belousov, V.P., & Panov, M.Yu. (1983). *Termodinamika vodnykh rastvorov neelektrolitov [Thermodynamics of aqueous solutions of non-electrolytes]*. Leningrad: Khimiia [in Russian].

14 Krestov, G.A. (1984). *Termodinamika protsessov v rastvorakh [Thermodynamics of processes in solutions]*. Leningrad: Khimiia [in Russian].

15 Bessonova, A.P., & Stas', I.E. (2010). Chastotnaia dispersiia fiziko-khimicheskikh svoistv vody, podverhsheisia EHM vozdeistviiu [Frequency dispersion of physico-chemical properties of water exposed to EM impact]. *Izvestiia vuzov. Khimiia i khimicheskaia tekhnolohiia — Reviews of HEI. Chemistry and chemical technology, 53, 4,* 48–50 [in Russian].

16 Stas', I.E., & Chirkova, V.Yu. (2012). Vliianie elektromahnitnoho polia na velichinu adsorbtsii spirtov iz vodnykh rastvorov [Influence of the electromagnetic field on the amount of adsorption of alcohols from aqueous solutions]. *Izvestiia AltGU — Reviews of Altay State University, 2, 3,* 138–141 [in Russian].

17 Stas', I.E., Shipunov, B.P., & Ivonina, T.S. (2003). Elektrodnye protsessy v vysokochastotnom elektromahnitnom pole [Electrode processes in a high-frequency electromagnetic field]. *Izvestiia vuzov. Ser. Khimiia i khim. tekhnolohiia — Reviews of HEI. Chemistry and Chemical Technology, 45, 5,* 61–66 [in Russian].

18 Anderson, R.C., & Simons, M.C.R. (1969). Study of the influence of the presence of alcohols on water structure. *Trans. Faraday Soc.*, *65(10)*, 2550–2557.

19 Glew, D.N., & Mak, H.D. (1968). *Hydrogen-Bonded Solvent Systems*. A.K. Covington and P. Jones (Eds.). London, United Kingdom.

20 Shatalov, V.M. (2009). Dehazatsiia biozhidkostei kak mekhanizm biolohicheskoho deistviia slabykh elektromahnitnykh polei [Degassing of biofluids as a mechanism of the biological effect of weak electromagnetic fields]. *Biofizichnii visnik — Biophysical bulletin, 23, 2,* 74–86 [in Russian].

UDC 541.6

V.V. Vazhev[1], B.G. Munarbaeva[1], E.M. Yergaliyeva[2], N.V. Vazheva[2], M.A. Gubenko[2]

[1]Z. Aldamzhar Kostanay Social and Technical University, Kazakhstan;
[2]Kostanay State Pedagogical Institute, Kazakhstan
(E-mail: v.vazhev@gmail.com)

Modeling of acute aqueous toxicity of organic compounds for *Daphnia magna*

Methods for the assessment of the environmental hazard of chemicals include the detection of acute aquatic toxicity of compounds for various small organisms, these are test objects. Experimental determination of toxicity presents significant difficulties; therefore, computational methods are developed. The article is devoted to predicting the toxicity parameter of organic substances of different classes in relation to the test organism from the class of crustaceans *Daphnia magna*. The possibility of using QSAR / QSTR (Quantitative Structure Activity Relationships / Quantitative Structure Toxicity Relationships) method for estimating the toxicity index of pLC_{50} using a large set of descriptors was investigated. To describe the structure of molecules, a set of 2644 descriptors generated by the Dragon 7 program was used. The calculations were carried out using the computer program Program Robustness Calculation (PROGROC). This program allows the number of descriptors to be used without preliminary selection exceeding the number of substances in the set. 546 Substances were used to construct the models, 170 compounds of which made up a control set, and 376 entered the training set. The obtained models are characterized by a high correlation between calculation and experiment. For a control sample of 170 compounds, the correlation coefficient is R = 0.952 and the standard deviation is s = 0.45, for a training sample of 376 compounds, R = 0.971 and s = 0.41. The model for all samples is characterized by the following statistical parameters: correlation coefficient is R = 0.966 and standard deviation is s = 0.42.

Keywords: organic compounds, toxicity, modeling, QSAR/ QSTR, predicting, pLC_{50}, *Daphnia magna,* PROGROC.

Introduction

Determination of acute toxicity of chemical compounds in relation to test objects is one of the methods for assessing the environmental hazard of substances. *Daphnia magna* daphnoids are often used as the objects of investigation. They are small organisms of the crustacean class.

Toxicity is usually assessed by the quantitative parameter LC_{50}, a semilethal concentration (mol/L), which causes half of the population to die within 24 (or 48) hours of exposure. The attractiveness of *Daphnia magna* as a test object is mainly due to the fact that it is grown without any special difficulties in the laboratory and is fairly stable in them, it gives a whole complex of test reactions and has a short life cycle that allows tracing the effects of toxic effects over a number of generations. Biotests on *Daphnia magna* are standardized in a number of countries. Nevertheless, like any experimental study, the definition of LC_{50} is a costly procedure. Therefore, alternative methods based on quantitative structure-activity relationships, such as QSAR-methods (Quantitative Structure Activity Relationships), are developed. In such studies, the measure of toxicity is $pLC_{50} = -\lg (LC_{50})$ — the toxicity parameter. The quality of calculations (modeling, prediction, estimation) is characterized by the correlation coefficient between the predicted and experimental values of the toxicity parameter R (or R^2) and the standard deviation s.

Vighi and Calamari [1] carried out one of the first studies on several organotin compounds using physical and topological parameters. Equations with a significant correlation $R^2 = 0.26–0.99$ and high prognostic ability were found. In [2] on the quantum-mechanical molecular descriptors, the toxicity models were constructed for 15 organophosphorus compounds with a correlation index of $0.80 < R^2 < 0.82$. In addition, the potential toxicity of 83 unstudied compounds was detected.

Cassani and Kovarich [3] simulated the toxicity of 97 triazoles and benzotriazoles using the multiple linear regression method with a maximum $R^2 = 0.83$. Moosus and Maran [4] in the study of 253 compounds of different classes reached the maximum value $R^2 = 0.74$ of all the models obtained. Toropov and Benfenati [5] have used topological indices as descriptors for predicting the toxicity of 262 pesticides. The best model had $R^2 = 0.7822$ and s = 0.849 for a training set of 220 substances and $R^2 = 0.7388$, s = 0.941 for a control set of 42 substances. Toropova et al. [6] used descriptors as functions of representing the structure of compounds in simplified molecular input line entry system (SMILES) and obtaining models with the highest value $R^2 = 0.7322$. Another article by Toropova et al. [7] used a hybrid representation of the structure of mole-

cules through SMILES and hydrogen-suppressed graph. The results for the obtained models are comparable with those of [6], while it was noted that hybrid descriptors are the best predictors.

Katritzky et al. [8] modeled the toxicity of EC_{50} against *Daphnia magna* for a series of 130 benzoic acids, benzaldehydes, phenylsulfonyl acetates, cycloalkane-carboxylates, benzanilides, and other esters. A general model with five descriptors, including all 130 compounds, was characterized by the following statistical parameters such as $R^2 = 0.712$, s = 0.6. Kar, Roy [9] investigated a large group of 297 chemical compounds, predictors were three-dimensional (electronic and spatial) and two-dimensional topological and information content indices, as well as n-octanol/water partition coefficient. When dividing the set into a training set of 222 substances and a control set of 75, the maximum value $R^2 = 0.75$ is reached. Kühne et al. [10] investigated a large collection of 1365 organic compounds with experimental data of toxicity and noted contradictions in the part of data obtained from various sources. They obtained local models for subsets of the entire set, with the maximum values $R^2 = 0.85$ and s = 0.66.

Cassotti et al. [11] subjected the existing toxicity data sets to examination and formed a MICHEM set of 546 substances that were most spared from discrepancies in the experimental data from various sources. When this set was divided into a training set of 436 substances and a control set of 110, they obtained a model with $R^2 = 0.78$.

Commenting the current state of the prediction of acute toxicity of chemical compounds for *Daphnia magna*, it can be noted that for heterogeneous and large sets of substances, the quality of forecasting cannot be considered sufficiently successful.

Assuming that the quality of predicting can be improved by increasing the number of descriptors and improving the computational technology, in this work we used a large set of 2644 descriptors generated by the Dragon 7 program to predict the pLC_{50} for *Daphnia magna*. The pLC_{50} toxicity values for *Daphnia magna* are derived from the appendix to the article [11].

Calculations were performed using the PROGROC (PROGgram RObustness Calculation) computer program developed by us [12], which was successfully applied to predict some parameters of biological activity, in particular, toxicity of organic compounds for *Tetrahimena pyriformis* [13]. An important and unique feature of this program is the possibility of using without a preliminary selection the number of descriptors exceeding the number of substances.

A number of models were built, for one of them the results of pLC_{50} prediction are shown in Figures 1 and 2. The training set included 376 compounds, the control set — 170. The statistical parameters of the model are given in Table 1.

Table 1

Correlation between the experimental and calculated pLC_{50} values

Correlation	Full set	Training set	Control set
R	0.966	0.971	0.952
s	0.42	0.41	0.45
Amount of substances	546	376	170

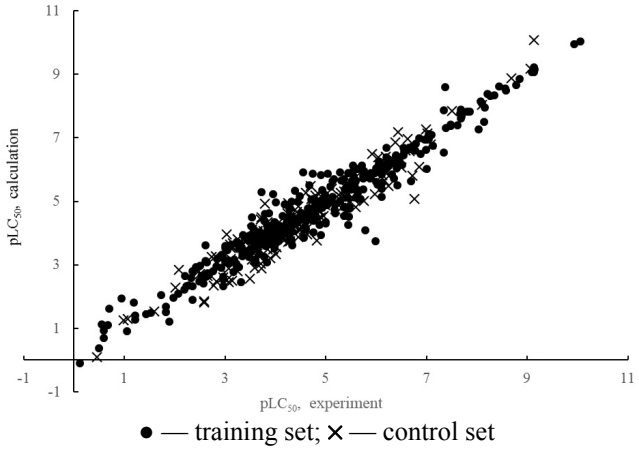

Figure 1. Correlation between the experimental values of pLC_{50} and calculated by molecular descriptors for the training and control sets

The frequency distribution of pLC_{50} prediction errors using molecular descriptors is shown in a histogram (Fig. 2).

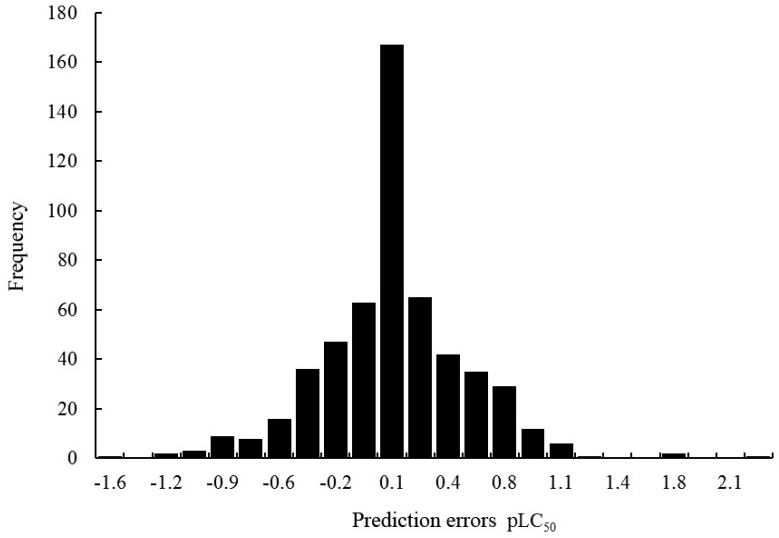

Figure 2. Histogram of frequency distribution of pLC_{50} prediction errors

The histogram of prediction error frequency distribution has edge emissions; the Table 2 shows the characteristics of the connections corresponding to these emissions.

T a b l e 2

Compounds with significant discrepancies between experimental [11] and calculated values of pLC_{50}

Compound	CAS*	Experiment	Calc.	Residual	Set
Acrylic aldehyde	107–02–8	5.99	3.74	2.25	Training
N-methylaniline	100–61–8	5.79	4.08	1.71	Training
Pyraclostrobin	175013–18–0	6.76	5.07	1.69	Control
Pendimethalin	40487–42–1	3.72	5.30	–1.57	Training
Bis(2-ethylhexyl)phthalate	117–81–7	4.55	5.92	–1.37	Training
9H-xanthene	92–83–1	3.95	5.22	–1.27	Training
Pyrethrin 2	121–29–9	7.37	8.59	–1.22	Training
1,2,4,5-Tetramethylbenzene	95–93–2	5.45	4.27	1.18	Training
Benzo[b]naphtho[1,2-d]furan	205–39–0	4.74	5.88	–1.15	Training
2-(6-Methoxy-2-naphthyl)propanoic acid	22204–53–1	3.79	4.93	–1.14	Control
Anthracene	120–12–7	6.70	5.63	1.07	Training
Methylcyclohexane	108–87–2	4.82	3.77	1.05	Control
1-Methyl-2-pyrrolidinone	872–50–4	4.91	3.93	0.98	Training
1-Propanol	71–23–8	0.94	1.95	–1.02	Training
1-Phenoxy-2-propanol	770–35–4	2.61	3.62	–1.01	Training

Note: CAS — registration number for Chemical Abstracts.

It is very likely that the listed in the table, or influencing them through links in the compound model, have errors in the experimental determination of the toxicity parameter.

Conclusion

In conclusion, we can note that the results obtained by us are superior to the literature data on the quality of predicting the toxicity parameter towards *Daphnia magna*. So, for example, in the most successful model [11], obtained on the same set of substances, but with a smaller sample size, the correlation coefficient is 0.88 ($R^2 = 0.78$).

References

1 Vighi M. QSARs for organotin compounds on *Daphnia magna* / M. Vighi, D. Calamari // Chemosphere. — 1985. — Vol. 14. — P. 1925–1932.

2 Zvinavashe E. Quantitative structure-activity relationship modeling of the toxicity of organothiophosphate pesticides to *Daphnia magna* and *Cyprinus carpio* / E. Zvinavashe, T. Du, T. Griff, H.H.J. van den Berg, A.E.M.F. Soffers, J. Vervoort et al. // Chemosphere. — 2009. — Vol. 75. — P. 1531–1538.

3 Cassani S. Daphnia and fish toxicity of (benzo)triazoles: validated QSAR models, and interspecies quantitative activity-activity modelling / S. Cassani, S. Kovarich, E. Papa, P.P. Roy, L. van der Wal, P. Gramatica // Journal of Hazardous Materials. — 2013. — Vol. 258–259. — P. 50–60.

4 Moosus M. Quantitative structure–activity relationship analysis of acute toxicity of diverse chemicals to *Daphnia magna* with whole molecule descriptors / M. Moosus, U. Maran // SAR and QSAR in Environmental Research. — 2011. — Vol. 22. — P. 757–774.

5 Toropov A.A. QSAR models for Daphnia toxicity of pesticides based on combinations of topological parameters of molecular structures / A.A. Toropov, E. Benfenati // Bioorganic & Medicinal Chemistry. — 2006. — Vol. 14. — P. 2779–2788.

6 Toropova A.P. QSAR models for toxicity of organic substances to *Daphnia magna* built up by using the CORAL freeware / A.P. Toropova, A.A. Toropov, E. Benfenati, G. Gini // Chemical Biology & Drug Design. — 2012. — Vol. 79. — P. 332–338.

7 Toropova A.P. CORAL: QSAR modeling of toxicity of organic chemicals towards *Daphnia magna* / A.P. Toropova, A.A. Toropov, S.E. Martyanov, E. Benfenati, G. Gini, D. Leszczynska et al. // Chemometrics and Intelligent Laboratory Systems. — 2012. — Vol. 110. — P. 177–181.

8 Katritzky A.R. Quantitative structure–activity relationship (QSAR) modeling of EC_{50} of aquatic toxicities for *Daphnia magna* / A.R. Katritzky, S.H. Slavov, I.S. Stoyanova-Slavova, I. Kahn, M. Karelson // Journal of Toxicology and Environmental Health, Part A. — 2009. — Vol. 72. — P. 1181–1190.

9 Kar S. QSAR modeling of toxicity of diverse organic chemicals to *Daphnia magna* using 2D and 3D descriptors / S. Kar, K. Roy // Journal of Hazardous Materials. — 2010. — Vol. 177. — P. 344–351.

10 Kühne R. Read-across prediction of the acute toxicity of organic compounds toward the water flea *Daphnia magna* / R. Kühne, R.-U. Ebert, P.C. von der Ohe, N. Ulrich, W. Brack, G. Schüürmann // Molecular Informatics. — 2013. — Vol. 32. — P. 108–120.

11 Cassotti M. Validation and extension of a similarity-based approach for prediction of acute aquatic toxicity towards *Daphnia magna* / M. Cassotti, V. Consonni, A. Mauri, D. Ballabio // SAR and QSAR in Environmental Research. — 2014. — Vol. 25(12). — P. 1013–1036.

12 Vazhev V.V. Estimation of flash points and molecular masses of alkanes from their IR spectra / V.V. Vazhev, M.K. Aldabergenov, N.V. Vazheva // Petroleum Chemistry. — 2006. — Vol. 46. — No. 2. — P. 136–139.

13 Важев В.В. Оценка токсичности органических соединений для *Tetrahymena pyriformis* методом QSAR / В.В. Важев, М.А. Губенко, Н.В. Важева, Э.М. Ергалиева, Е.А. Самсонюк // Вестн. Караганд. ун-та. Сер. Химия. — 2016. — № 3(83). — С. 39–44.

В.В. Важев, Б.Г. Мунарбаева, Э.М. Ергалиева, Н.В. Важева, М.А. Губенко

Daphnia magna үшін органикалық қосылыстардың өткір сулы улылығын модельдеу

Химиялық заттардың экологиялық қауіпсіздігін бағалау әдістерінің біріне әртүрлі ұсақ ағзалар — тест-объектілер үшін қосылыстардың өткір сулы улылығын анықтау жатады. Улылықты эксперименттік анықтау едәуір қиындықтар тудырады, сондықтан есептеу әдістері дамытылуда. Мақала әртүрлі класс органикалық заттарының улылық параметрін шаян тәрізділер класының өкілі болып табылатын *Daphnia magna* тестілік организміне қатысты болжауға арналған. Дескрипторлардың үлкен жиынтығын пайдаланып, QSAR/QSTR (Quantitative Structure Activity Relationships/ Quantitative Structure Toxicity Relationships) әдісін pLC_{50} улылық көрсеткішін бағалау үшін қолдану мүмкіндігі зерттелген. Молекулалардың құрылысын сипаттау үшін Dragon 7 бағдарламасы генерациялайтын 2644 дескрипторлар жиынтығы қолданылды. Есептеулер Program Robustness Calculation (PROGROC) компьютерлік бағдарламасы көмегімен жүргізілді. Бұл бағдарлама саны жиынтықтағы заттар санынан артық болатын дескрипторларды алдын ала іріктемей пайдалануға мүмкіндік береді. Модельдерді құру үшін 546 зат қолданылды, олардың ішінен 170 қосылыс бақылау іріктемесін, ал 376-ы жаттығу іріктемесін құрды. Алынған модельдер есептеу мен эксперимент арасындағы корреляцияның жоғары болуымен сипатталады. Бақылау іріктемесі үшін корреляция коэффициенті R = 0,952 және стандартты ауытқу s = 0,45, жаттығу іріктемесі үшін R = 0.971 және s = 0,41. Толық іріктеме үшін жасалған модель келесі статистикалық параметрлермен сипатталды: корреляция коэффициенті R = 0,966 және стандартты ауытқу s = 0,42.

Кілт сөздер: органикалық қосылыстар, улылық, болжау, QSAR/ QSTR, модельдеу, pLC_{50}, *Daphnia magna,* PROGROC.

В.В. Важев, Б.Г. Мунарбаева, Э.М. Ергалиева, Н.В. Важева, М.А. Губенко

Моделирование острой водной токсичности органических соединений для *Daphnia magna*

К числу методов оценки экологической опасности химических веществ относится выявление острой водной токсичности соединений для различных мелких организмов — тест-объектов. Экспериментальное определение токсичности представляет значительные трудности, поэтому развиваются вычислительные методы. Статья посвящена прогнозированию параметра токсичности органических веществ разных классов по отношению к тестовому организму из класса ракообразных *Daphnia magna*. Исследована возможность применения метода QSAR/QSTR (Quantitative Structure Activity Relationships/ Quantitative Structure Toxicity Relationships) для оценки показателя токсичности pLC_{50} с использованием большого набора дескрипторов. Для описания структуры молекул использован набор из 2644 дескрипторов, генерируемых программой Dragon 7. Расчеты выполнены с помощью компьютерной программы Program Robustness Calculation (PROGROC). Данная программа позволяет использовать без предварительного отбора число дескрипторов, превышающее число веществ в наборе. Для построения моделей использовано 546 веществ, из которых 170 соединений составили контрольную выборку, а 376 — вошли в тренировочную выборку. Полученные модели характеризуются высокой корреляцией между расчетом и экспериментом. Для контрольной выборки коэффициент корреляции R = 0,952 и стандартное отклонение s = 0,45, для тренировочной выборки R = 0,971 и s = 0,41. Модель для полной выборки характеризуется следующими статистическими параметрами: коэффициент корреляции R = 0, 966 и стандартное отклонение s = 0,42.

Ключевые слова: органические соединения, токсичность, моделирование, QSAR/QSTR, прогнозирование, pLC_{50}, *Daphnia magna,* PROGROC.

References

1 Vighi, M., & Calamari, D. (1985). QSARs for organotin compounds on *Daphnia magna. Chemosphere*, *14,* 1925–1932.

2 Zvinavashe, E., Du, T., Griff, T., van der Berg, H.H.J., Soffers, A.E.M.F., & Vervoort, J., et al. (2009). Quantitative structure-activity relationship modeling of the toxicity of organothiophosphate pesticides to *Daphnia magna* and *Cyprinus carpio*. *Chemosphere*, *75*, 1531–1538.

3 Cassani, S., Kovarich, S., Papa, E., Roy, P.P., van der Wal, L., & Gramatica, P. (2013). Daphnia and fish toxicity of (benzo)triazoles: validated QSAR models, and interspecies quantitative activity-activity modelling. *Journal of Hazardous Materials*, *258–259,* 50–60.

4 Moosus, M., & Maran, U. (2011). Quantitative structure–activity relationship analysis of acute toxicity of diverse chemicals to *Daphnia magna* with whole molecule descriptors. *SAR QSAR Environ. Res., 22,* 757–774.

5 Toropov, A.A., & Benfenati, E. (2006). QSAR models for Daphnia toxicity of pesticides based on combinations of topological parameters of molecular structures. *Bioorg. Med. Chem., 14,* 2779–2788.

6 Toropova, A.P., Toropov, A.A., Benfenati, E., & Gini, G. (2012). QSAR models for toxicity of organic substances to Daphnia magna built up by using the CORAL freeware. *Chem. Biol. Drug Des., 79,* 332–338.

7 Toropova, A.P., Toropov, A.A., Martyanov, S.E., Benfenati, E., Gini, G., & Leszczynska, D., et al. (2012). CORAL: QSAR modeling of toxicity of organic chemicals towards *Daphnia magna*. *Chemom. Intell. Lab. Syst., 110,* 177–181.

8 Katritzky, A.R., Slavov, S.H., Stoyanova-Slavova, I.S., Kahn, I., & Karelson, M. (2009). Quantitative structure–activity relationship (QSAR) modeling of EC_{50} of aquatic toxicities for *Daphnia magna*. *J. Toxicol. Environ. Health, Part A., 72,* 1181–1190.

9 Kar, S., & Roy, K. (2010). QSAR modeling of toxicity of diverse organic chemicals to *Daphnia magna* using 2D and 3D descriptors. *J. Hazard. Mater., 177,* 344–351.

10 Kühne, R., Ebert, R. -U., von der Ohe, P.C., Ulrich, N., Brack, W., & Schüürmann, G. (2013). Read-across prediction of the acute toxicity of organic compounds toward the water flea *Daphnia magna*. *Mol. Inform., 32,* 108–120.

11 Cassotti, M., Consonni, V., Mauri, A., & Ballabio, D. (2014). Validation and extension of a similarity-based approach for prediction of acute aquatic toxicity towards Daphnia magna. *SAR QSAR Environ. Res., 25(12),* 1013–1036.

12 Vazhev, V.V., Aldabergenov, M.K., & Vazheva, N.V. (2006). Estimation of flash points and molecular masses of alkanes from their IR spectra. *Petroleum Chemistry, 46(2),* 136–139.

13 Vazhev, V.V., Gubenko, M.A., Vazheva, N.V., Yergaliieva, E.M., & Samsoniuk, Ye.A. (2016). Otsenka toksichnosti orhanicheskikh soedinenii dlia *Tetrahymena pyriformis* metodom QSAR [Estimation of the toxicity of organic compounds to *Tetrahymena pyriformis* by QSAR method]. *Vestnik Karahandinskoho universiteta. Seriia Khimiia — Bulletin of the Karaganda University. Ser. Chemistry, 3(83),* 39–44 [in Russian].

UDC 541.11:546.244

E.S. Mustafin, D.A. Kaykenov, Kh.B. Omarov, R.Z. Kasenov,
A.T. Dyussekeyeva, S.B. Abeuova, A.S. Borsynbayev

Ye.A. Buketov Karaganda State University, Kazakhstan
(E-mail: edigemus@mail.ru)

Synthesis and electrophysical study of cobaltites of composition $LnM^{II}CoO_{3.5}$ (M^{II} — Mg, Ca, Sr, Ba)

This work is devoted to study of electrical properties, phases of $LnM^{II}CoO_{3.5}$ (M^{II} – Mg, Ca, Sr, Ba) which structure resembles to the structure of perovskite. The phases were obtained by solid-phase synthesis in accordance with the ceramic technology. The phase composition was determined by X-ray phase analysis. The diffractograms of the powders were indexed, the lattice parameters and its symmetry class were determined. It was found that the new compounds had a tetragonal symmetry, in the unit cell of which 16 structural units were located. Since complex oxides have high melting temperatures of about 1500–2000 ºC, it is impossible to obtain good quality single crystals suitable for measurements. For this reason, the study of their thermodynamic and electrophysical properties was carried out on samples in the form of sintered powders. In this study, the conductivity isotherms were measured by impedance spectroscopy at different temperatures. Resistance hodographs on the complex plane were constructed. Using the method of equivalent circuits, the grain boundaries and the bulk resistances of the sample grains were determined. The results showed that the new compounds had a small grain-boundary resistance. Using the temperature dependences, the activation energies of the conductivity of new cobaltites were calculated. The activation energy of conductivity for these compounds was 0.113–0.184 eV. The character of the dependence of the conductivity at moderate temperatures showed their thermal activation. In the Arrhenius coordinates, these sections of the graph were described by a straight line. An increase in the activation energy of the conductivity in the series of Mg^{2+}–Ca^{2+}–Sr^{2+}–Ba^{2+}cations was observed. The introduction of an alkaline earth ion with a large ionic radius led to a local distortion of the crystal lattice. This changed the value of the splitting of the d-levels of the transition metal-cobalt. This change in the activation energy as the alkaline earth metal cation changes can be explained by the change in the width of the forbidden band. Also, the replacement of rare-earth elements ions with alkaline-earth metal ions led to a structural disorder, to an increase in the formation of equilibrium charged point defects in the crystal structure, in which the strength of the bond with trapped charge carriers by electrons or holes in point defects in the crystal lattice with different alkaline-earth ions was different.

Keywords: solid-phase synthesis, rare-earth and alkali metals cobaltites, thermal dependence of electrical conductivity, complex oxides, impedance spectroscopy, Bode plots, conduction activation energy, conductivity isotherms.

Introduction

At present, electrochemical devices operating at elevated (> 30 ºC) and high (> 100 ºC) temperatures are beginning to be used in industry: solid electrolyte fuel cells, oxygen sensors, electrolyzers for oxygen production, oxygen pumps, etc. However, good materials for oxygen electrodes and switching elements capable of replacing metals, which are now used in these devices. These materials must be stable in highly oxidative and in some cases reducing media should have sufficient electrical conductivity. The latter should provide small ohmic losses at the electrodes and electrode-solid electrolyte contact, which should not change during long time operation. One of the promising materials for electrochemical elements operating at high

temperatures is complex oxides of transition and rare-earth elements of the type ABO_3 with a perovskite structure or close to it [1–3].

The purpose of this work is the synthesis, radiographic and electrophysical study of complex cobaltites of alkaline earth and rare earth metals of composition $LnM^{II}CoO_{3.5}$, where M^{II} are alkaline earth metals (M^{II} — Mg, Ca, Sr, Ba), which have promising electrophysical properties (semiconductor, ferroelectric, magnetic, superconducting, etc.).

Synthesis of compounds was carried out by solid-phase annealing in three stages at different temperatures. The initial components for the synthesis were lanthanum oxide of«puriss. spec.» grade, cobalt oxide (II) of «puriss.» grade and carbonates of alkaline earth metals of «puriss.» grade. The weights of the initial substances were weighed to the fourth decimal place. Their calculation was carried out in terms of specific final compositions of complex cobaltites. The mixtures of reagents were thoroughly rubbed in an agate mortar, and then they were quantitated into alundum crucibles for annealing in a selitic furnace. The synthesis was carried out as follows: the 1st stage — 10 hours, at 800 ºC, the 2nd stage at 1300 ºC — 10 hours with periodic grinding in a mortar; An annealing was carried out at 400 ºC for 20 hours in order to obtain stable compounds under normal conditions.

In order to control the phase composition of the synthesis products, X-ray studies were carried out on a MiniFlex-400 diffractometer in Cu $K_{\alpha 1}$ radiation at a voltage of 40 kV and a current of 40 mA. The survey was conducted in the interval $2\theta = 20º–80º$ in steps of 0.05º and exposure of 1 sec. to the point. To determine the phase composition at the synthesis stage, a set of specialized programs applied to the instrument for preliminary processing of experimental data was used. Performed phase analysis reveals the absence of initial reagents in the sample and the crystallinity of the reaction product. The diffraction patterns were detected and the unit cell parameters were determined by means of programs and checked by good agreement between the experimental and calculated values of $10^4/d^2$. Further, according to XRF data, types of syngony were determined, and parameters of the elementary cells of the cobaltites were studied. Their values are given in Table 1 below.

Table 1

Crystallochemical characteristics of synthesized compounds

Compound	Type of the system	Lattice parameters, Å		V^o, Å^3	$V^o_{unit\ cell}$, Å^3	Z
		A	c			
$LaMgCoO_{3,5}$	Tetragon.	10.77	16.25	1884.88	117.80	16
$LaCaCoO_{3,5}$	Tetragon.	10.86	16.75	1975.49	123.47	16
$LaBaCoO_{3,5}$	Tetragon.	10.89	17.10	2027.93	126.75	16
$LaSrCoO_{3,5}$	Tetragon.	10.81	16.92	1977.21	123.58	16

Experimental part

Tablets were obtained from the previously obtained solid-phase synthesis of powders on a hand press at a pressure of 20 kg/cm^2. As a plasticizer, a solution of natural rubber in toluene was used. The resulting disks were annealed in a muffle furnace at 1100 ºC for 6 hours. In order to make it sufficient for the experiment, the samples were held for 8 hours at a temperature of 600 ºC. Further, a thorough two-sided grinding was carried out. Platinum electrodes were applied to the ground surface of the sintered samples. For the preparation of platinum electrodes, finely dispersed platinum paste was used, mixed with an alcohol solution of rosin. The roasting of the electrodes was carried out in air at a temperature of 1100 for 1–1.5 hours.

Using the method of electrochemical impedance in the frequency range from 10 Hz to 1 MHz in a 2-contact cell, the temperature dependence of the electrical conductivity of the samples was investigated. The relative error in measuring the components of the impedance is in the range 0.3–0.5 %. Conductivity measurements were carried out in the temperature range 40–800 ºC. The shooting was carried out in the cooling mode. To measure the polytherm of the total conductivity, a dynamic mode with a cooling rate of 1.5 ºC/min was used. The study of the isotherms was carried out in a static mode with a step of 10–20 ºC and shutter speeds at each point before the onset of equilibrium. In the course of the experiment, the furnace temperature was set by the Varta TP403 temperature regulator. The temperature control near the sample was carried out using a platinum-rhodium-platinum thermocouple TPP-10. Figure 1 shows the hodographs of $LaMgCoO_{3.5}$ samples taken at different temperatures.

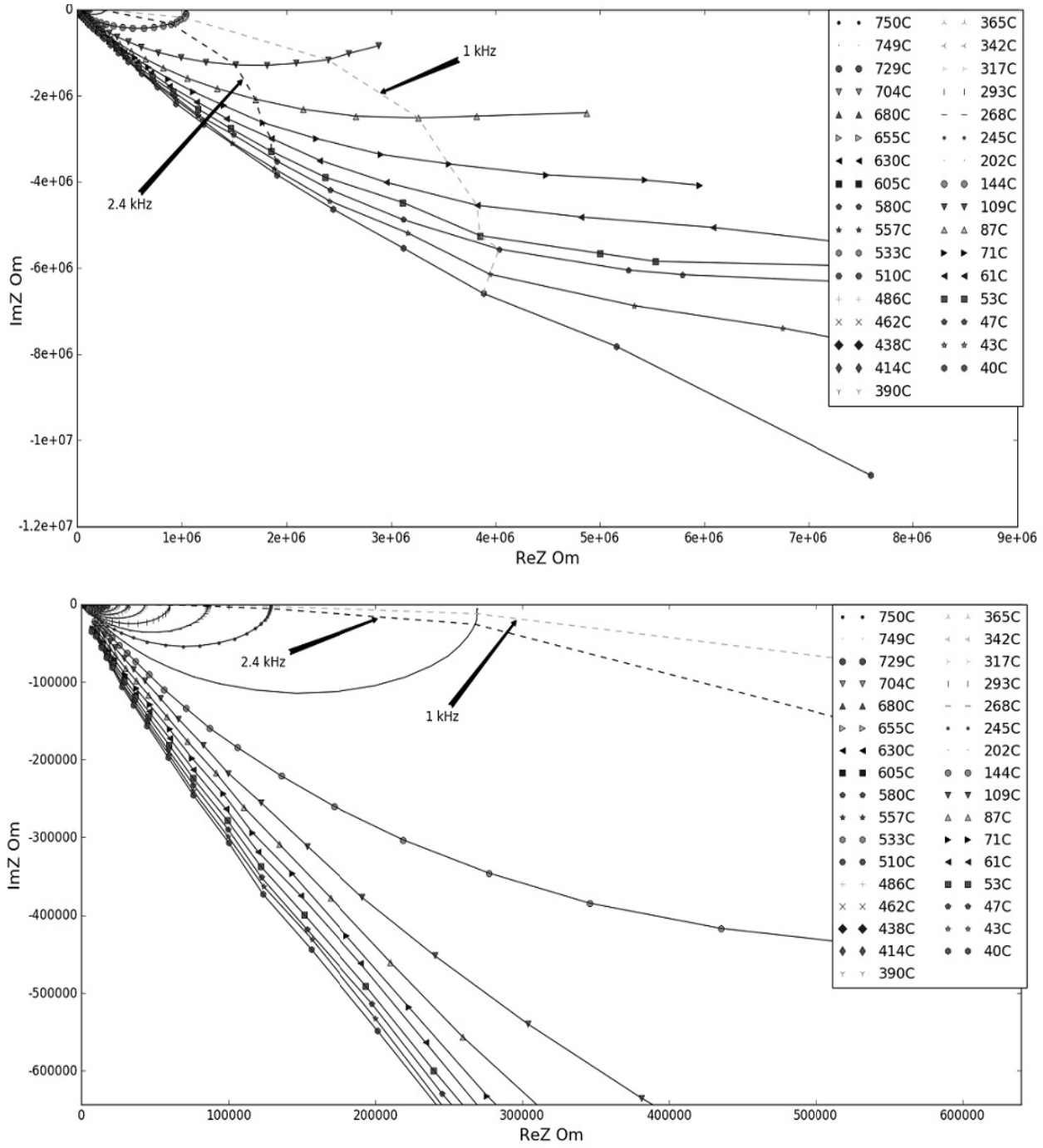

Figure 1. Hodographs sample $LaMgCoO_{3.5}$ obtained at different temperatures 40–750 ºC in different scales

The processing of data obtained in alternating current experiments is performed by representing them in the complex plane (the hodograph method) in coordinates. The imaginary part (for example, Im Z) is the real part (ReZ). The dotted line connects the points that correspond to measurements at a frequency of 1 kHz, 2.4 kHz.

To refine the study of the electrical characteristics of the samples, another installation has been assembled to study the temperature dependence of the electrical complex conductivity in a two-electrode method.

The furnace consists of a working chamber formed by a lining of a layer of refractory bricks, heaters and a thermal insulation layer insulated from the metal casing. The parts operating in the furnace chamber were made of heat-resistant materials. To measure the temperature, a chromel-alumel thermocouple was used with a TPM202 measuring regulator, which was connected to the computer by dint of interface converter (RS485 –> RS232) of the AC-3-M24. To exchange data and control signals between the regulator and the computer was carried out according to the protocol of the firm «Owen». The limit of the basic permissible

reduced error of TPM202 during the temperature measurement by the chromel-alumel thermocouple according to the converter meter documentation was 0.5 %.

The complex resistance was measured with the help of the RLC meter E7–21 by the voltmeter-ammeter method with an alternating current at a frequency of 1 kHz, in which the operating frequency voltage from the generator is applied to the measured object connected to the converter Y (conductivity) –> UT, UH. The converter generates two voltages, one of which (UT) is proportional to the current flowing through the measured object, the other (UH) is the voltage on it. The ratio of these voltages is equal to the complex conductivity (Y) or complex resistance (Z) of the object. The measurements were averaged over 10 measuring cycles. The heating rate of the sample is 5º/min.

Figure 2 shows the temperature dependence of the conductivity of cobaltite samples.

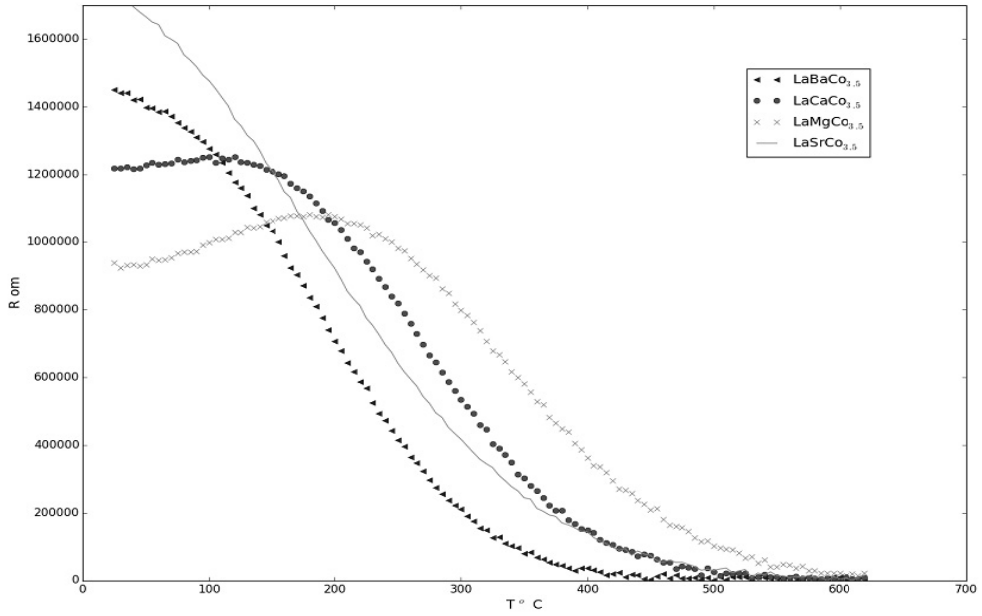

Figure 2. The dependence of the electrical resistance of $LaM^{II}CoO_{3.5}$ samples, where (M^{II} — Mg, Ca, Sr, Ba) on the temperature

Specific resistance of the sample was determined by the formula (1):

$$\rho = \frac{R \cdot S}{l}, \quad (1)$$

where R — is the resistance of the sample; S — is the cross-sectional area of the sample; l — is the length of the sample.

The specific conductivity of the sample δwas determined from formula:

$$\delta = \frac{1}{\rho}. \quad (2)$$

Results and Discussion

It can be seen from the graphs that at low frequencies at room temperatures the travel time curves represent inclined straight lines or arcs of circles of large radius, at high frequencies at high temperatures of the semicircle. The curves of the resistance versus temperature at 1 kHz show a sharp decrease in resistance. In the experiments we used electrochemical cells with blocking platinum electrodes. The equivalent circuitry of the cell corresponding to high temperatures can be represented by a series connection of resistances and the presence of a capacitance. Also the kind of impedance shows a significant contribution of electronic conductivity at high temperatures. At low temperatures, the effect of the capacitance of the double electrode/sample layer and the weak electronic conductivity is manifested. The activation energy of electrical conductivity was calculated from the slope of the dependence of lnσ on the reciprocal temperature. The activation energies of

conductivity for new compounds are determined using the obtained data and the values of activation energies are given in Table 2.

Table 2

Energy of activation of high-temperature electrical conductivity of cobaltites

Compound	The activation energy of conductivity, eV
$LaMgCoO_{3.5}$	0.113
$LaCaCoO_{3.5}$	0.147
$LaSrCoO_{3.5}$	0.169
$LaBaCoO_{3.5}$	0.184

The character of the dependence of the conductivity at moderate temperatures shows their thermal activation, in the Arrhenius coordinates these sections of the graph are described by a straight line. An increase in the activation energy of the conductivity in the series of Mg^{2+}–Ca^{2+}–Sr^{2+}–Ba^{2+} cations was observed. The introduction of an alkaline earth ion with a large ionic radius led to a local distortion of the crystal lattice. This changed the value of the splitting of the *d*-levels of the transition metal-cobalt. This change in the activation energy as the alkaline earth metal cation changes can be explained by the change in the width of the forbidden band. Also, the replacement of rare-earth elements ions with alkaline-earth metal ions led to a structural disorder, to an increase in the formation of equilibrium charged point defects in the crystal structure, in which the strength of the bond with trapped charge carriers by electrons or holes in point defects in the crystal lattice with different alkaline-earth ions was different.

References

1 Пальгуев С.Ф. Высокотемпературные оксидные электронные проводники для электрохимических устройств: учеб. пособие / С.Ф. Пальгуев, В.К. Гильдерман, В.И. Земнов. — М.: Наука, 1990. — 197 с.

2 Mitchell R.H. Perovskites modern and ancient / R.H. Mitchell. — Canada: Almaz press Inc., 2002. — 262 p.

3 Иванов-Шиц А.К. Ионика твердого тела / А.К. Иванов-Шиц, И.В. Мурин // ЖФХ. — 2010. — Т. 2, № 15. — С. 619–623.

Е.С. Мустафин, Д.А. Кайкенов, Х.Б. Омаров, Р.З. Касенов,
А.Т. Дюсекеева, С.Б. Абеуова, А.С. Борсынбаев

$LnM^{II}CoO_{3.5}$ (M^{II} — Mg, Ca, Sr, Ba) құрамды кобальтиттерін синтездеу және электрфизикалық зерттеу

Мақала құрылысы перовскиттің құрылысына ұқсас $LnM^{II}CoO_{3.5}$ (M^{II} — Mg, Ca, Sr, Ba) қосылыстары фазаларының электрлік қасиеттерін зерттеуге арналған. Фазалар керамикалық технологиялар бойынша қатты фазалық синтездеу әдісімен алынды. Фазалық құрам рентгенфазалық талдау әдісімен анықталды, ұнтақтардың дифрактограммаларын индицирлеу жүргізілді, кристалдық тордың параметрлері және симметрия класы анықталды. Жаңа қосылыстар тетрагоналды симметрияға ие, элементарлы ұяшықтарында 16 құрылымдық бірліктер орналасқандығы анықталды. Күрделі оксидтер шамамен 1500–2000 ºС жоғары балқу температурасына ие болғандықтан, өлшеулер жүргізуге болатын сапасы жақсы монокристалдар алу мүмкін емес. Сондықтан олардың термодинамикалық және электрфизикалық қасиеттерін зерттеу күйдірілген ұнтақтар түріндегі үлгілермен жүргізіледі. Берілген жұмыста өткізгіштіктің изотермалары әртүрлі температураларда импедансты спектроскопия әдісімен өлшенді. Кешенді жазықтықта кедергінің годографтары салынды. Эквивалентті нұсқалар әдісін пайдаланып, үлгі дәндерінің дәндішекаралық және көлемдік кедергілері анықталды. Нәтижелер жаңа қосылыстар төмен дәндішекаралық кедергіге ие екендігін көрсетті. Температуралық тәуелділік нәтижелерін пайдалана отырып, жаңа кобальттиттердің өткізгіштіктерінің активтену энергиялары есептелінді. Берілген қосылыстар үшін өткізгіштіктің активтену энергиялары 0,113–0,184 eV тең. Орта температураларда өткізгіштіктің тәуелділік сипаттамалары олардың термиялық активтенуін көрсетті, Аррениус координаттарында графиктің бұл аймақтары тік сызықпен сипатталды. Mg^{2+}–Ca^{2+}–Sr^{2+}–Ba^{2+} катиондары қатарында өткізгіштіктің активтену энергиясының жоғарылауы байқалады. Иондық радиусы үлкен сілтілікжер ионын енгізу кристалдық тордың жергілікті қисаюына себеп болды. Бұл ауыспалы металл — кобальттің *d*-деңгейінің ыдырау мәнін өзгертеді. Сілтілікжер металл

катионы өзгерген сайын активтену энергиясының байқалған өзгерістерін тыйым салынған аймақтың жалпақтығымен түсіндіруге болады. СЖЭ иондарын сілтілікжер металдарының иондарымен ауыстыру құрылымдық ретсіздікке әкеледі, кристалдық құрылыста тепе-теңдіктегі нүктелік бұзылымның пайда болуының артуына себеп болады, олардағы кристалдық тордағы нүктелік бұзылымдарда электрондар мен тесіктердің зарядты тасымалдаушыларды ұстап алу байланыстардың беріктігі әртүрлі сілтілікжер иондары үшін әртүрлі.

Кілт сөздер: қатты фазалық синтез, сирекжер және сілтілік металдардың кобальтиттері, электрөткізгіштіктің термиялық тәуелділігі, күрделі оксидтер, импедансты спектроскопия, Боде диаграммалары, өткізгіштіктің активтену энергиясы, өткізгіштік изотермалары.

Е.С. Мустафин, Д.А. Кайкенов, Х.Б. Омаров, Р.З. Касенов,
А.Т. Дюсекеева, С.Б. Абеуова, А.С. Борсынбаев

Синтез и электрофизические исследования кобальтитов состава $LnM^{II}CoO_{3.5}$ (M^{II} — Mg, Ca, Sr, Ba)

Статья посвящена изучению электрических свойств фаз $LnM^{II}CoO_{3.5}$ (M^{II} — Mg, Ca, Sr, Ba), имеющих структуру, близкую к структуре перовскита. Фазы были получены методом твердофазного синтеза в соответствии с керамической технологией. Фазовый состав был определен методом рентгенофазового анализа, проведено индицирование дифрактограммы порошков, определены параметры решетки и ее класс симметрии. Обнаружено, что новые соединения имеют тетрагональную симметрию, в элементарной ячейке которой расположены 16 структурных единиц. Так как сложные оксиды обладают высокими температурами плавления порядка 1500–2000 ºС, монокристаллы хорошего качества, пригодные для проведения измерений, получить невозможно. Поэтому изучение их термодинамических и электрофизических свойств проводят на образцах в виде спеченных порошков. В данной работе проведены измерения изотерм проводимости методом импедансной спектроскопии при разных температурах. Построены годографы сопротивлений на комплексной плоскости. Используя метод эквивалентных схем, определены зернограничные и объемные сопротивления зерен образца. Результаты показали, что новые соединения имеют малое зернограничное сопротивление. Используя температурные зависимости, вычислены энергии активации проводимости новых кобальтитов. Энергия активации проводимости для данных соединений составляет 0,113–0,184 eV. Характер зависимости проводимости при средних температурах показывает их термическую активацию, в координатах Аррениуса эти участки графика описываются прямой линией. Наблюдается увеличение энергии активации проводимости в ряду катионов Mg^{2+}–Ca^{2+}–Sr^{2+}–Ba^{2+}. Введение щелочноземельного иона с большим ионным радиусом приводит к локальному искажению кристаллической решетки. Это меняет величину расщепления *d*-уровней переходного металла — кобальта. Наблюдаемое изменение энергии активации по мере изменения катиона щелочноземельного металла можно объяснить изменением ширины запрещенной зоны. Также замещение ионов РЗЭ ионами щелочноземельных металлов приводит к структурной неупорядоченности, к увеличению образования в кристаллической структуре равновесных заряженных точечных дефектов, в которых прочность связи с захваченными носителями заряда электронами или дырками у точечных дефектов в кристаллической решетке с разными щелочноземельными ионами различна.

Ключевые слова: твердофазный синтез, кобальтиты редкоземельных и щелочных металлов, термическая зависимость электрической проводимости, сложные оксиды, импедансная спектроскопия, диаграммы Боде, энергия активации проводимости, изотермы проводимости.

References

1 Palguev, S.F., Gilderman, V.K., & Zemnov, V.I. (1990). *Vysokotemperaturnye oksidnye elektronnye provodniki dlia elektrokhimicheskikh ustroistv [High-temperature oxide electronic conductors for electrochemical devices]*. Moscow: Nauka [in Russian].

2 Mitchell, R.H. (2002). *Perovskites modern and ancient*. Canada: Almaz press Inc.

3 Ivanov-Shits, A.K., & Murin, I.V. (2010). Ionika tverdoho tela [Ionica of a solid]. *Zhurnal Fizicheskoi khimii — Journal of Physical Chemistry*, *2*, 619–623 [in Russian].

UDC 669.712.543.226

N.I. Kopylov[1], E.P. Solotchina[2]

[1]*Institute of Solid State Chemistry and Mechanochemistry of the Siberian Branch of the Russian Academy of Sciences, Novosibirsk, Russia;*
[2]*V.S. Sobolev Institute of Geology and Mineralogy of the Siberian Branch of the Russian Academy of Sciences, Novosibirsk, Russia*
(E-mail: kolyubov@narod.ru)

Study of the thermal properties of clays from the Krasnoyarsk and Sukpak deposits of Tuva

The most important factor in the development of industry and the construction industry of individual and hard-to-reach regions is the availability of their respective raw materials and energy base. Their possible effective use can often be difficult due to difficult geological conditions, lack of required transport connections and removal from industrial centers. So, in particular, more than a dozen industrial deposits of fossil raw materials and clay rocks located in hard-to-reach areas are known on the territory of the Republic of Tuva and their extraction is currently not cost-effective. Therefore, available low-grade raw materials with the introduction of various additional components can be used as the main raw material. The latter requires a certain amount of complex research, namely, the study of the dynamics of the behavior of the initial components, their mixtures, the batching compositions during roasting, the development of technology parameters using new raw materials, etc. In this connection, in the first stage of the research in this paper using a number of methods of physicochemical analysis the dynamics of the phase transformations occurring in the material of the rare-earth clays of the Sukpak and Krasnoyarsk deposits of Tuva is studied, with their heating in the temperature range up to ~ 1020–1025 °C. As a result, the stages of successive thermal decomposition of the material were determined, namely, the removal of sorption and hydrated moisture, the destruction of hydroaluminosilicates, the decomposition of magnesian calcite, and the initial formation of high-temperature aluminosilicate structures.

Keywords: thermal, X-ray phase analysis, X-ray fluorescent analysis, clays, oxides, carbonates, silicates, aluminosilicates.

Introduction

One of the most important factors for the development of the construction industry of remote and hard-to-reach regions is the availability of an appropriate raw materials base and its efficient use. However, often existing internal sources of raw materials are not used enough in regions. So, in particular, more than a dozen industrial deposits of clay rocks are known on the territory of Tuva [1–4]. The presence of 45–62 % of SiO_2 and 13–18 % of Al_2O_3 in them allows them to be attributed to semi-acid clays (herein and after, % wt.). They contain significant concentrations of alkaline earth metal compounds (5–10 %), iron oxides (6–9 %). Similar clay rocks are divided into two groups:

- smectite, with predominance of the mineral nontronite $(Fe, Al)_2[Si_4O_{10}]\cdot(OH)_2\cdot nH_2O$ in the clays of this group;
- micaceous, rock-forming mineral in which is illite (a kind of hydromuscovite) — $K_{<1}Al_2[(Si, Al)_4O_{10}]\cdot OH_2\cdot nH_2O$.

The latter in terms of plasticity refer to a moderately and slightly plastic group. They are also light-binder material. Their refractory temperatures are in the range of 1180–1250 ºC and have a small sintering interval (~ 30–50 ºC).

At a firing temperature of smectite clay up to 1100 ºC, the crock of the cake has water absorption (B) equal to 8–10 %, which indicates its porous structure. Therefore, in order to obtain a dense crock (B <5 %), as a rule, clays of the hydromica group are used.

An analysis of the geography of occurrence of clay rocks of Tuva showed that the existing clays of the micaceous group on the territory of the Republic were in hard-to-reach areas of the region and their extraction was currently not possible. Therefore, mainly montmorillonite clays of the Krasnoyarsk and Sukpak deposits are used as the main plastic raw material in practice. These clays are low-dispersed, moderately and low-plastic, with high and medium sensitivity to drying, characterized by a small interval of sintering.

For effective work of production on this raw material it is necessary to work out for it the required technological mode of roasting. And to obtain the specified technological properties of the material of these

clays, it is necessary to additionally produce specially selected effective additives for them. Natural fluxescan be these additives. Deposits of qualitative natural fluxes — pegmatites (a mixture of quartz and feldspars) are found in the Republic, but are in inaccessible mountainous terrain and are not yet developed due to the difficulty of their development. Therefore, low-quality raw materials with the addition of various man-made materials such as quarry wastes, asbestos and other technological products are used as additives in practice.

By the time, only solid brick of M75 grade is produced from ceramic materials in the amount of ~2–3 thousand pieces per year by the construction industry of Tuva, with the annual requirement of about 20–22 thousand pieces of conditional brick. Missing requirements are covered by income from other regions. At the same time the cost of material increases by 1.5–1.7 times due to transportation costs [2].

With the purpose of more efficient use of raw materials for the construction industry, a number of works on improving the production of ceramic materials have been carried out recently [2, 3, 5]. Also, attempts were made to use the Khovu-Aksy dump slurry (plant «Tuvakobalt» wastes) in the production process of ceramic materials instead of natural fluxes [6, 7].

These preliminary experiments have shown the possibility of obtaining a ceramic material of a dense crock based on local clays and dump sludge of Khovu-Aksy. However, these experiments were of a trial nature. At the same time, the ecological factor was not taken into account, although the sludge of the Khovu-Aksy dumps contains 3.0 to 6.3 % of arsenic [8]. How will the arsenic compounds present in the sludge behave in the process of production and further exploitation of ceramic products? This question remains open. Therefore, at the subsequent stage of research on the use of Khovu-Aksy dump wastes in the production of ceramic building materials, the environmental factor should be decisive, along with the study of the physical and technological properties of the materials of the initial charge and the products obtained.

In order to study the possibility of using the wastes of the Khovu-Aksy dump for the production of ceramic products and building materials as a flux at the initial stage of the research program, there was made a study of the phase transformations occurring during roasting, the initial components of the production of ceramic materials (clays of Sukpak and Krasnoyarsk deposits of Tuva, dump products of Khovu-Aksy), as well as their mixtures.

This report presents the results of studying the phase transformations occurring in the material of the clays under investigation during their calcination.

Experimental

Initial samples of clays were subjected to quantitative analysis for oxides by X-ray fluorescent method and X-ray phase analysis (XRD) to determine their mineral composition. The obtained results on the content of oxides in the samples of the investigated clays are presented in the Table.

T a b l e

X-ray fluorescence analysis of starting materials

No.	Starting material	Analysis data, % mass														
		SiO_2	Al_2O_3	Fe_2O_3	MgO	CaO	TiO_2	Na_2O	K_2O	SO_3	NiO	CuO	Co_3O_4	P_2O_5	MnO	Amorphous phase
1	Krasnoyarsk Clay	55.73	14.26	6.20	2.48	6.36	0.75	2.17	2.24	0.51	0.006	Undefined	Undefined	0.22	0.10	8.22
2	Sukpak Clay	49.76	14.83	7.26	3.22	8.24	0.83	1.15	2.17	0.26	0.008	Undefined	Undefined	0.32	0.16	11.05

X-ray fluorescence silicate analysis of the samples was performed on an ARL-9900-XP ARL (Applied Research Laboratories) X-ray spectrometer. The sample was dried at 105 ºC for 1.5 hours, then it was calcined at 960 ºC for 2.5 hours and mixed with a flux (66.67 % of lithium tetraborate, 32.83 % of lithium metaborate, and 0.5 of lithium bromide) in a ratio of 1:9 (the total weight of the mixture is 5 g). The mixture was melted in platinum crucibles in an induction furnace (Lifumat-2,0-Ox, Germany). State standard samples of the rock composition were used to verify the correctness of the analysis.

X-ray phase analysis was performed on an ARLXTRA powder diffractometer of Thermo Scientific ARL Products (Switzerland). The samples were ground in alcohol in an agate mortar and applied to a glass substrate of 2×2 cm in size. The thickness of the preparation was ~20 mg/cm^2. The samples were scanned (CuK_a radiation) in the range from 2° to 65° (2Θ) in steps of 0.05°, the scanning time at the point was 3 sec.

The interpretation of X-ray diffraction patterns of minerals was compared with the reference cards of the International powder database «Power diffraction files» (PDF).

Thermal studies (DTA) were carried out using the Pauliick model derivatograph, Pauliick Erdei (Hungary), MOM-1000 type. The conditions are standard: the heating rate is ~10 deg/min, the air environment; the temperature limit is 900–1025 ºC. The samples of the cinders of the investigated clays after thermal analysis were also studied for the phase composition by X-ray diffraction analysis. The data on the chemical, physical, chemical and thermochemical properties of individual natural compounds, minerals and clays available in the reference and scientific literature were used to process the results of the thermal analysis of the products under study [9–15].

Thermal analysis of the Sukpak clay

According to X-ray fluorescence analysis:

- The basis of the average sample of the Sukpak clay is quartz (α-SiO_2) and magnesium containing calcite — (Mg, Ca)CO_3;
- it contains a considerable amount of plagioclase, the sum of albite ($NaAlSi_3O_8$) and anorthite ($CaAl_2Si_2O_8$) = (100 – *n*) $NaAlSi_3O_8$ + *n*$CaAl_2Si_2O_8$, where «*n*» can vary from 0 to 100;
- kaolinite — $Al_4[Si_4O_{10}](OH)_8$ is also present; potassium feldspar, which represents aluminosilicates mainly of potassium (orthoclase, microcline — $K[AlSi_3O_{10}]$, etc.); mica (aluminosilicates $AB_{2-3}[T_4O_{10}](OH, F)$, where A — K, Na, Ca and others, B — Al, Mg, Fe; T — Si, Al); smectite, illite-smectite (solid solution of mica-like minerals, the compositions of which, according to the bibliography, belong to the high-silica mica: montmorillonites and saponites);
- the presence of hematite α-Fe_2O_3 is noted.

According to the data of X-ray fluorescence analysis (see Table), the sample with relatively equal content of alumina (14.83 %) with Krasnoyarsk clay has lower contents of silicon oxide (49.76 %), sodium (1.15 %), but in somewhat larger amounts oxides of a number of other metals (iron, magnesium, calcium, potassium).

After carrying out the thermal analysis within the temperature up to 900 ºC, the mineral composition of the resulting cinder according to the X-ray phase analysis has undergone the following changes. There is a complete absence of magnesian calcite and kaolinitein the sample with the dominance of the quartz phase. Along with quartz, the dominant mineral is plagioclase. The product of thermolysis shows the presence of potassium feldspar, hematite, traces of mica, illite-smectite, and also the possible presence of karosite-$KFe_3[SO_4]_2(OH)_6$.

The DTA curve of the thermogram (Fig. 1) shows a number of endothermic effects with temperature peaks at 100, 540, 680, and ~795 ºC. The stages of mass loss (see curves of TG and DTG) are fixed by the final temperatures of 250, 540, 750 and 800 ºC. Sorbed and crystallization moisture is removed from the clay materialin the interval up to ~ 250 ºC. In the temperature range ~ 435–620 ºC, decomposition of kaolinite takes place: decomposition of weakly formed structures occursup to ~ 500 ºC, and further (at ~500–600 ºC), the ordered forms are destroyed with removal of structural (molecular) water and the release of amorphous phases of Al_2O_3 and SiO_2.

Apparently, the process of decomposition of magnesian calcite beginsalready at temperatures of ~ 620–650 ºC. Initially, the decomposition process occurs with the release of MgO as an amorphous phase. Further, the decomposition of magnesian calcite is completed by the release of CaO and complete distillation of CO_2 within the limits of temperatures ~ 750–795 ºC.

The DTGA of a sample of Sukpak clay subjected to additional abrasion in a mortar and heated in the temperature range up to 1025 ºC (see Fig. 2), practically confirmed the course of the thermal decomposition described by the curves of the thermogram curves of the first experiment (Fig. 1). However, there is an increase in mass loss in the temperature range of 80–250 ºC and a decrease in mass loss in the high-temperature stages of heating. As a result, the total mass loss was also significantly reduced. This is due to the fact that with additional processing (abrasion), there was a partial destruction of hydrated hydrosilicate structures and at the same time an increase in the sorption capacity of the material [15]. Analysis of the TG curve shows that the decomposition process of magnesian calcite is more clearly divided into two stages. At the temperature stage from temperatures of ~ 580–600 ºC the effect of decomposition of magnesian calcite with the release of the amorphous phase of MgO is manifested. A fairly clear endoeffect at 740–770–820 ºC is due to further decomposition of calcite with the formation of an amorphous phase of CaO and CO_2 distilling off. And further, at ~ 900 ºC the decomposition of the residual calcite is completed. Subsequent

small effects at 900, 930 ºC, apparently, can be attributed to the residual decomposition of the most stable aluminosilicate phases and the formation of structures such as spinel or mullite based on amorphous active oxides formed during the decomposition of aluminosilicates and carbonates.

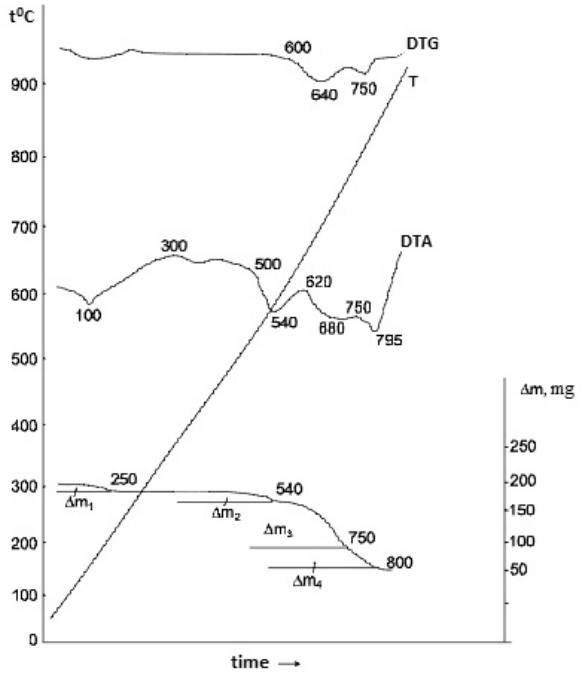

Figure 1. The thermogram of the Sukpak clay sample without additional treatment

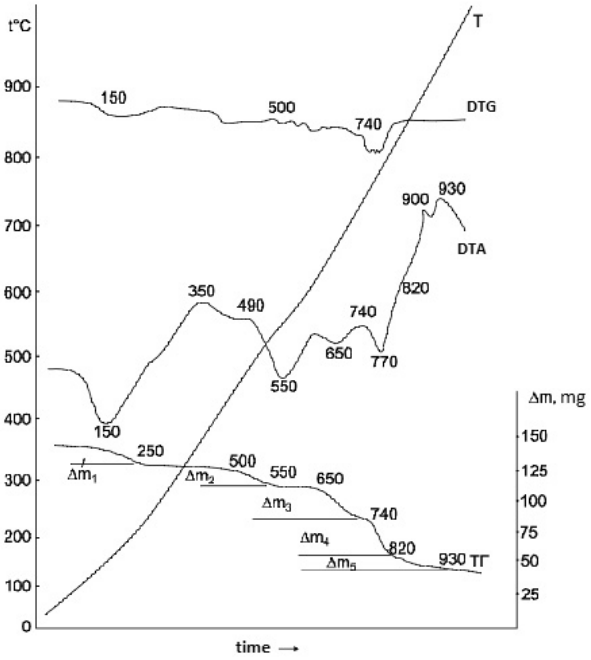

Figure 2. The thermogram of the Sukpak clay sample subjected to additional abrasion

The drop in the mass of the material when heated according to the TG curve is in accordance with the dynamics of the thermal decomposition of the sample presented above. It is carried out sequentially in several stages in the temperature intervals: ~ 80–250 ºC, ~ 440–600 ºC, ~ 650–750 ºC, ~ 770–900 ºC with a loss of mass, respectively: 0.8–1.7 %; 2.2 %; 2.8–6.7 %; 4.9–5.6 %. The main weight loss (~ 80 %) occurs at the last stage. The total mass loss is in the range of ~ 11.7–15.2 %, depending on the conditions for the preliminary preparation of the sample and the temperature limit of heating at DTGA.

Thermal analysis of the Krasnoyarsk clay

According to the X-ray fluorescence analysis in the original sample of the Krasnoyarsk clay:

- quartz (α-SiO_2); potassium feldspar (in particular, microcline and orthoclase-K [$AlSi_3O_{10}$]), plagioclase (albite — $Na[AlSi_3O_8]$ and anorthite — $Ca[Al_2Si_2O_8]$), magnesian calcite — $(Mg, Ca)CO_3$ dominate;
- there are such minerals as chlorite — $(Mg, Fe^{2+}, Fe^{3+})_6 \cdot [AlSi_3O_{10}](OH)_8$; kaolinite — $Al_4[Si_4O_{10}](OH)_8$; dioctahedral mica (muscovite type — $KAl_2[(Si, Al)_4O_{10}](OH, F)$); smectite and traces of illite-smectite;
- traces of hematite — Fe_2O_3, siderite — $FeCO_3$ and goethite — FeO(OH) are noted.

In contrast to the Sukpak clay, potassium feldspar and plagioclase dominate in the composition of the Krasnoyarsk clay along with quartz and calcite. These minerals in the Sukpak clay are contained in a small amount. In addition, there are still chlorite and goethite, as well as sideritein the Krasnoyarsk clay. They were not found in the Sukpak clay.

Comparing the content of element oxides in the Krasnoyarsk and Sukpak clays (see Table), it should be noted that there is a greater content of quartz, sodium oxides and a fewer oxides of iron, magnesium and calciumin the Krasnoyarsk clay.

The character of the DTGA curve of the sample of the Krasnoyarsk clay subjected to preliminary abrasion (Fig. 3) is rather close to the character of the DTGA curves of the Sukpak clay, although it has some differences. Thus, with similar low-temperature endoeffects with temperature peaks at 160 and 540º, the subsequent course of the DTA and TG curves changes somewhat. High-temperature endoeffects of DTA (in the

temperature range of 600–850 ºC) are insignificant and weakly manifested. Only endoeffect with a peak at 750 ºC is relatively clearly manifested. The TG curve smoothly extends from 440 to 600 ºC and further from 700 to 800 ºC with the continuation of some decrease in mass up to 900 ºC, in contrast to the TG curves of the sample of the Sukpak clay.

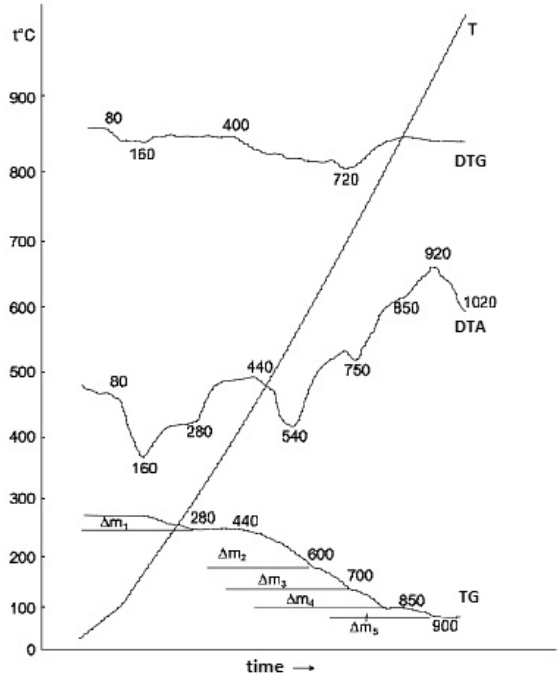

Figure 3. Thermocouple sample of the Krasnoyarsk clay subjected to additional abrasion

After the thermal analysis of the sample of the Krasnoyarsk clay, carried out in the temperature range up to 900 ºC, the phases of quartz, plagioclase dominate in the cinder material, the content of potassium feldspar is somewhat lowered, calcite, kaolinite, siderite, hematite, goethite, illite-smectiteare completely absent. The material retains traces of mica and a magnetite phase appears.

Based on the data obtained from the thermal analysis of the samples of the Krasnoyarsk clay (Fig. 3) and X-ray phase analysis data, the following sequence of thermal transformations occurring when the material of the Krasnoyarsk clay is heated can be represented.

Adsorbed water is removed in the temperature range of ~ 80–160 ºC. Subsequently, within a range of up to 300 ºC, a partial removal of the crystallization water takes place. In the temperature range of ~ 400–600 ºC, the destruction of mineral phases such as kaolinite occurs with the removal of structural (molecular) water and the formation of amorphous Al_2O_3 and SiO_2. The decomposition of chlorite and magnesian calcite takes place with a further rise in temperature within 600–850°C. The degradation products (Al_2O_3, SiO_2, MgO, CaO) formed in these temperature ranges are likely to acquire a plagioclase structure after subsequent heating (> 900 °C), which explains the increase in its content in the material as a result of thermal exposure to the product under study.

The weight loss of the material occurs in the following sequence: within the limits of temperatures up to 280 ºC — 3,3 %, to 600 ºC — 6,7 %, to 700 ºC — 4,4 %, to 850 ºC — 3,3 % and to ~ 920 ºC — 2,2 %. The total mass loss is 19.9 %, which significantly exceeds (within ~ 5–6 %) the decrease in the mass of the Sukpak clay.

Subsequent heating, exceeding 900 ºC, leads to complete decomposition of carbonate and hydrosilicate phases and promotes the process of transformation of amorphous phases formed as a result of the destruction of a wide range of aluminosilicates into plagioclase, spinel or mullite structures.

The stage-by-stage loss of mass that occurs during heating is due to the following factors, namely, removal of adsorption and crystallization water (endoeffects at ~ 80–400 ºC) and decomposition of structures of aluminosilicates with removal of structural (molecular) moisture (endoeffects at ~ 440–600 ºC); decomposition of magnesium calcite and siderite with the removal of CO_2 (endoeffects at ~ 600–850 ºC).

Conclusion

The dynamics of the phase transformations in the clay samples of the clays of the Sukpak and Krasnoyarsk deposits that occur when they are heated in the temperature range up to ~ 1020–1025 ºC is generally carried out according to the general scheme. Sorption and crystalline hydrate moisture is mainly removed in the region of low temperatures up to ~ 400–450 ºC. At temperatures in the region of ~500–600 ºC and with subsequent heating, the destruction of hydroaluminosilicate structures with the removal of crystallization (molecular) water, the release of amorphous oxide phases of silicon, aluminum and other metals included in these aluminosilicates occur. At subsequent heating in the temperature range of ~ 600 ºC and higher, the decomposition of magnesian calcite with the removal of CO_2 into the gas phase and the formation of successively amorphous magnesium oxide structures (up to ~ 700–800 ºC) and, further, calcium oxide (in the range above 800–850 ºC) take place. At temperatures above 900 ºC in the material of the samples, new high-temperature aluminosilicate structures such as spinel, mullite, and plagioclase begin to form amorphous oxides. However, this does not lead to a volumetric and aggregate change. The material, as a rule, slightly hardened, but there was no appearance of liquid phases and even minimal sintering («grasping»). The products formed after the experiment with a little effort are scattered.

Some differences in the dynamics of phase transformations and in the composition of firing products of the Sukpak and Krasnoyarsk clays are determined by the difference in the phase composition of these clays.

References

1 Кара-сал Б.К. Химико-минералогические особенности месторождения глин и суглинков Тувы / Б.К. Кара-сал, В.И. Кудрявцев // Состояние и перспективы освоения природных ресурсов Тувы: сб. науч. тр. — Кызыл: ТувИКОПР СО РАН, 2002. — С. 100–105.

2 Кара-сал Б.К. Керамические строительные материалы, получаемые обжигом при пониженном давлении: автореф. дис. … д-ра техн. наук: 05.23.05 — «Строительные материалы и изделия (технология, структура и изделия)» / Б.К. Кара-сал. — Новосибирск: СибСТРИН, 2007. — 36 с.

3 Кара-сал Б.К. Влияние пониженного давления на процессы газовыделения при обжиге глин / Б.К. Кара-сал // Стекло и керамика. — 2004. — № 9. — С. 18–20.

4 Лебедев В.И. Природные ресурсы Республики Тува: проблемы и перспективы их освоения: монография / В.И. Лебедев. — Кызыл: ТувИКОПР СО РАН, 2007. — 77 с.

5 Кара-сал Б.К. Прогнозирование технологических свойств керамических масс на основе химико-минералогических особенностей глинистых пород / Б.К. Кара-сал, Д.Х. Сат, У.Д. Чульдум // Естественные и технические науки. — 2009. — № 1. — С. 371–375.

6 Кара-сал Б.К. Керамический материал на основе отходов извлечения кобальтового концентрата / Б.К. Кара-сал, Э.Э. Ондар, К.Л. Сат // Известия вузов. Строительство. — 2009. — № 8. — С. 32–36.

7 Кара-сал Б.К. Керамический материал на основе отходов кобальтового концентрата / Б.К. Кара-сал, М.С. Иргит, Ю.Д. Каминский // Техника и технология. — 2005. — № 5. — С. 63–66.

8 Копылов Н.И. Проблемы мышьяк-содержащих отвалов: монография / Н.И. Копылов. — Новосибирск: Академ. изд-во «ГЕО», 2012. — 182 с.

9 Atlas of thermoanalytical curves. — London; New York; Budapest: Akademiai Kiado, 1974. — Vol. 1–5.

10 Куликов Б.Ф. Минералогический справочник технолога-обогатителя: справ. изд. / Б.Ф. Куликов, В.В. Зуев, И.А. Вайншенкер, Г.А. Митенков. — Л.: Недра, 1985. — 264 с.

11 Бетехтин А.Г. Минералогия: монография / А.Г. Бетехтин. — М.: Гос. изд-во геолог. лит., 1950. — 956 с.

12 Горшков В.С. Термография строительных материалов: монография / В.С. Горшков. — М.: Изд-во лит. по строительству, 1968. — 237 с.

13 Пашкевич Л.А. Термография продуктов глинозёмного производства: справ. / Л.А. Пашкевич, В.А. Броневой, И.П. Краус. — М.: Металлургия, 1983. — 129 с.

14 Годовиков А.А. Минералогия: учебник / А.А. Годовиков. — М.: Недра, 1983. — 647 с.

15 Иванова В.П. Термический анализ минералов и горных пород: монография / В.П. Иванова, Б.К. Касатов, Т.Н. Красавина, Е.Л. Розинова. — Л.: Недра, 1974. — 399 с.

Н.И. Копылов, Э.П. Солотчина

Туваның Сукпак және Красноярск кен орындары топырақтарының термиялық қасиеттерін зерттеу

Жеке және алыс аймақтардың өнеркәсібі мен құрылыс индустриясы дамуы үшін маңызды факторлары болып шикізаттық және энергиялық базаларының болуы табылады. Әдетте, оларды тиімді пайдалану мүмкіндігі күрделі геологиялық жағдайлармен, қажетті транспорттық қатынасудың және өнеркәсіптік орталықтардан алыс орналасуымен қиындатылады. Мысалы, нақтылап айтқанда, Тува Республикасы өңірінде, алыс өңірлерде орналасқан және сондықтан олардың өңделуі қазіргі кезде тиімді болмайтын, шикізат кендерінің және топырақ шығарындаларын ондаған өнеркәсіптік қазбалар кені бар. Сондықтан негізгі шикізат көзі ретінде қолжетімді төмен сұрыптағы шикізатын әртүрлі қосымша компоненттер енгізу ақылы қолданылуы мүмкін. Осыған байланысты кешенді зерттеулердің белгілі көлемі қажет: бастапқы компоненттердің сипатталу динамикасын, олардың қоспаларын, қыздырғандағы шихталайтын құрамдарын зерттеу, жаңа шикізаттың қолдануымен технологиялар параметрлерін өңдеу т.б. Осыған байланысты осы жұмыстың бастапқы сатыларында физика-химиялық талдаулардың бірқатар әдістерін қолданып, Тувадағы Сукпак және Красноярск кен орындары топырақтарының төмен сұрыпты материалдарында, оларды ~1020–1025 ºС дейін қыздырғандағы фазалық өзгерістердің динамикасы зерттелген. Нәтижесінде материалдың біртіндеп термиялық ыдырауындағы сатылары анықталды: сорбциялық және гидратты ылғалды жою, гидроалюмосиликаттарды деқұрылымдау, магнезиалды кальцитті ыдырату және жоғары температуралық алюмосиликатты құрылымдарды жаңадан қалыптастыру.

Кілт сөздер: рентгенфлуоресцентті, рентгенфазалық және термиялық талдаулар, топырақтар, оксидтер, силикаттар, алюмосиликаттар.

Н.И. Копылов, Э.П. Солотчина

Изучение термических свойств глин Сукпакского и Красноярского месторождений Тувы

Важнейшим фактором развития промышленности и стройиндустрии отдельных и труднодоступных регионов является наличие у них соответствующей сырьевой и энергетической базы. Их возможное эффективное использование зачастую может быть затруднено вследствие сложных геологических условий, отсутствия требуемого транспортного сообщения и удаления от промышленных центров. Так, в частности, на территории Республики Тува известно более десятка промышленных залежей ископаемого сырья и пород глин, находящихся в труднодоступных районах, и их добыча в настоящее время нерентабельна. Поэтому в качестве основного сырья может быть использовано доступное низкосортное сырьё с введением различных дополнительных компонентов. Последнее требует определённого объёма комплексных исследований, таких как изучение динамики поведения исходных компонентов, их смесей, шихтующих составов при обжиге, отработка параметров технологии с использованием нового сырья и т.д. В связи с этим на первом этапе исследований в данной работе с использованием ряда методов физико-химического анализа изучена динамика фазовых преобразований, происходящих в материале низкосортных глин Сукпакского и Красноярского месторождений Тувы, при их нагреве в области температур до ~1020–1025 ºС. В результате были определены этапы последовательного термического разложения материала: удаление сорбционной и гидратной влаги, деструктуризация гидроалюмосиликатов, разложение магнезиального кальцита и начальное формирование высокотемпературных алюмосиликатных структур.

Ключевые слова: термический, рентгенофазовый, рентгенофлуоресцентный анализы, глины, оксиды, карбонаты, силикаты, алюмосиликаты.

References

1 Kara-sal, B.K., & Kudriavtsev, V.I. (2002). Khimiko-mineralohicheskie osobennosti mestorozhdeniia hlin i suhlinkov Tuvy [Chemical and mineralogical features of the clay and loam deposits of Tuva]. *Sostoianie i perspektivy osvoeniia prirodnykh resursov Tuvy — State and prospects of natural resources development in Tuva*. Kyzyl: TIKOPR SB RAS [in Russian].

2 Kara-sal, B.K. (2007). Keramicheskie stroitelnye materialy, poluchaemye obzhihom pri ponizhennom davlenii [Ceramic building materials obtained by firing under reduced pressure]. *Extended abstract of Doctor's thesis.* Novosibirsk [in Russian].

3 Kara-sal, B.K. (2004). Vliianie ponizhennoho davleniia na protsessy hazovydeleniia pri obzhihe hlin [Influence of a reduced pressure on the processes of gas evolution during clays firing]. *Steklo i keramika — Glass and ceramics*, *9*, 18–20 [in Russian].

4 Lebedev, V.I. (2007). *Prirodnye resursy Respubliki Tyva: problemy i perspektivy ikh osvoeniia [Natural resources of the Republic of Tuva: problems and prospects for their development]*. Kyzyl: TIKOPR SB RAS [in Russian].

5 Kara-sal, B.K., Sat, D.Kh., & Chuldum, U.D. (2009). Prohnozirovanie tekhnolohicheskikh svoistv keramicheskikh mass na osnove khimiko-mineralohicheskikh osobennostei hlinistykh porod [Prediction of technological properties of ceramic masses on the basis of chemical-mineralogical features of clay rocks]. *Yestestvennye i tekhnicheskie nauki — Natural and technical sciences*, *1*, 371–375 [in Russian].

6 Kara-sal, B.K., Ondar, E.E., & Sat, K.L. (2009). Keramicheskii material na osnove otkhodov izvlecheniia kobaltovoho kontsentrata [Ceramic material based on cobalt concentrate waste]. *Izvestiia vuzov. Stroitelstvo — Proceedings of universities. Building, 8*, 32–36 [in Russian].

7 Kara-sal, B.K., Irgit, M.S., & Kaminskii, Yu.D. (2005). Keramicheskii material na osnove otkhodov kobaltovoho kontsentrata [Ceramic material based on the waste of cobalt concentrate]. *Tekhnika i tekhnolohiia — Engineering and technology*, *5*, 63–66 [in Russian].

8 Kopylov, N.I. (2012). *Problemy myshiak-soderzhashchikh otvalov [Problems of arsenic-containing dumps]*. Novosibirsk: Akadem. izdatelstvo «GEO» [in Russian].

9 *Atlas of thermoanalytical curves* (1974). (Vols. 1–5). London; New York; Budapest: Akademiai Kiado.

10 Kulikov, B.F., Zuyev, V.V., Vainshenker, I.A., & Mitenkov, G.A. (1985). *Mineralohicheskii spravochnik tekhnolohaobohatitelia [Mineralogical handbook of the enriching technologist]*. Leningrad: Nedra [in Russian].

11 Betekhtin, A.G. (1950). *Mineralohiia [Mineralogy]*. Moscow: Hos. izdatelstvo heolohicheskoi literatury [in Russian].

12 Gorshkov, V.S. (1968). *Termohrafiia stroitelnykh materialov [Thermography of building materials]*. Moscow: Izdatelstvo literatury po stroitelstvu [in Russian].

13 Pashkevich, L.A., Bronevoi, V.A., & Kraus, I.P. (1983). *Termohrafiia produktov hlinoziomnoho proizvodstva [Thermography of products of alumina production]*. Moscow: Metallurhiia [in Russian].

14 Godovikov, A.A. (1983). *Mineralohiia [Mineralogy]*. Moscow: Nedra [in Russian].

15 Ivanova, V.P., Kasatov, B.K., Krasavina, T.N., & Rozinova, Ye.L. (1974). *Termicheskii analiz mineralov i hornykh porod [Thermal analysis of minerals and rocks]*. Leningrad: Nedra [in Russian].

UDC 573.6.086.83:550.7; 546.22–162.25

V.M. Shaikhutdinov[1], N.K. Zhappar[1, 2], O.A. Ten[1], D.S. Balpanov[1], Ye.N. Kanafin[1, 2], R.A. Khannanov[1], R.Sh. Erkasov[2], A.A. Bakibaev[3], A.T. Kezdikbaeva[4]

[1]*«BioGeoTec» LLP, Stepnogorsk, Kazakhstan;*
[2]*L.N. Gumilyov Eurasian National University, Astana, Kazakhsnan;*
[3]*Tomsk State University, Russia;*
[4]*Ye.A. Buketov Karaganda State University, Kazakhstan*
(E-mail: nariman_zhappar@mail.ru)

Pilot-scale tank biooxidation of gold bearing arsenopyrite concentrates

This article shows the results of experimental tests of bacterial oxidation of arsenopyrite gold concentrate that contains gold (60 g/t), sulfides (23 %), iron (26 %) and arsenic (11 %). A consortium, consisting of the mesophilic strain *Acidithiobacillus ferrooxidans* AF-2 and moderately thermophilic strains of *Sulfobacillus thermosulfidooxidans* OT-1 and *Sulfobacillus thermosulfidooxidans* SK-4, was used in the test. The tests were carried out on the equipment, consisting of 6 reactors with a volume of 1.5 m^3 each. The concentration of solids in the pulp was maintained at 20 % (w/w). In the process of optimizing the parameters of the bacterial oxidation plant, the retention time of the concentrate was reduced from 12 to 6 days. During the test, the destruction of sulfides was over 90 %, which provided gold recovery from biooxidation products by cyanide leaching over 94 %. In addition, the average gold recovery rate reached 95 %. The removal of arsenic from the leaching solutions was carried out by means of two-stage neutralization with calcium carbonate. Due to high oxidation degree maintained throughout the entire operation of the experimental plant, a high ratio of iron to arsenic concentration in the solution was observed, which provided ideal conditions for arsenic precipitation in the form of trivalent iron arsenate. Determination of the stability of precipitate residuals was carried out according to the protocol Toxicity Characteristic Leaching Procedure (TCLP). The precipitate obtained after neutralization of the leaching solution does not require special disposal, since the final concentration of arsenic in the extracts of TCLP tests was 0.14 mg/L.

Keywords: arsenopyrite concentrate, biooxidation, tank leaching, *Acidithiobacillus ferrooxidans, Sulfobacillus thermosulfidooxidans,* gold, arsenic, pilot-scale.

Introduction

The main problem of gold mining in Kazakhstan is that in most cases (65 %) the gold-bearing ores are classified as refractory ores. The deposits with these stubborn ores are hardly developedin our country [1]. In this regard, a necessity to use additional procedures at the processing of these ores arises. Currently, there are several approaches to «open» the refractory ores; these are physicochemical methods (oxidation under the high temperature and high pressure) and biological method (bioleaching) [2].

Pressure leaching is the method of oxidative decomposition of the sulphide minerals of iron and non-ferrous metals, with which the particles of gold associate in the ore. It occurs in industrial autoclaves under the high pressure (1 MPa or higher) and high temperatures (150–200 ºC).

Bacterial leaching (bioleaching) is a relatively new and promising method based on the use of the ability of some natural bacteria (iron-and sulfur-oxidizing) to oxidize sulfide minerals and to produce energy at normal temperatures and pressures:

$$2FeAsS + 7O_2 + H_2SO_4 + 2H_2O \rightarrow 2H_3AsO_4 + Fe_2(SO_4)_3$$

$$4FeS + 9O_2 + 2H_2SO_4 \rightarrow 2Fe_2(SO_4)_3 + 2H_2O$$

$$4FeS_2 + 15O_2 + 2H_2O \rightarrow 2Fe_2(SO_4)_3 + 2H_2SO_4$$

However, for refractory gold ores and concentrates with a low arsenic content, the choice between the two technologies (the physicochemical and bacterial) has an individual character for each particular deposit, depending on size and physicochemical characteristics of the deposit. Moreover, for arsenopyrite ore with a high arsenic content, the use of physical and chemical methods is limited by both environmental problems and economical issues. It poses a risk of the release of highly toxic arsenic into the surroundings [3].

Tank method of bacterial leaching is a relatively new and promising method for the processing of arsenic-containing ores and concentrates. In this process, the gold extraction occurs by the destruction of the crystal lattice of sulfide minerals which finely disseminate the gold. One of the benefits of this method is that it can be used for the cleaning of the concentrates from the harmful compounds such as arsenic. Finally, the bioleaching is the up-to-date tool for the selective extraction of metals from collective concentrates or industrial products [4].

Methods

The microbial culture, used in this study, were mixed culture of mesophilic and moderately thermophilic microorganisms: *Acidithiobacillus ferrooxidans*AF-2 (B-RKM 0797), *Sulfobacillus thermosulfidooxidans* OT-1 (B-RKM 0794) and SK-4 (B-RKM 0796), which was deposited in the official collection at the RSE «Republican Collection of Microorganisms» of the Committee of Science of Ministry of Education and Science of the Republic of Kazakhstan.

The pH and redox potential (Eh) were determined by the analyzer «Mettler Toledo Seven Multi S47-K». The concentration of metals in solid samples and solutions was determined using atomic emission spectrometry on the spectrometer iCAP 7200 ICP-OES Analyzer of «Thermo Scientific» company and using the method of atomic absorption with atomization in a graphite furnace using the «QUANTUM-2AT» atomic absorption spectrometer [5]. The concentrations of Fe^{3+} and Fe^{2+} ions in the liquid phase were determined spectrophotometrically on «KFK-3–01» colorimeter (at wavelength λ=510 nm) [6]. The sulfur content in the sulfide concentrate and in the residues of leaching was determined gravimetrically [7].

During the pilot test, the arsenopyrite concentrate was obtained from the Bestobe deposit (JSC «Mining and Metallurgical Complex «Kazakhaltyn»). The average gold content is 60 g/t, the content of sulfides is 23 %, iron is 26 %, arsenic is 11 %. The concentration of solids in the pulp of the pilot plant was maintained at 20 % (w/w).

The pilot plant for bacterial oxidation of arsenopyrite concentrates consisted of 6 reactors with a volume of 1.5 m^3 each. The bioreactors are equipped with stirring devices, bubbling rings for air supply and heaters to maintain the temperature at 40 ºC. Pulp preparation was carried out in a 2 m^3 conditioning tank, provided with a stirring device.

First three bioreactors worked in parallel and formed the first stage. A combined stream from these bioreactors was then cascaded into a series of three bioreactors. The use of the first three bioreactors in parallel had a crucial role in the growth and stability of bacterial populations due to the fact that the retention time at first stage increases threefold. Schematic diagram of the installation is shown in Figure 1.

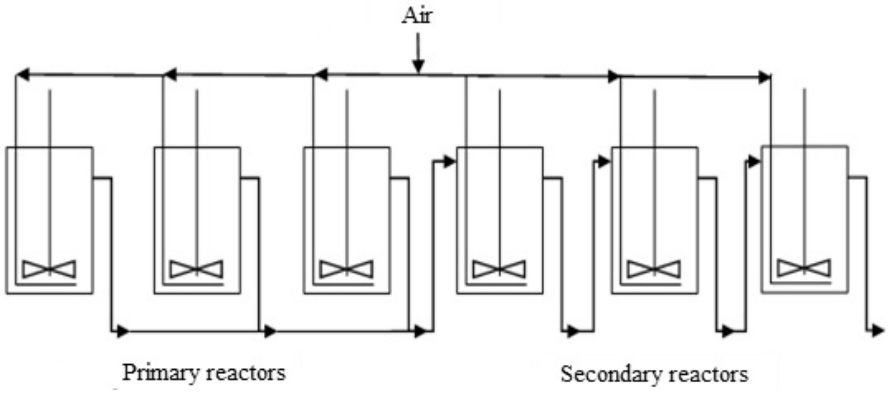

Figure 1. The scheme of pilot-scale plant

The cyanidation of bacterial leach residues and untreated concentrates was carried out in 100 ml Erlenmeyer flasks at a working volume of 40 ml with 40 % pulp on a shaker at 25 ºC and 200 rpm for 24 hours. The pH of the pulp was maintained at pH 10.5–11.0 by the addition of 10N sodium hydroxide.

Results

Initially, the retention time of the concentrate in the plant was 12 days. Due to the slow flow rate into the primary reactor, the feed was supplied hourly from the pre-weighed packages of the concentrate, and the water was added continuously. After the stable operation with a certain retention time was demonstrated, the feed rate had increased.

In the process of bacterial oxidation special attention was accentuated on the maintenance of the optimum acidity of the pulp (pH 1.0–1.5). Controlling the acidity of the pulp is necessary to prevent a decrease in the activity or death of acidophilic bacteria, as well as the precipitation of iron and arsenic compounds with an increase in acidity [8]:

$$2H_3AsO_4 + Fe_2(SO_4)_3 \rightarrow 2FeAsO_4 + 3H_2SO_4$$

$$3Fe_2(SO_4)_3 + 12H_2O + M_2SO_4 \rightarrow 2MFe_3(SO_4)_2(OH)_6 + 6H_2SO_4$$

where M^+ — is K^+, Na^+, NH_4^+or H_3O^+.

Samples were taken from each reactor for chemical analysis on a daily basis. The analysis included the determination of total iron, total sulfur, sulfide sulfur and arsenic in the solid samples and iron, sulfate sulfur and arsenic were analyzed in the solutions. The parameters of the bacterial oxidation process are shown in Table 1.

Table 1

Parameters of bacterial oxidation in a pilot plant

Pulp density, %	20
Retention time, days	6
Temperature, °C	40
Iron, g/L	45–49
Arsenic, g/L	16–19
pH	1.2–1.3
Eh, mV	640–720
The concentration of dissolved oxygen, ppm	2.0–5.0
Weight loss, %	38
Sulfide oxidation, %	90
Removal of As, %	92
Average recovery of Au, %	95

In the process of optimizing the parameters of the pilot bacterial oxidation plant, the retention time of the concentrate was reduced from 12 to 6 days. The recovery of gold was determined by standard bottle tests. Gold recovery, obtained from bacterial oxidation products, is shown in Figure 2.

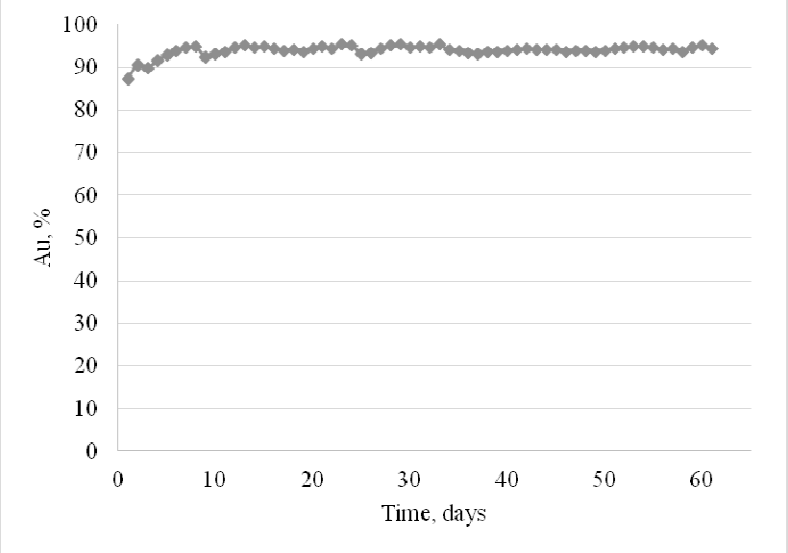

Figure 2. The gold recovery obtained from the bottle tests

According to the data presented in Figure 2, it can be seen that high levels of the gold recovery were observed throughout the test period. Figure 3 shows the graph of the gold recovery, depending on the total oxidation of sulfides.

According to the data presented in Figure 3, it can be seen that during the tests, the destruction of sulphides was over 90 %, which ensured the recovery of gold frombiooxidation products over 94 %. The average gold extraction was about 95 %.

Many researchers have shown that in order to effectively remove arsenic from the solution and obtain a stable precipitate of iron (III) arsenate, neutralization should be carried out step by step [8–11].

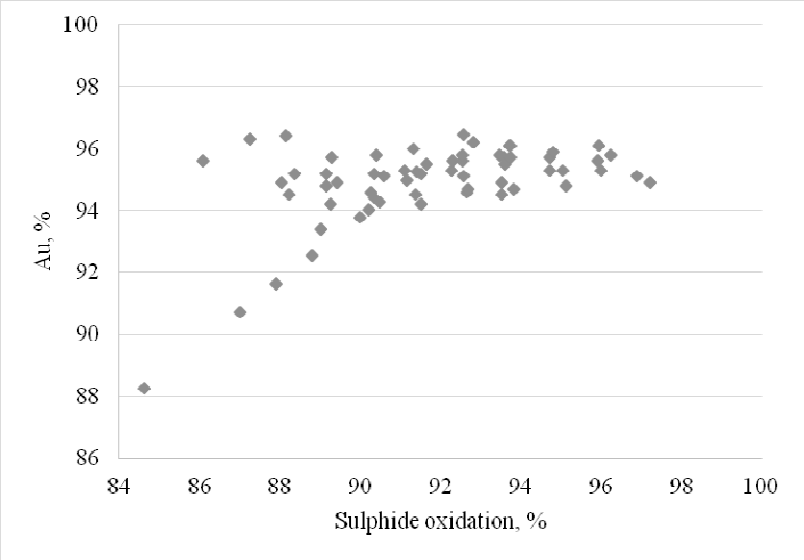

Figure 3. Dependence of the gold recovery on the oxidation state of sulfides

In the first stage, arsenic is deposited in the form of stable iron arsenate at pH 3–5, after that, the pH is raised to 6–8, in order to reach an environmentally acceptable level. The chemical processes that occur in this case can be described by the following equations:

Stage 1: Neutralization to pH 3–5

$$Fe_2(SO_4)_3 + H_3AsO_4 + CaCO_3 + 2H_2O \rightarrow$$
$$\rightarrow Fe(OH)_3(s) + CaSO_4(s) + FeAsO_4(s) + 2H_2SO_4 + CO_2$$

Stage 2: Neutralization to pH 6–8

$$H_2SO_4 + CaCO_3 \rightarrow CaSO_4(s) + CO_2 + H_2O$$

The formation of calcium arsenate $Ca_3(AsO_4)_2$ should be avoided during the neutralization of the arsenic solutions. Calcium arsenate is more soluble than iron (III) arsenate and is not a suitable form for long-term storage due to decomposition to carbonate under the influence of carbon dioxide contained in the air. The formation of calcium arsenate can be prevented with a molar ratio of iron (III): arsenic above 3: 1 and an increase in pH in the first stage of no more than 4–5 [12].

Due to high oxidation degree is maintained throughout the entire operation of the experimental plant, a high ratio of iron to arsenic concentration in the solution was observed, which provided ideal conditions for the arsenic precipitation in the form of trivalent iron arsenate. Determination of residual precipitation stability was carried out according to the protocol U.S. EPA-TCLP. The threshold concentration of TCLP for arsenic is 5 mg/L. The test results are shown in Table 2.

Table 2

Data of solution and residue analysis

Biooxidation solution			In solution after precipitation	In TCLP extract
Fe, g/L	As, g/L	pH	As, mg/L	As, mg/L
47	18	1.2	0.05	0.14

According to Table 2, the precipitate obtained after neutralization of the leaching solutions does not require special disposal, since the final concentration of the arsenic in the extracts of TCLP tests was 0.14 mg/L.

Conclusion

The pilot test have shown a high efficiency of biooxidative pretreatment of the arsenopyrite concentrate using *Acidithiobacillus ferrooxidans* AF-2, *Sulfobacillus thermosulfidooxidans* OT-1 and *Sulfobacillus thermosulfidooxidans* SK-4 for the gold extraction. 92 % of arsenic was recovered in 6 days of treatment. Only 47 % of gold is recovered through the direct cyanidation of the concentrate, while cyanidation after biooxidation has shown 95 % of the gold recovery.

References

1 Тусупова Б.Х. Анализ современного состояния добычи и кучного выщелачивания золота / Б.Х. Тусупова, Ж.Д. Байгурин // Вестн. КазНТУ. — 2009. — № 5. — С. 2, 3.

2 Лодейщиков В.В. Технология извлечения золота и серебра из упорных руд / В.В. Лодейщиков. — Иркутск: Иргиредмет, 1999. — 342 с.

3 Bhalerao S.A. Bioleaching: An Economic Alternative for the Mining Industry: A Review / S.A. Bhalerao // International journal of biotechnology and biosciences. — 2011. — Vol. 1. — P. 67–72.

4 Kaksonen A.H. The role of microorganisms in gold processing and recovery-A review / A.H. Kaksonen, B.M. Mudunurua, R. Hackl // Hydrometallurgy. — 2014. — Vol. 142. — P. 70–83.

5 Гарифзянов А.Р. Эмиссионная фотометрия пламени и атомно-абсорбционная спектроскопия / А.Р. Гарифзянов. — Казань: Казанский гос. ун-т, 2009. — 94 с.

6 Vogel A.I. Vodel's textbook of quantitative chemical analysis / A.I. Vogel. — Longman Group UK Limited, 1989. — 690 p.

7 Алексеев В.Н. Количественный анализ / В.Н. Алексеев. — М.: Химия, 1972. — 504 с.

8 Zeng W. Detection and analysis of attached microorganisms on the mineral surface during bioleaching of pure chalcopyrite with moderate thermophiles / W. Zeng, S. Tan, M. Chen, G. Qiu // Hydrometallurgy. — 2011. — Vol. 106. — P. 46–50.

9 GrËafe M. Formation of metal-arsenate precipitates at the goethite–water interface / M. GrËafe, M. Nachtegaal, D.L. Sparks // Environ. Sci. Technol. — 2004. — Vol. 38. — P. 6561–6570.

10 Jia Y. Coprecipitation of arsenate with iron (III) in aqueous sulfate media: Effect of time, lime as base and co-ions on arsenic retention / Y. Jia, G.P. Demopoulo // Water research. — 2008. — Vol. 42. — P. 661–668.

11 Moldovan B.J. Characterizing and quantifying controls on arsenic solubility over a pH range of 1–11 in a uranium mill-scale experiment / B.J. Moldovan, M.J. Hendry // Environ. Sci. Technol. — 2005. — Vol. 39. — P. 4913–4920.

12 Rawlings D.E. Biomining: Theory, Microbes and Industrial Processes / D.E. Rawlings. — Berlin: Springer-Verlag Berlin Heidelberg, 2007.

В.М. Шайхутдинов, Н.К. Жаппар, О.А. Тен, Д.С. Балпанов, Е.Н. Канафин,
Р.А. Ханнанов, Р.Ш. Еркасов, А.А. Бакибаев, А.Т. Кездикбаева

Арсенпиритті алтын концентратты күбіде биототықтырудың тәжірибелі сынағы

Мақалада құрамында алтын 60 г/т, сульфидтер 23 %, темір 26 %, күшәлә 11 % арсенпиритті алтын концентратты күбіде биототықтыру сынақтарының нәтижелері көрсетілген. Сынақ кезінде *Acidithiobacillus ferrooxidans* AF-2 мезофилді штаммнан және орташа-термофилді штаммдардан тұратын консорциум пайдаланды. Сынақтардың әрбірі 1,5 м^3 көлемді 6 реактордан тұратын қондырғыда жүргізілді. Қондырғы қуат көзінде қатты заттар концентрациясын 20 % (мас./мас.) деңгейінде ұстады. Күбіде бактериялық тотықтыру қондырғысының оңтайландыру барысында концентратты ұстау уақыты 12-ден 6 тәулікке дейін қысқартылды. Сынақ үстінде сульфидтер бұзылуы 90 % жоғары, бұл биототықтыру өнімнен алтынды алу 94 % жоғары, сынақ ішінде алтынды орташа алуы 95 % құрады. Шаймалау ерітінділерден күшәләні арылту кальций карбонатымен екі кезеңді бейтараптандыру жолымен жүргізілді. Эксперименттік қондырғының бар жұмысы бойы ұсталынатын тотықтырудың жоғары деңгейінен үш валентті темір арсенаты түрінде күшәләнің тұнуына кемшіліксіз жағдайды тудырған ерітіндіде күшәләға үш валентті темір концентратының жоғары қатынасы байқалды. Сонымен бірге темір арсенатының (III) тұрақты тұнбасы пайда болды. Тұну тұнбасының тұрақтылығын анықтау Toxicity Characteristic Leaching Procedure (TCLP) хаттамасы бойынша жүргізілді. Шаймалау ерітіндісін бейтараптандыру нәтижесінде алынған тұнба TCLP тесттер сірінділерінде күшәләнің соңғы концентрациясы 0,14 мг/л құрағандықтан, арнайы сақтауды талап етпейді.

Кілт сөздер: арсенпиритті концентрат, биототықтыру, шанда шаймалау, *Acidithiobacillus ferrooxidans, Sulfobacillus thermosulfidooxidans,* алтын, күшәлә, сынамалы сынау.

В.М. Шайхутдинов, Н.К. Жаппар, О.А. Тен, Д.С. Балпанов, Е.Н. Канафин,
Р.А. Ханнанов, Р.Ш. Еркасов, А.А. Бакибаев, А.Т. Кездикбаева

Опытное испытание чанового биоокисления арсенопиритного золотого концентрата

В статье приведены результаты опытных испытаний чанового бактериального окисления арсенопиритного золотого концентрата: содержание золота 60 г/т, сульфидов 23 %, железа 26 %, мышьяка

11 %. При испытании использовали консорциум, состоящий из мезофильного штамма *Acidithiobacillus ferrooxidans* AF-2 и умеренно-термофильных штаммов *Sulfobacillus thermosulfidooxidans* ОТ-1 и SK-4. Испытания проводились на установке, состоящей из 6 реакторов, объемом 1,5 м^3 каждый. Концентрацию твердых веществ в питании установки поддерживали на уровне 20 % (мас./мас.). В процессе оптимизации параметров установки чанового бактериального окисления время удержания концентрата было сокращено с 12 до 6 суток. В ходе испытания разрушение сульфидов составило свыше 90 %, которое обеспечило извлечение золота из продуктов биоокисления при цианировании свыше 94 %, среднее извлечение золота в течение испытаний составило 95 %. Удаление мышьяка из растворов выщелачивания проводили путем двухстадийной нейтрализации раствора карбонатом кальция. Из-за высокой степени окисления, поддерживаемой на протяжении всей работы экспериментальной установки, наблюдалось высокое отношение концентрации трехвалентного железа к мышьяку в растворе, что обеспечило идеальные условия для осаждения мышьяка в виде арсената трехвалентного железа. Определение стабильности осадков осаждения проводили по протоколу Toxicity Characteristic Leaching Procedure (TCLP). Осадок, полученный в результате нейтрализации раствора выщелачивания, не требует специального захоронения, так как конечная концентрация мышьяка в экстрактах TCLP тестов составила 0,14 мг/л.

Ключевые слова: арсенопиритный концентрат, биоокисление, чановое выщелачивание, *Acidithiobacillus ferrooxidans, Sulfobacillus thermosulfidooxidans,* золото, мышьяк, опытное испытание.

References

1 Tusupova, B.Kh., & Baygurin, Zh.D. (2009). Analiz sovremennoho sostoianiia dobychi i kuchnoho vyshchelachivaniia zolota [Analysis of the current state of mining and heap leaching of gold]. *Vestnik KazNTU — Bulletin of KazNTU, 5,* 2–3 [in Russian].

2 Lodeyshchikov, V.V. (1999). *Tekhnolohiia izvlecheniia zolota i serebra iz upornykh rud [Technology of extraction of gold and silver from refractory ores]*. Irkutsk: Irhiredmet [in Russian].

3 Bhalerao, S.A. (2011). Bioleaching: An Economic Alternative for the Mining Industry: A Review. *International journal of biotechnology and biosciences*, *1*, 67–72.

4 Kaksonen, A.H., Mudunurua, B.M., & Hackl, R. (2014). The role of microorganisms in gold processing and recovery. A review. *Hydrometallurgy*, *142*, 70–83.

5 Garifzyanov, A.R. (2009). *Emissionnaia fotometriia plameni i atomno-absorbtsionnaia spektroskopiia [Emission photometry of a flame and atomic absorption spectroscopy]*. Kazan: Kazan State University [in Russian].

6 Vogel, A.I. (1989). *Vodel's textbook of quantitative chemical analysis*. Longman Group UK Limited.

7 Alekseev, V.N. (1972). *Kolichestvennyi analiz [Quantitative analysis]*. Moscow: Khimiia [in Russian].

8 Zeng, W., Tan, S., Chen, M., & Qiu, G. (2011). Detection and analysis of attached microorganisms on the mineral surface during bioleaching of pure chalcopyrite with moderate thermophiles. *Hydrometallurgy*, *106*, 46–50.

9 GrËafe, M., Nachtegaal, M., & Sparks, D.L. (2004). Formation of metal-arsenate precipitates at the goethite–water interface. *Environ. Sci. Technol*., *38*, 6561–6570.

10 Jia, Y., & Demopoulo, G.P. (2008). Coprecipitation of arsenate with iron (III) in aqueous sulfate media: Effect of time, lime as base and co-ions on arsenic retention. *Water research*, *42*, 661–668.

11 Moldovan, B.J., & Hendry, M.J. (2005). Characterizing and quantifying controls on arsenic solubility over a pH range of 1–11 in a uranium mill-scale experiment. *Environ. Sci. Technol*., *39*, 4913–4920.

12 Rawlings, D.E. (2007). *Biomining: Theory, Microbes and Industrial Processes*. Berlin: Springer-Verlag Berlin Heidelberg.

UDC 546.19

N.I. Kopylov[1], M.O. Moldurushku[2]

[1]Institute of Solid State Chemistry and Mechanochemistry of the Siberian Branch of the Russian Academy of Sciences, Novosibirsk, Russia;
[2]Tuva Institute of Integrated Development of Natural Resources of the Siberian branch of the Russian Academy of Sciences, Kyzyl, Russia
(E-mail: kolyubov@narod.ru)

Study of the influence of initial contents of arsenic of the Khovu-Aksy dumps on effectiveness of the developed regimes of their dearsenization

Dumps of arsenic-containing wastes from the former Tuvakobalt combine are one of the most dangerous objects of Tuva. The combine's wastes were accumulated in ponds (dumps) for 20 years of operation of the combine. After its closure, the ponds were drained and are now exposed to the external environment, namely, groundwater, precipitation and wind erosion. The accumulated dumps contain industrial contents of nonferrous metals and about 50 thousand tons of arsenic. Due to natural precipitation, toxic compounds are flushed to the lower layers of dump maps with subsequent ingress into groundwater and the environment. Long-term studies carried out at the Institute of Solid State Chemistry and Mechanochemistry and the Tuvinian Institute for Exploration of Natural Resources of the Siberian Branch of the Russian Academy of Science were devoted to the issue of dearsenization of arsenic dumps of Khovu-Aksy of the «Tuvakobalt» combine with the aim of processing them and obtaining the secondary raw materials for the production of materials on their basis that can be used as recyclables in the national economy such as cake — as a flux in the production of ceramic and arsenic sulphide in the production of antiseptics in the processing of wood or biocide for antifouling coatings of hulls of ships and hydrotechnical structures. Studies carried out using initial samples of dumps sludge taken from different burial sites and differing in the content of arsenic (1.88 and 4.21 %) showed the possibility of effective dearsenization of slurry materials on the tested technological regimes of the process, regardless of the concentration of arsenic in them, with the formation of cake (with a content of As ≤ 0.3 %) and arsenic sulfide (IV degree of toxicity).

Keywords: sludge, cake, arsenic sulfide, soda, roasting, leaching, solution pH.

Introduction

According to the technology designed for the Khovu-Aksy deposit (the Republic of Tuva, Russia), the arsenic was withdrawn from autoclave leaching solutions by magnesian «milk» precipitation at S:L = 1:4 and manganese oxide consumption ~13 kg/kg of arsenic [1]. The residual arsenic content in the carbonate pulp in terms of the dry mass should be no more than 2.4 % (herein and after, % wt.).

The washed sludge (tails of thickening pulp of autoclave leaching), comprising up to 93–97 % of the mass of the ore, was sent to the dump. In the tails, as a rule, 10 to 25 % of cobalt was remained from the content in the ore (~ 0.1 % of the sludge mass) in the initial arsenide form [2]. The arsenic-magnesian precipitate of the solution dearsenization was sent to the dump along with the autoclave leaching sludges.

Over 20 years of operation of the combine, more than 2 million m^3 of wastes were stored in the Khovu-Aksy dumps [3] with a content of As in the range of 3.5–6.4 % and metals on average, %: Co — 0.18; Ni — 0.22; Cu — 0.11 as well as Ag — 45 g/t and Au is 60 mg/t. As field investigations of the dumps have shown [4] pore waters that area complex magnesia-calcium ammonia-hydrocarbonate type of solutions are formed

as a result of waste storage. A high content of arsenic was found there (2.2 mg/L). Also, high levels of arsenic are found in water extracts (5.5 mg/L). This indicates the presence of soluble forms of arsenic in the dumps. There was also an increase in arsenic content in the drying slag of dumps (Map No. 5) to 29.5 mg/L, which corresponds to 50 MPC for this type of storage [3].

Thus, there is an intensive leaching of arsenic of various types by solutions formed or coming from outside, and its subsequent migration with drainage waters into the environment. Consequently, the arsenic-containing waste of the combine in conditions of constant contact with the environment represents a serious environmental hazard for the region. In addition, the dump wastes of Khovu-Aksy contains high iron contents (up to ~ 10 %) and alkaline earth oxides (CaO, MgO, total 25–30 %) and moderate concentrations of refractory oxides (SiO_2 and Al_2O_3), which determines their low refractory temperature ~ 1180 ºC) and fusibility. Therefore, the removal of arsenic, its neutralization and the possible integrated use of dumps as technogenic raw materials with extraction of metals from them, obtaining marketable products (building materials, ceramics, etc.) is an actual problem.

Fundamental work on the removal of arsenic from technological processes was carried out in the second half of the 20th century within the framework of the All-Union Program MP-16/20 (CMC USSR) [5], in particular, on the removal of arsenic from concentrates of heavy non-ferrous metals in the head of the process by sulphidizing firing and transfer it into a slightly soluble (4 hazard category) sulphide form [6, 7 etc.].

Using this positive experience, later studies were carried out on the application of this technology to neutralize the Khovu-Aksy dumps. The possibility of deep removal of arsenic from the materials of the dumps was shown. The content of arsenic in the initial material (on average ~ 5 %) was decreased to 0.80–0.28 %, respectively, at a ratio of the sulphidizer to the product from 1:6 to 1:2 at a roasting temperature of 900–950 ºC [8]. At the same time, the simultaneous burning of the sludge without a sulphidizer showed the absence of magnesium arsenates (initially the main dump form of arsenic according to the technology of dearsenization of autoclave solutions [1]), which should decompose with distillation of arsenic trioxide at 450–600 ºC according to the reactions [9]:

$$2MgNH_4AsO_46H_2O = 2NH_3 + 7H_2O + 2MgO + As_2O_3$$
$$Mg_3(AsO_4)_24H_2O = 3MgO + As_2O_3 + 4H_2O + O_2$$

Since this is not observed in our case, this is explained by the fact that in the dumps during storage magnesian arsenates decompose as a result of hypergenes with the formation of secondary arsenic compounds such as vivianite forms of arsenates.

In the technological aspect, the sulphitizing roasting process must be carried out in the kinetic conditions of the countercurrent solid-gas. For this purpose, a shaft type furnace can serve as an optimal unit, and appropriate equipment is required for condensation and trapping of arsenic sulphide fumes and utilization of sulfurous anhydride [6]. All this requires certain initial financial investments. Therefore, despite the high performance, its practical use is currently quite problematic.

In the metallurgy of lead, as early as the beginning of the 20th century, a method was developed for the processing of spikes, including burning-sintering at a temperature of red heat of a mixture of spice with soda and subsequent aqueous leaching of the formed sinder [10, 11]. In the experiments carried out on this method, the Khovu-Aksy dumps of the Tuvakobalt combine obtained leaching cakes of a soda-slime cake with a content of 0.47 to 0.71 % of arsenic in them. More than 90 % of the arsenic contained in the sludge of the heap is concentrated in the leach solution [12].

As the practice of research has shown, the phase and chemical compositions of the dumping products of metallurgical industries, in particular the Khovu-Aksy dumps are determined by the initial composition of the raw materials, the processing technology, and also depend on the time and storage conditions. While storing wastes in dumps, their chemical and mineral compositions can be sharply different both in the area of the dump and its vertical section, as well as from the trench to the trench, from the map to the map. So, for example, (according to the data of 2006 [13]), in the volume of the last map No. 5 of the Khovu-Aksy dumps, iron and arsenic are distributed in the following order. In terms of the surface layer, the iron content is fixed by a 2-fold concentration spread (the average content is 4.4 %, the maximum is 6.2 %, the minimum is 3.1 %), and the arsenic content is 16-fold (with an average content of 2.1 %, the maximum is 4.8 % and the minimum is 0.3 %).

The average borehole test at a depth of ≥ 1 m contains 5.1 % of iron — and 2.5 % of arsenic. Despite the short shelf life, leaching and washing out of elements in the lower layers of the map, their vertical migration and possible interaction, in particular arsenic with natural and technological solutions, have already been

noted. According to the results of the study, it is concluded in [4] that the bulk of the elements (metals) of the upper horizons is assimilated by pore solutions and, as they are deposited in the maps, are gradually washed out into the lower layers by natural precipitation, where they concentrate on the active surfaces of the formed mineral rocks as a result of sorption. In this regard, it seems interesting to consider the influence of the formed composition of the sludge material on the process of its processing, with the transfer of arsenic to the sulphide according to the technology being developed.

At the same time, all work on the development of arsenic removal technology from the Khovu-Aksy dumps and optimization of optimal process regimes was carried out on samples with high arsenic concentrations (within ~ 3–4.5 %) [14, 15]. No experiments were performed on the material with low concentrations of arsenic (within ~ 1–2 % of As). In this connection, it is of interest to check the effectiveness of previously worked out technology regimes on the material of the dump with a low initial arsenic content.

Experimental

The study was carried out on samples of sludge from the dump of map No. 5, selected (06.2012) from different horizons and differing in their arsenic content: 1.88 % is an average sample taken from a depth of ~0.1–0.15 m from the upper horizon, and 4.21 % is the average sample from the lower horizons of the dump (>1.0 m).Firing sludge mixtures with soda and adding coal was carried out at the ratio sludge:soda:coal = = 1:1:0.1. Further, aqueous leaching, cake separation, arsenic precipitation from the solution with sodium sulphide was carried out. Experiments to check the effect of the initial slurry composition on the arsenic content on the final indicators of the technology were carried out on the following regimes obtained earlier as a result of joint research by the Institute of Solid State Chemistry and Mechanochemistry and the Tuvinian Institute for Exploration of Natural Resources of the Siberian Branch of the Russian Academy of Science [14, 15]:

- roasting procedure with the ratio of components in the initial charge, sludge:soda:coal = 1:1:0.1, in the temperature range 650–850 ºC and holding time 1.0 h;
- the operation of aqueous leaching at S:L = (1:6)–(1:10); temperature 70–80 ºC and time 1–1.5 hours, followed by separation by filtration of cake and arsenic-containing aqueous solution and aqueous washing of cake at a temperature of 40–50 ºC;
- sulphidation operation by introducing into an aqueous arsenic-containing sodium sulphide solution heated to ~50 ºC, calculated from 1.7 to 2.0, stoichiometrically necessary to bind arsenic to As_2S_3 sulphide;
- removal of the silicic acid formed in the process by introducing an acid (HCl) into the solution until the pH of the solution decreases from 11–12 to 8–9;
- precipitation of arsenic sulphide from the solution by further lowering the pH to a value of 2–3, its removal by filtration from the solution into a separate solid, environmentally less hazardous product.

There are a series of experiments using an average sample of sludge from the lower horizons of the dump. The initial sample of the sludge contained 4.21 % As. The cinder (soda flake) obtained after heat treatment of the charge in the prescribed regimes practically completely retains arsenic in the range of 2.27–2.38 % (on average 2.31 %) according to the chemical analysis.

The resulting firing products were leached with distilled water at stirring. After the operation, the pulp was filtered; the cake was washed with hot water and dried. The minimum arsenic content in the cake was obtained at a firing temperature of 720 ºC. The chemical analysis gives the following average content of elements in the cake: 0.34 % — As; 6.04 % — Fe; 16.20 % — Ca; 0.075 % — Co; 0.069 % — Ni; 3.73 % — Al. The resulting arsenate solution is alkaline with a pH of ~12 and a content of As ~4 g/L.

Since it was found that during the operation of sulphidation of the resulting arsenate solution together with arsenic sulphide precipitation of a silicon dioxide impurity takes place, therefore, prior to sulphiding, it was necessary to remove the siliceous constituents from the solution. To this end, the solution, heated to ~60 ºC, was acidified (with a concentrated solution of hydrochloric acid) to pH 8–9. Upon subsequent cooling to room temperature, formation and subsequent structuring of the silicic acid precipitate occurred. The precipitate was separated and calcined at ~800 ºC. The sample of the obtained silica precipitate contained: O_2 — 55.2 %; Si — 35.12 %. A certain amount of impurity of sodium and chlorine was also found in the resulting solid product. The silicon dioxide content in it is about 85 %.

From the filtrate, after the removal of silicon dioxide, arsenic is precipitated by introducing into the solution at 100 % excess of sodium sulfite and acidifying the solution to pH = 2–3, by adding the necessary amount of hydrochloric acid. The degree of separation of arsenic in the form of sulphide precipitate from the

solution was 99.5 %, with the content of arsenic being up to 40 % arsenic and up to 60 % sulphur. According to elemental chemical analysis, the sulphide precipitate, in addition to arsenic sulphide, contains about 10 % of elemental sulphur.

There are experiments using an average sample of the upper horizon sludge. The initial sample of the sludge contained 1.88 % — As; 0.057 % — Co and Ni; 0.048 % — Cu; 5.0 % — Fe; 3.98 % — Al; 4.78 % — Mg; 14.0 % — Ca; 18.0 % — Si. Analysis shows the presence of quartz, calcite, a number of silicate, aluminosilicate mineral constituents in the material, as well as the vivian form of arsenates.

After calcination-sintering of the prepared charge (sludge:soda:coal = 1:1:0.1), products were obtained whose average elemental composition is as follows 1.13 % — As; 5.0 % — Ca; 2.01 % — Mg; 6.88 % — Si; 2.13 % — Fe; 1.41 % — Al; 21.09 % — Na; 14.31 % — C. According to the X-ray analysis phases of quartz, silicates and aluminosilicates, vivianite forms of arsenate have been preserved in the material. There is no calcite.

The cake of the aqueous leaching of the soda ash contains: 0.27 % — As; 16.20 % — Ca; 6.04 % — Fe; 3.73 % — Al; 0.075 % — Co; 0.069 % — Ni; 0.074 % — Cu; 16.22 % — Si; 7.24 % — Na; 5.48 % — Mg; 0.08 % — C. According to the analysis, the material is mainly represented by quartz, silicate and aluminosilicate mineral constituents. The phases of arsenides and arsenates in the cake material are absent.

After the extraction of the cake from the arsenate solution, then, at a temperature of ~60 ºC, the removal of silicon by a solution of hydrochloric acid (an aqueous solution in a ratio of 1:1) was carried out with a decrease in the pH of the solution to 9–8. The silica residue obtained after cooling and daily settling was calcined at 800 ºC. The resulting sample of the silica precipitate contains up to 37 % of Si. The sample also contains impurities of sodium and chlorine. The content of silicon dioxide is of the order of ~83 %.

For deposition of arsenic sulphide from the solution, its pH was further reduced to 3–2 at a solution temperature of 60 ºC, followed by exposure (during the day at room temperature). The product obtained contained 45.7 % of As, which approximates As to the composition of arsenic pentasulphide.

Results and discussion

Thus, in order to determine the effect of arsenic content in the initial sample of the sludge on extracting it into a separate, slightly toxic product, experiments on sludge dearsenization were carried out on a number of initial samples of sludge (map 5), taken from the surface and lower horizons of the dump, which differed sharply in content of arsenic in them (1.88 and 4.21 %, respectively).

In work previously elaborated the following optimal modes of technology were used:

– composition of the charge and the ratio of components in it: sludge:soda:coal = 1:1:0.1;
– aqueous leaching at S:L = (1:6)–(1:10), temperature 70–80 ºC, time 1.5 h and the subsequent filtration with allocation of a cake from a solution;
– precipitation of silica from the solution by lowering the pH of the solution to 9–8 and subsequent removal of the silica precipitate by filtration;
– sulphidization of the solution with sodium sulphide with 100 % excess of reagent;
– precipitation of arsenic sulphide with a decrease in the pH of the solution to 3–2 and its subsequent isolation from the solution by filtration.

As a result, it was shown that this technology provides the maximum withdrawal of arsenic into a separate low-toxic product, with its any content in the original sludge. When calcining the charge (in the composition of sludge:soda:coal = 1:1:0.1) and subsequent aqueous leaching of the resulting cinder, the residual arsenic concentration in the formed cake is in the range from 0.23 to 0.34 %. The extraction of arsenic from the slurry into the solution is of the order of 90–95 %. With further acidification of the leach solution to pH = 8–9, precipitation of a white precipitate occurs. After its calcination at 800 °C, it contains up to 85 % of SiO_2 according to the chemical analysis. Subsequent decrease in the pH of the solution to 2–3 leads to a complete (by 98–99 %) precipitation of arsenic in the form of sulfide from a solution. According to the chemical analysis a certain amount of sulphuris present in the sediment, which is close to its content in the product corresponding to the composition of pentlandite (As_2S_5).

Conclusions

The studies carried out using initial samples of slurry of the Khovu-Aksy dumps of the Tuvakobalt combine selected from different burial sites and differing in their arsenic content (1.88 and 4.21 %) have shown the possibility of effective dearsenization of the slurry materials of the given dumpson the tested process regimes, regardless of the concentration of arsenic in them, with the formation of practically low-toxic

cake (with a content of As ≤ 0.3 %) and arsenic sulphide (hazard of IV category).The obtained materials can be used as recyclables in the national economy: cake as a smelter in the production of ceramic products, and arsenic sulphide in the production of antiseptics for woodworking or biocide of anti-fouling coatings for hulls of ships and hydraulic structures.

References

1 Кобальт: монография: в 2-х т. Т. 2. / И.Д. Резник, С.И. Соболь, В.М. Худяков. — М.: Машиностроение, 1995. — 470 с.

2 Лазарев М.И. Повышение эффективности передела в схеме производства кобальта гидрометаллургического цеха: монография / М.И. Лазарев. — Свердловск: МЦМ СССР, 1979. — 42 с.

3 Забелин В.И. Экология и здоровье: монография / В.И. Забелин, В.В. Заика, В.И. Лебедев. — Кызыл: Тувинское книжн. изд-во, 1995. — 89 с.

4 Гаськова О.Л. Экспериментальное моделирование окислительного выщелачивания хвостов передела никель-кобальтовых руд / О.Л. Гаськова, Е.П. Бортникова, С.Б. Бортникова, Н.В. Андросова // Химия в интересах устойчивого развития. — 2000. — Т. 8, № 3. — С. 184.

5 Копылов Н.И. Мышьяк: монография / Н.И. Копылов, Ю.Д. Каминский; под ред. акад. РАН Г.А. Толстикова. — Новосибирск: Сиб. универ. изд-во, 2004. — 367 с.

6 Исабаев С.М. Физико-химические основы сульфидирования мышьяксодержащих соединений: монография / А.С. Пашинкин, Э.Г. Мильке, М. Жамбеков. — Алма-Ата: Наука, 1986. — 184 с.

7 Каминский Ю.Д. Технологические аспекты извлечения золота из руд и концентратов: монография / Ю.Д. Каминский, Н.И. Копылов; под ред. чл.-корр. РАН Г.Л. Пашкова. — Новосибирск: Изд-во СО РАН, 1999. — 123 с.

8 Копылов Н.И. Сульфидизирующий обжиг отвальных промпродуктов комбината «Тувакобальт» / Н.И. Копылов, Ю.Д. Каминский // Вестн. Караганд. ун-та. Сер. Химия. — 2016. — № 81(1). — С. 65–70.

9 Набойченко С.С. Мышьяк в цветной металлургии: монография / С.С. Набойченко, С.В. Мамячиков, С.В. Карелов. — Екатеринбург: УрО РАН, 2004. — 240 с.

10 Litvill K. // Trans. Amer. Inst. Min. and Met. Eng. — 1925. — Vol. 71. — P. 953 (цит. по: Гофман Г.О. Металлургия свинца /пер. с нем., под ред. и дополнением акад. АН СССР Г.Г. Уразова. — М.-Л.: Цветметиздат, 1932. — С. 656–658).

11 Пономарёва Е.И. Мышьяк в свинцово-цинковой промышленности: монография / Е.И. Пономарёва, В.Д. Соловьёва, В.В. Боброва и др. — Алма-Ата: Наука, 1975. — 101 с.

12 Копылов Н.И. Вывод мышьяка из отвалов комбината «Тувакобальт» комбинированным способом / Н.И. Копылов, Ю.Д. Каминский // Вестн. Караганд. ун-та. Сер. Химия. — 2016. — № 81(1). — С. 60–64.

13 Бортникова С.Б. Геохимия техногенных систем: монография / С.Б. Бортникова, О.Л. Гаськова, Е.П. Бессонова. — Новосибирск: Академ. изд-во «Гео», 2006. — 169 с.

14 Копылов Н.И. Комбинированный способ извлечения мышьяка из отвалов / Н.И. Копылов, Ю.Д. Каминский, А.П. Очур-оол // Химическая технология. — 2011. — Т. 12, № 8. — С. 498–500.

15 Копылов Н.И. Проблемы мышьяксодержащих отвалов: монография / Н.И. Копылов; отв. ред. акад. Г.А. Толстиков. — Новосибирск: Академ. изд-во «Гео», 2012. — С. 127, 128.

Н.И. Копылов, М.О. Молдурушку

Хову-Аксы үйінділеріндегі күшәләнің бастапқы құрамдарын оларды деарсенизациялаудың өңделген тәртібінің тиімділігіне әсерін зерттеу

Туваның ең қауіпті нысандарының бірі болып бұрынғы «Тувакобальт» комбинатының күшәлә-құрамды қалдықтарының үйінділері табылды. Комбинат қалдықтары комбинаттың 20 жыл жұмысы барысында қалдықтарды көму тоғанды үйінділерінде жинақталды. Комбинат жабылған соң тоғаншалар кептіріліп, осы уақытқа дейін сыртқы ортаның әсері: ағын сулар, атмосфералық жауын-шашын, жел эрозиясы жатады. Жинақталған үйінділерде түсті металдардың өнеркәсіптік құрамдары және күшәләнің 50 мың тоннаға жуық мөлшері бар. Табиғи жауын-шашындардың салдарынан улы қосылыстар төменгі қабаттарға шайылады, соңынан ағын суларға және қоршаған ортаға түседі. РҒА СБ ХТТМИ және ТувКОПРИ жүргізілген көпжылдық зерттеулер «Тувакобальт» комбинатының Хову-Аксы күшәләқұрамды үйінділерін деарсенизациялау, олардың өңделу және солардың негізінде халық шаруашылығында екіншілік шикізат ретінде қолданылуы мүмкін, материалдарды өңдеуге қажет екіншілік заттарды: кекті-керамикалық өнімдерді алуда немесе жол салу саласында қолданылатын плавеньдер ретінде, ал күшәлә сульфиді-теңіз жайықтарының өсетін жабындарын немесе гидротехникалық құрылғылар үшін, ағаштарды немесе биоцидті өңдеуге қажет антисептиктер өндірісінде қолданылатын заттарды алу мәселесіне арналған. Үйінділер шламдарының, көмудің әртүрлі деңгейлерінен алынған және олардың құрамындағы күшәләнің құрамы бойынша ажыратылатын (1,88 және 4,21 %), сынамаларын қолданып жүргізілген зерттеулер әртүрлі технологиялық режимдерде зерттеліп, нәтижесінде құрамындағы күшәләнің мөлшеріне қарамастан, шлам

материалдарын тиімді деарсенизациялау мүмкіндігі бар екенін және құрамында (As≤ 0,3 % және улылығы IV күшәлә сульфиді бар) кек түзілетінін көрсетті.

Кілт сөздер: шламдар, кек, күшәлә сульфиді, сода, күйдіру, сілтісіздендіру, ерітіндінің pH, өнеркәсіптік құрамы.

Н.И. Копылов, М.О. Молдурушку

Изучение влияния исходных содержаний мышьяка отвалов Хову-Аксы на эффективность разработанных режимов их деарсенизации

Одним из наиболее опасных объектов Тувы являются отвалы мышьяксодержащих отходов бывшего комбината «Тувакобальт». Отходы комбината накапливались в прудковых захоронениях (отвалах) в течение 20 лет работы комбината. После его закрытия прудки были осушены и в настоящее время подвергаются воздействию внешней среды: грунтовых вод, атмосферных осадков и ветровой эрозии. В накопленных отвалах содержатся промышленные содержания цветных металлов и порядка 50 тыс. т мышьяка. За счёт естественных осадков происходит смывание токсичных соединений в нижние слои карт отвала с последующим попаданием в грунтовые воды и окружающую среду. Многолетние исследования, проводимые в ИХТТМ и ТувИКОПР СО РАН, были посвящены вопросу деарсенизации мышьяксодержащих отвалов Хову-Аксы комбината «Тувакобальт» с целью их переработки и получения на их основе вторичного сырья для производства материалов, которые могут быть использованы в качестве вторсырья в народном хозяйстве: кека — в качестве плавня при производстве керамической продукции или дорожного строительства, а сульфида мышьяка — в производстве антисептиков при обработке древесины или биоцида для противообрастающих покрытий корпусов морских судов и гидротехнических сооружений. Проведенные исследования с использованием исходных проб шлама отвала, отобранных из различных уровней захоронения и отличающихся по содержанию в них мышьяка (1,88 и 4,21 %), на отработанных технологических режимах процесса показали возможность эффективной деарсенизации шламовых материалов, вне зависимости от величины концентрации в них мышьяка, с образованием кека (с содержанием ≤ 0,3 % As) и сульфида мышьяка (IV степени токсичности).

Ключевые слова: шламы, кек, сульфид мышьяка, сода, обжиг, выщелачивание, pH раствора, промышленное содержание.

References

1 Reznik, I.D., Sobol', S.I., & Khudiakov, V.M. (1995). *Kobalt [Cobalt]*. (Vols. 1–2). Moscow: Mashinostroenie [in Russian].

2 Lazarev, M.I. (1979). *Povyshenie effektivnosti peredela v skheme proizvodstva kobalta hidrometallurhicheskoho tsekha [Increase of efficiency of redistribution in the scheme of production of cobalt hydrometallurgical shop]*. Sverdlovsk: MTSM USSR [in Russian].

3 Zabelin, V.I. (1995). *Ekolohiia i zdorovie [Ecology and health]*. Kyzyl: Tuvinskoe knizhnoe izdatelstvo [in Russian].

4 Gaskova, O.L., Bortnikova, Ye.P., Bortnikova, S.B., & Androsova, N.V. (2000). Eksperimentalnoe modelirovanie okislitelnoho vyshchelachivaniia khvostov peredela nikel-kobaltovykh rud [Experimental modeling of oxidative leaching of tailings of redistribution of nickel-cobalt ores]. *Khimiia v interesakh ustoichivoho razvitiia — Chemistry in the interests of sustainable development*, *8, 3,* 184.

5 Kopylov, N.I., & Kaminsky, Yu.D. (2000). *Myshiak [Arsenic]*. G.A. Tolstikov (Ed.). Novosibirsk: Sibirskoe universitetskoe izdatelstvo [in Russian].

6 Isabaev, S.M., Pashinkin, A.S., Milke, E.G., & Zhambekov, M. (1986). *Fiziko-khimicheskie osnovy sulfidirovaniia myshiaksoderzhashchikh soedinenii [Physicochemical bases of sulfidation of arsenic-containing compounds]*. Alma-Ata: Nauka [in Russian].

7 Kaminskii, Yu.D., & Kopylov, N.I. (1999). *Tekhnolohicheskie aspekty izvlecheniia zolota iz rud i kontsentratov [Technological aspects of gold recovery from ores and concentrates]*. G.L. Pashkov (Ed.). Novosibirsk: Publishing house of the SB RAS [in Russian].

8 Kopylov, N.I., & Kaminskii, Yu.D. (2016). Sulfidiziruiushchii obzhih otvalnykh promproduktov kombinata «Tuvakobalt» [Sulphidizing firing of dumping industrial products of the «Tuvakobalt»]. *Vestnik Karahandiskoho universiteta. Seriia Khimiia — Bulletin of the Karaganda University. Ser. Chemistry*, *81(1),* 65–70 [in Russian].

9 Naboichenko, S.S., Mamiachikov, S.V., & Karelov, S.V. (2004). *Myshiak v tsvetnoi metallurhii [Arsenic in nonferrous metallurgy]*. Yekaterinburg: UrB RAS [in Russian].

10 Litvill, K. (1925).*Trans. Amer. Inst. Min. and Met.Eng*., *71*, 953 (cited in: Hoffman, G.O. (1932). *Metallurhiia svintsa [Metallurgy of lead]*. (Urazova G.G., Trans.). Moscow-Leningrad: Tsvetmetizdat [in Russian]).

11 Ponomareva, Ye.I., Soloviov, V.D., & Bobrova V.V. (1975). *Myshiak v svintsovo-tsinkovoi promyshlennosti [Arsenic in the lead-zinc industry]*. Alma-Ata: Nauka [in Russian].

12 Kopylov, N.I., & Kaminskii, Yu.D. (2016). Vyvod myshiaka iz otvalov kombinata «Tuvakobalt» kombinirovannym sposobom [The withdrawal of arsenic from the dumps of the plant «Tuvakobalt» in a combined way]. *Vestnik Karahandiskoho universiteta. Seriia Khimiia — Bulletin of the Karaganda University. Ser. Chemistry*, *81(1),* 60–64.

13 Bortnikova, S.B., Gaskova, O.L., & Bessonova, Ye.P. (2006). *Heokhimiia tekhnohennykh system [Geochemistry of technogenic systems]*. Novosibirsk: Akadem. izd-vo «Heo» [in Russian].

14 Kopylov, N.I., Kaminskii, Yu.D., & Ochur-ool, A.P. (2011). Kombinirovannyi sposob izvlecheniia myshiaka iz otvalov [Combined method of extracting arsenic from dumps]. *Khimicheskaia tekhnolohiia — Chemical technology*, *12, 8*, 498–500.

15 Kopylov, N.I. (2012). *Problemy myshiaksoderzhashchikh otvalov [Problems of arsenic-containing dumps]*. G.A. Tolstikov (Ed.). Novosibirsk: Akadem. izdatelstvo «Heo» [in Russian].

UDC 378.1

G.T. Kokibasova, A.T. Dyussekeyeva, S.Kh. Kaztayeva

Ye.A. Buketov Karaganda State University, Kazakhstan
(E-mail: kokibasova@mail.ru)

Formation of critical thinking skills at the lesson of the discipline «Chemistry of Elements»

A methodology for conducting classes using new forms of work that promote the development of critical thinking has been developed. The first year students took part in the experiment. Pedagogical experiment consisted of three stages, namely, ascertaining, formative and control. Classes were held with the use of various techniques such as schemes, diagrams, presentations, clusters, which made the classes more interesting, cognitive and diverse. Questionnaires and questions for testing the level of components development of critical thinking were designed. They helped to determine the level of educational motivation and to test the effectiveness of supporting abstracts. These tasks were applied before the beginning of the experiment to determine the initial level of development of critical thinking, as well as after the formation stage. The results of the present stage of the experiment showed that the level of critical thinking of first-year students was not sufficiently developed. The obtained data of research can be used at creation of a technique of students' critical thinking development in the chemistry course teaching. In comparison with the traditional form of teaching, where an authoritarian approach to learning is used, this technology provides a free liberal form of conducting a lesson that leads to the awakening of students' cognitive activity. Traditional evaluation technique can be used to assess students when using new forms of work, since the components of critical thinking cannot be evaluated specifically. The technology helps to establish a discussion between students, through a form of work such as oral presentation.

Keywords: critical thinking, motivation, introspection, reflection, technology, Venn diagram, cluster, presentation.

Introduction

Lecture, seminar, practical classes, laboratory work, independent work of students are traditional forms of teaching chemistry in high school. Lecture is a basic form of teaching students. The main purpose of a lecture is to provide a theoretical basis for training, develop interest in the learning process and a certain academic discipline, and motivate students to develop self-directed activities during the course [1]. In addition, a lecture is a convenient way of obtaining the basic information in a compressed form, which activates the process of cognitive activity in practical exercises. All of these are a significant plus of lecture classes. However, it is possible to identify a number of disadvantages inherent in the lecture form of training, for example, getting involved in passive perception of the information received, inability to think critically, and almost complete absence of independent work. At the lecture classes the students do not try to comprehend the material, but simply mechanically write down the lecturer's information. This means that there is simply an imitation of the cognitive process. There is a need for a new format arises for conducting lecture classes to use the teaching time effectively, which is provided to familiarize students with new material by reading the lecture of a teacher.

Experimental

The pedagogical experiment was conducted on the discipline «Chemistry of Elements» in which the first-year students took part. The first-year students of the Kazakh department were chosen to participate in the experiment, because there are class-lesson forms of the organization of the educational process at schools, where students study subjects strictly sequentially in a specific volume for a certain period in classroom conditions. In the university, students are trained in the credit system of education, which is aimed at increase the level of self-education and individualizing the pace of student learning. Therefore, first-year students are the least prepared for an individual form of training organization, where they must independently master the knowledge. Also another reason why first-year students took part in the experiment is that at school students use one or two textbooks, when they come to the university, as such, they have no single textbook on which they can study. This is one of the difficulties in finding and studying information. One of the tasks of the experiment was that the students of the Kazakh department should learn to write lecture notes from textbooks not only in Kazakh, but in Russian too.

Before applying the technology of critical thinking at the lesson of chemistry, it is necessary to find out at what level of development critical thinking exists. Especially, in the first year students with a different level of education from different schools study. In this regard, the pedagogical experiment was divided into three stages, namely, ascertaining, formative and control. For each stage, various tasks were developed, which served as diagnostic and forming tools [2].

The goal of the ascertaining stage of the experiment is to determine the initial level of development of critical thinking among students in the process of teaching chemistry of elements. In accordance with the goal, the main tasks of the ascertaining stage of the experiment are outlined:

– to determine the level of motivational readiness of students for the formation of critical thinking in the process of studying the chemistry of elements;
– define criteria and indicators of the level of development of critical thinking of students;
– select the diagnostic material with which it's possible to determine the qualitative characteristics and are unique to each of the critical thinking levels;
– define the initial level of development of critical thinking in first-year students.

At this stage of the experiment, students' learning motivation was studied, also the ability to compose abstracts, and the ability to work in a group. A questionnaire [3] to study the motivation of students was used, where students were required to answer «yes» or «no» to the following questions:

1) Are you interested in studying chemistry?
2) Can you apply the knowledge gained in chemistry in life?
3) Do you ask questions to the teacher if you do not understand something?
4) Do you read additional literature on chemistry?
5) Do you like solving complex chemistry problems?
6) Are you interested in the achievements of scientists in the field of chemistry?
7) Are you trying to find answers to your questions?
8) Do you apply knowledge gained in chemistry classes while studying another subject?
9) Do you limit the information in the textbook to answer on the lesson?
10) Do you practice self-education?
11) Do you consider the information presented in the textbooks is interesting?
12) Do you think good knowledge will help you in your future professional work?

For each question with a «yes» answer, one point is awarded, with a negative answer, the points are not credited. Levels of motivation: high (from 10 to 12), medium (from 6 to 9), low (from 0 to 5).

It is possible to monitor positive changes in the students' educational motivation in comparison with the initial state after processing the results of the questionnaire (Table 1).

Table 1

The level of motivation of students before and after the experiment

Levels	Number of Students	
	before the experiment	after the experiment
High	6	7
Average	14	15
Low	4	2

As the results of the research show, the motivation of the majority of students at the beginning of the experiment is at an average level, where students' interest in the learning process is inactive and the activities of students are not meaningful, and then there are positive changes.

There are a huge number of techniques and strategies for students to develop their critical thinking. At the beginning of the study, we selected forms of independent work that contributed to the development of the ability to think critically, which would result in mastering the skills of presenting the results of our analysis in various ways such as writing a summary, a collective presentation, a Venn diagram and diagrams, clusters.

Writing and drawing up a summary before each lecture was offered to students at home. Students can use any sources of information that must be presented in the form of a lecture. The amount of information learned by students in self-writing notes, the degree of understanding of the material studied, as well as those questions and facts that students could not understand in the course of independent work were determined by asking leading questions. Preliminary acquaintance with the material through the drafting of the abstract first caused the students great difficulties. Therefore, at the initial stage of the application of this methodology, the independent writing of abstracts was organized. Mandatory requirements for the content of the abstract was a thesis of the theoretical material with the derivation of formulas, laws, questions arising during the study of the material, the availability of examples of practical application of the material [4].

Evaluation of the abstracts was organized as follows. Four groups of students were trained, who were trained to write abstracts, according to the following criteria:

– there is no abstract;
– the abstract is not complete (not all material is reflected in the abstract);
– the summary is complete, but it has some drawbacks (the material is poorly structured, there are no conclusions, few examples, its attitude to the material is not shown in the form of questions, additions);
– the abstract is mostly without shortcomings. Improvements in learning outcomes were recorded.

When comparing the results of the study of preliminary processing of educational material, one can observe an increase in the number of students whose abstracts are mostly deficient, which leads to the development of the capacity for self-organization and critical analysis of one's own activity (Table 2).

Table 2

The results of the evaluation of abstracts before and after the experiment

Evaluation Criteria	Number of Students	
	before the experiment	after the experiment
There is no abstract	2	0
Abstract is incomplete	11	8
Abstract is complete	7	7
Abstract basically has no shortcomings	4	9

To assess the effectiveness of the compiled abstracts, we conducted a test work, where students had to answer a series of questions on the topic, using only their own abstracts. Within 10 minutes, using their own notes, the students had to answer the following 6 questions:

1) Why, in comparison with other elements of the VA group, the maximum valence of nitrogen in compounds is III, whereas, for example, the maximum valence of phosphorus is V?
2) Why does molecular nitrogen show a low reactivity?
3) What single oxide can be obtained by direct interaction of nitrogen and oxygen at high temperatures?
4) What reaction underlies the use of hydrazine as a rocket fuel?
5) Why is nitric acid stored in dark bottles? What reaction equation underlies this storage condition?
6) The most common nitrate, which is used as a nitrogen fertilizer?

Verification work carried out at the end of the experiment showed also improvements in comparison with the ascertaining stage.

Presentation as a kind of educational retelling puts the task to convey from the perceived text the main thing, using the language means of generalized content transfer. It occupies a special place in the teaching of coherent speech and contributes to the improvement of general communicative skills: to disclose the topic, the main idea of the text, to plan the utterance, to improve the created text.

Presentation lasting about 15–20 minutes was prepared by students, who were previously divided into groups. For example, in the lesson on «Elements of Group V», where the main representatives are nitrogen and phosphorus, we used the oxidation states characteristic of these elements as a basis for dividing students into groups. If a student came across a card with a «+5», he was in a group that needed to characterize all the nitrogen compounds, where he exhibited an oxidation state of «+5».

In preparing the presentation, students were given the opportunity to use various sources of information, including their own abstracts.

From each group, 2 to 3 representatives were elected who were to go to the board and provide information about the element, its representatives, properties and applications. After their speech, students from other groups asked them questions on interesting or incomprehensible facts.

The main requirements for the presentation were: own critical analysis of information, close communication with the audience, persuasiveness and creative submission of information using examples. The greatest number of skills and competencies helps to get work on a collective presentation, as apart from analytical abilities, the ability to distribute duties, skills of effective oral presentation is also developed.

Also one of the new forms of work was the development of schemes (Fig. 1).

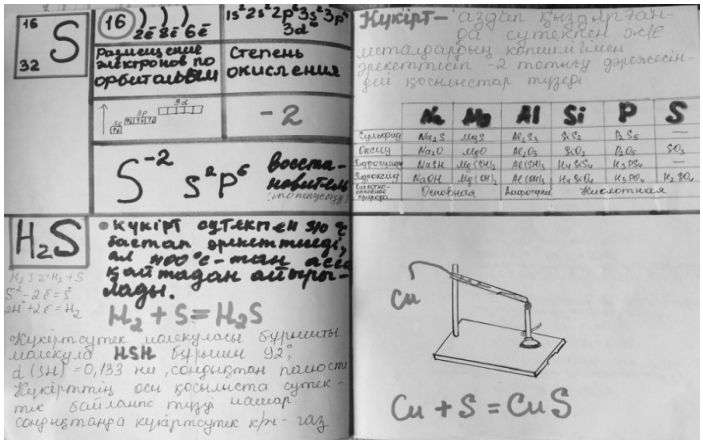

Figure 1. Presentation of the training material in the form of a schema

The scheme is used to visually structure a topic, highlight the main structural elements and establish links between them. These schemes help students to see not only the distinctive features of objects, but also allow faster and stronger storage of information [5].

The Venn diagram was used to compare two or more elements that have similar physical and chemical properties. The lesson reveals two or more concepts, terms, phenomena that need to be compared. For example, in the task «Compare properties and structure that are inherent in nitrogen and phosphorus», students draw rings, fill in graphs. At the stage of reflection, the diagrams in the groups are discussed (Fig. 2).

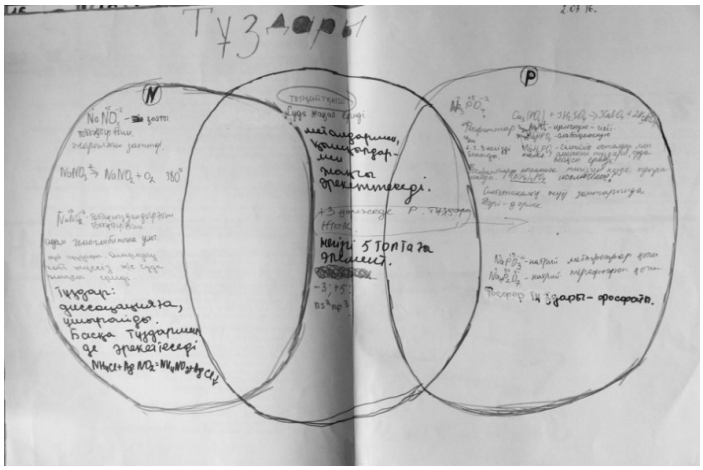

Figure 2. Venn diagram on the subject «Elements of the VA group»

Another of the new forms of work was the reception of Clusters. On the lesson, we tried to characterize the s-elements. Students had to write in notebooks all the associations that they cause these metals (work within 2 minutes). The teacher builds clusters on the board according to the ideas expressed by the students (Fig. 3).

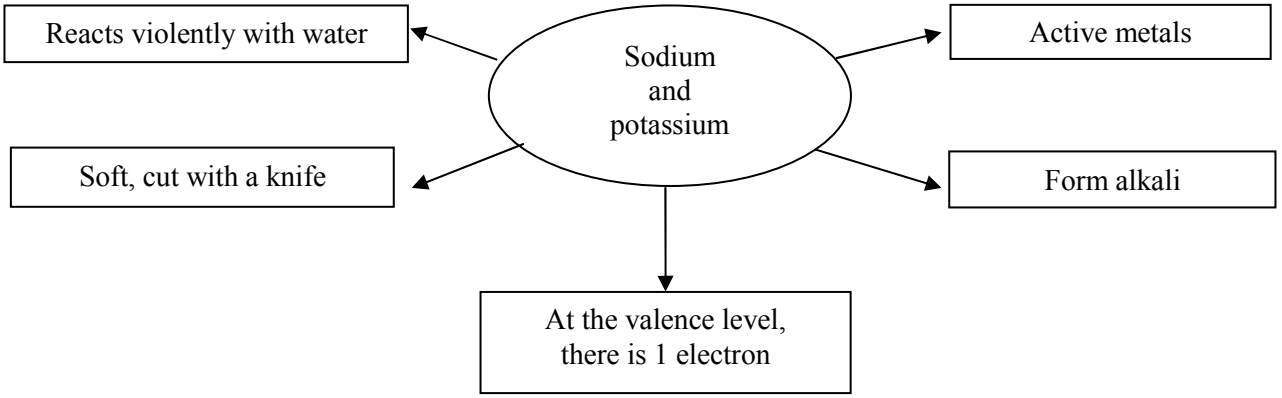

Figure 3. Cluster on «Sodium, potassium and their properties»

At the end of each lesson, students were asked questions for self-analysis of the effectiveness of their own abstracts and their participation in the work of the group when applying the presentation of the material.

1) Has your reference abstract helped you in answering questions on the topic of the lecture?

2) Do you think that the teaching material is fully reflected in your abstract?

3) Do you think you have learned reflect the training material briefly and at the same time fully?

4) Do you participate in the preparation of the group for the presentation?

5) Do you present your thoughts aloud when discussing a group of questions of a lecture?

6) Do you participate in the distribution of roles and the definition of the function of each member of the group?

7) Do you like the pace of the work of the group you were assigned to?

For clarity, the results of the study of the effectiveness of the abstracts are presented in the form of a diagram in Figure 4.

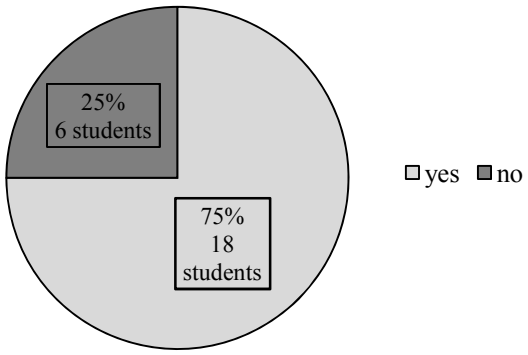

Figure 4. Efficiency of abstracts

The number of students who believe that the quality of their abstracts had improved markedly increased. Perhaps this was due to the fact that the number of students who believed that they had coped well with the questions of verification work had increased.

After processing the results of the questionnaire, the following data were obtained: 79 % of students rate their learning activity in the group as high, 21 % — as low.

On the last lesson we held a reflection in order to identify students' perception of new forms of work. For this purpose, students were given questionnaires with the following questions [6]:

1) Did you like the new forms of work with information?

2) Did you easily manage to present information in the form of diagrams, diagrams and presentations?

3) Do you think that these forms of work contribute for improving the quality of knowledge in this discipline?

4) Would you like to continue using these forms of work in class?

The results of this survey are shown in Figure 5.

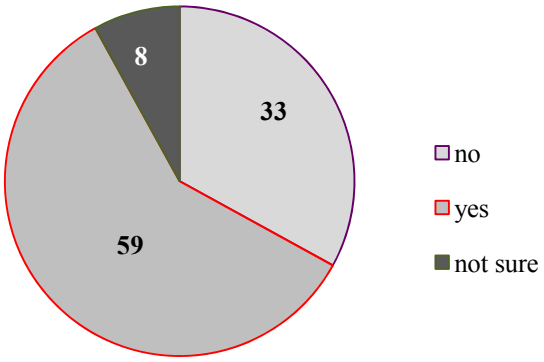

Figure 5. Perception of new forms of students work

Conclusions

Approbation of methods for developing students' critical thinking (abstract, clusters, schemes, Venn diagram and presentations) has proved the possibility of purposeful development of critical thinking of first-year-students in the process of teaching chemistry. The most difficult for the students was the task — the Venn diagram and the preparation of lecture notes. By the end of the experiment, students have learned to compose such abstracts that can be used in practical exercises without resorting to additional sources.

The results of testing all components of critical thinking at the control stage confirm the success of the experiment. Also, these techniques help to interest more passive students, who in the course of time in the process of learning may appear personal functions, in particular, motivation for learning. When applying these strategies independence of judgments, creative abilities are developed. If the teacher uses these techniques in the educational process, they can also identify individual gaps in the knowledge of each student.

It is necessary to use different methods and techniques to develop critical thinking among students not only in lectures, but also in practical exercises.

A small disadvantage of this technology is the teacher's time spent preparing for the lesson, since there are almost no didactic or teaching aids, which give examples of ready-made assignments that could be used to prepare the lesson plan. All the tasks the teacher needs to think through independently and to foresee questions that can raise doubts among students.

References

1 Халперн Д.А. Психология критического мышления: учеб. пособие / Д.А. Халперн. — СПб.: Наука, 2000. — 512 с.

2 Нечитайлова Е.В. Использование технологии развития критического мышления на уроках химии / Е.В. Нечитайлова // Химия в школе. — 2011. — № 6. — С. 12–18.

3 Омарова В.К. Инновационные подходы в образовании: учеб. пособие / В.К. Омарова. — Павлодар: Ғылым, 2012. — 253 с.

4 Калашникова Н.А. Методология формирования критического мышления у студентов вузов / Н.А. Калашникова // Вестн. ВолГУ. — 2010. — № 8. — С. 25, 26.

5 Полицинский Е.В. Активизация познавательной деятельности студентов на лекционных занятиях/ Е.В. Полицинский, Е.А. Румбешта // Вестн. ТГПУ. — 2011. — № 6. — С. 37–40.

6 Kokibasova G.T. Implementation of new forms of works for formation of skills of information critical analysis / G.T. Kokibasova, K.K. Serikova, M.M. Abisheva // Вестн. Караганд. ун-та. Сер. Химия. — 2017. — № 4(88). — С. 108–112.

Г.Т. Кокибасова, А.Т. Дюсекеева, С.Х. Казтаева

«Элементтер химиясы» пәні бойынша сабақтарында сын тұрғысынан ойлау қабілеттерін қалыптастыру

Сын тұрғысынан ойлауды дамытуға ықпал ететін жаңа жұмыс түрлерін қолданатын сабақтарды өткізу әдістемесі жасалды. Экспериментке бірінші курс студенттері қатысты. Педагогикалық тәжірибе үш кезеңнен тұрды: анықтау, қалыптастыру және бақылау. Сабақтар әр түрлі әдістерді қолданумен өткізілді: схемалар, диаграммалар, презентациялар, кластерлер, олар сабақты қызықты және когнитивті етуіне ықпал етті. Сыни тұрғыдан ойлау компоненттерінің даму деңгейін тексеру үшін сауаттылықты дамытудың деңгейін анықтау және рефераттардың тиімділігін тестілеу сұрақтары бойынша сауалнама өткізілді. Бұл міндеттер эксперимент басталғанға дейін сыни ойлаудың бастапқы деңгейі, сондай-ақ қалыптасу кезеңінен кейін анықталды. Тәжірибенің қазіргі кезеңінің нәтижелері бірінші курс студенттерінің сын тұрғысынан ойлау деңгейі жеткіліксіз дамығанын көрсетті. Зерттеудің алынған деректерін химияны оқыту барысында студенттердің сыни ойлауды дамыту әдісін құру кезінде қолдануға болады. Оқудың авторитарлық әдісі қолданылатын дәстүрлі оқыту әдісімен салыстырғанда, бұл технология оқушылардың танымдық белсенділігін оятуға әкелетін сабақты өткізудің еркін либералды нысанын қамтамасыз етеді. Оқушылардың жаңа жұмыс формаларын пайдаланған кезде бағалау үшін дәстүрлі бағалау әдісін қолдануға болады, себебі сыни ойлаудың компоненттері нақты бағалануы мүмкін емес. Технология ауызша презентация сияқты жұмыс түрлерімен студенттер арасында пікірталас құруға көмектеседі.

Кілт сөздер: сын тұрғысынан ойлау, мотивация, өзін-өзі талдау, рефлексия, технология, Венна диаграммасы, кластер, презентация.

Г.Т. Кокибасова, А.Т. Дюсекеева, С.Х. Казтаева

Формирование навыков критического мышления на занятиях дисциплины «Химия элементов»

Разработана методика проведения занятий с применением новых форм работ, способствующих развитию критического мышления. В эксперименте принимали участие студенты первого курса. Педагогический эксперимент состоял из трех этапов: констатирующего, формирующего и контрольного. Занятия проходили с применением различных приемов: схемы, диаграммы, презентации, кластеры, которые делали занятие более интересным, познавательным и разнообразным. Для проверки уровня развития компонентов критического мышления были разработаны анкеты для определения уровня развития учебной мотивации и вопросы для проверки эффективности опорных конспектов. Данные задания применялись перед началом эксперимента для определения исходного уровня развития критического мышления, а также после проведения формирующего этапа. Результаты констатирующего этапа эксперимента показали, что уровень критического мышления первокурсников недостаточно развит. Полученные данные исследования могут быть использованы при создании методики развития критического мышления студентов в процессе обучения химии. В отличие от традиционной формы преподавания, где используется авторитарный подход к обучению, данная технология обеспечивает свободную либеральную форму проведения занятия, которая ведет к пробуждению когнитивной деятельности студентов. Для оценивания студентов при использовании новых форм работы можно пользоваться традиционной методикой оценивания, так как компоненты критического мышления невозможно оценивать конкретно. Технология способствует установлению дискуссии между студентами посредством такой формы работы, как устная презентация.

Ключевые слова: критическое мышление, мотивация, самоанализ, рефлексия, технология, диаграмма Венна, кластер, презентация.

References

1 Khalpern, D.A. (2000). *Psikholohiia kriticheskoho myshleniia [Psychology of critical thinking]*. Saint Petersburg: Nauka [in Russian].

2 Nechitaylova, Ye.V. (2011). Ispolzovanie tekhnolohii razvitiia kriticheskoho myshleniia na urokakh khimii [Using technology to develop critical thinking in chemistry lessons]. *Khimiia v shkole — Chemistry at School, 6*, 12–18 [in Russian].

3 Omarova, V.K. (2012). Innovatsionnye podkhody v obrazovanii [Innovative approaches in education]. Pavlodar: Gylym [in Russian].

4 Kalashnikova, N.A. (2010). Metodolohiia formirovaniia kriticheskoho myshleniia u studentov vuzov [Methodology for the formation of critical thinking in university students]. *Vestnik VolGU — Bulletin VolSU*, 8, 25–26 [in Russian].

5 Politsinskiy, Ye.V., & Rumbeshta, Ye.A. (2011). Aktivizatsiia poznavatelnoi deiatelnosti studentov na lektsionnykh zaniatiiakh [Activation of cognitive activity of students in lecture classes]. *Vestnik TGPU — Bulletin of TSPU*, 6, 37–40 [in Russian].

6 Kokibasova, G.T., Serikova, K.K., & Abisheva, M.M. (2017). Implementation of new forms of works for formation of skills of information critical analysis. *Vestnik Karagandinskoho universiteta. Seriia Khimiia — Bulletin of the Karaganda University. Ser. Chemistry, 4(88)*, 108–112.

АВТОРЛАР ТУРАЛЫ МӘЛІМЕТТЕР
СВЕДЕНИЯ ОБ АВТОРАХ
INFORMATION ABOUT AUTHORS

Abeuova, S.B. — PhD, Senior lecturer of the Inorganic and Technical Chemistry department, Ye.A. Buketov Karaganda State University, Kazakhstan.

Adekenov, S.M. — Laureate of the State Prize of the RK, Honored Worker of the RK, Academician of the National Academy of Sciences, Dr. Chem. Sci., Professor, Chairman of the Board of JSC «International Research and Production Holding "Phytochemistry"», Karaganda, Kazakhstan.

Arystanova, Zh.T. — MSc., Engineer of Technological incubator, Ye.A. Buketov Karaganda State University, Kazakhstan.

Baizhigit, E.A. — Master student, Engineer of the Laboratory of Chemistry of Steroid Compounds, JSC «International Research and Production Holding "Phytochemistry"», Karaganda, Kazakhstan.

Bakibaev, A.A. — Dr. Chem. Sci., Professor, Tomsk State University, Russia.

Balpanov, D.S. — Cand. Chem. Sci., Senior Researcher, «BioGeoTec» LLP, Stepnogorsk, Kazakhstan.

Blagikh, Ye.V. — MSc, Institute of Polymer Materials and Technology, Almaty, Kazakhstan.

Bolatbay, A.N. — Master student, Ye.A. Buketov Karaganda State University, Kazakhstan.

Borsynbayev, A.S. — Researcher of the Laboratory of the engineering profile «Physical and chemical methods of research», Ye.A. Buketov Karaganda State University, Kazakhstan.

Burkeyev, M.Zh. — Dr. Chem. Sci., Professor, Director of Research Institute of chemical problems, Ye.A. Buketov Karaganda State University, Kazakhstan.

Burkeyeva, G.K. — Senior lecturer of the Organic Chemistry and Polymers department, Ye.A. Buketov Karaganda State University, Kazakhstan.

Chirkova, V.Yu. — Postgraduate of the Department of Physical and Inorganic Chemistry, Chemical Faculty, Altai State University, Barnaul, Russia.

Dyussekeyeva, A.T. — Cand. Chem. Sci., Assistant Professor of the Department of Inorganic and Technical Chemistry, Ye.A. Buketov Karaganda State University, Kazakhstan.

Erkasov, R.Sh. — Dr. Chem. Sci., Professor, L.N. Gumilyov Eurasian National University, Astana, Kazakhstan.

Gubenko, M.A. — MSc in Chemistry, Senior lecturer of the Department of Natural Sciences, Kostanay State Pedagogical Institute, Kazakhstan.

Ismagulov, B.M. — Master student of the Chemical faculty, Ye.A. Buketov Karaganda State University, Kazakhstan.

Issagulov, A.Z. — Dr. Tech. Sci., Professor, First pro-rector, Karaganda State Technical University, Kazakhstan.

Kanafin, Ye.N. — Junior Researcher, «BioGeoTec» LLP, Stepnogorsk, Kazakhstan.

Kasenov, R.Z. — Cand. Chem. Sci., Associate Professor, Laboratory of the engineering profile «Physical and chemical methods of research», Ye.A. Buketov Karaganda State University, Kazakhstan.

Kasymova, L.G. — Lecturer, Karaganda State Technical University, Kazakhstan.

Kaykenov, D.A. — Researcher of the Laboratory of the engineering profile «Physical and chemical methods of research», Ye.A. Buketov Karaganda State University, Kazakhstan.

Kazhikenova, S.Sh. — Dr. Tech. Sci., Professor, Head of the Higher Mathematics department, Karaganda State Technical University, Kazakhstan.

Kaztayeva, S.Kh. — MSc, Department of Inorganic and Technical Chemistry, Ye.A. Buketov Karaganda State University, Kazakhstan.

Kezdikbaeva, A.T. — Cand. Chem. Sci., Assistant Professor, Ye.A. Buketov Karaganda State University, Kazakhstan.

Khannanov, R.A. — Senior Researcher, «BioGeoTec» LLP, Stepnogorsk, Kazakhstan.

Klimentova, J. — Mgr., PhD, Department of Inorganic Chemistry, Faculty of Science, Charles University, Prague, Czech Republic.

Klivenko, A.N. — PhD, Teacher, Shakarim State University of Semey, Kazakhstan, Kazakhstan.

Kokibasova, G.T. — Cand. Chem. Sci., Associate Professor, Professor of the department of Inorganic and Technical Chemistry, Ye.A. Buketov Karaganda State University, Kazakhstan.

Kopylov, N.I. — Dr. Tech. Sci., Professor, Institute of Solid State Chemistry and Mechanochemistry of the Siberian Branch of the Russian Academy of Sciences, Novosibirsk, Russia.

Kudaibergen, G.K. — PhD student, Ye.A. Buketov Karaganda State University, Kazakhstan.

Kudaibergenov, S.E. — Dr. Chem. Sci., Professor, Director, Institute of Polymer Materials and Technology, Laboratory of engineering profile of Satbayev University, Almaty, Kazakhstan.

Kurmanova, A.F. — Cand. Chem. Sci., Assistant Professor of the Physical and Analytical Chemistry department, Ye.A. Buketov Karaganda State University, Kazakhstan.

Kutzhanova, K.Zh. — Cand. Chem. Sci., Assistant Professor of the Physical and Analytical Chemistry department, Ye.A. Buketov Karaganda State University, Kazakhstan.

Makhmetova, G.Sh. — Lecturer, Karaganda State Technical University, Kazakhstan.

Minayeva, Ye.V. — Cand. Chem. Sci., Assistant Professor of the Organic Chemistry and Polymers Department, Ye.A. Buketov Karaganda State University, Kazakhstan.

Moldurushku, M.O. — Research Fellow, Tuva Institute of Integrated Development of Natural Resources of the Siberian branch of the Russian Academy of Sciences, Kyzyl, Russia.

Mukhanova, D.A. — MSc., Engineer of LLP Biotron Group, Stepnogorsk, Kazakhstan.

Munarbaeva, B.G. — Cand. Ped. Sci., Head of the Department of Natural Sciences, Z. Aldamzhar Kostanay Social and Technical University, Kazakhstan.

Mustafin, E.S. — Dr. Chem. Sci., Professor, Head of the Laboratory of the engineering profile «Physical and chemical methods of research», Ye.A. Buketov Karaganda State University, Kazakhstan.

Nurakhmetova, Zh.A. — MSc, Engineer, Institute of Polymer Materials and Technology, Almaty, Kazakhstan.

Omarov, Kh.B. — Vice-rector for scientific work, Corresponding Member of the National Academy of Sciences of the Republic of Kazakhstan, Dr. Tech. Sci., Professor, Ye.A. Buketov Karaganda State University, Kazakhstan.

Omasheva, A.V. — Cand. Chem. Sci., Associate Professor of the Organic Chemistry and Polymers department, Ye.A. Buketov Karaganda State University, Kazakhstan.

Pushchina, A.V. — Graduate student of the Physical and Analytical Chemistry department, Ye.A. Buketov Karaganda State University, Kazakhstan.

Pustolaikina, I.A. — Cand. Chem. Sci., Assistant Professor of the Physical and Analytical Chemistry department, Ye.A. Buketov Karaganda State University, Kazakhstan.

Sadakbayeva, Zh.K. — PhD, Institute of Macromolecular Chemistry of the Academy of Sciences, Prague, Czech Republic.

Salkeyeva, L.K. — Dr. Chem. Sci., Professor, Head of the Organic Chemistry and Polymers department, Ye.A. Buketov Karaganda State University, Kazakhstan.

Shaikhova, G.S. — Cand. Tech. Sci., Senior Lecturer, Karaganda State Technical University, Kazakhstan.

Shaikhutdinov, V.M. — Junior Researcher, «BioGeoTec» LLP, Stepnogorsk, Kazakhstan.

Shtobbe, I.A. — Assistant Professor of the Physical and Inorganic Chemistry department, Altai State University, Barnaul, Russia.

Sigitov, V.B. — Dr. Chem. Sci., Researcher, Institute of Polymer Materials and Technology, Almaty, Kazakhstan.

Solotchina, E.P. — Doctor of Geological and Mineralogical Sciences, Leading researcher, V.S. Sobolev Institute of Geology and Mineralogy of the Siberian Branch of the Russian Academy of Sciences, Novosibirsk, Russia.

Stas', I.E. — Doctor of Chemistry, Associate Professor of the Physical and Inorganic Chemistry department, Altai State University, Barnaul, Russia.

Tazhbayev, Ye.M. — Dr. Chem. Sci., Professor, Dean of Chemical faculty, Ye.A. Buketov Karaganda State University, Kazakhstan.

Temirgaziev, B.S. — PhD student, Master of technical sciences, Ye.A. Buketov Karaganda State University; Junior researcher of the Laboratory of Chemistry of Steroid Compounds, JSC «International Research and Production Holding «Phytochemistry», Karaganda, Kazakhstan.

Ten, O.A. — Candidate of Biological Sciences, Senior Researcher, «BioGeoTec» LLP, Stepnogorsk, Kazakhstan.

Tuleuov, B.I. — Head of the Laboratory of Chemistry of Steroid Compounds, Dr. Chem. Sci., Professor, Corresponding Member of NAS RK, JSC «International Research and Production Holding «Phytochemistry», Karaganda, Kazakhstan.

Tuleuov, U.B. — Student, Ye.A. Buketov Karaganda State University, Kazakhstan.

Vazhev, V.V. — Dr. Chem. Sci., Professor of the Department of Natural Sciences, Z. Aldamzhar Kostanay Social and Technical University, Kazakhstan.

Vazheva, N.V. — Candidate of pedagogical sciences, Associate Professor of the Department of Natural Sciences, Kostanay State Pedagogical Institute, Kazakhstan.

Vojtisek, P. — Assoc. Prof., RNDr., CSc., Department of Inorganic Chemistry, Faculty of Science, Charles University, Prague, Czech Republic.

Yergaliyeva, E.M. — MSc in Chemistry, Senior Teacher of the Department of Natural Sciences, Kostanay State Pedagogical Institute, Kazakhstan.

Yesentayeva, N.A. — Master student, Ye.A. Buketov Karaganda State University, Kazakhstan.

Zhaparova, L.Zh. — PhD, Assistant Professor of the Organic Chemistry and Polymers department, Ye.A. Buketov Karaganda State University, Kazakhstan.

Zhappar, N.K. — Junior Researcher, «BioGeoTec» LLP, Stepnogorsk, Kazakhstan.

Zhumagalieva, T.S. — Cand. Chem. Sci., Associate Professor of the Organic Chemistry and Polymers department, Ye.A. Buketov Karaganda State University, Kazakhstan.